THE UNIVERSITY OF LIVERPOOL

Interaction of circulating galectin-3 and cancer-associated MUC1 in cancer metastasis

Thesis submitted in accordance with the requirements of the University of Liverpool for the degree of Doctor in Philosophy by

Qi Cheng Zhao

April

2010

ACKNOWLEGEMENTS

First, I would like to thank Cancer Research UK for funding this work, and for its continual and increasing support throughout my PhD, even during my thesis writing up period. As an international student paying international tuition fee, this financial support is very important to me. Also I would like to thank Henry Lester scholarship for their financial supporting during my PhD.

Then I would like to thank my supervisors Dr Lugang Yu and Professor Jonathan M Rhodes for their guidance, ideas and help. Dr Yu, you teach me so much during my PhD, especially at the starting days in the basic research fields here, I met so many difficult. Your continual encouragement, patience and friendly help, that make me successfully deal with the entire situation, have been invaluable. I shall never forget the times working for you. And in personal, I am grateful for you given a helping hand whenever I need, even don't mention fantastic time enjoyed in your house. Professor Jonathan Rhodes, your enthusiasm and dedication to this work has been an inspiration.

I would also like to show my appreciation to those who have supported my work in the division of Gastroenterology, both colleagues and friends, I want to thank you for creating an environment which was productive in which to work. I would like to say special thank you to Monica, who don't work here now, for her teaching and assistance in using flow cytometry. I would also like to thank Dr Barry Campbell and Professor Mark Prichard and Professor Alastair Watson for their advices given in my presentation or panel meeting.

I would like to thank Professor Gerard B. Nash, Mr Philip C. Stone in University of Birmingham helped in flow condition experiment, John Hilkens from Netherlands kindly provide the cells line, Dr. Thecla Lesuffleur (INSERM U560, Lille, France) for the HT29-5F7 cells and Dr. Mark Reddish (Biomira, Edmonton, Canada) for the B27.29 mAb. Xiuli Guo in Shandong University of China conducted the animal experiments. I would like to thank my friend Shaohui Wang for her encouragement and helping in my thesis format.

Finally, my biggest thank you is reserved for my family, my lovely son Yinuo Zhao, my parents Yu Sheng Zhao, Xing Zhen Wang, my brother Qijun Zhao, for all your encouragement and support, in so many ways, over years.

DECLARATION

I hereby declare that this thesis is a presentation of my original work. All experimental work was performed by myself apart from flow condition experiment performed by Mr Philip C. Stone and me in University of Birmingham. The animal experiments performed by Xiuli Guo in Shandong University of China. Wherever contributions of others are involved, every effort has been made to indicate this clearly, with due reference to the literature.

The work was done under the guidance of Dr Lugang Yu and Professor Jonathan M Rhodes, both of the school of Clinical sciences at the University of Liverpool.

ABSTRACT

The concentrations of the galactoside-binding galectin-3 are greatly increased in the circulation of cancer patients and in particular those with metastasis. It shows here that galectin-3 at pathologically-relevant concentrations induces marked increase of cancer cell homotypic aggregation, heterotypic adhesion to vascular endothelium and trans-endothelial invasion *in vitro* under static and flow conditions and decreases the latency of experimental metastasis in athymic nude mice. These effects are shown to be a consequence of the interaction between galectin-3 and TF antigen on cancer-associated MUC1 by inducing MUC1 cell surface re-localization/polarization thus revealing the otherwise concealed cell adhesion molecules including CD44 and E-Cadherin. These findings suggest that interaction between circulating galectin-3 and cancer-associated MUC1 is an important mechanism in promoting haematogenous dissemination of tumour cells to remote sites.

It also shows here that peanut agglutinin, a-TF-binding lectin from peanut, at concentrations similar to that observed in the blood circulation of people who ingested 200g peanuts induces homotypic aggregation and heterotypic adhesion to vascular endothelial cells *in vitro*. The cell aggregates induced by PNA increases the survival and resistance of cancer cells to anoikis initiation under anchorage-independent conditions. These results suggest a detrimental effect of the presence of peanuts in the diet of cancer patients on patients' survival.

ABBREVIATIONS

ABA	*A. bisporus* agglutinin
ABL	*Agaricus bisporus* lectin
AGE	Advanced glycosilation end products
ASF	asialofetuin
BSA	Bovine serum albumin
CAMs	cell adhesion molecules
CEA	Carcino-embrionic antigen
CEC	colonic epithelial cell
CRDs	carbohydrate recognition domains
CTCs	Circulating tumour cells
DISC	death-inducing signalling complex
DMEM	Dulbecco's modified Eagle's medium
DMSO	Dimethyl sulfoxide
ECL	enhanced chemiluminescence
ECM	extracellular matrix components
EDTA	ethylenediaminetetraacetic acid
EGM	Endothelial growth media
ELISA	Enzyme-linked immunosorbent assay
FADD	Fas-associated death domain protein
FasL	Fas Ligand
FCS	Fetal Calf Serum
FOV	fields of view
GlcNAc	*N*-acetylglucosamine
HA	Hyaluronan
HIPK2	homeodomain-interacting protein kinase 2
HMVEC-L	human microvascular lung endothelial cells
HSC-3	human squamous carcinoma
HUVEC	human umbilical vein endothelial cells
ICAM-1	with intercellular adhesion molecule-1 (ICAM-1)
IDC	invasive ductal carcinoma
MGAT5	beta1,6N-acetylglucosaminyltransferase V
MPM	Malignant pleural mesothelioma
MUC1-C	MUC1 COOH-terminal subunit
MUC1CT	MUC1 cytoplasmic tail
NECDS	non-enzymatic cell dissociation solution
NF-kB	nuclear factor kB
O.D.	optical density
OMM	mitochondrial membrane
PI	propidium iodide
PNA	peanut agglutinin
poly-HEMA	poly-2-hydroxyethyl methacrylate

SDS	sodium dodecyl sulfate
TEER	trans-endothelial electrical resistance
TEMED	Tetramethylethylenediamine
TF	Thomsen-Friedenreich oncofetal carbohydrate (Galβ1,3GalNAc-)
Tn	GalNAc-
TNFR	tumour necrosis factor-a receptor
TNF-α	tumour necrosis factor-alpha
VNTR	variable numbers of tandem repeat peptides

CONTENT

CHAPTER 1

1. Introduction

1.1. Metastasis of epithelial cancers

1.1.1. Cancer and metastasis

Twenty-three per cent of all deaths in the US (US Mortality Data 2006, National Center for Health Statistics, Centers for Disease Control and Prevention, 2009. http://www.cdc.gov/) and 27% of all deaths in the UK are due to cancer (1-3). About 293,600 new cancer cases were diagnosed in the UK in 2006 (1, 2, 4). This means one new cancer case every two minutes in the UK. Metastasis is the main reason for cancer-related fatality. Although the mortality rate for all neoplasm fell by 10% in the UK from 1998 to 2007, cancer-associated casualty remains one of the major disease-associated mortality in UK (1-3).

1.1.2. The metastasis cascade

Cancer metastasis from primary to remote tumour sites is a sequential interrelated multi-stepped process (5). The major steps are as follows: (a) neoplastic cells transform and grow progressively at the primary tumour sites, (b) extensive vascularization occurs when the tumour mass exceeds 2 mm in diameter, (c) tumour cells invade through the host blood vessel wall into the blood/lymphatic circulation, (d) cancer cells survive in the circulation with formation of tumour microemboli, (e)tumour microemboli adhere to the blood

vessel wall endothelium at a distant site, (f) extravasion and growth of the tumour cells at the remote site (5).

Thus, homotypic cell–cell aggregation of cancer cells and their heterotypic adhesion to the vascular endothelium are two of the key steps in the cancer metastasis cascade.

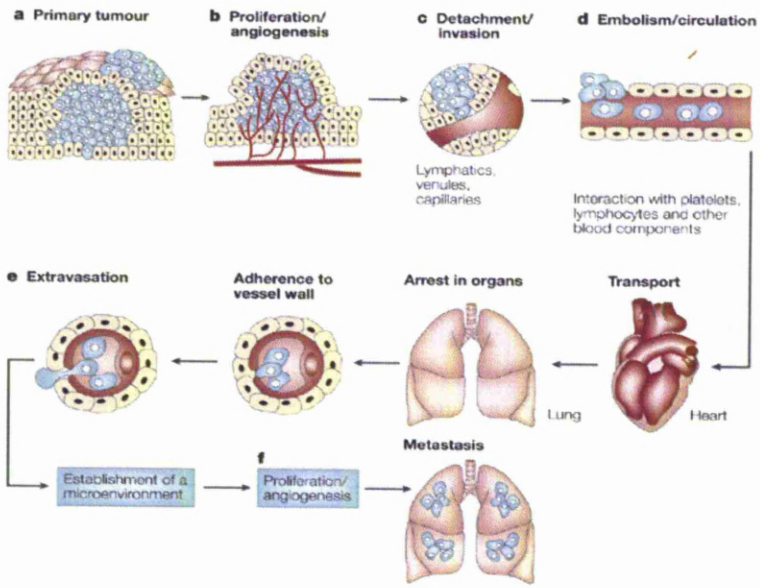

Fig 1-1, Metastatic cascade (from Fidler 2003) (5)

1.1.3. Cancer cell heterotypic adhesion to endothelial cells

Cancer cell heterotypic adhesion to the vascular endothelium is facilitated by a variety of cell surface adhesion molecules (6) (7). Cancer metastasis often occurs in an organ-specific manner. For example, the regional lymph nodes, bone marrow, lung and liver are the specific metastasis organs for breast cancer,

whereas preferred metastatic sites for colon cancer are the lung, liver, brain, adrenal glands and skeleton (8).

Three mechanisms have been proposed in the past to explain the organ-specific manner of cancer metastasis: circulation patterns, mechanical trapping and cell adhesion.

The circulation pattern, for example the direction and connection of lymphatic or venous drainage, is clearly a significant factor determining the site of metastasis. However, direct connection alone provides only a partial explanation for organ-specific metastasis (5). For example, the preferred metastasis organs of breast cancer are the lungs, bones, liver and brain (9), some of which do not have a direct circulatory connection to the breast. Experimental intravenous injection of melanoma cells in animal models demonstrated that, although tumour cells reached the vasculature of all organs, metastases developed in the orthotopic and grafted lungs and ovaries, but not in the kidneys (10). Thus, cancer spread to secondary tumour sites cannot be explained solely by circulation patterns.

The mechanical trapping theory hypothesizes that the initial site of tumour arrest depends heavily on the relative size of the tumour cells and tumour cell clusters (11). Thus, cancer cell clusters/aggregates, by acting as microemboli, produce more metastases than single cell populations (12-14). However, it has been observed that colon carcinoma cells with different metastatic capacities preferentially arrest in lung and liver capillaries, although the diameters of

involved microvessels were larger than the adherent tumour cells (8). This indicates that a mechanical trap alone cannot explain organ-specific metastasis of all types of cancers.

The cell adhesion mechanism suggests that the tumour cell arrest in the target organs in metastasis may be controlled primarily by the specific expression of cell adhesion molecules on cancer cells as well as on the vascular endothelial cells (15-17). In a recent study of breast cancer, 344 primary breast tumours of lymph node-negative patients were classified into different molecular subtypes (including luminal A) according to the 'intrinsic' gene list describing the subtypes. Luminal A subtype was abundant in bone relapse but absent in lung relapse,while focal adhesion was found up-regulated in the luminal A subtype but down-regulated in lung relapse (18). This indicates (a) that molecular subtypes cause preferential metastasis at different sites and (b) rate of metastasis in the lung is reduced as a consequence of down-regulation of local adhesion in the luminal A relapse. Although the exact adhesion molecules involved in cancer cell adhesion to endothelial cells are still unclear, four families of adhesion molecules, including E-selectin, cell adhesion molecules (CAMs) (19), CD44 (16) and integrins (17), are believed to be involved.

E-selectin is an important endothelial cell surface adhesion molecule whose physiological role is known to mediate the rolling of neutrophils, monocytes and memory T cells on the endothelium before their extravasation at sites of inflammation (20, 21). There is evidence that E-selectin is also involved in cancer-endothelial adhesion in metastasis (15, 22, 23). For example, E-selectin-

mediated binding of colonic carcinoma cells to human and mouse endothelial cells has been shown to correlate with the metastatic potential of the cells (24). Addition chimeric molecules containing extracellular regions of E-selectin coupled with the Fc portion of human IgGl, inhibits colon carcinoma HT-29 cell adhesion to the endothelium monolayer and the formation of lung metastases, while control L-selectin-immunoglobulin had no effect, although it can still bind to the HT29 cells (25). Murine carcinoma H-59 cell adhesion to the endothelial cells pre-activated with tumour necrosis factor-alpha (TNF-α, a cytokine that stimulates the acute phase reaction) could be completely and specifically abolished by a neutralizing monoclonal antibody to murine E-selectin (MAb 9A9) in vitro. The presence of the MAb 9A9 reduced the median number of liver metastases of H-59 cells by 97% in comparison to the control group in syngeneic mice (15).

Cell surface CD44 molecules have been shown to be involved cell–cell and cell–matrix interaction. The cell surface CD44 promotes tumour cell survival in invaded tissue (26) and metastasis. Several experiments using animal metastasis models have shown a correlation between increased CD44 expression and metastatic capability in cultured human melanoma (27), lymphoma cell lines (28) and rat pancreatic carcinoma cells (29). CD44 is also involved in the adhesion of cancer cells to a wide range of extracellular matrix (ECM) components (30). Hyaluronan (HA) is the major ligand of CD44 (31). There are many reports showing that the CD44-associated metastasis is linked to its binding to HA (32-35). Interactions between HA/CD44-stimulated p300 (acetyltransferase) and resveratrol-activated SIRT1 (deacetylase) play critical

roles in regulating the balance between cell survival and apoptosis, and between multi-drug resistance and sensitivity in breast tumor cells (36). Hyaluronan-mediated CD44 activation of RhoGTPase signalling and cytoskeleton function promotes tumour progression (37). Heregulin-mediated ErbB2-ERK signalling activates hyaluronan synthases leading to CD44-dependent ovarian tumour cell growth and migration (38).

There are also reports showing that the effect of CD44 on metastasis may not be dependant on its binding to HA(39, 40). The CD44 proteins have multiple protein isoforms as a result of their various splicing variants and it has been suggested that splicing variation and glycosylation play an important role in determining CD44-ligand binding (41). CD44 cross-linking with the CD44 receptor on the human breast tumour cell line (MDA-MB-435s) has been shown to lead to the enhanced expression and relocation of MMP-9 in human breast tumour cells and increased tumour invasion and metastasis (42). There are also studies showing that the degradation products of tumour-associated ECMs (extracellular matrix components) interact with CD44 and are involved in CD44-mediated tumour progression (43).

1.1.4. Cancer cell homotypic aggregation in metastasis

There are strong links between the ability of tumour cells to form homotypic aggregation and metastasis. Homotypic cancer cell aggregation at the sites of their primary attachment to the endothelium has been shown in *vitro*, ex *vivo* and in *vivo* with metastatic breast and prostate carcinoma cells (44). It shows

that cancer cells selected in *vitro* for an enhanced homotypic aggregation kinetics produce significantly higher in *vivo* experimental metastasis than the less aggregated parental cells, and also in *vivo* selection of tumour cells for high metastatic potential exhibiting increased homotypic aggregation properties (45-47). Aggregates of cancer cells have been shown to have higher survival rates in the blood circulation than single cells (13, 14). Intraportal injection of aggregated DHD/K12/TRb colon cancer cells into syngeneic BD IX rats produced over four times more liver metastases than injection with the same numbers of single cells (12).

It has been demonstrated that the aggregates of cancer cells arrest more efficiently in the small vasculature and increase metastasis (48). It has been suggested that the enhanced metastatic potential of cancer cell aggregates may be linked to resistance of the cells to the anoikis (suspension-induced apoptosis) (49). Anoikis is a specific type of apoptotic process induced by loss of cell adhesion or inadequate cell-matrix interactions (50). It has been suggested that anoikis is the dominant mechanism of removing disseminating tumour cells from the circulation (51).

It is well known that after invasion of the primary tumour cells into the circulation, only very few of them can survive in the circulation and eventually cause metastasis at remote organs in cancer patients (52, 53). Studies using cancer cell labelling with 125iodineiodo-deoxyuridine have shown that less than 0.1% of tumour cells are still viable 24 hours after their injection into the animal, and that less than 0.01% of these cells can survive to eventually produce

metastases (54). The ability of cancer cells to avoid destruction and survive from blood circulation would represent an important factor in the process of cancer metastasis (55). Prolonged survival of tumour cells in the circulation is directly associated with increased metastasis in BALB/c nude mice (56).

E-cadherin is a transmembrane glycoprotein that plays a major role in calcium-dependent, epithelial cell–cell interaction (57, 58). Several reports have shown that E-cadherin is expressed on the cell membrane of tumour cells at metastatic sites but not in the primary carcinoma sites (59-62). This indicates that E-cadherin may play different roles at different stages of cancer development.

1.1.5. Cancer cell extravasations (trans-endothelial invasion)

Cancer cell extravasations metastasis is a vital metastatic stage in which tumour cells penetrate the vascular wall at remote organs. It does not matter that some people add that extravasion starts from morphological change of the cells, such as flattening to increase contact areas, followed by migration through the vascular wall (63) and growth in the new organ.

1.1.6. Cancer cell anoikis in metastasis

1.1.6.1. Anoikis

Anoikis, a Greek word meaning homeless, is an apoptotic process induced by loss or improper contact of the cells with the extracellular matrix (64). Anoikis is an important mechanism in removing disseminating tumour cells from the

circulation (51, 65). Resistance to anoikis is an important feature of metastatic cancer cells (52, 66).

As a special type of apoptosis, anoikis-mediated cell death acts through the activation of either the intrinsic or extrinsic apoptosis pathways (67, 68). The intrinsic apoptosis pathway acts through mitochondria membrane permeabilization and cytochrome C release. Following cell detachment from the extracellular matrix (ECM) under the anoikis condition, Bid and Bim, members of the BH3-only family of proteins, are activated and promote the assembly of the pro-apoptotic Bax and Bak oligomers on the outer mitochondrial membrane (OMM) (69, 70). This creates channels on OMM (71) and the release of cytochrome C. Released cytochrome C then contributes to the apoptosome with caspase-9 and the cofactor apoptosis protease activating factor (Apaf), which activates the executioner caspases, caspase-3 (72-74). The anti-apoptotic Bcl-2 protein protects OMM (70, 75, 76) or sequesters the activator Bid and Bim and prevents Bax and Bak oligomerization (77, 78). On the other hand, sensitizer BH3-only proteins such as Bad, Bik, Bmf, Noxa, Puma and Hrk inhibit the action of Bcl-2 by competing for the BH3 domain of Bcl-2, thus allowing the action of BH3-only proteins to induce Bax-Bak oligomer formation (79, 80).

The extrinsic apoptosis pathway acts through the extracellular death ligands on the cell surface and caspase-8. Following detachment of the cells from ECM, the extracellular death ligands, such as Fas Ligand (FasL) and tumour necrosis factor-a (TNF-a), bind to their transmembrane death receptors, namely Fas and TNF-a receptor (TNFR). This results in the assembly of the death-inducing

signalling complex (DISC). The formation of DISC attracts other adaptor proteins such as the Fas-associated death domain protein (FADD), recruiting several molecules of caspase-8, which activate caspase-8, caspase-3 and -7 and apoptosis (70, 81). There are cross-talks between the extrinsic and intrinsic apoptotic signalling in some cells (82). In such cases, activation of the death receptor ligand on the cell surface is not essential in anoikis initiation. Caspase-8 activation comes from activating the intrinsic pathway (83); the extrinsic apoptotic signalling could be induced by positive feedback from mitochondrial membrane damage (84, 85).

1.1.6.2. Cell aggregation and anoikis

The majority of the cancer cells that have invaded the blood circulation are rapidly destroyed by anoikis or by the immune surveillance system and only a very small fraction of the invaded cells can survive and eventually cause metastasis at remote sites (54, 71).

It has been shown that cancer cells in aggregated forms develop the ability to evade anoikis. For example, aggregated human squamous carcinoma (HSC-3) cells shows less apoptosis than the single cell population when cultured for 36 hours under suspension conditions (86). This enhanced ability of cell aggregates to evade anoikis has been suggested to be due to decreased FAK phosphorylation and increased p53 levels (86). Malignant pleural mesothelioma (MPM) cultured in suspension on poly-HEMA coated tissue culture plates form well-organized aggregates in which the cellular PI3K/Akt, ERK and SAPK/JNK

signalling pathways are found to be inactivated. Impairment of cell aggregation by culturing the cells in suspension but under spinning conditions is seen to activate SAPK/JNK and Bim and induce anoikis (87). Claudia Hofmann et al. have revealed that colonic epithelial cell (CEC) crypts freshly isolated from surgical specimens and centrifuged into aggregation pellets show less anoikis in comparison to the CEC crypts liberated (passed over the mesh filter 80μm pore size) in suspension (88). Thus, formation of cell aggregates results in enhanced ability of the cells resistant to anoikis initiation.

1.2. Alteration of cell surface glycosylation in cancer

1.2.1. General:

Glycosylation is a post-translational process in which sugar residues are attached to proteins or lipids. Altered glycosylation occurs in neoplastic and inflammatory conditions such as cancer, Crohn's disease, rheumatoid arthritis and tuberculosis. It is believed that more than half of the mammalian proteins are modified by glycosylation of *O*- or *N*-linked glycans (89). *N*-linked glycosylation occurs via attachment of complex and diverse sugar chains through *N*-acetylglucosamine (GlcNAc) to the amide group of asparagine residues. *N*-linked glycosylation occurs on a large number of membrane-associated and secreted proteins in eukaryote cells (90). *N*-linked glycans share a common branched trimannosyl core

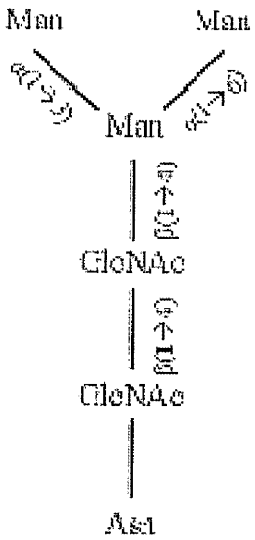

Fig. 1-2 The trimannosyl core, common to all *N*-linked glycans(89)

Man3GlcNAc2-Asn (Fig. 1-2), which may be elaborated to form a diversity of heterogeneous, often quite large and bulky, bi-, tri- or tetra-antennary glycans (89).

O-linked glycosylation occurs in many cell membrane and secreted proteins. The *O*-linked glycans tend to be smaller and less branched than *N*-linked glycans. *O*-glycans are more diverse than *N*-linked glycans. The mucin-type *O*-glycans are the most common *O*-linked glycans and are characterized by the attachment of α-*N*-acetylgalactosamine (α-GalNAc) to serine and threonine residues of proteins. Mucin type *O*-linked glycosylation is seen in (amongst others) epithelial cells, leukocytes and vascular endothelia (90, 91). Membrane-bound and secreted mucins carry many *O*-linked glycans which typically comprise more than 50% of the mucin molecular weight (92).

Glycans modulate various aspects of the proteins they attach to, for example

O-glycans may confer protease resistance of the proteins by protecting thermolysin-sensitive regions of the polypeptide (93).

At least eight different core structures have been reported to occur on mucin type glycans. All these core structures are based on the core-α-GalNAc residue, which is further substituted at C3, C6 or at both positions with β-galactose (Gal) at C3, β-GlcNAc at C3 and/or C6, and α-GalNAc at C3 or C6 (Fig1-3 (94)). This results in the formation of either core 1, core 2 or core 3 structures. Some of the mucin-type *O*-linked glycans are cancer-associated antigens, this includes GalNAc- (Tn), sialyl-GalGAc (sialyl-Tn) and Galβ1,3GalNAc- (Thomsen-Friedenreich or TF) antigens (95). Some of these carbohydrate antigens have been studied as therapeutic targets for cancer treatment (96).

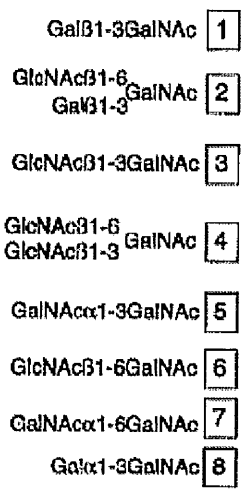

Fig 1-3: Core structure of the Mucin-Type O-Glycans

(94)

1.2.2. TF antigen

1.2.2.1. TF expression and carrier proteins

The TF disaccharide (also called the Thomsen-Friedenreich, TF or T antigen) is the core I structure of *O*-linked mucin-type glycans. It is concealed in normal epithelium by sialic acids, sulphates or other sugar chains that form branched and complex *O*-glycans (97). In cancer, unsubstituted Galβ1-3GalNAc occurs in about 90% of all human cancers, including colon, breast, bladder, prostate, liver, ovary and stomach. (98) Cancer-associated MUC1 is to date one of only two cell surface proteins known to carry the unsubstituted TF disaccharide; the other is the high molecular weight splice variant of the cell surface adhesion molecule CD44v6 (99). Alternative splicing of CD44 can produce a large number of different isoforms, some of which are overexpressed during colorectal tumorigenesis. Overexpression of CD44v6, one of the high molecular weight variant CD44 isoforms, is associated with poor prognosis (100). CD44v6 is shown to express TF antigen and sialyl-Tn in HT29 human colon cancer cells (99).

Cancer-associated MUC1 is the predominant carrier of the TF antigen in mammary, gastric, pancreatic and colorectal adenocarcinomas, thyroid, renal and bladder carcinomas (101, 102). Investigations by Baldus et al. with anti-MUC1 antibody BW835 [(which defines a site-specific Thomsen-Friedenreich disaccharide linked to threonine within the VTSA motif of MUC1 tandem repeats (103)] and HMFG-2 and anti-TF antibody A78G/A7 [specific for both anomeric forms of this disaccharide (TF alpha and TF beta, including related structures on glycolipids)(104)] and TF-binding PNA have shown that the anti-MUC1 and anti-TF antibodies reacted significantly more

strongly with adenoma of high grade dysplasia while faintly or negatively with adenomas of low grade dysplasia in 45 colorectal adenomas and 48 carcinomas. Mucins extracted from three individual moderately differentiated native cancer specimens of colorectal origin show relative binding activity with all three reagents of BW835 and HMFG-2 and A78G/A7 (105). Baldus et al. have also shown that TF antigens may be, at least in part, carried by MUC1 peptide cores in gastric carcinomas after staining 208 specimens from primary gastric adenocarcinoma patients with BW835 and A78G/A7 (106).

1.2.2.2. TF in cancer metastasis

TF expression correlates with cancer progression and metastasis (97). TF expression on MUC1, as revealed by immunohistochemical studies using an antibody (BW835) specific for TF on MUC1(103), correlates with the presence of lymph node metastases and an unfavourable prognosis in patients with gastric cancer (106) and with increased Pathological Tumor-Node-Metastasis (pTNM) Staging, histologic grading and lower survival probability in patients with colorectal carcinoma (107). Investigations of the specimens from 264 patients with colorectal carcinoma using primary monoclonal antibodies (MAbs) A78-G/A7, which bind to TF-alpha and TF-beta antigens, the latter present in glycolipids, irrespective of the carrier, and BW835, which detects TFalpha on MUC1 repeat peptide, show that BW835 reactivity exhibited a significant correlation with increasing pTNM staging and histologic grading. In univariate survival analysis, reactivity with A78-G/A7 anti-TF antibody correlated significantly with increasing pTNM staging,

histological grading and lower survival probability (107). A similar study using 208 specimens from primary gastric adenocarcinoma patients demonstrated that BW835 binding correlated with tumour progression from pT1 to pT2, from pTNM stage I to stage II, and that the presence of lymph node metastases decreased survival probability in stage I and tubular/papillary carcinomas (106).

1.2.2.3. The effects of TF expression in cancer metastasis

The TF antigen is a natural ligand of a group of dietary TF binding lectins, including that from peanut (Arachis hypogea) (PNA) (108, 109), Amaranth (Amaranthus caudatus) (110), mushroom *Agaricus bisporus* (ABL) (111) and jackfruit (jacalin) (110). Interaction of cancer-associated TF with TF-binding PNA and amaranth stimulates human colonic cancer cell proliferation(110, 112), while TF interaction with other TF-binding ABL and jacalin inhibits cell proliferation(110, 111).

The TF antigen is also a ligand of the mammalin galactoside-binding galectins and the interaction between TF and cancer-associated galectin-3 expressed by cancer cells and endothelial cells has been shown to promote cancer cell proliferation, adhesion and aggregation (97). Galectin-3 promotes cancer cell proliferation *in vitro* when added exogenously (113, 114). Down-regulation of galectin-3 expression by antisense technology suppresses cancer cell proliferation in human breast carcinoma MDA-MB-435 cells in soft agar and in nude mice (115). Interactions of cancer-associated-TF with galectin-3

expressed in human breast carcinoma MDA-MB-435 cells and by endothelial cells have been reported to increase cancer cell adhesion to the monolayer of the vascular endothelium and to enhance homotypic cancer cell aggregation (116). Highly metastatic human breast carcinoma MDA-MB-435 cells which express high levels of both TF and galectin-3 show significantly increased adhesion to the endothelial monolayer under static and sheer flow conditions and increased homotypic cell–cell aggregation. The MDA-MB-435 cells were shown to produce a high rate of metastasis when transplanted into nude mice by allografts when compared with less TF-expressing MDA-MB-468 cells (116). It was reported that initial attachment of the cancer cells to the endothelial monolayer causes rapid clustering of endothelial-associated galectin-3 at the cancer endothelium contacts, whilst the cancer-associated galectin-3 is accumulated at the homotypic cancer–cancer cell contacts (44, 116).

Introduction of a TF antigen-binding peptide (HGRFILPWWYAFSPS), or a synthetic TF antigen-mimicking peptide (lactulosyl-l-leucine) or TF antigen-expressing glycoproteins (117, 118), significantly inhibits rolling and stable adhesion of MDA-MB-435 cells to the endothelial monolayer under static (119, 120) and flow conditions (121). *In vivo*, intravenous co-inoculation of breast or prostate cancer cells together with antibodies against either TF or galectin-3 decreases the formation of cancer cell deposits in mouse lung and bones (97). Treatment of colon 26 carcinoma cells (BALB/c-derived tumor cells subcultured by subcutaneous implantation) with neuraminidase led to the exposure of TF, and consequently to a higher frequency of liver metastases in

syngeneic Balb/c mice. This effect could be prevented by an antibody to TF (A78-G/A7), but not by a control antibody (122). These studies suggest that metastatic cancer cell adhesion to target organ microvessels and homotypic cancer cell aggregation at the cancer–endothelium adhesion sites are regulated by the interaction of cancer-associated TF antigen with endothelial- and cancer-associated galectin-3 (97).

1.2.3. Molecular mechanism of altered glycosylation in cancer

Alteration of cellular glycosylation is a common feature in cancer cells. Alteration of *N*-glycosylation in tumours includes increased expression of β1-6 branched complex-type sugar chains (123) and increased expressions of the three β-*N*-acetylglucosaminyltransferases GnT-III, -IV and -V are reported in cancer cells (124).

The molecular mechanism of the changes in *O*-linked glycosylation in cancer is much more complex. Cancer cells are normally shown to carry shorter and less branched *O*-linked carbohydrate chains, with increased sialylation and reduced sulfation (125-127). Altered expressions or activities of the relevant glycosyltransferases was initially thought to be the primary reason causing altered *O*-linked glycosylation in cancer. Brockhausen and colleagues found that many glycosyltransferase activities present in the normal mammary cell line are also expressed at variable levels in breast cancer cells (128). The activity of a sialyltransferase (CMP-sialic acid Gal beta 1-3GalNAc alpha 3-sialyltransferase) was increased several-fold in three breast cancer cell lines,

BT20, MCF-7 and T47D. The Gal beta 1-3GalNAc (GlcNAc to GalNAc) beta 6-GlcNAc-transferase activity was found to be lacking in mammary cancer cell lines BT20 and T47D but expressed in MCF-7 breast cancer cells (128).

The expressions of Tn (GalNAcα-Ser/Thr), sialosyl-Tn and TF antigens are often increased in cancer cells. Interestingly, it was found that the levels of the relevant glycotransferases that control the biosynthesis of Tn, sialosyl-Tn and T antigens were similar in paired specimens of normal and cancerous tissues (129). Furthermore, in cancerous tissues, the enzyme activities of the glycotransferases were found not to be in correlation with tumour location, stage or histologic type (129). Those studies suggest that the expressions of the glycosyltransferase alone may not account for the altered glycosylation changes in cancer cells.

There are reports showing that redistribution of the glycotransferases in the Golgi apparatus may contribute to the abnormal glycosylation of proteins (130) (131).

Several studies suggest that the inappropriate Golgi pH may be responsible for altered glycosylation potential (132-134). Perturbing of the Golgi pH causes increased expression of some cancer-associated carbohydrate antigens and also causes structural disorganization of the Golgi apparatus in otherwise normally glycosylating cells. Disturbance of the Golgi pH has been shown to cause altered glycosylation in colorectal cancer cells *in vitro* and *in vivo* (in patients) (132). Elevation of the Golgi pH by treatment of the cells with bafilomycin A or pH calibration buffers has been shown to induce an increase

of TF antigen expression in breast and colorectal cancer cells (133, 134). All those studies indicate that altered glycosylation in cancer cells is attributed to relocalization of glycosyltransferases within the Golgi (135).

TF antigen on colon cancer cells has been shown to be expressed specifically on high molecular weight splice variants (CD44v6) of the adhesion molecule CD44, but not on the standard CD44 from both normal and colon cancer tissues (99). This suggests that splicing of CD44 may be involved in altered cell surface glycosylation in cancer cells. Tumour necrosis factor alpha (TNF-α) is a pre-inflammatory cytokine and can induce cancer-associated glycosylation changes in cancer cells (136). Addition of TNF-a in cell culture results in aberrant mucin expression, increased expression of TF and decreased sulphation in cultured goblet cell-differentiated colon cancer cell lines (137). TNF-a has also been shown to increase expression of the cancer-related sialyl Lewis-x antigen in human lung cancer cell lines QG-95 (136) and Lewis-y on the surface of the colorectal carcinoma cell lines HT29, LoVo and SW480 (138). Interestingly, the expression of CD44v10 has been shown to be significantly up-regulated by recombinant human interferon-gamma and rTNF-alpha in colon carcinoma cells (139).

1.2.4. Roles of altered glycosylation in cancer

The beta 1-6 branched *N*-linked oligosaccharides are consistently increased in neoplasias of human breast and colon and have been shown to correlate with the pathological staging of human breast and colon neoplasia (140). While

tumour growth and metastasis were inhibited in Mgat5-deficient mice, Golgi beta1,6N-acetylglucosaminyltransferase V (MGAT5) is required in the biosynthesis of beta1,6GlcNAc-branched N-linked glycans (141). The increased expression of the highly branched *N*-glycans at cell surface is correlated with the rapidity of tumour formation and altered adhesive properties of tumour cells in *vivo* (142). Increased expression of cell surface *N*-glycans has been shown to contribute directly to reducing contact-inhibition cell growth in an immortalized lung epithelial cell line (143). Overexpressions of sialyl-Le^x, sialyl-Le^a and sialyl-Le^x on the surface of tumour cells, including human adenocarcinoma of colon (144, 145), breast cancer (146) et al., were used as a marker for tumour diagnosis (145, 147). The increased cell surface expression and binding to E-selectin of sialyl-Le^x have been shown to correlate with the metastatic potential of human colon cancer cells (148). Several clinical studies have shown that the expressions of sialyl-Le^a and sialyl-Le^x in tumours are correlated to enhanced cancer progression and metastasis (124).

Alteration of cellular glycosylation is a common characteristic of human cancer (149-151). Amongst the commonest glycosylation changes are the increased occurrence of GalNAcα1-Ser/Thr(Tn antigen), Neu5Acα2-6GalNAc (sialyl-Tn antigen) and Galβ1-3GalNAcα1-Ser/Thr (TF or T antigen) (97). Sialyl-Tn antigen is expressed in breast cancer patients but not in normal mucosa (152). Overexpression of sialyl-Tn has been shown to be related to resistance of the cancer cells to chemotherapy (153). In experimental mouse

models, inhibition of sialylation (154) and enhancement of mucin glycosylation (155) reduce cancer cell metastasis.

1.3. MUC1 in normal and cancer epithelia

1.3.1. Mucin protein

The surface of epithelial cells is covered and protected by a layer of mucus (156). The major content of mucus is mucins. Mucins are high molecular weight glycoproteins with a tandem repeat peptide rich in threonine, serine and proline (157). Mucins carries a large number of short oligosaccharides (which account for 50–90% of the molecular weight of mucins) that are *O*-glycosidically linked to the serine and threonine residues. By cDNA cloning, at least 18 human mucin genes have been identified. They are MUC1, MUC2, MUC3A, MUC3B, MUC4, MUC5AC, MUC5B, MUC6, MUC7, MUC8, MUC12, MUC13, MUC15, MUC16, MUC17, MUC19, MUC20 and MUC21 (158, 159). Secreted gel-forming mucins (MUC2, MUC5AC, MUC5B, MUC6, MUC19) and transmembrane mucins (MUC1, MUC3A, MUC3B, MUC4, MUC12, MUC17 and MUC21) are two structurally and functionally distinct classes of mucins. Some MUC gene products do not fit well into either class (MUC7, MUC8, MUC13, MUC15, MUC16, MUC20) (157-161). cDNAs designated MUC11 and MUC12 may be derived from two closely related genes or may be parts of the same gene. Murine Muc10 and Muc14 as yet have no human counterparts. MUC9, encoding the mucin-like glycoprotein oviductin, has been renamed OVGP1. MUC18, now named

MCAM, was the original designation of a cell adhesion molecule in the immunoglobulin gene superfamily, not a mucin (157).

1.3.2. MUC1 structure

MUC1 is a large, heavily glycosylated transmembrane mucin protein. It has a large extracellular domain, a transmembrane region and a short cytoplasmic tail (162). The extracellular domain of MUC1 consists of variable numbers of 20-amino acid tandem repeat peptides (VNTR) that are rich in serines, threonines and prolines and are heavily glycosylated with complex *O*-glycans (150, 163). 50–90% of the molecular mass of MUC1 comes from carbohydrates. The MUC1 protein has a very large extracellular domain (1000 to 2200 amino acids) made of a variable number of highly conserved tandem repeats (25–125) of 20 amino acid residues (HGVTSAPDTR-PAPGSTAPPA). Its cytoplasmic domain is made of 72 amino acids that contain signalling motifs (164). The extracellular domain of MUC1 can extend 200 to 500 nm above the plasma membrane (165).

The tandem repeats of MUC1 extracellular domains are rich in serines, threonines and prolines and are heavily glycosylated with complex *O*-glycans (151, 163). The initial glycosylation occurs by addition of an *N*-acetylgalactoside residue to serine or threonine residues (Tn antigen). The Tn antigen is then modified by either a Galactose (Gal) residue to form a core 1 structure (Galß1, 3GalNAc-O-Ser/Thr), an N-acetylglucosamine residue to form a core 3 structure, or a sialic acid residue for chain termination. Then

core 1 and core 3 structures are further modified by other carbohydrate residues to form branched complex glycans or core 2 glycans (166).

The *O*-glycosylation of MUC1 is a step-by-step process occurring in the cis to trans Golgi. Each MUC1 VNTR contains five potential O-glycosylation sites(167). There are unique active site conformations for each member of distinct GalNAc-transferases. The extended backbone conformations assigned to the VTSA motif are preferable for the GalNAc-T1; polyproline II–like conformations assigned to the GTSA motif are primarily recognized by the GalNAc-T2; and relatively folded conformations assigned to γ -turn-like structure of the PDTR motif are required for the efficient recognition and binding by the GalNAc-T4(168). The recombinant polypeptide N-acetylgalactosaminyltransferase rGalNAc-T1(169, 170), rGalNAc-T2, rGalNAc-T4(171) preferentially glycosylates Thr within the VTSA peptide motif, Thr in GSTA, Ser within the VTSA and Thr within the PDTR motif separately.

The addition of GalNAc to the five potential O-glycosylation positions of the MUC1 tandem repeat include two pathway. Addition of Gal or GlcNAc residue to GalNAc forms core 1 or core 2 structures and exerts inhibitory effects on initial glycosylation at proximal sites. This pathway results in the low-density glycosylation as found on human milk mucin. In breast cancer cells on the other hand, a deletion or under-expression of the core2-specific β6-GlcNAc-transferase and a concomitant over-expression of the α3-sialyltransferase could account for the higher degree of site substitution by the concerted action of the ppGalNAc-Ts(167).

1.3.3. MUC1 distribution in normal epithelium

MUC1 is normally expressed on the apical surface of most normal secretory epithelial cells, including those in the mammary gland (172) and the gastrointestinal, respiratory, urinary and reproductive tracts (173). MUC1 expression is generally investigated by MUC1 immunohistochemistry using anti-MUC1 antibodies. MUC1 detected by 139H2 (Mouse Mab anti-core 1 protein) and DF3 anti-MUC1 antibody (Mouse Mab anti-core 1 protein ± carbohydrate) was seen to be expressed on the apical membranes of most secretory epithelial tissues, such as the ductular and glandular tissue of bronchus, breast, pancreas, prostate and uterus, and less frequently in gastric surface epithelium, gallbladder, small and large intestinal epithelium (173).

The lack of activity of the 139H2 anti-MUC1 antibody in intestinal tissue, which however shows relatively high levels of steady-state MUCI mRNA, suggests that immunohistochemical detection of MUC1 may be largely influenced by MUC1 glycosylation, which could result in concealment of antibody recognition sites (173).

1.3.4. MUC1 in epithelium cancer

Compared with the MUC1 in normal epithelium, cancer-associated MUC1 loses its apical membrane polarization and becomes over-expressed around the entire cell surface (174, 175). The MUC1 mRNA and detectable protein levels are frequently shown to be altered in adenocarcinomas compared with

corresponding normal tissues (173, 176). MUC1 overexpression is found in more than 80% of breast, gastric, colonic, pancreatic and prostate adenocarcinomas, bile duct neoplasms, esophageal squamous cell carcinomas and 50% of ovarian mucinous cystadenocarcinomas (173, 176). This increased MUC1 expression is seen to be associated with high metastatic potential and poor prognosis (155, 176, 177).

Interestingly, cancer-associated MUC1 was found to be overexpressed on the entire cell surface of tumour cells compared to polarization of MUC1 on the apical surface in the normal epithelium (162, 174, 175). Recently, Yonezawa has reported that MUC1 in invasive ductal carcinoma of the pancreas (IDC) by MUC1/DF3 immunohistochemistry was not only expressed at the cell apex but also at the cytoplasm and lateral membrane, in comparison to the MUC1 expression only at the cell apex in the normal tissues (176).

Cancer-associated MUC1 also shows reduced expression of complex *O*-glycans and increased expression of short oligosaccharides such as GalNAcα- (Tn antigen), sialylated GalNAcα- (sialyl-Tn) and Galβ1,3GalNAcα- (T or TF antigen) (127). MUC1 in cancer cells is shown to carry more core 1-related O-glycans while it carries predominatly core 2-related O-glycans in normal tissue (178, 179).

1.3.5. The function of MUC1

1.3.5.1. Anti-adhesive

Overexpression of cancer-associated MUC1 has been shown to inhibit cancer cell–cell and cancer-extracellular matrix interactions (174, 180). A normal mammary epithelial cell line (HBL-100) and a melanoma cell line (A375) transfected with cDNA-encoding MUC1/episialin have been shown to undergo less cell aggregation in comparison to their control cells which do not express MUC1 (181). MUC1 overexpression in transfectants of a melanoma cell line (A375), a ras-transformed Madin-Darl-canine kidney cell line (MDCK-ras-e) and a human breast epithelial cell line (HBL-100) reduces integrin-mediated adhesion to the extracellular matrix (174). Furthermore, E-cadherin-mediated adhesion of two breast cancer cell lines, YMB-S and ZR-75-1S, was functionally suppressed by overexpression of MUC1 but resumed after MUC1 expression was reduced by MUC1 antisense oligonucleotide (180) . Thus, MUC1 expression on the cell surface inhibits cell adhesion.

MUC1-mediated inhibition of cell adhesion may be a result of its shielding of the small adhesion molecular cell membrane due to its massive size. This may also be contributed to by the negative charge of its heavy content of sialic acids and/or sulphates (182). The anti-adhesive property of MUC1 may also involve competition of its cytoplasmic tail with adhesion molecules for cytoskeletal components. The latter is, however, less likely as truncated MUC1/episialin which does not express its cytoplasmic tail is still able to inhibit cell adhesion (174). The contribution of the negative charge of the sialic acids may also be limited, as removal of the MUC1 sialic acid residues by neuraminidase only partly restores cell adhesion (181).

MUC1 is known to protrude 200–500 nm above the plasma membrane (165). In contrast, the typical cell adhesion molecules extend less than 30 nm above the plasma membrane (183, 184). Hence the typical adhesion molecules are likely to be largely concealed by the large and long MUC1 molecules on the cell surface. MUC1 transfectants of cL929 fibroblast cells that contain three tandem repeats showed a comparable level of aggregation in comparison with the MUC1 negative control cells. However, the MUC1 transfectants that contain eight repeats (LUD8/B1 and LUD8/D4), 15 repeats (LUD15/4.2) and 36 repeats (LUE6/10 and LUE6/15) displayed decreasing levels of cell–cell interactions. These results strongly support a role of the extracellular domain of MUC1 in its anti-adhesion functions (175).

1.3.5.2. Adhesive properties of MUC1

MUC1 has also been shown to mediate cell adhesion. MUC1 has been shown to interact with intercellular adhesion molecule-1 (ICAM-1) and increase adhesion of cancer cells to HUVEC cells in cell culture under static conditions (185, 186) and under fluid flow conditions (187), and enhances cancer cell transendothelial migration (188). Migration of human breast cancer MCF7 cells across a gelatin-coated transwell membrane could be increased by the sequential addition of ICAM-1-expressing cells (primary human breast fibroblasts and primary human umbilical vein endothelial cells) (188). Antibodies against MUC1 or ICAM-1, but not a control antibody, could abrogate cell migration in those cases (188). It has also been demonstrated that MUC1–ICAM1 interaction initiates Src-CrkL-Rac1/Cdc42–Mediated

Actin Cytoskeletal Protrusive Motility, an effect that can be exclusively abrogated by an anti–ICAM-1 antibody (189). MUC1–ICAM1 interaction has also been shown to enhance cancer cell interaction with B lymphocytes (190) and fibroblasts (Rahn et al., 2004) in cell culture under static conditions.

Thus, cell surface MUC1 can act as an anti-adhesive molecule by preventing cancer cell adhesion and can also act as an adhesion molecule by interaction with ICAM1 and increase cell–cell interactions. The anti-adhesive property of MUC1 has been shown to promote epithelial tumour cell adhesion to the basement matrix at the primary tumour sites and their subsequent invasion into the circulation (181).

1.3.5.3. Signal transduction by MUC1

MUC1 is also a signalling protein and can transduce extracellular signals into the cells through interaction of its cytoplasmic domain with intracellular signalling proteins, such as P53 and b-catenin.

p53 is a tumour suppressor and its expression is up-regulated in response to various stresses such as DNA damage, hypoxia and oncogene activation. Activated p53 initiates several different transcriptional programs that can result in either cell cycle arrest, cellular senescence or apoptosis (191). The MUC1 COOH-terminal subunit (MUC1-C) can interact with p53 through binding to the PE21 element in the p53 proximal promoter and suppress p53 activation (192).

The MUC1 cytoplasmic tail can also interact with β-catenin (193) and transduce cell signalling through the Wnt/β-catenin signalling pathway and regulate the expressions of a number of downstream genes essential for cell proliferation and differentiation (194). The Wnt/b-catenin signalling pathway is known to be perturbed in a number of disease conditions such as cancers, bone diseases (differentiation of osteoblasts and regulation of bone mass) and cardiovascular diseases (194). The MUC1 cytoplasmic tail (MUC1CT) has also been shown to be involved in several other signalling pathways, such as those involved in Ras, p120 catenin and estrogen receptor (195). Furthermore, MUC1 expression has been shown to regulate intracellular oxidant levels, and to decrease the apoptotic response of the cells to oxidative stress (196).

Thus MUC1 is involved in signal transduction via interaction of its cytoplasmic tail with important intracellular signalling proteins such as p53 (Wei et al., 2005) and β-catenin (Yamamoto et al., 1997; Singh and Hollingsworth, 2006) and suppresses cellular apoptosis in response to DNA damage (Ren et al., 2004; Raina et al., 2006; Yin et al., 2007).

1.4. Galectins and cancer

1.4.1. Galectin structure

Galectins are a family of animal lectins that have binding affinity for β-galactosides and share conserved carbohydrate recognition domains (CRDs). The CRDs of galectins are about 130 amino acids and are responsible for recognition of galectins to carbohydrates (120). To date, 15 mammalian

galectins have been identified which are subdivided into prototype galectins (galectin-1, -2, -5, -7, -10, -11, -13, -14 and -15), which have one CRD and exist as monomers or non-covalent homodimers, a chimera-type galectin (galectin-3) that is composed of a non-lectin domain connected to one CRD, and tandem-repeat-type galectins (galectin-4, -6, -8, -9 and -12) that consist of two CRDs in a single polypeptide chain (197). Galectins are either bivalent or multivalent in their carbohydrate-binding activities as a result of molecular polymerization. In this way, galectins can form ordered arrays/lattices of complexes when they bind to multivalent glycoconjugates (120).

1.4.2. Galectin-3

Galectin-3 is a chimera type of galectin containing one-CRD domain which is fused to a stretch of unusual tandem repeats of short amino-acid stretches (198).

1.4.3. Distribution of galectin-3

Galectin-3 is expressed by a wide variety of mammalian cells. These include monocytes and macrophages (199), gastric epithelium (200), colonic epithelium (201), mammary epithelium (202), prostatic cells (203) and a range of neoplastic tissues, including anaplastic large cell lymphoma (204), thyroid carcinoma (205), breast carcinoma (202, 206), gastric carcinoma (200), colon carcinoma (201), ovarian carcinoma (207), prostate carcinoma (203) and

melanoma (208). Galectin-3 is found inside cells, extracellularly (but cell surface associated) and in the circulation (209, 210).

1.4.4. Role of galectin-3 in cancer

There is increasing evidence showing that galectin-3 contributes to cancer cell transformation, development and metastasis (120, 211).

1.4.4.1. Intracellular galectin-3:

Intracellular galectin-3 is an apoptosis inhibitor (212, 213). Tumour cells transfected with a cDNA-encoding galectin-3 reduced cellular apoptosis(212). cells transfected with a gene encoding an amino-terminal truncated galectin-3 increased cell sensitivity to apoptotic stimuli (120). Repression of galectin-3 by homeodomain-interacting protein kinase 2 (HIPK2) activated tumour suppressor gene p53 is required in p53-induced apoptosis (214). Galectin-3 acts as a selective binding partner of activated K-Ras, an important Ras oncoprotein (215). NF-kB (nuclear factor kB) is known to play a role in tumour cell resistance to apoptosis (216). Galectin-3 expression has been shown to regulate the expression of NF-kB transcription factor (217, 218). Galectin-3-mediated inhibition of apoptosis has been shown to be involved in protecting mitochondrial membrane integrity by preventing cytochrome c release and caspase activation in human breast carcinoma cells (219).

Intracellular galectin-3 is also an mRNA splicing promoter (220). Cell-free-splicing assays using HeLa cell nuclear extracts and 32P-labelled MINX as the pre-mRNA substrate demonstrate that galectin-3 is required in pre-mRNA splicing (220). In this splicing assay, the addition of carbohydrates with high galectin-3 binding affinity inhibits product formation of the splicing complexes, while the addition of carbohydrates without galectin-3 binding affinity does not. Nuclear extracts that are depleted of galectin-3 are deficient in splicing activity. This splicing deficiency could be restored by the addition of recombinant galectin-3, but not other lectins with a similar saccharide binding specificity (soybean agglutinin) or with a different specificity (wheat germ agglutinin) (220).

Galectin-3 is involved in tumour cell transformation. Inhibition of galectin-3 expression suppresses the phenotypes of transformation of human breast carcinoma cells and thyroid papillary carcinoma cells in cell culture (115, 221). Conversely, galectin-3 overexpression by transfection of galectin-3 cDNA in a normal thyroid follicular cell line induces the phenotypes of transformation (222). It has been suggested that galectin-3-mediated cell transformation is related to its interaction with –Ras (215), an oncogenic protein that plays a vital role in transformation (223, 224).

1.4.4.2. Cell surface-associated galectin-3

Cancer cell-associated galectin-3 is reported to play an important role in tumour cell heterotypic adhesion to endothelium and cancer cell homotypic

aggregation. It was found that the highly metastatic human breast carcinoma cells of MDA-MB-435 that express higher levels of galectin-3 show a higher level of adhesion to monolayers of endothelial cells in vitro compared to their nonmetastatic counterparts MDA-MB-468 (116). Addition of synthetic galectin-3 carbohydrate recognition domain-specific peptides significantly inhibited rolling and stable heterotypic adhesion of human MDA-MB-435 breast carcinoma cells to endothelial cells under flow conditions, as well as homotypic tumor cell aggregation in vitro (Zou et al., 2005). Addition of the galectin-3 inhibitor - synthetic lactulose amine prevents galectin-3-mediated homotypic cell aggregation (225). Liver metastasis of adenocarcinoma cell lines XK4-A3 and RPMI4788 was reduced by alpha-lactose and anti-galectin-3 treatment (226).

Cancer cell-associated galectin-3 has also been shown to increase cancer cell adhesion and invasion. Overexpression of galectin-3 in lung cancer cells enhances the cell motility and invasiveness in vitro (227). Overexpression of galectin-3 in human breast carcinoma cells results in the remodelling of the cellular cytoskeletal elements that are associated with cell spreading (228, 229). Introduction of recombinant galectin-3 inhibits the adhesion of tumour cells to extracellular matrix proteins of various human cancer cells (230-232). This effect of galectin-3 has been suggested to be related to its interaction with the adhesive molecular integrin$\alpha 1\beta 1$ (229). Galectin-3 when added exogenously in solution or when bound within a three-dimensional matrix markedly enhanced the migration of the primary tumour cell lines through a Matrigel barrier (233). By contrast, another study showed that exogenously

added galectin-3 (Matrigel-coated with 0.15μg/cm2 gal-3) reduced the migration of human colon cancer cell lines (234).

Reduction of galectin-3 expression in LsiM6 and HM7 human colon cancer cells is associated with decreased liver colonization and spontaneous metastasis in athymic mice after splenic-portal inoculation, whilst elevation of galectin-3 expression in low metastatic LS174T colon cancer cells results in increased liver metastasis (Bresalier et al., 1998). Thus, cell-associated galectin-3 contributes to cancer cell motility and invasiveness by interaction with the cell-surface proteins expressed on the same or adjacent cells.

1.4.4.3. Circulating galectin-3

The concentration of circulating galectin-3 has been shown to be increased up to fivefold in the sera of patients with breast, colorectal and lung cancers (209), melanoma (235), thyroid malignancy (236), bladder cancer (237) and head and neck squamous cell carcinomas (HNSCCs) (238).

Serum galectin-3 concentrations in various cancers (Table1-1)

	Normal individuals	Non metastasis	Metastasis	Total of malignant	Reference
Breast cancer	62 ng/ml (20-313)	40 ng/ml (20-170)	170 ng/ml (20-620)	100 ng/ml (20-620)	Iurisci et al. 2000
Gastrointestinal cancer	62 ng/ml (20-313)	75 ng/ml (20-328)	320 ng/ml (20-950)	185 ng/ml (20-950)	Iurisci et al. 2000
Lung cancer	62 ng/ml (20-313)			171.5 ng/ml (20-807)	Iurisci et al. 2000
Head and neck squamous cell carcinoma	2.39 ng/ml (1.3-6.4)			3.2 ng/ml (0.8-7.9)	Saussez et al. 2008
Bladder	584 pg/ml (range 259-1262)			1068 pg/ml (range 551-2028)	Sakaki et al. 2008
Melanoma	6.9 ng/ml (5.9-8)			12 ng/ml (9.4-15.5)	Vereecken et al. 2006
Thyroid cancer	2.22 ng/ml (1.4-3.1)			3.4 ng/ml (2.4-7.8)	Saussez et al. 2008

Interestingly, the increased galectin-3 concentration in the circulation of cancer patients is seen to be closely correlated with cancer progression. Those patients with metastatic disease have significantly higher circulation of galectin-3 than those with localized tumours (209, 239). Until very recently, it remained unknown whether this increased circulation of galectin-3 had any functional implications in cancer progression.

Recent studies in our group have demonstrated that the cancer-associated transmembrane mucin protein MUC1 is a natural ligand of galectin-3 in human cancer cells (Yu et al., 2007). The interaction between galectin-3 and MUC1 is via binding of galectin-3 to the Thomsen-Friedenreich oncofetal carbohydrate (Galβ1,3GalNAc-, T or TF) antigen on MUC1. The interaction between exogenously introduced galectin-3 and MUC1 increases cancer cell adhesion to the monolayer of human umbilical vein endothelial cells (HUVECs) in culture. It was found that binding of galectin-3 to MUC1 causes MUC1 cell surface polarization and consequent revealing of the smaller adhesion molecules that are otherwise concealed by the large size and length of MUC1 (Yu et al., 2007).

CHAPTER 2

2. Hypothesis and aims

2.1 Hypothesis

The huge size and heavy glycosylation of the transmembrane mucin protein MUC1, which protrudes over 10 times higher from the surface of the epithelial cancer cells than classical adhesion molecules, may shield these adhesion molecules and thus prevent interaction of disseminating cancer cells with each other and with endothelial cells. Binding to MUC1, via the oncofetal Thomsen-Friedenreich (Galβ1,3GalNAcα1, TF) antigen, of circulating galectin-3, whose concentration is markedly increased in the circulation of cancer patients, causes MUC1 polarization and subsequent exposure of the smaller adhesion molecules thus increasing cancer cell homotypic aggregation, heterotyic adhesion to endothelium and trans-endothelial invasion (extravasation) hence promoting cancer metastasis.

2.2 The aims of the study

To investigate the effects of MUC1 expression and MUC1-galectin-3 interaction on cancer cell homotypic aggregation (see chapter 5), heterotypic adhesion to vascular endothelial cells and trans-endothelial migration and on metastasis (see chapter 4).

To assess the effects of the TF-binding peanut agglutinin (PNA) on cancer

cell-cell interaction and metastasis (see chapter 6).

CHAPTER 3

3. Materials and methods.

3.1. Materials.

Full-length recombinant galectin-3 (Cat No. 1154-GA/CF, carrier free), monoclonal antibodies against CD44H (Cat No. BBA10), E-cadherin (Cat No. MAB1838) and E-selectin (Cat No. BBA16), ICAM-1 (Cat No. BBA3), VCAM-1 (Cat No. BBA5), integrin-β (Cat No. MAB17782), anti-human galectin-3 antibody (Cat No.MAB1154) and biotinylated anti-human galectin-3 antibody (Cat No. BAF1154) were all from R & D Systems Europe Ltd (Abingdon, United Kingdom). B27.29 anti-MUC1 antibody, which binds to the epitope **RPAP within the tandem repeat region (240)**, was kindly provided by Dr. Mark Reddish (Biomira Inc., Edmonton, Canada). CT-2 anti-MUC1 cytoplasmic tail antibody was from NeoMarkers (Fremont CA). Anti-TF antibody (TF5) was kindly provided by Dr. Bo Jansson (BioInvent Therapeutic, Lund, Sweden) (241). Peanut agglutinin (PNA) was purchased from Sigma. Florescence-conjugated peanut lectin, peroxidase-conjugated PNA, AMCA anti-mouse IgG(H+L) made in horse (Cat No. CI-2000), AMCA anti-hamster IgG(H+L) made in goat (Cat No. CI-9100) and mounting medium for fluorescence H1200 with DAPI were purchased from Vector Laboratories Ltd (Peterborough, UK). *Streptococcus pneumoniae* Endo-*N*-acetyl-galactosaminidase (EC 3.2.1.97), *O*-glycanase, was obtained from Prozyme Inc (Oxford, UK). The trypsin-EDTA solution (10×) with 5% porcine trypsin, 2% EDTA (Cat No. T4174, dilute to 1× with PBS before

using) and the Non-Enzymatic Cell Dissociation Solution were from Sigma. The Vybrant DIO (octadecyl oxacarbocyanines) and DiI (1,1¢ -dioctadecyl-3,3,3¢ ,3¢ -tetramethylindocarbocyanine perchlorate) Cell-labelling Solutions were from Molecular Probes (Cambridge, UK). Calcein (AM) was obtained from Invitrogen. The 24 wells Cell culture insert was from BD (CAT No. (35)3097). Asialofetuin was bought from Sigma.

3.2. Medium (All were from Sigma except where particularly specified)

a) Dulbecco's modified Eagle's medium (DMEM). A) Complete culture medium contains 10% FCS (fetal calf serum), penicillin 100U/ml, streptomycin 100 μg/ml, glutamine 2 mM. B) Serum-free DMEM contains 0.5% bovine serum albumin, penicillin 100U/ml, streptomycin 100 μg/ml, glutamine 2 mM. C) Antibiotic-free DMEM contains 10% FCS, glutamine 2 mM. D) Antibiotic-free and serum-free DMEM contains glutamine 2mM. The cell lines HT-29, HT29-5F7, HCA1.7+, HCA1.7-, ACA19+, ACA19- and SW620 were cultured with this medium.

b) McCoy's 5a. A) Complete medium contains 10% FCSpenicillin 100U/ml, streptomycin 100 μg/ml, glutamine mM. B) Antibiotic-free medium contains 10% FCS, glutamine 2 mM. The cell lines HCT116 were cultured with this medium.

c) Endothelial growth media (EGM) supplemented with BBE 2 ml, hEGF 0.5 ml, Hydrocortisone 0.5ml, FBS 25 ml, GA-1000 0.5 ml (EGM Bullet kit,

Cambrex Bio Sciences, UK) were used for the culture of human umbilical vein endothelial cells (HUVEC).

d) EGM-2 endothelial growth media supplemented with FBS 25 ml, hEGF 0.5 ml, Hydrocortisone 0.2ml, hFGF-B 2ml, VEGF 0.5ml, R^3-IGF-1 0.5ml, ascorbic acid 0.5ml, GA-1000 0.5 ml (EGM-2 Bullet kit, Cambrex Bio Sciences, UK) were used for human microvascular lung endothelial cells (HMVEC-Ls)

3.3. Cell lines

HT-29 and HT29-5F7: The HT-29 human colon cancer cell line was obtained from the European Cell Culture Collection via the Public Health Laboratory Service (Porton Down, Wiltshire, UK). HT29-5F7 cells, kindly provided by Dr. Thecla Lesuffleur (INSERM U560, France), are enterocyte-like subpopulations of HT29 cells that express mainly MUC1 and MUC5B and were isolated as a consequence of their resistance to 5-fluorouracil. The cells were cultured in DMEM supplemented with 10% FCS, 100 units/ml penicillin, 100μg/ml streptomycin and 4mM glutamine at 37°C in a humidified atmosphere of 5% CO_2. The culture medium was changed two to three times a week.

HUVECS and HMVEC-L: Human umbilical vein endothelial cells (HUVECs) and human microvascular lung endothelial cells (HMVEC-L) were obtained from Cambrex Bio Sciences Wokingham Ltd (Wokingham, UK). HUVEC cells were cultured in endothelial growth media (EGM Bullet kit, Cambrex Bio Sciences, UK). HMVEC-L cells were cultured in EGM-2 endothelial

growth media (EGM-2 Bullet kit, Cambrex Bio Sciences, UK). Less than five passages of the cells were used in all the experiments. The culture medium was changed every two days.

HCA1.7+/HCA1.7- and ACA19+/ACA19-: MUC1 transfection of HBL-100 human breast epithelial cells and human melanoma A375 cells with full-length cDNA encoding MUC1 either variant A or B with about 40 repeats, which is similar to the amount present in the small allele of T47D cells(182), and the subsequent selection of the MUC1 positive transfectants HCA1.7+, ACA19+ and the negative revertants HCA1.7- and ACA19- were as described previously(174).

SW620: Human colon cancer cells were obtained from the European Cell Culture Collection via the Public Health Laboratory Service (Porton Down, Wiltshire, UK).

HCT116: Human colon carcinoma cells were from the European Collection of Cell Cultures. HCT116 cells are malignant cells isolated from a male with colonic carcinoma. HCT116 cells are tumourigenic in nude mice and form colonies on agarose. Growth and plating efficiency are enhanced by using a feeder layer of murine fibroblasts (242).

3.4. Cell thawing and plating

The cell culture medium was warmed to 37°C in the waterbath (about 30 minutes) before use. The freezing vial of cells from the N2 cell bank was warmed up at 37°C in the waterbath. The cell suspension was then added into 10ml pre-warmed cell culture medium in a 15ml tube. (For defrosting

HUVEC cells, the cells were added directly into one or two T25 cell culture flasks.) After centrifugation of the cell suspension for 5 minutes at 1000RCF(×g), the supernatant was discard. The cell pellet was re-suspended in 10ml pre-warmed cell culture medium and seeded into a T25 cell culture flask. The cells were incubated at 37°C in a humidified atmosphere of 5% CO_2. The culture medium was changed two to three times a week.

3.5. Detachment of the cells with trypsin or non-enzymatic cell dissociation solution

Sub-confluent cells in T-25 cell culture flasks were rinsed twice with 10ml each time PBS before 2ml Trypsin (with 0.5% porcine trypsin and 0.2% EDTA) or non-enzymatic cell dissociation solution (NECDS) was added into each T25 flask for 5-10 minutes at 37°C until the cells became detached from the flasks. After addition of 10ml pre-warmed culture medium, the cell clumps were dispersed by sucking up and blowing down the cell suspension 10 times using a 10ml pipette, to produce a single cell suspension.

3.6. Cell aliquoting

After detachment of the cells with trypsin (see cell detachment), 10ml complete cell culture medium was added. The cell numbers were counted and re-suspended in 5×10^5/ml concentration in complete culture medium. 1ml (0.5ml for HCA1.7- cells) was added into each T25 flask 10ml complete

culture medium and the cells were incubated at 37°C in a humidified atmosphere of 5% CO_2.

3.7. Cell freezing

After detachment of the cell with trypsin 10ml complete cell culture medium was added. The cell suspension was centrifuged at 1000RCF(×g) for 5 minutes. After removal of the supernatants, the cell pellet was re-suspended in cell freezing medium (20% FCS, 7% Dimethyl sulfoxide (DMSO) in culture medium) at cell density 1×10^6/ml for HT-29, HT29-5F7, HCA1.7+, HCA1.7-, SW620, HCT116. 3×10^5/ml for HUVEC and HMVEC-L cells. One 10ml cell suspension was transferred into a Cryotube. The cells were stored at -80°C overnight before being transferred to a N2 cell bank.

3.8. Cell counting

Cell numbers were counted using a haemacytometer. The number of cells was obtained with the following equation: Cells Density (cells/ml) = number of cells per square × 10^4.

3.9. Assessment of cell aggregation by flow cytometry

3.9.1. After detachment of the cells with 2 ml cell dissociation solution at 37°C for 5–10 mins, 10ml serum-free DMEM medium was added and cell

clumps were dispersed by sucking up and blowing down the cell suspension several times using a 10ml pipette. The cells were then washed twice with PBS 10ml each time. The PBS was removed by spinning the cell suspension for 5 minutes at 1000g (RCF). After cell counting, the cells were removed then diluted to 1×10^6/ml cells with serum-free medium. 0.2ml cell suspension was taken and diluted into 5×10^5/ml with 1ml serum-free medium to be used as unstained control cells in later flow cytometry analysis. Two aliquots of (2ml or more according to the experiments needed) 1×10^{6}/ml cells were transferred into two 15ml tubes. One tube was added in 5ul/ml Dil cell-labelling solution and another in 5ul/ml DiO cell-labelling solution. After 30 mins incubation at 37°C, 10ml PBS was added into each tube; after centrifugation of the cell suspension for 5 minutes at 1000rpm, the supernatants were removed. The cells were washed a second time with PBS. The cell pellets were re-suspended at about 1×10^6/ml with serum-free DMEM medium. The cell numbers were re-counted and the cells were diluted with serum-free medium to 5×10^5/ml. 500 μl of each cell suspensions were taken as unmixed Dio- and Dil- labelled cells for later use to identify the single dye-labelled cell population by flow cytometry. 1.5ml of each cell suspension was then mixed by gently sucking up and blowing down the cell suspension several times with a pipette. The cell suspension was then divided into different tubes with 1ml/tube (5×10^5/ml) and incubated with the presence or absence of recombinant galectin-3, antibodies, lactose or PNA in a rotating incubator (Julabo Temp SW23, Julabo labortechnic GMBH, Seelbach, Germany) at 100 REVS /min at 37°C for 1 hour.

3.9.2. At the end of the incubation, the cell suspension was cooled on ice and cell aggregation was analysed by flow cytometry (Becton-Dickinson FACS Vantage SE). Unlabelled cells and cells labelled with DiI- or DiO- only dye were used to identify the position of the unlabelled (bottom-left), DiO-labelled (top-left) and DiI-labelled (bottom-right) cell populations in the bi-variant correlation plot. The cell population containing both DiO and DiI fluorescence (upper-right) in the correlation plot was defined as cell aggregates in this study. The percentage of each cell population was obtained using the FACS software (Cell Quest).

It should be mentioned that this method measures cell aggregates containing both DiO- and DiI-labelled cells. Although this method may underestimate the total cell aggregates by having eliminated the aggregates formed by the cells labelled with the same fluorescent dye, it more accurately measures the percentage of cell aggregates formed after the two cell populations (DiO- and DiI-labelled) are introduced together (which is a key part of this study) by reducing experimental errors potentially caused due to 1) cell aggregation formed before introduction of recombinant galectin-3 and 2) differences in the abilities of the cells to be labelled with the two fluorescent dyes.

When assessing the cell aggregation, a 200μM nozzle was selected because the larger sizes of cell aggregation easily clog the nozzle.

3.10. Epithelial cell-endothelial adhesion - Method one:– counting cell numbers

a) After detachment of the endothelial cells from a T25 flask with Trypsin, 5ml endothelial culture medium was added and the cell clumps were dispersed by sucking up and blowing down the suspension 10 times with a 10ml pipette. The cell numbers were counted with a haemocytometer and the cells were diluted into 5×10^4/ml in endothelial culture medium.

b) 13mm glass cover slides were inserted into the wells of a 24-well cell culture plate followed by gentle addition of the endothelial cell suspension (1ml/well). The culture medium was changed the next day and the cells were added with or without 10ng/ml TNF-α for 12 hours at 37°C before the adhesion assay.

c) Sub-confluent cancer cells or MUC1 transfectants were released from the culture flasks by 2ml cell dissociation solution as discussed earlier. After the cell clumps were dispersed by pipetting, cell numbers were counted with a haemocytometer.

d) The cells were then diluted to 1×10^6/ml cells with serum-free medium and added to 5ul/ml DIO cell-labelling solution at 37°C for 30 minutes.

e) The cells were washed twice with 10ml PBS each time by centrifugation for 5 minutes at 1000RCF(×g).

f) The cells were then re-suspended into about 2×10^6/ml with serum-free DMEM medium. Re-count the cells with a haemocytometer and dilute the labelled cells into 5×10^4/ml with serum-free medium.

g) The endothelial monolayer was washed twice with PBS 1ml/well. 250ul cancer cells suspension (1.25×10^4/well in serum-free medium) was then incubated with or without galectin-3 for 30 min at 37°C before addition of the whole cell suspension into the monolayer of endothelial cells for 1 hr at

37°C. The medium was removed and the cells were washed twice with 1ml/well PBS and fixed with 2% paraformaldehyde 0.5ml/well for 15 minutes at room temperature.

h) After removal of the paraformaldehyde and washing once with 0.5ml PBS/well, the glass cover slides were taken out from the wells and mounted with mounting medium for fluorescence (H1200 with DAPI from VECTOR). The cover slides were covered with a new 22mm cover slide. The slides were blinded with tapes and fluorescence-labelled cells remaining on the endothelial monolayer were counted in 10 random fields of view (FOV) under fluorescence microscopy (Olympus B51 fluorescence microscope).

3.11. Epithelial cell-endothelial adhesion –Method two: Calcein-AM labelling

a) After detachment of the cells and washing with PBS, the cells were diluted into 1X 10^6/ml cells with serum-free medium before addition of 10μl/ml Calcein AM cell labelling solution at 37°C for 30 minutes. The cells were washed twice with 10ml PBS each time by centrifugation for 5 minutes at 1000RCF(×g).

b) The cells were then re-suspended into about 1×10^6/ml with serum-free DMEM medium. Re-count the cells with a haemocytometer and dilute labelled cells into 5×10^4/ml with serum-free medium.

c) The endothelial monolayer was washed twice with PBS 1ml/well. 100µl cancer cells suspension (5×10^3/well in serum-free medium) was then incubated with or without galectin-3 for 30 min at 37°C before addition of the whole cell suspension into the monolayer of endothelial cells.

d) After 1 hour's incubation of the cells at 37°C, the medium was removed and the cells were washed twice with PBS 1ml/well before 0.1ml/well cell lysis buffer (2×sample buffer without Bromthymol blue) was added. After 30 minutes shaking of the plate at speed 200REVS/minute on Orbital shaker SO3 at room temperature, the fluorescence density of the cell lysates was measured using a TECAN infinite F200 microplate reader with

Excitation Wavelength	485	nm
Emission Wavelength	535	nm
Excitation Bandwidth	20	nm
Emission Bandwidth	25	nm
Gain	50	Manual

The background (from medium and endothelial monolayer) was deducted before analysis of the data.

3.12. Cell adhesion under flow conditions

3.12.1. This was assessed with a flow-based video-microscopic model (243, 244). Human umbilical vein endothelial cells (HUVECs) were isolated from freshly obtained human umbilical cords by collagenase digestion of the interior of the umbilical vein (245). The cells were maintained in medium 199

(M199; Invitrogen, Paisley, UK) containing 20% fetal calf serum, 28μg/mL gentamicin, 2.5μg/mL amphotericin B, and 1 ng/mL epidermal growth factor (all from Sigma) until confluent (246). The cells were dissociated with trypsin/EDTA (ethylenediaminetetraacetic acid) and seeded approximately at 4×10^6/ml (a total of 45μl) into rectangular glass capillaries (microslides; internal width 3 mm, depth 0.3 mm) which had been coated with collagen/gelatin (bovine skin gelatine from Sigma in deionized water at 1% w/v) for 24 hrs at 37°C to allow the cells to form a monolayer. The HUVEC monolayer was stimulated with 100U/ml TNF-α for 24 hrs at 37°C before being used in the cell adhesion experiments. (All these were conducted by Philip Stone at Birmingham University.)

3.12.2. Sub-confluent ACA19+/- cells were detached from the T25 cell culture plate 5ml/flask with non-enzyme cell dissociation solution. After washing with 10ml PBS twice, the cells were re-suspended in 5ml serum-free medium and the cell numbers were counted using a haemocytometer. The cells were then diluted into 1×10^6/ml with serum-free DMEM and incubated with or without 1 μg/ml recombinant galectin-3 for 30 mins at 37°C before being perfused through the microslides at the chosen volumetric flow rate to deliver a desired wall shear stress. After 4 minutes of washing with PBS, the micro slides were video-recorded and the number of the adhered cells was quantified and normalized by the number of cells perfused.

3.13. Electrophoresis and lectin/immunoblotting

3.13.1. Cell lysis: up to 90% confluence cells in a T25 flask were washed with PBS 10ml twice. 0.7ml/T25 flask SDS(sodium dodecyl sulfate)-sample buffer was added and incubated for 20 minutes at room temperature. The cell lysates were collected into 1.5ml tubes and kept at -20°C until use.

SDS-Sample buffer:

	2 fold	4 fold
Stacking buffer	2.5ml	0ml
Glycerol	1.0ml (20%)	2ml
Mercaptoethanol	0.5ml (10%)	1ml
20% SDS	1.0 (4%)	2ml
1% Bromthymol blue	50µl	0.1ml

3.13.2. Gel preparation:

Separating gel	4%	7.50%	10%	15%
Deionized water	6ml	4.85ml	4.20ml	2.35ml
1.5M Tris-HCL resolving gel buffer	2.5ml	2.5ml	2.5ml	2.5ml
10% (w/v) SDS	100ul	100ul	100ul	100ul
30% acrylamide/bisacrylamide	1.35ml	2.5ml	3.33ml	5ml
TEMED	5µl	5µl	5µl	5µl
10% ammonium persulfate	65µl	50µl	50µl	50µl

Stacking gel	3.75%	4.00%
Deionized water	3.09ml	3.05ml
0.5M Tris-Hcl stacking gel buffer	1.25ml	1.25ml
10% (w/v) SDS	50ul	50ul
30% acrylamide/bisacrylamide	0.625ml	0.665ml
TEMED	10µl	10µl
10% ammonium persulfate	65µl	50µl

After the glass plates and spacers (1.0mm thick) were assembled, the running gel was poured to about 1cm below the wells of the comb (~4.9ml). Then 80ul water-saturated butanol-1 was added on top of the gel (adding from the corner of the gel). When the gel had set (~ 40 mins), the butanol was poured off and the gel was rinsed with about 2ml deionized water three times. Stacking gel was added and the 1.0mm thick comb inserted immediately. When the stacking gel had set, the glass plates were placed in a gel rig and immersed in buffer. Prior to running the gel, the wells were flushed out thoroughly with running buffer.

Running buffer:

Tris-Base	30.67
Glycine	64.04
SDS	2.2
Make up	4L

3.13.3. Running the gels

The samples were heated at 100°C for 10 mins before being loaded to the gels.

The proteins separated on the gels were transfered to nitrocellulose membrane using a transfer buffer compounded of following ingredients.

Transfer buffer

Tris-Base	12.12g
Glycine	57.65g
Methanol	800ml
Make up	4L

The gel was sandwiched as negative pole (black) – Sponge – filter paper – gel – nitrocellulose membrane – filter paper – sponge – positive pole (white) and transferred at 100V for 1 hr.

After electrode transfer, the nitrocellulose membrane was stained with Ponceau S (0.1% Ponceau S in 1% acetic acid) solution for 2–3 minutes to visualize the protein bands. To get a clearer view of the bands, the blots were washed several times with 1% acetic acid. The Ponceau staining was removed by washing the blot several times with PBS.

3.13.4. Immunobloting

The membrane was blocked in Blocking Buffer (1% BSA in 1% TWEEN20 in PBS) for 30 minutes at room temperature or 4°C overnight.

The first antibody in 1% BSA in TWEEN20 in PBS was then applied to the membrane according to the concentrations specified in the results section for 1 hour at room temperature. The blot was washed three times with 1% TWEEN20 in PBS 100ml/time with rolling on a rolling machine for 10 minutes per time. After removal of the solution, the secondary antibody

diluted in 1% BSA in TWEEN20 in PBS was applied for 1 hour at room temperature. After 3–5 times with 1% TWEEN20 in PBS 100ml each time, the binding was visualized using enhanced chemiluminescence (ECL).

3.14. MUC1 and E-Cadherin cell surface localization

a) Sub-confluent cells were released from culture plates with 2ml non-enzymatic cell dissociation solution for 5–10 minutes at 37°C until the cells became detached from the flask.

b) 10ml serum-free DMEM medium was added and the cell clumps were dispersed by sucking up and blowing down the cell suspension several times using a 10ml pipette. The cells were then re-suspended in 5 ml serum-free DMEM medium and cell numbers were counted with a haemocytometer.

c) For MUC1 localization in single cells, the cells were diluted into 5×10^5/ml with serum-free medium; go to step h) directly.

d) For the MUC1 localization in cell aggregation, the cells were diluted into 1×10^6/ml cells with serum-free medium. Two aliquots (2ml each) of 1×10^6/ml cells suspension were taken into two 15ml tubes. To one was added 5μl/ml DiL cell-labelling solution and to the another was added DiO 5 μl/ml cell-labelling solution for 30 mins at 37°C.

e) The cells were washed twice by 10ml PBS each tube and centrifuged for 5 minutes at 1000RCF(×g) to remove the supernatants.

f) Each cell pellet was re-suspended into 5×10^5/ml (4ml) with serum-free medium. The two cell suspensions were then mixed by gently sucking up

and blowing down several times with a pipette and divided into several tubes with 1ml/tube.

g) The cell suspension was then incubated in the presence or absence of recombinant galectin-3 1μg/ml, anti-MUC1 (B27.29) antibodies 1μg/ml in a rotating incubator (Julabo Temp SW23, Julabo labortechnic GMBH, Seelbach, Germany) at 100 REVS /min at 37°C for 1 hr.

h) Two 1cm diameter circles were drawn on poly-lysine-coated glass slides with thin black marker pen. 100μl cell suspensions were dropped in the marked circle on the poly-lysine coated slides for 30 minutes at room temperature.

i) After gentle removal of the medium from the slides, 150μl 2% paraformaldehyde was applied to fix the cells for 15 minutes at a flow hood at room temperature. The paraformaldehyde was removed and the cells were washed twice with PBS. 100μl 5% normal goat serum/PBS was applied to block the non-specific binding for 30 minutes at room temperature.

j) After removal of the solution, 100ul/circle of primary antibody diluted in 1% goat serum in PBS (anti-MUC1 B27.29 (5mg/ml) 1:2000, anti-E-Cadherin antibody (1mg/ml) 1:400) was applied for 1 hr at room temperature.

k) The slides were rinsed with PBS in a tank. Tissues were used to dry the slide around the circle, 100ul/circle FITC- (1:400) or AMCA- (1:400) labelled secondary antibody in 1% goat serum in PBS (for the purpose of counting the MUC1 localization % in single cells, using anti-mouse immunoglobin FITC; for MUC1 localization or E-Cadherin distribution on

the cell membrane of cell aggregation, using anti-mouse immunoglobin AMCA) were applied for 1 hr at room temperature. The slides were washed three times by rinsing with PBS and mounted in a mounting medium H-2000 (Vector Laboratories Ltd), then the slides were covered with another cover slide. The slides were blinded and the MUC1 localization was observed under a fluorescent microscope with the same microscope settings. The percentage of cells lacking a continuous rim of MUC1 in 500 cells was scored in randomly selected low power fields with 15X objective under fluorescent microscopy, as previously described (Yu et al., 2007).

3.15. Cell surface expressions of MUC1, E-Cadherin, E-selectin and CD44

Sub-confluent cells were released by 2ml non-enzymatic cell dissociation solution incubated for 5–10 minutes at 37°C and washed twice with PBS 10ml each time. After removal of the supernatant, 5ml 2% paraformaldehyde was added to fix the cells for 15 minutes at room temperature. After washing the cells twice with 10ml PBS and centrifugation at 1500RCF(×g) to remove the supernatants, the cells (10^6/ml) were incubated with 5% goat serum for 30 minutes at room temperature on the roller mixer. After removal of the supernatant following centrifugation at 1500RCF(×g) for 5 mins, the cells were re-suspended into 10^6/ml in the 1% goat serum in PBS and divided 1ml/tube in 1.5ml tubes. Antibodies against E-Cadherin (1mg/ml), E-selectin (1mg/ml) or CD44H (1mg/ml) were all in 1:400. Anti-MUC1 antibody B2729

(5mg/ml) in 1:2000 working concentration was applied to the cells solution for 1 hr at room temperature on the roller (or overnight at 4°C). After washing twice with PBS, fluorescence-conjugated secondary antibodies (1:400 in 1% BSA in PBS) were applied for 1 hour at room temperature. After three washes with PBS, the cells were re-suspended in PBS in 0.5ml/tube. The cell surface expression of MUC1, E-selectin, E-Cadherin or CD44H was analysed by flow cytometry. Fluorescent conjugated secondary antibody was used as a negative control in all the experiments.

3.16. siRNA MUC1 and E-Cadherin transfection

Plate Format		Tube 1 Volumes per well		Tube 2 Volumes per well		Plating Volume (µL/well)
Plating Format(wells/plate)	Surface Area (cm^2/well)	2 µM siRNA (µL)	Serum-free Medium (µL)	Dharma*F* *ECT* (µL)	Serum-free Medium (µL)	Transfection Medium
96	0.3	5	5	0.05 – 0.5	9.95 – 9.5	100
24	2	25	25	0.5 – 2.0	49.5 – 48.0	500

*Note: 100 nM = 100 nmol/L = 100 pmol/mL = 100 fmol/µL

All steps of the protocol were performed in a laminar flow cell culture hood using sterile technique. Each experiment included the following samples in triplicate: mock-transfection (without siRNA), non-specific control siRNA

(iCONTROL™ Non-Targeting siRNA, Cat. # D-001210-01-05) and test siRNA.

The cells were released by trypsinization and cell numbers were counted. The cells were diluted in antibiotic-free complete medium to 5.0 x 10^4 cells/mL (ACA19+ cells 3.0 x 10^4 cells/ml). 100 µL cell suspension was seeded into each well of a 96-well plate, or 1ml/well for a 24-well plate. The cells were incubated at 37°C with 5% CO_2 overnight. Transfection (all calculations are shown for triplicate samples in 96-well format. 24-well cell plate format adjusted by a 10 fold increase) 20 µM siRNA stock siRNA was diluted into 2 µM siRNA solution in 1× siRNA buffer. In separate tubes, the appropriate amount of 2 µM siRNA (Tube 1) and DharmaFECT 4 (Tube 2) was diluted with antibiotic-free and serum-free medium as follows: a. Tube 1 – Add 17.5 µL of 2 µM siRNA to 17.5 µL serum-free medium. The total volume was 35 µL. b. Tube 2 – Add 1.4 µL of DharmaFECT 4 to 33.6 µL serum-free medium. The total volume was 35 µL. The contents of each tube was mixed gently by pipetting carefully up and down and incubate for 5 minutes at room temperature. Contents of Tube 1 were added to Tube 2. In this example, the total volume was 70 µL. The contents were mixed by pipetting carefully up and down and incubate for 20 minutes at room temperature. 280µL antibiotic-free complete medium was added to the mix in step 4 for a total volume of 350 µL transfection volume. The complete culture medium were removed from the wells of the 96-well plate and 100 µL of the appropriate transfection medium replaced to each well. The cells was incubated at 37°C in 5% CO_2 for 48–96 hrs for protein analysis. After transfection, the cells were either lysed and the expressions of the target protein were analysed by immunoblotting or

the cells were labelled with DiO and DiI followed by the assessment of cell aggregation or adhesion in the presence or absence of recombinant galectin-3, as described in the earlier protocol.

3.17. Cell viability, caspase assays

The CellTiter-Glo® Buffer was thawed, and equilibrated to room temperature prior to use. The lyophilized CellTiter-Glo® Substrate was equilibrated to room temperature prior to use. All of the CellTiter-Glo® Buffer was transferred into the amber bottle containing CellTiter-Glo® Substrate to reconstitute the lyophilized enzyme/substrate mixture. This formed the CellTiter-Glo® Reagent.

Mixed by gently vortexing, swirling or by inverting the contents to obtain a homogeneous solution. 100ul/well of cells solution in concentration 2×10^5/ml was added to each flat white (block) transparent 96-well plate. The control wells were added with medium only to obtain a value for background luminescence. The plate and its contents was equilibrated at room temperature for approximately 30 minutes. 100ul CellTiter-Glo® Reagent was added to the cell culture medium present in each well. Contents was mixed for 2 minutes on an orbital shaker to lyse the cells. The plate was allowed to incubate at room temperature for 30 minutes to equilibrate.

Luminescent reading with Tecan infinite 200 (**Note:** Uneven luminescent signal within standard plates can be caused by temperature gradients, uneven

seeding of cells or edge effects in multiwall plates.)

Application:	Tecan i-Control, 1.3.3.0
Device:	infinite 200
System	MED17-86467C
Plate	Corning 96 Flat bottom Transparent Polystyrol
Mode	Luminescence
Attenuation	NONE
Integration Time	500ms
Settle Time	0ms

3.18. Anoikis detection by Annexin V-FITC cell surface binding

The cells were released by NECDS and either treated or not treated, after suspension in a poly-HEMA coated cell culture plate for the desired time (see Chapter 5 and Chapter 6). Collect 2.5 x 10^5 cells by centrifugation. The cells were re-suspended in 500 µl of 1X Binding Buffer (from Biovision) at a concentration of 5 x 10^5 cells/ml. 5 µL of Annexin V-FITC and 5 µL of propidium iodide (PI 50µg/ml) were added into 0.5ml cell solution and incubated at room temperature for 5 mins in the dark before analysis of annxin-V cell surface binding by flow cytometry (Ex = 488 nm; Em = 530 nm) using FITC signal detector (usually FL1) and PI staining by the phycoerythrin emission signal detector (usually FL2).

Cell without staining and cells stained only with Annexin V-FITC or propidium iodide(PI) were used to identify the position of without staining (bottom-left panel), Annexin V-FITC (bottom-right panel) and PI (upper-right panel) labelled cell populations in the bivariate correlation plot. Annexin-V positive and PI negative (early apoptotic, at the bottom right in the bivariate correlation plot) and Annexin-V positive and PI positive (late apoptotic, at the top right in the correlation plot) cells are considered as apoptotic cells (Fig3-

1).

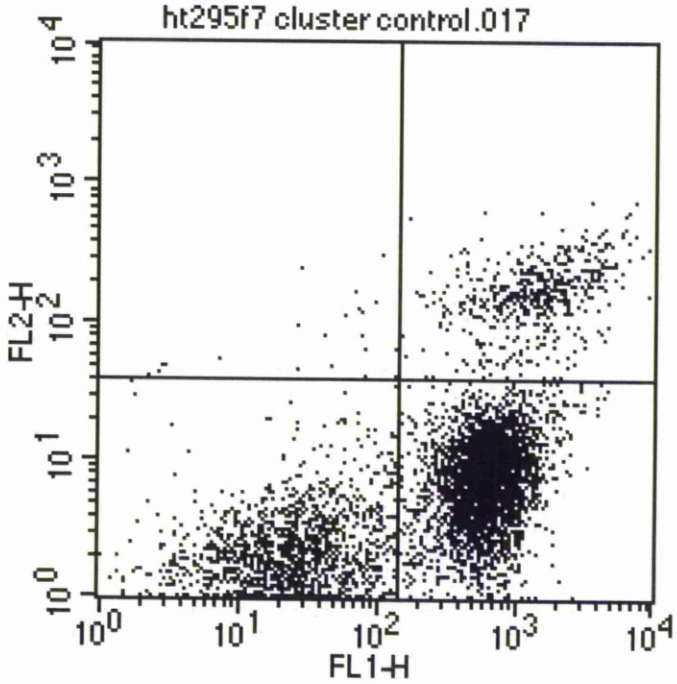

Fig 3-1. An example of flow cytometry plots from the anoikis assessments of HT29-5F7 cells. Annexin-V positive and PI negative (early apoptotic, at the bottom right in the bivariate correlation plot) and Annexin-V positive and PI positive (late apoptotic, at the top right in the correlation plot) cells are considered as apoptotic cells.

3.19. Trans-endothelial invasion

The trans-endothelial invasion assays were performed in transwell cell culture inserts (BD Falcon, MA) with 8-μm pore filters. HUVEC cells were cultured in the inserts 50000/well for 3 days to allow tight formation of the cell monolayer. The monolayer integrity and permeability were monitored by

measuring the trans-endothelial electrical resistance (TEER) using a voltohmmeter (EVOM, World Precision Instruments, UK).

Epithelial cells were released by Non-Enzymatic Cell Dissociation solution, labelled with DiO-fluorescent dye 5μl/ml (1×10^6/ml in serum-free medium) for 30 mins at 37°C. Then the cells were washed twice with PBS and diluted into 5×10^4/ml in serum-free medium, and incubated with or without recombinant galectin-3 for 30 mins at 37°C before the cells were applied to the HUVEC monolayer. The cancer cells 250μl/well were added directly (without removing the endothelial culture medium) on the HUVEC monolayer for 16 hrs at 37°C. The cells inside the inserts were scraped with cells scraper (reformed from 16cm 2-position blade cell scraper from Sarstedt, Inc. Newton, NC 28658) and removed from the upper side of the transwell membrane with a cotton swab. The transwell membrane of the insert was fixed with 2% paraformaldehyde at room temperature for 15 minutes in the fume hood. The inserts membrane was then cut down from the insert housing and put on glass slides, bottom side up. The slides were sealed with mounting medium for fluorescence (H1200 with DAPI from VECTOR) and the fluorescent cells migrated to the bottom side of the transwell membrane were counted under fluorescence microscopy.

3.20. Assessment of secreted galectin-3 from cells by ELISA

The Anti-Gal3 antibody (RD MAB1154 from R&D) was diluted to 2.5μg/ml with coating buffer (1.6 Na2CO3, 1.46g NaHCO3 in 1L, PH9.6). 100ul/well was added into an ELISA plate. The plate was sealed with Parafilm and

incubated overnight at room temperature. The wells were washed 3 times with 300ul/well PBS with complete removal of the liquid at each step. After removing the solution in the last wash, the plate was inverted and blotted against paper towel to remove the residue of the solution.

The wells were then added in 300μL/well of 5% BSA in PBS (Blocking Buffer) at room temperature for a minimum of 1 hour. The wells were washed three times with PBS before addition of the testing samples. Both samples to be tested and standard recombinant galectin-3 were diluted in polypropylene tubes. 100 μL of samples or standard of recombinant galectin-3 (250,125,62.5,31.25,15.6,7.8,3.9,2,1,0.5,0.25μg/ml) in 1% BSA in PBS was added. The solution was mixed by gently tapping the plate frame for 1 minute. The plate was covered and incubated for 2 hours at room temperature. The plate was washed with 300μl/well PBS three times. 100 μL (0.4μg/ml in 1% BSA/PBS) of the biotinylated anti-Gal3 antibody (BAF 1154 from R&D) was added to each well for 2 hours at room temperature. The plate was then washed with 300μl/well PBS three times. 100 μL of Extra Avidin-HRP (R&D Systems, dilute 1:1000 in 1% BSA in PBS) was added into each well for 20 minutes at room temperature. The plate was washed with 300ul PBS three times.

100 μL SigmaFAST OPD (Sigma) Solution was added into each well for 20–30 minutes at room temperature. 50 μL 4M sulphuric acid was then added into each well to stop the reaction. The plate was gently tapped to ensure thorough mixing before the optical density (O.D.) was read (within 30 minutes) with a Sunrise microplate reader at 452 nm. Wavelength correction set to 540 or 570 nm. The concentration of the testing samples was obtained from the standard

curve.

CHAPTER 4.

4. Effects of galectin-3 on cancer cell heterotypic adhesion to endothelium and trans-endothelial migration

4.1. Aims

To assess the influence of cell surface MUC1 expression and MUC1-galectin-3 interaction with recombinant galectin-3 at pathologically-relevant circulating galectin-3 concentrations on cancer cell heterotypic adhesion to vascular endothelial cells and trans-endothelial migration.

4.2. Introduction

One of the critical steps in cancer metastasis is the adhesion of disseminating tumor cells to the blood vessel endothelium in distant organs. This process is thought to be regulated by the mechanical properties of the cancer cells and also by the specific expression of various adhesion molecules and/or ligands to adhesion molecules on the surface of cancer cells and endothelial cells (247).

Previous studies from our group have shown that MUC1 is a natural ligand of galectin-3 in human cancer cells. Binding of recombinant galectin-3 to cancer-associated MUC1, via the TF antigen, induces MUC1 cell-surface polarization, thus revealing underlying adhesion molecules on the cell surface, and increases the adhesion of human epithelial cells to human umbilical vein endothelial cells (HUVEC) under static cell culture conditions(248). Previous investigations have indicated that the great size and length of MUC1 allows it to form a protective shield on the cell surface and inhibit cancer cell-cell and

cancer cell-matrix interactions (174, 175). We therefore investigated the effects of MUC1 expression and MUC1-galectin-3 interactions on cancer cell heterotypic adhesion to endothelial cells.

4.3. Materials and methods

Materials. Recombinant full-length human galectin-3 and monoclonal antibodies (mAb) against human CD44H (BBA10) and E-selectin (BBA16) were from R&D Systems. B27.29 anti-MUC1 mAb was kindly provided by Dr. Mark Reddish (Biomira, Inc.). Nonenzymatic Cell Dissociation Solution was from Sigma. Vybrant DiO Cell-Labeling Solutions were from Molecular Probes.

Cell lines. Human colon cancer HT29 and HT29-5F7 cells. Macrovascular HUVECs and human microvascular lung endothelial cells (HMVEC-L) Cells that had been passaged less than five times were used in the experiments. $ACA19^{+}$, and $ACA19^{-}$,all as described in chapter 3

Cancer cell-endothelial adhesion. Cancer cell-endothelial adhesion was assessed as described at chapter 3. At the end of the experiments, the samples were blinded and the fluorescently labeled cells remaining on the endothelial monolayer were counted in 10 randomly selected fields of view using fluorescent microscopy (Olympus B51). The ability of the cells to be labeled by the fluorescent dye was different between any two human cell lines tested

in our pilot experiment. As comparison of the cell adhesion between different MUC1-expressing cells is an important part of this study, the actual number of the fluorescently labeled cells adhered to endothelial monolayer, rather than the reading of the fluorescent density, was used as the end point.

Small interfering RNA MUC1 knockdown. $ACA19^{+}$ cells (3×104/ml,1ml/well in 24Wells cell culture plate after 24 hours cultured in incubator at 37°C in Anti-biotic free complete DMEM)were transfected with 100 nmol/L MUC1 small interfering RNA (siRNA) or scrambled control non-targeting siRNA (siCONTROL, Dharmacon) for 48 h at 37°C in serum-free and anti-biotic free DMEM medium. The cells were lysed and the expression of MUC1 was assessed by MUC1 immunoblotting with the B27.29 anti-MUC1 antibody (5mg/ml 1:15000 in 1%BSA in PBS) followed by goat anti-mouse HRP-conjugated antibody1:1000 in 1% BSA in PBS. See in details at chapter 3.

Cell adhesion under flow conditions (Experiment performed in University of Birmingham in collaboration with Prof G Nash, I traveled there to do part of those experiments with them together). HUVECs, cultured in flattened glass capillaries for 24 h at 37°C to allow the cells to form monolayers as described previously(243), were unstimulated or stimulated with 10 ng/mL tumor necrosis factor-α (TNF-α) for 24 h at 37°C before the introduction of cancer cells. $ACA19^{+/-}$ cells were incubated with or without 1 μg/mL galectin-3 for 30 min at 37°C. The cells were then perfused through glass capillaries at a flow rate to deliver 0.05-Pa shear wall stress. After 4 min of washing with PBS, the capillaries were video-recorded and the number of adherent cells was

quantified and expressed as the number of adherent cells per square millimeter per 10^6 cells perfused.

Cell-surface expressions of E-selectin and CD44. Cells released with Nonenzymatic Cell Dissociation Solution were fixed with 2% paraformaldehyde for 0.5 h, blocked with 5% normal goat serum/PBS for 0.5 h, and incubated with antibodies against E-selectin (1mg/ml 1:400 in 1%BSA in PBS)or CD44H(1mg/ml 1:400 in 1%BSA in PBS) for 1 h at room temperature. After application of fluorescence-conjugated secondary antibody 1:400 for 0.5 h, the expression of cell-surface E-selectin or CD44 was analyzed by flow cytometry (Cells treated without primary anti-E-selectin or anti-CD44H antibody used as control in the cytometry analysis).

Trans-endothelial invasion. HUVECs (50000/ml, 0.5ml/well in EBM medium) were cultured in Transwell inserts with 8-μm-pore filters (BD Falcon) for 3 d to allow tight formation of cell monolayers. Monolayer integrity was monitored by measuring transendothelial electrical resistance using a volt-ohm meter (EVOM, World Precision Instruments), and monolayers with transendothelial electrical resistance >800 Ω /cm^2 were used for transendothelial assessment. Epithelial cells (1×10^6/ml in serum-free medium), labeled with DiO (5μl/ml), were incubated with or without galectin-3 (concentrations)for 30 min at 37°C before application of the cells to the HUVECs for 16 h at 37°C. The cells at the upper side of the Transwell membrane were removed with a cotton swab and fluorescent cells migrated to the bottom side of the Transwell membrane were counted using an Olympus

B51 fluorescence microscope after removal of the transwell membrane from the transwell inserts.

Measurement of galectin-3 concentration in the cell culture supernatant by ELISA:

Sample preparation: HT295F7 cells (5.0 $\times 10^5$ cells/mL) in serum-free DMEM medium were incubated for 1.5 hours at 37°C. The cells suspension was spun at 1500RCF(×g) for 5 minutes. Then the supernatant was collected and froze at -20°C for galectin-3 test.

100 μL/well of Anti-Gal3 antibody 2.5μg/ml(RD MAB1154 from R&D) in coating buffer(1.6 Na2CO3, 1.46g NaHCO3 in 1L, PH9.6) in PBS, use immediately) was transferred to an ELISA plate. The plate was sealed and incubated overnight at room temperature. Each well was aspirated and washed 3 times by forcefully filling each well with PBS (300 μL) using a multi-channel pipette. The liquid was completely removed at each step. After the last wash, the remaining PBS was removed by inverting the plate and blotting it against clean paper towelling. The plates was blocked by adding 300 μL of 5% BSA in PBS of Blocking Buffer to each well and incubated at room temperature for a minimum of 1 hour. After washing, the plates was ready for sample addition. Dilutions of unknowns and standards was carried out in polypropylene tubes.100 μL of sample or standards of Recombinant Galectin-3 in 1% BSA in PBS was added per well. The samples were mixed by gently tapping the plate frame for 1 minute. The plate was covered with an adhesive strip and incubated 2 hours at room temperature. The plate was washed 3 times by forcefully filling each well with PBS (300 μL) using a

multi-channel pipette. 100 μL of the Biotinylated anti-Gal3 antibody(BAF 1154 from R&D) 0.4μg/ml, diluted in 1%BSA in PBS, was added to each well. The plate was covered with a new adhesive strip and incubated for 2 hours at room temperature. The plate was washed 3 times by forcefully filling each well with PBS (300 μL) using a multi-channel pipette. 100 μL of Extra Avidin-HRP (R&D Systems, dilute 1:1000 in 1% BSA in PBS) was added to each well. The plate was covered and incubated for 20 minutes at room temperature. The plate was avoided placing in direct light. The plate was washed 3 times by forcefully filling each well with PBS (300 μL) using a multi-channel pipette. 100 μL SigmaFAST OPD (from Sigma-Aldrich) Solution was added to each well. The plate was incubated for 20 - 30 minutes at room temperature. The plate was avoided placing in direct light. 50 μL 4M sulphuric acid was added to each well. The plate was gently tapped to ensure thorough mixing. The optical density (O.D.) of each well was determined within 30 minutes. The Sunrise microtiter plate reader was set to 452 nm. wavelength correction set to 540 or 570 nm. The values of the unknown samples were assigned in relation to the standard curve. Various methods (*e.g.*, linear, semi-log, log/log, 4 parameter logistic) in Excel were tried to see which curve best fits the data. One way to determine if the curve fit is correct is to back fit the standard curve O.D. values. To do this, the standard curve was first plotted. Next, standards were treated as unknowns and interpolate the O.D. values from standard curve. The readings were close to the expected values (+/-10%). The data reduction method that gave the best correlation (r) value and backfitted was used.

Statistical analysis. Paired or unpaired *t* test for single-comparison, one-way ANOVA followed by Newman-Keuls' test for multiple comparisons, χ^2 test, and Kaplan-Meier analysis followed by log-rank test (StatsDirect for Windows, StatsDirect) were used where appropriate. Differences were considered significant when 2-tailed $P < 0.05$

4.4. Results

4.4.1 Effect of MUC1 expression and MUC1-galectin-3 interaction on cancer-endothelial adhesion under static conditions

Immuno/lectin blots of MUC1-positive transfectants ACA19^{+} and MUC1-negative transfectants (ACA19^{-}) cells of A375 human melanoma cells with B27.29 anti-MUC1 mAb (5mg/ml 1:15000 in 1%BSA in PBS) and TF-binding PNA (1mg/ml 1:1000 in 1%BSA in PBS) showed that MUC1 in ACA19^{+} cells is abundantly decorated with TF antigens (Fig4-1). MUC1-positive transfectants ACA19^{+} showed abundant expression of MUC1 while the negative transfectants ACA19- showed no detectable expression of MUC1 (Fig4-1).

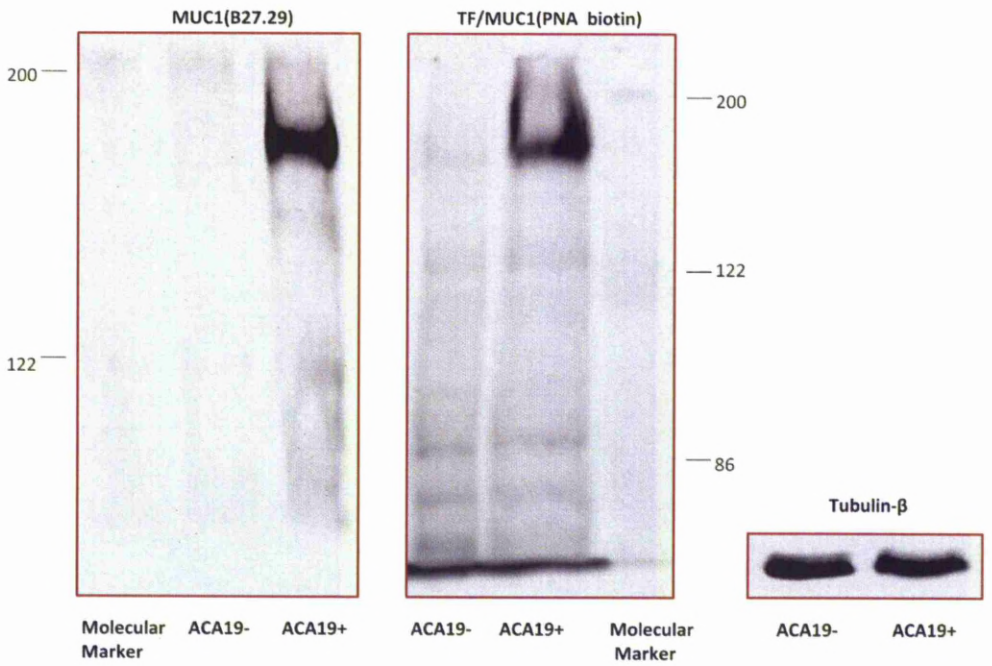

Fig4-1 Expression of MUC1 and MUC1-associated TF in ACA19+/- transfectants. Immunoblots of ACA19+/- cell lysates were probed with biotinylated TF-binding peanut agglutinin (PNA), B27.29 anti-MUC1 antibody or anti-tubulin antibody (1mg/ml 1:1000 in 1%BSA in PBS).

HUVEC cells (Red) were seeded on the glass cover slipes inserted in 24 well culture plates till confluence after three days (Fig4-2). The $ACA19^{+}$ and $ACA19^{-}$ were labeled with DiO (green) fluorescence labeling solution separately for 30minutes before applied HUVEC monolayer (Only for presentation purposes HUVEC prelabelled with DiL for 30minutes, not labeled in every real adhesion experiment).

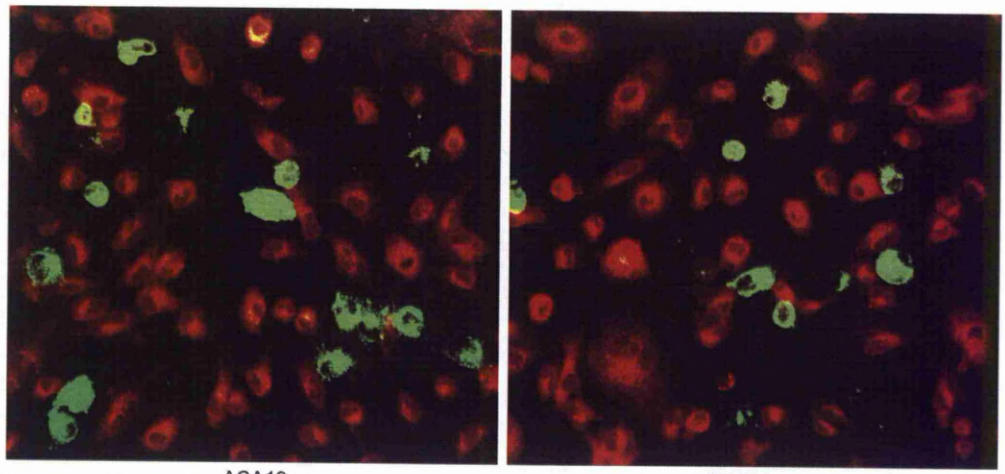

Fig 4-2. ACA19^{+} cells adhere less than ACA19^{-} cells to monolayer of HUVECs. ACA19+or- cells (green) were labeled with DiO and dropped on the HUVEC monolayer (red) on the slides for 1 hour at 37°C , The cells were washed and the adhesion cells on the HUVEC monolayer were counted under fluorescence microscope.

ACA19^{+} cells showed significantly less adhesion to unstimulated and TNF-α– prestimulated HUVECs compared with the ACA19^{-}. (Fig 4-2, and 4-3)

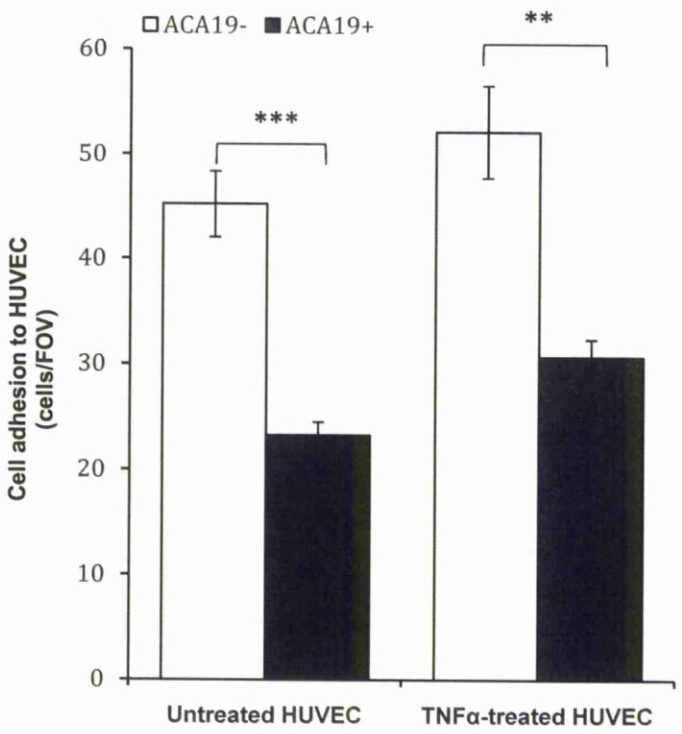

Fig 4-3. Effects of MUC1 expression on cancer cell-HUVEC adhesion under static conditions. $ACA19^+$ cells adhere less than $ACA19^-$ cells to HUVECs. *Columns,* mean of triplicate determinations from three independent experiments; *bars,* SE. *, $P < 0.05$; **, $P < 0.01$; ***, $P < 0.001$ (one-way ANOVA compare means).

To determine the effect of circulating galectin-3 on cancer cell adhesion to endothelium, we pretreated the cells with recombinant galectin-3 at several pathologically relevant circulating galectin-3 concentrations. Earlier investigation by Iurisci and colleagues (209) has shown that the concentration of circulating galectin-3 increases up to 5-fold in the sera of cancer patients with melanoma, breast, or gastrointestinal cancer (range, 20–950 ng/mL) compared with healthy people. Our own investigation has indicated that the

concentrations of circulating galectin-3 in the sera of colorectal cancer patients are >14-fold higher (up to 5 μg/mL) than in healthy people (Barrow et al, unpublished data). We found that pretreatment of the cells with galectin-3 at concentrations >100 ng/mL resulted in significant increase of $ACA19^{+}$, but not $ACA19^{-}$, cell adhesion to HUVECs (Fig4-4).

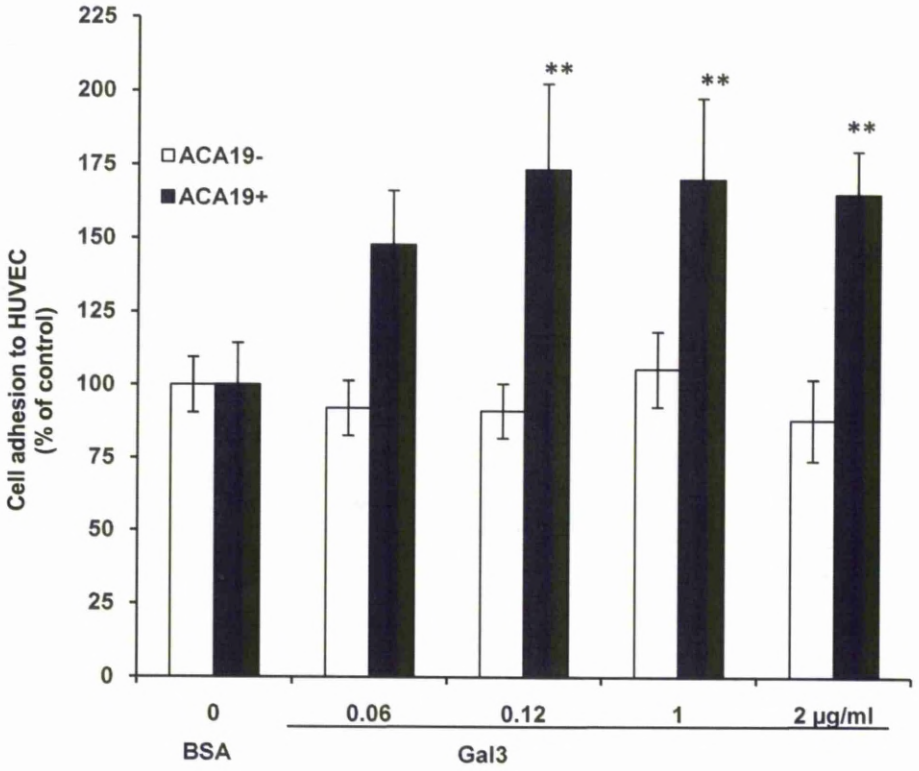

Fig4-4. Effects of MUC1-galectin-3 interaction on cancer cell-HUVEC adhesion under static conditions. Pretreatment of the cells with galectin-3 increases $ACA19^{+}$, but not $ACA19^{-}$, cell adhesion to HUVECs. *Columns,* mean of three independent experiments; *bars,* SE. *, $P < 0.05$; **, $P < 0.01$; ***, $P < 0.001$ (one-way ANOVA followed by Newman-Keuls' test for multiple comparisons).

Treatment of ACA19+ with MUC1 siRNA results in 63% reduction of MUC1 expression in comparison with cells treated with control siRNA (fig 4-5).

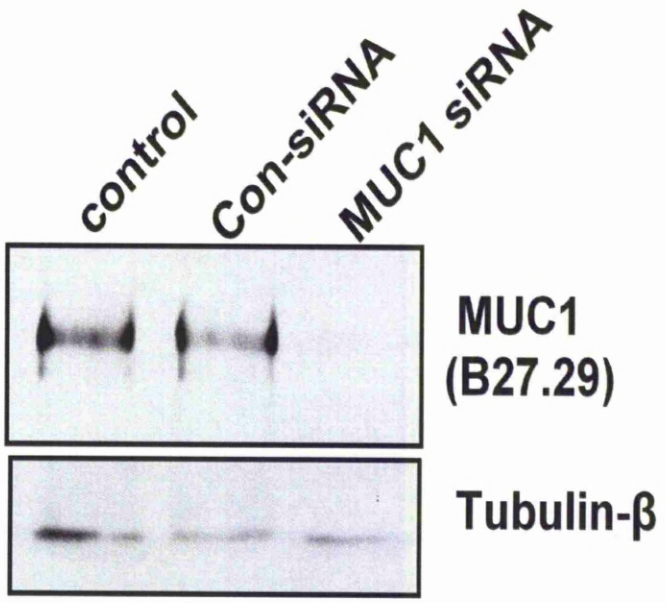

Fig4-5. siRNA MUC1 suppression in ACA19$^+$ cells. ACA19$^+$cells were treated with siRNA MUC1 or control non-targeting siRNA for two or three days before the cellular muc1 expression was determined by B27.29 immunoblotting. Selected representative blots of three experiments.

Suppression of MUC1 expression by siRNA in ACA19$^+$ cells was seen to be associated with 47% increased adhesion of the cells to HUVECs(Fig4-6), and this prevented the increase of cell adhesion in response to galectin-3 (Fig4-7).

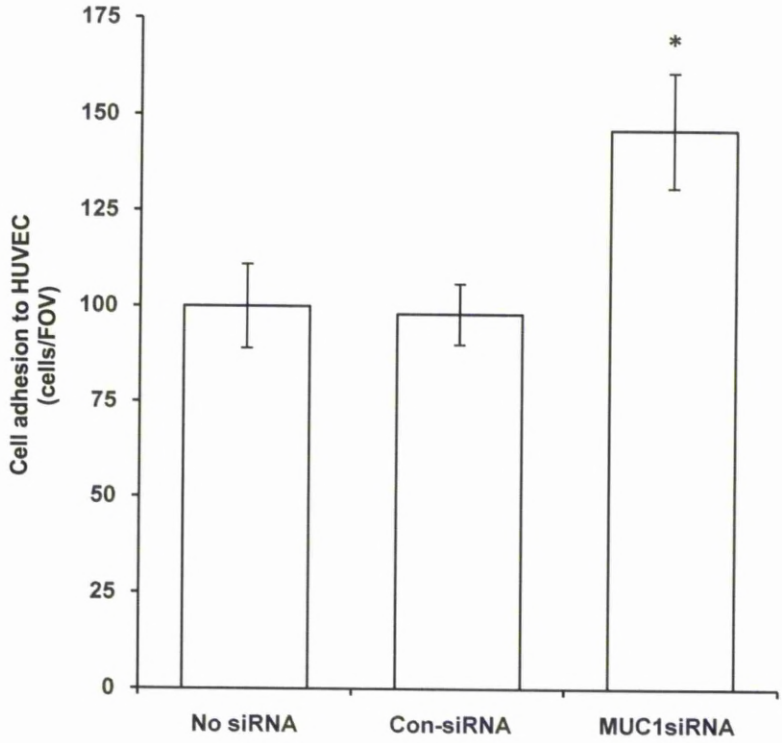

Fig4-6 Effects of MUC1 expression on cancer cell-HUVEC adhesion under static conditions. MUC1 suppression increases ACA19$^+$ cell adhesion, mean of three independent experiments; *bars,* SE. *, $P < 0.05$; **, $P < 0.01$; ***, $P < 0.001$. (one-way ANOVA to compare means).

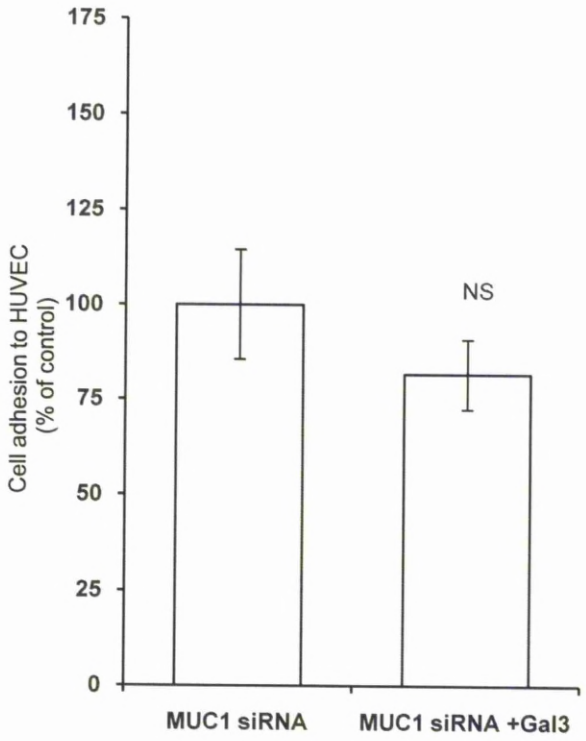

Fig4-7 SiRNA MUC1 suppression in ACA19$^+$ cells. MUC1 suppression abolishes galectin-3–induced cell adhesion. *Columns,* mean of three independent experiments; *bars,* SE. *, $P < 0.05$; **, $P < 0.01$; ***, $P < 0.001$. (one-way ANOVA compare means).

Thus, the presence of extracellular free galectin-3, by its interaction with MUC1, counteracts the antiadhesive effect of MUC1 expression on cancer cell adhesion.

To determine whether MUC1-galectin-3 interaction has similar effects on cell

adhesion in cancer cells that naturally express MUC1, we compared the adhesion of human colon cancer HT29 and HT29-5F7 cells in the presence or absence of recombinant galectin-3. HT29-5F7 is a HT29 subline selected by its resistance to 5-fluorouracil and has much greater MUC1 than the parental HT29 cells (249)(Fig 4-8).

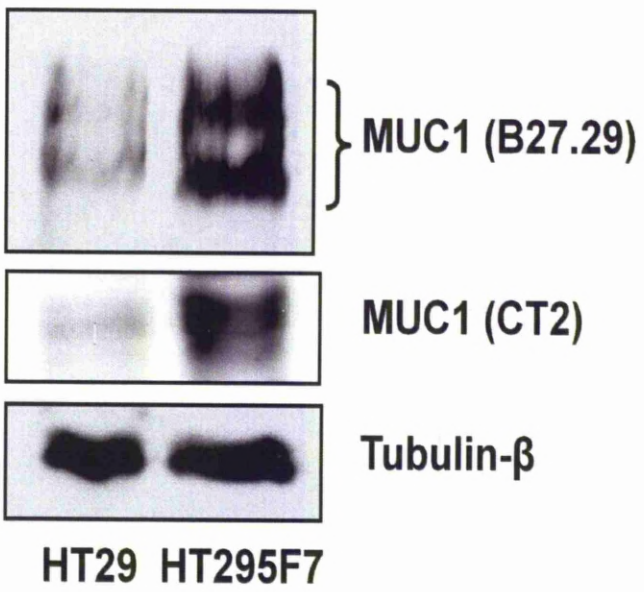

Fig4-8 Expression of MUC1 in HT29 and HT29-5F7 cells. Higher MUC1 expression in HT29-5F7 than in parental HT29 cells. HT-29 and HT29-5F7 cell lysates were probed with B27.29 anti-MUC1 antibody(5mg/ml, 1:15000), CT-2 anti-MUC1 antibody against the cytoplasmic tail of MUC1 (0.5mg/ml, 1:1000. NeoMarkers, Fremont, CA) or anti-β-tubulin antibody (1mg/ml, 1:1000).

HT29 cells showed significantly more adhesion to unstimulated and TNF-α–prestimulated HUVECs than HT29-5F7 cells (Fig4-9).

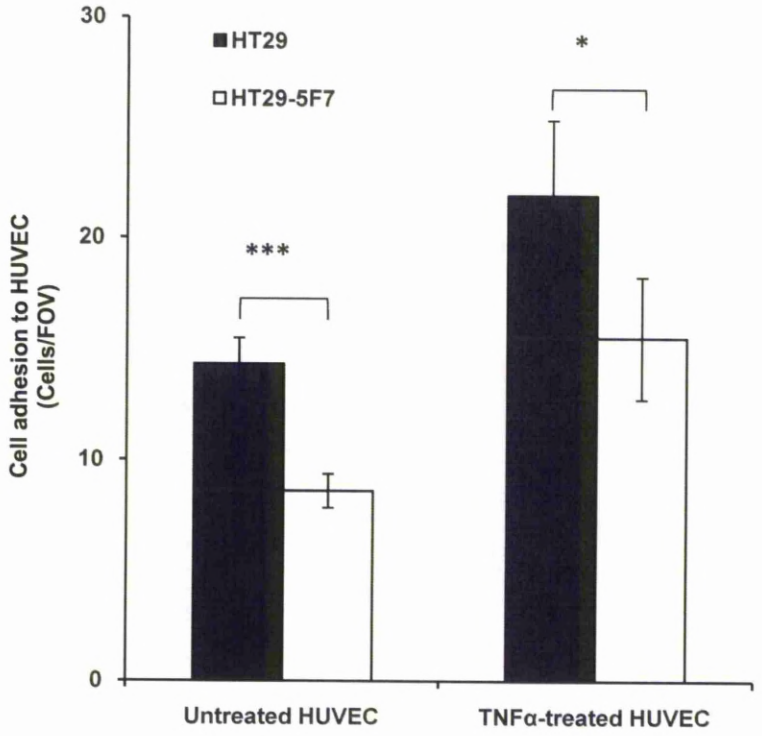

Fig4-9 Effects of MUC1 expression on HT29 and HT29-5F7 cell adhesion to HUVECs. HT29-5F7 cells show less adhesion than HT29 cells to HUVECs unstimulated or pre-stimulated with 10ng/ml TNFα for 16 hr. Data are expressed as total number of the adhered cells/FOV as mean ± SEM from two independent experiments. The difference was analysed by unpaired *t* test.

Pretreatment of the cells with galectin-3 significantly increased adhesion of HT29-5F7, but not HT29, cells to HUVECs(Fig4-10), and this effect was abolished by the presence of TF-expressing Asialofetuin (Fig4-11).

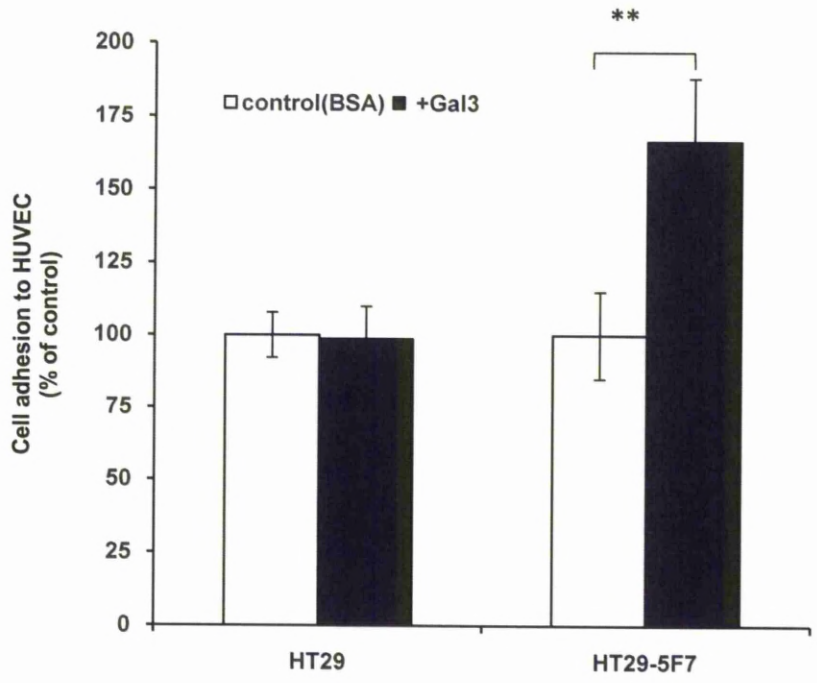

Fig4-10 Effects of MUC1-galectin-3 interaction on HT29 and HT29-5F7 cell adhesion to HUVECs. Galectin-3 (1μg/ml) treatment increases adhesion of HT29-5F7 but not HT29 cells to HUVECs. Data are expressed as percentage of the adhered cells compared to that in the controls (mean ± SEM of triplicate determinations from three independent experiments). The difference was analysed by paired *t* test. *p<0.05, **p<0.01, ***p<0.001. (one-way ANOVA compare means).

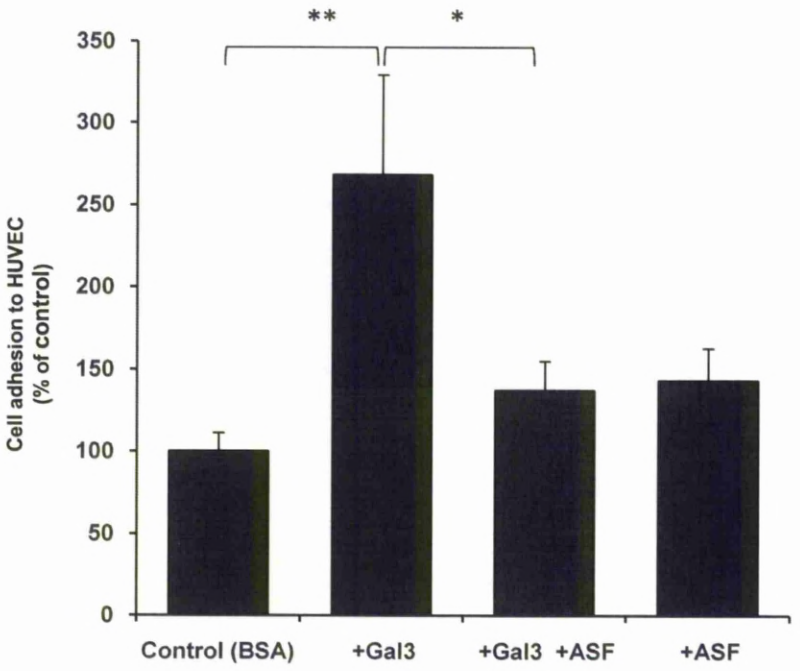

4-11 Effects of MUC1-galectin-3 interaction on HT29 and HT29-5F7 cell adhesion to HUVECs. Galectin-3-induced cell adhesion was blocked by the presence of galectin-3-binding ligand asialofetuin (ASF). HT29-5F7 cells were treated without or with 1 μg/ml galectin-3 in the presence or absence of 20μg/ml ASF before the assessment of cell adhesion. Data are as percentage of the adhered cells compared to that in the controls (mean ± SEM of triplicate determinations from six independent experiments). The difference was analysed by ANOVA, Newman and Keuls. *$p<0.05$, **$p<0.01$, ***$p<0.001$.

To see whether the effects of MUC1–galectin-3 interaction on cancer cell adhesion to HUVECs also occur with microvascular endothelium, a model that is probably closer to the *in vivo* situation in metastasis, we analyzed cell

adhesion to HMVEC-L. Again, ACA19^{+} cells showed significantly less adhesion to unstimulated and TNF-α–prestimulated HMVEC-Ls than ACA19^{-} cells (Fig 4-13).

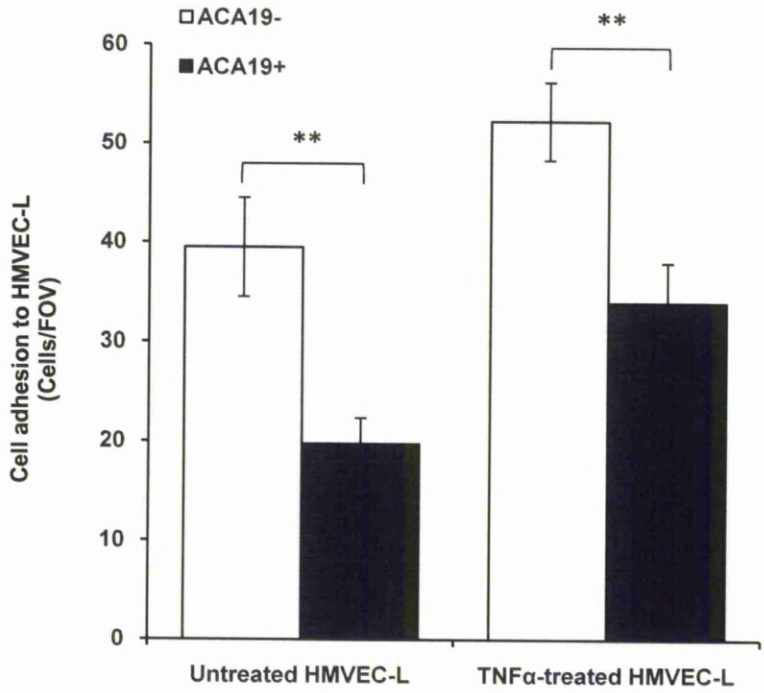

Fig 4-13. Effects of MUC1 on cancer cell-HMVEC-Ls adhesion under static conditions.ACA19^{+} cells adhere less than ACA19^{-} cells to HMVEC-Ls prestimulated with or without TNF-α. *Columns,* mean of three independent experiments; *bars,* SE. *, $P < 0.05$; **, $P < 0.01$; ***, $P < 0.001$. (one-way ANOVA compare means).

Pretreatment of the cells with galectin-3 (1 μg/mL) increased adhesion of $ACA19^+$ cells but not of $ACA19^-$ cells comparing with control(Fig 4-14)

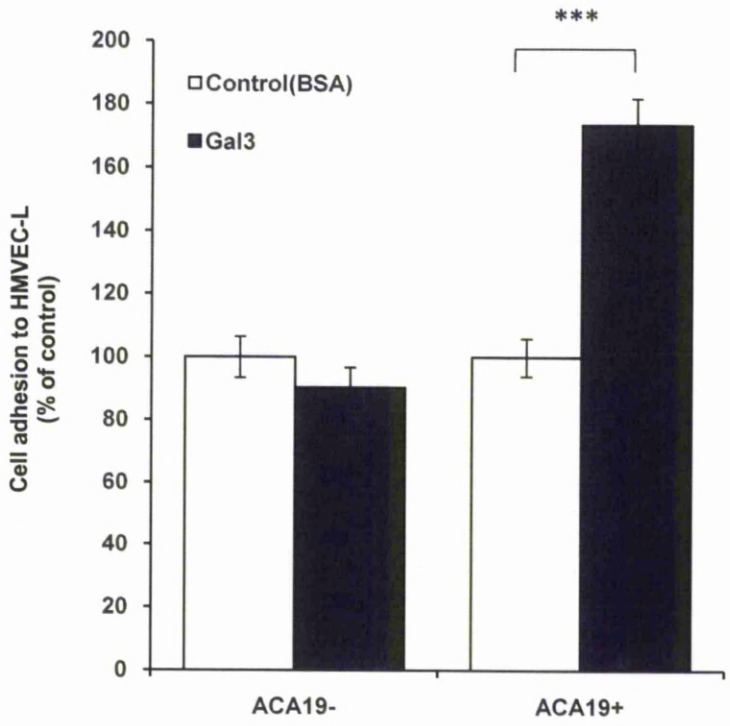

Figure 4-14. Effects of MUC1-galectin-3 on cancer cell-HMVEC-Ls adhesion under static conditions: Galectin-3 (1 μg/mL) increases ACA19+, but not ACA19–, cell adhesion to HMVEC-Ls. Columns, mean of two independent experiments; bars, SE. *, $P < 0.05$; **, $P < 0.01$; ***, $P < 0.001$. (one-way ANOVA compare means).

Collectively, these results indicate that MUC1 expression prevents cancer cell adhesion to macrovascular and microvascular endothelium and that MUC1-galectin-3 interaction reduces this protective effect of MUC1.

4.4.2 Assessment of galectin-3 secretion.

We also assessed whether galectin-3 is secreted into the medium by the cancer cells. 5×10^5/ml cells suspension 1ml of HT295F7, HT29, ACA19+ or ACA19- cell were incubated for 1.5 hour at 37°C, the culture medium (Serum-free DMEM)was collected after spin of the medium at 1500RCF(×g) for 5 min and the concentrations of galectin-3 in the medium was assessed by ELISA. Recombinant galectin-3 was used to generate a standard curve (Fig 4-12)

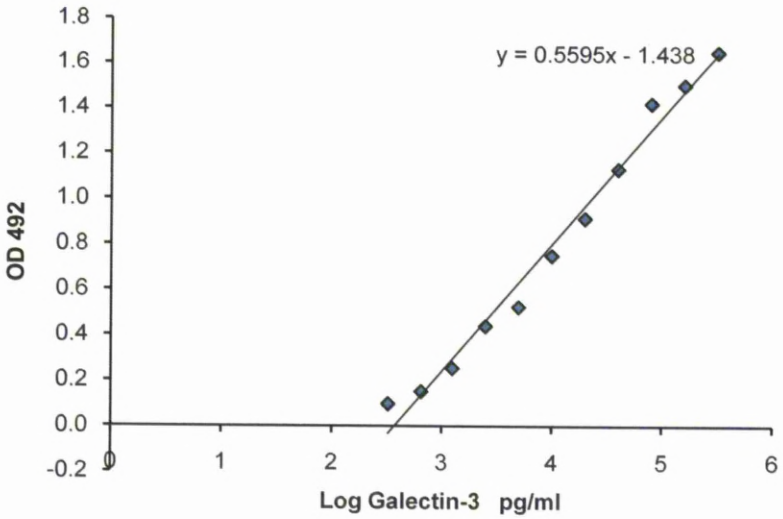

Fig4-12 Standard curve of recombinant Galectin-3 tested by ELISA(Triplicate)

It was found that galectin-3 secrected into the mediun with the 1.5 hr incubation time was all less than 0.325 ng/mL (the detectable limit of the assay) Thus, the contribution of endogenously secreted galectin-3 to recombinant galectin-3–mediated cell adhesion in these assessments is minimal.

4.4.3 Effect of MUC1 and MUC1-galectin-3 interaction on cancer-endothelail adhesion under sheer flow conditions

10^6 cells were perfumed through HUVEC monolayers pre-treated with TNFa for 24 hours on glass capillaries in PBS at 0.5 ba for 4 mins. The HUVEC monalyers were washed by PBS for 1minutes before video-recorded. The numbers of adhesion cells per square millimeter per 10^6 cells perfused was calculated. The results are shown in Fig4-15. Under 0.05 Pa shear flow conditions, very few $ACA19^+$ or $ACA19^-$ cells showed adhesion to unstimulated HUVECs, but their adhesion was markedly (68%) increased when HUVECs were pretreated with TNF-α(Fig 4-15).

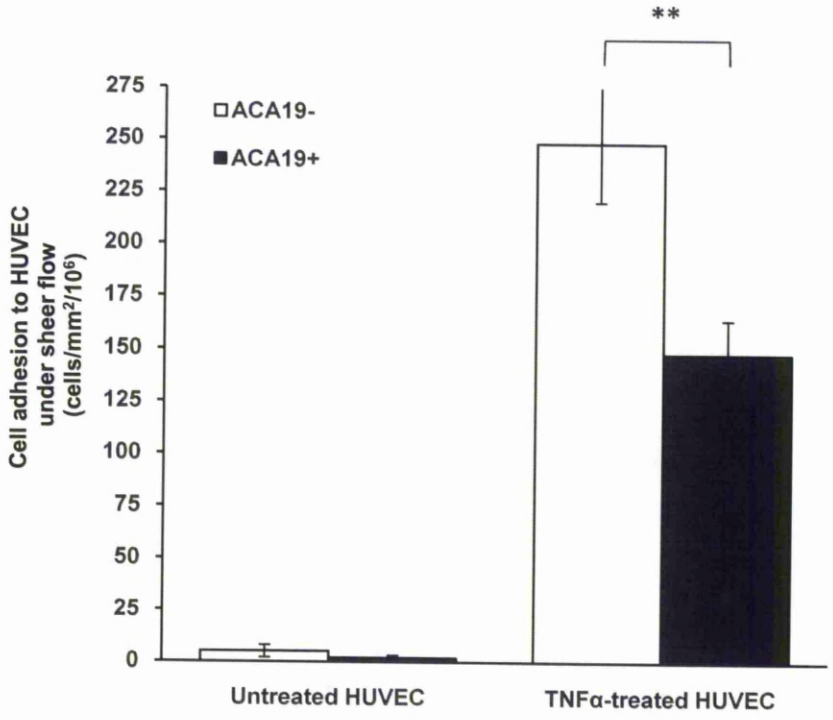

Figure 4-15. Effects of MUC1 expression on cancer cell-HUVEC adhesion under flow conditions.ACA19$^+$ cells adhere less than ACA19$^-$ cells to HUVECs at 0.05-Pa shear stress flow conditions. *Columns,* mean of seven independent experiments; *bars,* SE. *, $P < 0.05$; **, $P < 0.01$; ***, $P < 0.001$. (one-way ANOVA compare means).

Moreover, ACA19$^+$ cells showed 68% less adhesion than ACA19$^-$ cells to TNF-α–stimulated HUVECs under such conditions. Pretreatment of the cells with 1 μg/mL galectin-3 resulted in 55% increased adhesion of ACA19$^+$ cells but not of ACA19$^-$ cells(Fig 4-16)

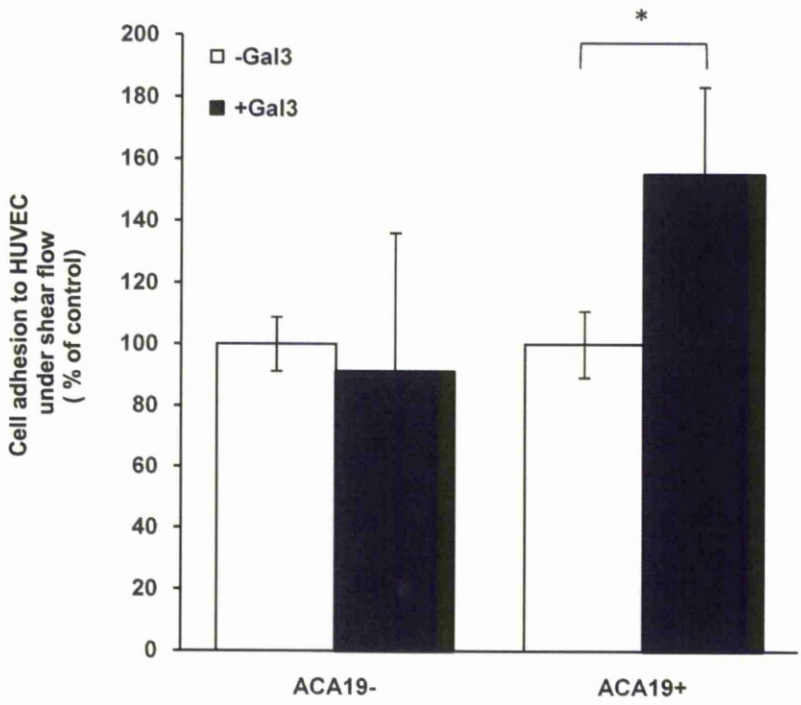

Fig 4-16. Effects of MUC1-galectin-3 interaction on cancer cell-HUVEC adhesion under flow conditions. galectin-3 (1 μg/mL) treatment increases adhesion of $ACA19^+$, but not $ACA19^-$, cells to HUVECs under flow conditions. *Columns,* mean of five $ACA19^+$ and six $ACA19^-$ independent assessments; *bars,* SE. *, $P < 0.05$; **, $P < 0.01$; ***, $P < 0.001$.

Thus, Cancer cell-endothelial adhesion under flow conditions is inhibited by MUC1 expression but increased by MUC1-galectin-3 interaction. The effects of MUC1 expression and galectin-3-MUC1 interaction on cancer cell-endothelial adhesion seen under static conditions also hold true under flow conditions.

4.4.4 Effect of Galectin-3 and B27.29 anti-MUC1 mAb on MUC1 cell-surface polarization and on cell adhesion.

Previous studies in our group has shown shown that galectin-3-MUC1 interaction induces change in MUC1 cell-surface localization (248). To see whether this change in MUC1 localization is associated with altered cell adhesion to endothelium, we compared MUC1 cell-surface clustering in response to galectin-3 and cell adhesion to HUVECs.

It was found that 10% (48 of 500) $ACA19^+$ cells showed spontaneous clustering of MUC1 on the cell surface, as illustrated by discontinuity of MUC1 cell-surface staining when cultured in suspension for 1 h at 37°C (Table4-1).

Table 4-1. Galectin-3 and B27.29 anti-MUC1 antibody induce discontinuous MUC1 cell surface localization on ACA19+ cells.

	Control	Gal-3 (1μg/ml)	B27.29 (1μg/ml)
	% (n)	% (n)	% (n)
37°C	10 (48)	14(68)*	26(128)**
Pre-fixed	7 (36)	8 (39)	9 (43)

After pretreatment with galectin-3 (1 μg/mL) at 37°C for 1 h, 40% more (68 of 500; $P < 0.05$) cells showed MUC1 cell-surface polarization than control cells. Introduction of B27.29 anti-MUC1 mAb also resulted in significant increase (128 of 500; $P < 0.01$) in the number of cells showing MUC1 cell-

surface polarization. This effect of B27.29 on MUC1 cell-surface polarization is in keeping with previous reports that the presence of 214D4 anti-MUC1 mAb, which also recognizes the VNTR region of MUC1, induces MUC1 cell-surface polarization in MUC1-transfected human melanoma cells (175). The B27.29 mAb recognizes the PDTRPAP epitope in the VNTR region of MUC1(250), and nuclear magnetic resonance analysis has indicated an enhanced binding affinity of B27.29 to MUC1 in the presence of short sugar chains within the VNTR region(251).

It was found that the increases in MUC1 cell-surface polarization in response to galectin-3 and to B27.29 mAb are both associated with increased adhesion of $ACA19^{+}$ cells to HUVECs (Fig 4-17). Furthermore, introduction of galectin-3 or B27.29 mAb to paraformaldehyde-prefixed cells, which would be unable to undergo changes in the MUC1 cell-surface localization, failed to induce cell adhesion to HUVECs compared with the control cells. These results support a direct link between discontinuous cell-surface localization of MUC1 and increased cell adhesion in response to galectin-3 and B27.29 mAb.

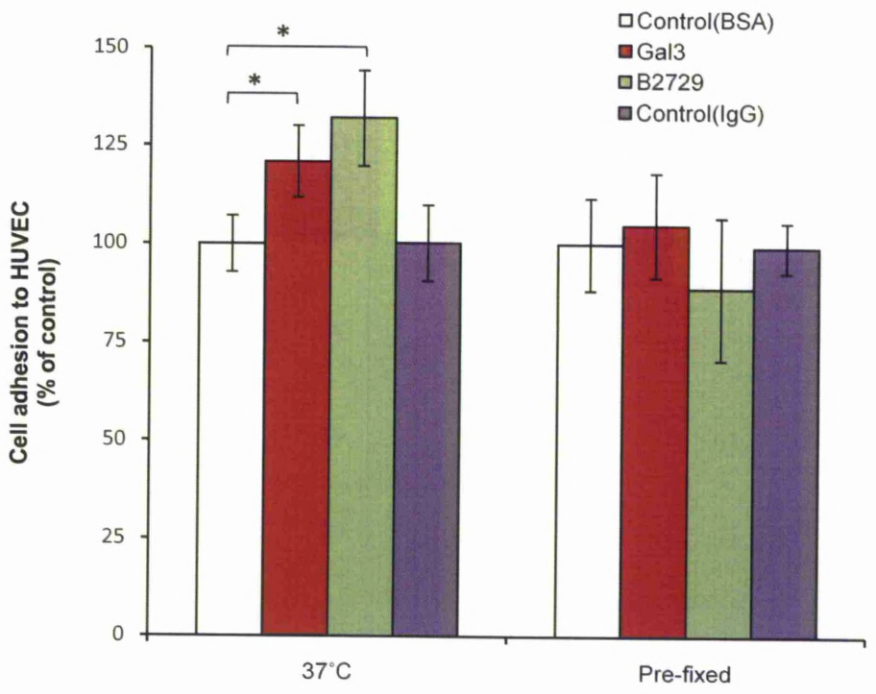

Fig 4-17. Galectin-3 and B27.29 anti-MUC1 mAb both induce increased adhesion to HUVECs of live, but not prefixed, ACA19$^+$ or ACA19$^-$ cells. Live or paraformaldehyde-prefixed ACA19$^{+/-}$ cells were pretreated with 1 μg/mL recombinant galectin-3, B27.29 mAb, bovine serum albumin (*BSA*), or control mouse IgG before adhesion to HUVECs. *Columns,* mean of four independent experiments; *bars,* SE. *, $P < 0.05$(one-way ANOVA).

4.4.5 Aassessment of the cell adhesion molecules involved in galectin-3-mediated cancer-endothelial adhesion.

Since the galectin-3 caused MUC1 localization, the effect of the presence of antibodies against the cell surface adhesion molecules was tested. The presence of 25 μg/mL anti-CD44H mAb (BBA10), which recognizes all CD44 isoforms, caused 26% ($P < 0.05$) inhibition of ACA19$^-$, but not

ACA19^{+}, adhesion to HUVECs, but largely blocked ACA19^{+} cell adhesion induced by galectin-3(Fig 4-18).

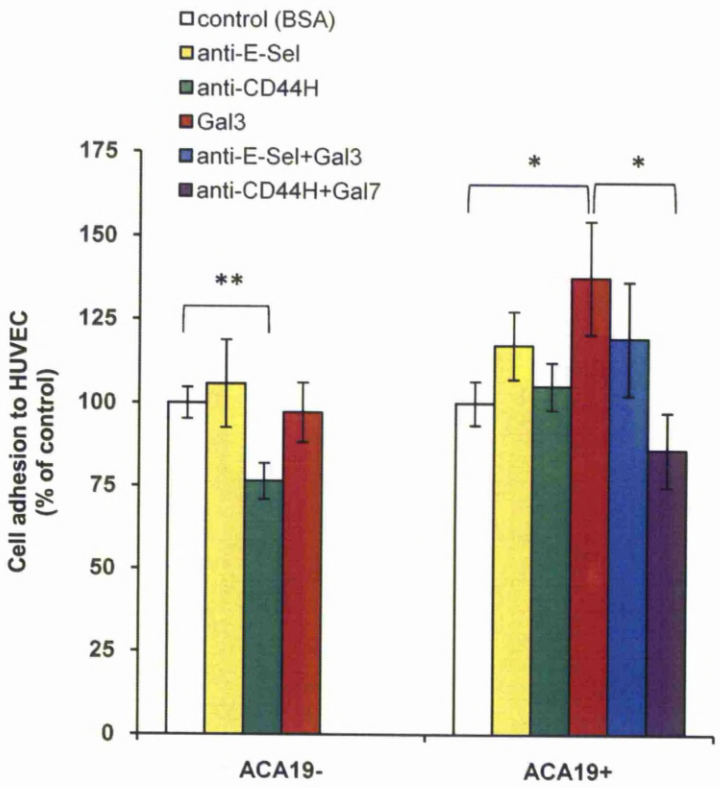

Fig4-18. Involvement of cell-surface CD44 and ligand(s) to endothelial-E-selectin in galectin-3–induced cancer cell-endothelial adhesion. The presence of 25 μg/mL anti-CD44H, but not anti–E-selectin mAb reduces $ACA19^-$ cell adhesion and adhesion of $ACA19^+$ cells induced by 1 μg/mL galectin-3. *Columns,* mean of three independent experiments; *bars,* SE. *, $P < 0.05$; **, $P < 0.01$; ***, $P < 0.001$. (one-way ANOVA followed by Newman-Keuls' test for multiple comparisons)

The presence of 25 μg/mL anti–E-selectin antibody, however, failed to block the adhesion of either $ACA19^-$ or $ACA19^+$ cells and also showed no significant inhibition ($P = 0.47$) of galectin-3–induced $ACA19^+$ adhesion(Fig

4-17). The presence of either anti-CD44H or anti–E-selectin antibody inhibited HT29 cell adhesion to HUVECs(Fig 4-19)

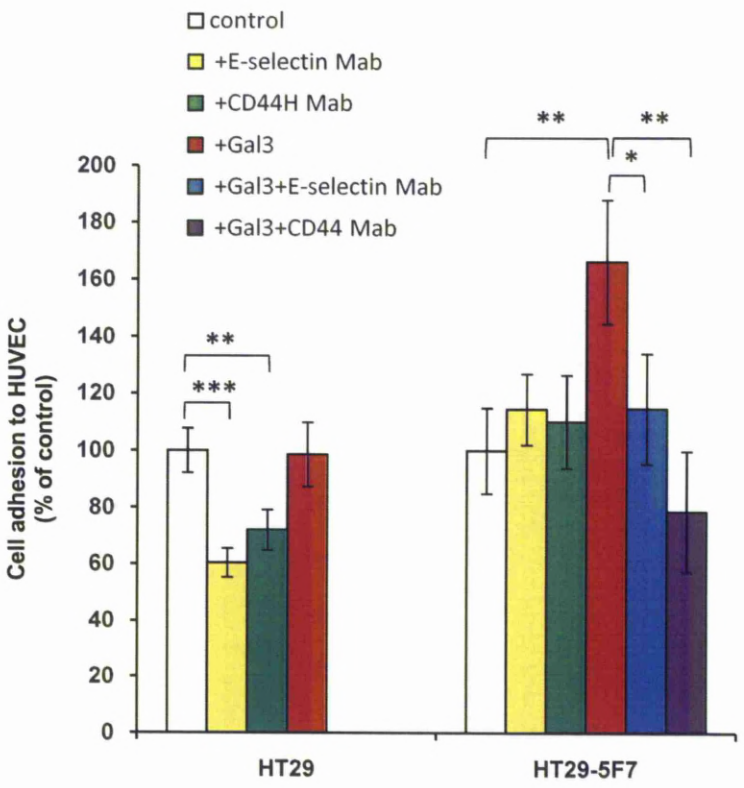

4-19. Involvement of cell-surface CD44 and ligand(s) to endothelial-E-selectin in galectin-3–induced cancer cell-endothelial adhesion. the presence of 25 μg/mL anti-CD44H or anti–E-selectin antibody inhibits HT29 and HT29-5F7 cell adhesion and adhesion of HT29-5F7 cells induced by 1 μg/mL recombinant galectin-3. *Columns,* mean of three independent experiments; *bars,* SE. *, $P < 0.05$; **, $P < 0.01$; ***, $P < 0.001$. (one-way ANOVA followed by Newman-Keuls' test for multiple comparisons)

Neither of these antibodies at this concentration showed significant inhibition of HT29-5F7 cell adhesion to HUVECs, but their presence completely

prevented the increase of HT29-5F7 cell adhesion in response to galectin-3(Fig4-18).

Antibody binding followed by flow cytometry analysis showed similar CD44 cell-surface expression and antibody accessibility between HT29 and HT29-5F7 and between ACA19$^-$ and ACA19$^+$ cells (Fig4-20)

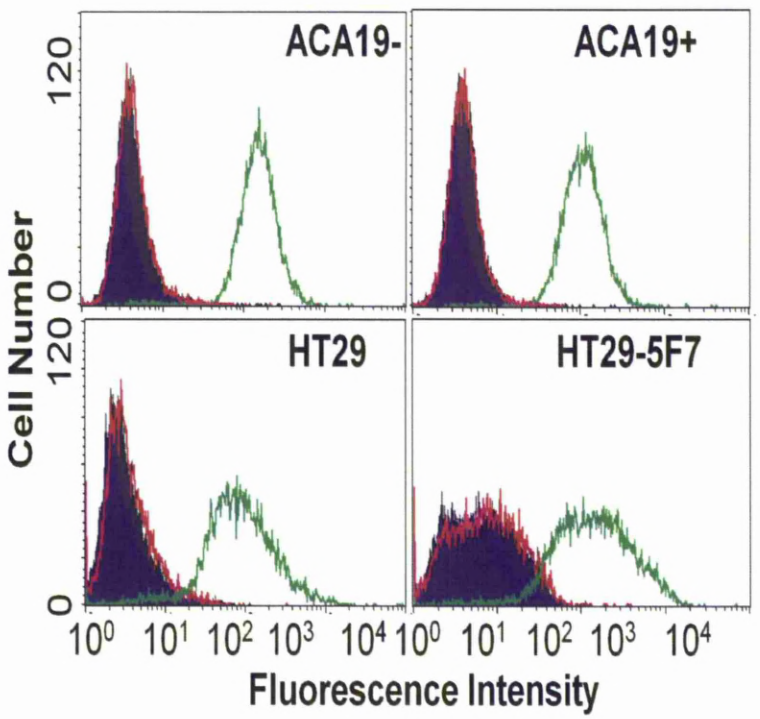

Fig 4-20. Expression of cancer cell-surface CD44 and E-selectin. cell-surface expression of E-selectin and CD44 are similar between HT29 and HT29-5F7 cells and between ACA19$^+$ and ACA19$^-$ cells. *Green,* CD44; *red,* E-selectin; *purple,* isotype control.

Thus, the lack of effect of the anti-CD44H antibody on the adhesion of HT29-5F7 and ACA19$^+$ cells to HUVECs is likely due to the inability of cell-surface

CD44 to gain access to its receptor on HUVECs as a result of functional concealment of cell-surface CD44, for example, by the presence of adjacent MUC1. The inhibition by the anti-CD44H antibody of galectin-3–induced cell adhesion, in which cell-surface CD44 is functionally exposed following MUC1 cell-surface polarization, supports this conclusion. The relatively modest inhibition of the anti-CD44 antibody at 25 μg/mL on ACA19$^-$ adhesion indicates that cell-surface CD44 may represent just one of several cell adhesion molecules involved in melanoma cell-endothelial adhesion.

We found that anti-CD44H antibody pretreatment of HT29 cells, but not of HUVECs, caused a significant inhibition of subsequent HT29 cell adhesion to HUVECs (Fig4-21).

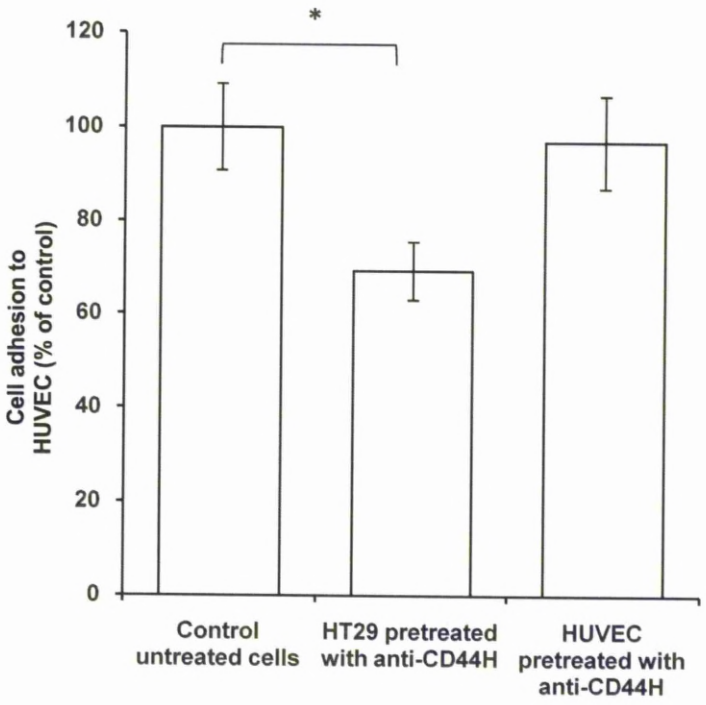

Fig4-21. Involvement of cancer cell-surface CD44 in galectin-3–induced cancer cell-endothelial adhesion. Pretreatment of HT29 cells, but not of HUVECs, with 25 μg/mL anti-CD44H antibody inhibits HT29 cell adhesion to HUVECs. *Columns,* mean of three independent experiments; *bars,* SE. *, $P < 0.05$; **, $P < 0.01$; ***, $P < 0.001$. (one-way ANOVA)

This indicates the involvement of HT29-associated, but not HUVEC-associated, CD44 molecules in HT29-endothelial interaction and in galectin-3–mediated cancer cell-endothelial adhesion. This is in keeping with earlier

reports of a role for cancer-associated CD44 in the initial endothelial adhesion of human prostate, breast, and colon cancer cells(252, 253). Neither HT29/HT29-5F7 nor $ACA19^{-}$/$ACA19^{+}$ cells express E-selectin on their cell surface (Fig4-19). The HT29 adhesion to HUVECs and the HT29-5F7 adhesion to HUVECs induced by galectin-3 were, however, inhibited by the presence of the anti–E-selectin antibody(Fig4-18). This suggests the involvement of endothelial-E-selectin in these cell adhesion events. The different effects of the anti–E-selectin antibody on HT29/HT29-5F7 and $ACA19^{-/+}$ adhesions to HUVECs likely reflect differences in the expression of E-selectin ligands on the surface of HT29 colon and ACA19 melanoma cells.

4.4.6 Assessment of effects of MUC1 and MUC1-galectin-3 interaction on Cancer cell transendothelial invasion

The HUVECs were cultured in an invasion chamber (Fig 4-23) and the monolayer integrity of the cells were measured by transendothelial electric resistance with a vol-ohm meter (Fig4-22) . Good monolayers were seen under microscope to be achieved after 3 days culture of the cells.

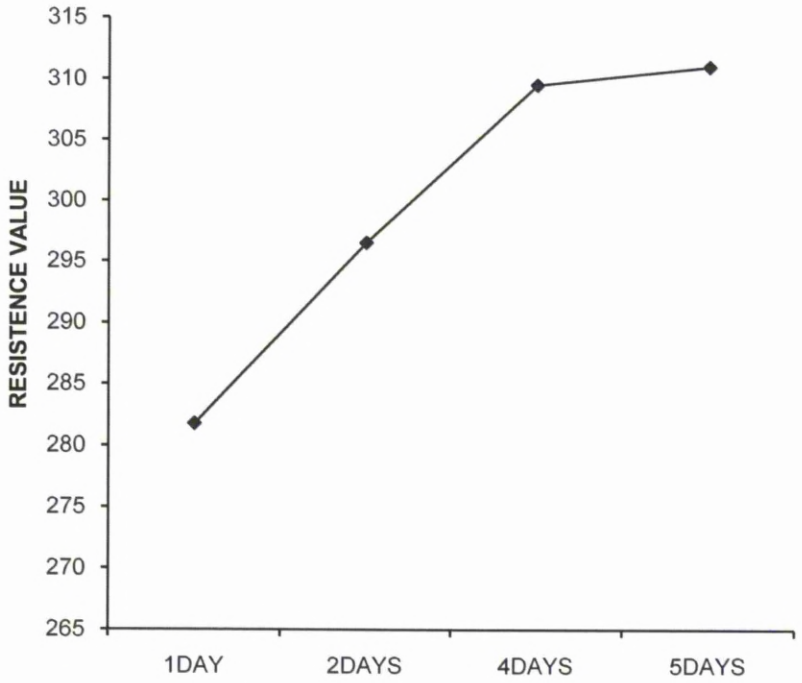

Fig4-22. Transendothelial electric resistance of HUVEC monolayers at different times.

Then, the tumor cells labeled with Dio cell labeling solution were dropped on the HUVECs and incubated for 16 h at 37°C(Fig4-23).

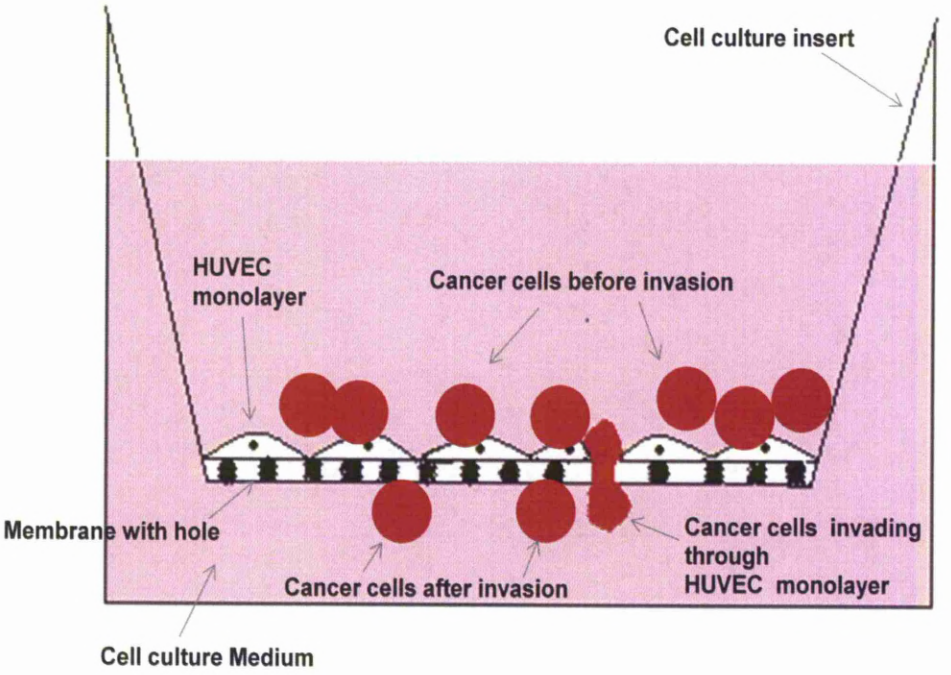

Fig4-23. The set up of the invasion chamber.

$ACA19^+$ cells showed less trans-HUVEC invasion than $ACA19^-$ cells (Fig4-24) after 16 hr culture.

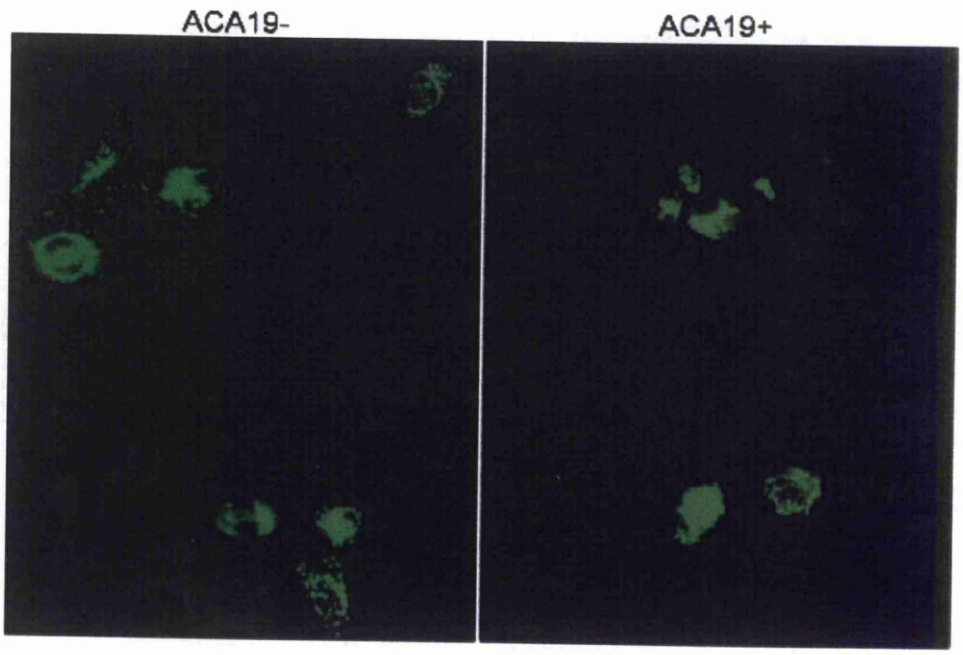

Fig4-24. Effects of MUC1 expression on cancer cell transendothelial invasion. $ACA19^+$ cells showed less trans-HUVEC invasion than $ACA19^-$ cells (Picture of the bottom outside of the Transwell membrane after 16 hr).

ACA19$^-$ showed 46% greater trans-HUVEC invasion than ACA19$^+$ cells(Fig4-25)

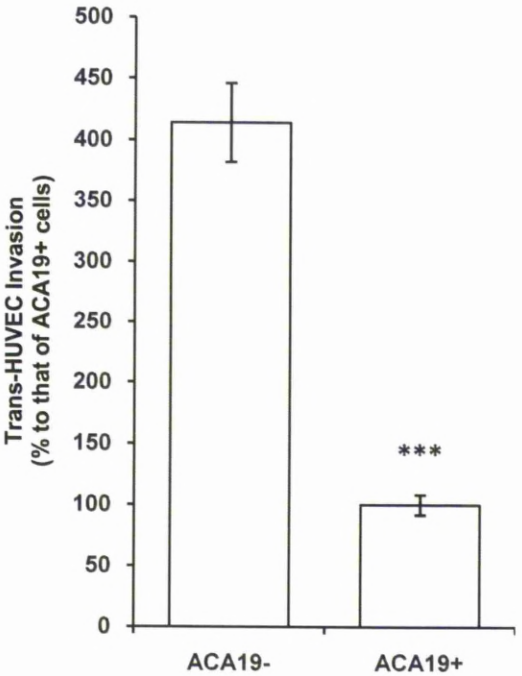

Fig4-25. Effects of MUC1 on cancer cell transendothelial invasion.ACA19$^+$ cells show less trans-HUVEC invasion than ACA19$^-$ cells. *Columns,* mean of triplicate determinations from six independent experiments; *bars,* SE. *, $P < 0.05$; ***, $P < 0.0001$. (one-way ANOVA compare means (bonferroni))

Pretreatment of the cancer cells with galectin-3 (1 μg/mL) before their application to the HUVEC monolayers resulted in 64% increased invasion of $ACA19^+$ cells but not of $ACA19^-$ cells (Fig4-26).

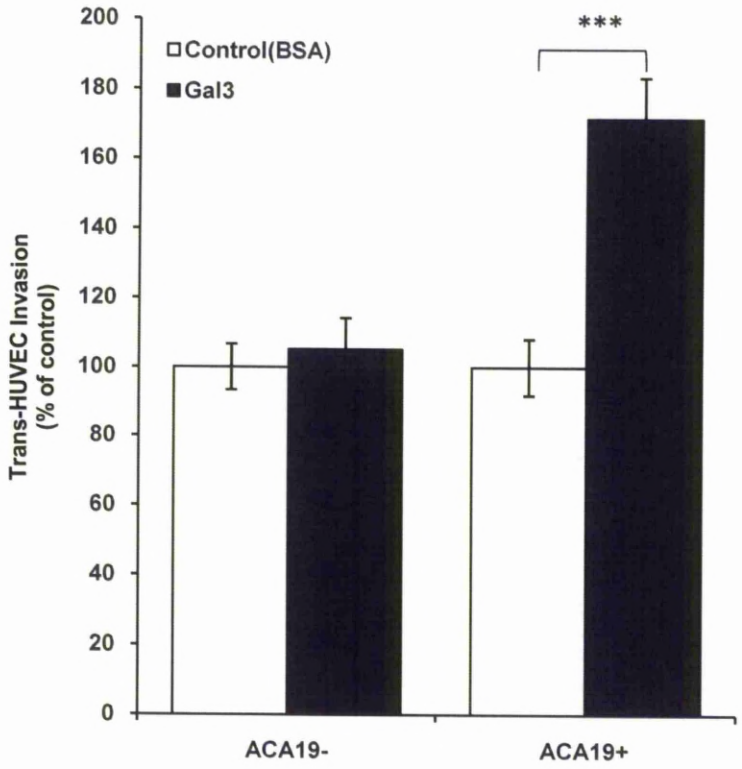

Fig4-26. Effects of MUC1-galectin-3 on cancer cell transendothelial invasion. galectin-3 (1 μg/mL) pretreatment increases $ACA19^+$, but not $ACA19^-$, cell trans-HUVEC invasion. *Columns,* mean of six independent experiments; *bars,* SE. *, $P < 0.05$; ***, $P < 0.0001$. (one-way ANOVA compare means)

This effect of galectin-3 was completely prevented by the presence of lactose(Fig4-27).

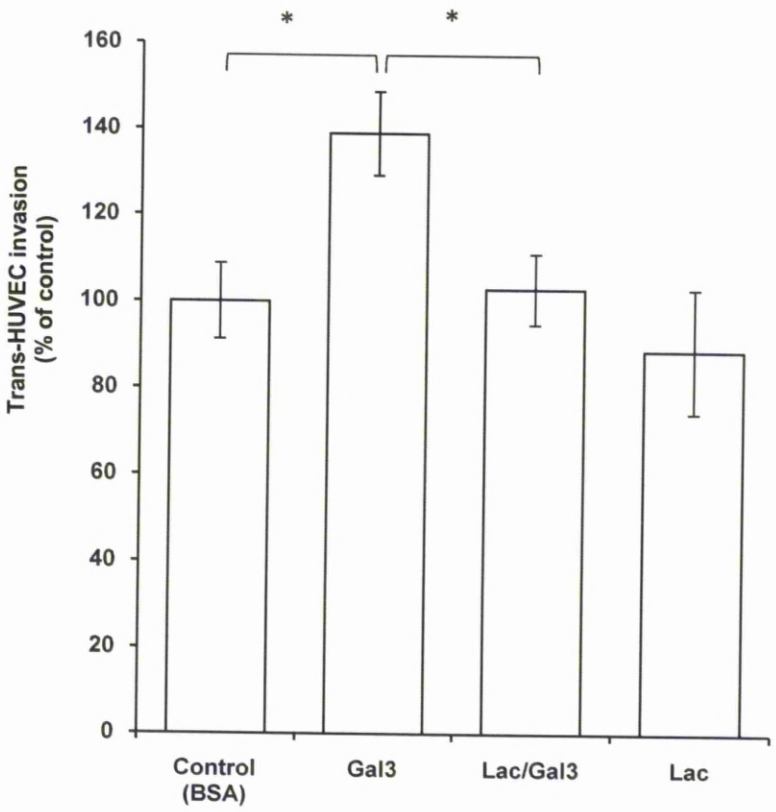

Fig4-27. Lactose inhibition of the galectin-3 induced cancer cell transendothelial invasion. Galectin-3–mediated transendothelial invasion of ACA19+ is inhibited by the presence of (10 μg/mL) lactose. Columns, mean of four independent assessments; bars, SE. *, $P < 0.05$; ***, $P < 0.0001$. (one-way ANOVA followed by Newman-Keuls' test for multiple comparisons).

4.4.7 Effect of MUC1 expression and MUC1-galectin-3 interaction on metastasis in vivo in nude mice see appendix 1.(this part of the study was conducted by Pr Xiuliguo et al in Shangdong University of China)

4.5 Discussion:

This study shows that overexpression of cell-surface MUC1 is associated with reduced cancer cell-endothelial adhesion under static and flow conditions and with decreased cancer cell transendothelial invasion. Work by our collaboratiors subsequently showed (appendix 1) that increased MUC1 expression correlated with and increased survival of athymic nude mice inoculated i.v. with malignant melanoma cells. The interaction of cell-surface MUC1 with circulating galectin-3 at pathologically relevant concentrations reduces the protective effects of MUC1 on cancer cell adhesion, transendothelial invasion, and metastasis. These effects of galectin-3 are mediated by MUC1 cell-surface clustering and the consequent exposure of cell-surface adhesion molecules including CD44 and the ligand(s) for endothelial-E-selectin. Thus, the enhanced molecular interaction between circulating galectin-3 and cancer-associated MUC1 in the bloodstream of cancer patients, occurring as a result of the increased expression of MUC1 by cancer cells, the increased expression of the galectin-3-ligand TF antigen by cancer-associated MUC1, and the increased concentration of circulating galectin-3, all of which are common features in cancer, promotes metastasis.

Cancer cell adhesion to endothelium is a vital step in metastasis and is mediated by a range of adhesion molecules and their ligands, including selectins and integrins expressed on cancer cells and endothelial cells, which in turn are regulated by circulating molecules such as cytokines(247). The inhibitory effect of MUC1 expression and the stimulatory effect of galectin-3-MUC1 interaction on cancer cell-endothelial adhesion shown in this study suggest that MUC1 cell-surface polarization, which leads to uncovering of the smaller adhesion molecules and/or ligands to adhesion molecules, represents an essential first step in the process of cancer cell-endothelial adhesion. Given the variable expression of MUC1 in different cancer cell lines(254), the lack of inhibitory effect of anti-selectin antibodies on cancer cell-endothelial adhesion observed in several previous investigations (255) may be, to a large extent, due to the concealment of the cell-surface selectin ligands by MUC1.

MUC1 can carry sialyl Lewis–related carbohydrate structures that act as ligands for selectins (256). However, an interaction between cancer-associated MUC1 and endothelial-E-selectin will probably not induce tight cell adhesion, a process that is believed to require the involvement of cell-surface integrins as has been well established for leukocyte-endothelial adhesion (257). Tight cancer cell-endothelial adhesion may only occur after MUC1 cell-surface polarization and exposure of integrins and other smaller cell adhesion molecules. Our previous demonstration (248)that MUC1 is absent at the cancer cell-endothelial contact point supports this.

The protective effect of the MUC1 "shield" and the "deprotective" effect of the galectin-3-TF/MUC1 interaction on cancer cell adhesion provide

explanations at the molecular level for several recent clinical and experimental observations related to metastasis, for example, the correlation between increased apical MUC1 cell-surface polarization and increased lymphatic invasion, recurrence rate, and lower overall survival in breast cancer patients (258). The correlation of increased concentrations of circulating anti-TF antibodies, which would inhibit galectin-3–mediated TF/MUC1 interactions, with improved prognosis in gastric cancer(259) is also consistent with our model. The association of MUC1 sialylation with a better prognosis in breast cancer(260) is also in keeping with a reduced galectin-3-TF/MUC1 interaction as a consequence of concealment of TF by sialic acid, thus inhibiting MUC1-galectin-3 interaction(248). The significant extension of animal survival induced by i.p. coinjection of an anti-TF antibody with metastatic 4T1 breast cancer cells(261) could be the consequence of the blockade of the galectin-3-TF/MUC1 interaction.

Because increased occurrence of the TF glycan is one of the commonest glycosylation changes in cancer(97), this study also highlights the functional importance of cancer-associated changes in cellular glycosylation (151, 262)and indicates a potential for glycan profiling in predicting cancer metastasis and prognosis. Furthermore, as the increased concentrations of circulating galectin-3 in cancer patients are probably produced not only by the tumor cells but also by the peritumoral inflammatory and stromal cells(209), this also reinforces the importance of the tumor microenvironment for metastasis(263, 264).

It should be emphasized that this study focuses on the role of circulating galectin-3 on cancer cell adhesion and metastasis. The functional importance of cancer cell-associated galectin-3 in metastasis is well documented (120, 211). For example, antisense suppression of galectin-3 in metastatic LSLiM6 human colon cancer cells before inoculation of the cells into athymic mice results in reduced liver colonization and metastasis(265), whereas suppression of galectin-3 expression by short hairpin RNA in melanoma cells reduces tumor cell invasiveness and capacity to form tube-like structures on collagen, so-called vasculogenic mimicry(266). Similarly, reduction of galectin-3 expression in highly malignant human breast cancer MDA-MB-435 cells leads to loss of serum- and anchorage-independent growth *in vitro* and tumor growth in nude mice(115).

Thus, galectin-3 released into the bloodstream of cancer patients promotes cancer cell hematogenous dissemination by its interaction with TF-expressing MUC1 on cancer cell surface. This provides insight into the molecular regulation of metastasis and has important implications for the development of therapeutic strategies to prevent metastasis.

CHAPTER 5

5. Effects of galectin-3 on cancer cell homotypic aggregation

5.1. Aims

To assess the effect of MUC1 expression and MUC1-galectin-3 interaction at pathologically relevant concentrations on tumour cell homotypic aggregation

5.2. Introduction

Formation of tumour cell aggregation/emboli in the circulation prolongs the survival of tumour cells and allows their physical trapping in the micro-vasculature and contributes to cancer cell hematogenous dissemination (5, 267).

Our discovery that the interaction between cancer-associated MUC1 and galectin-3 increases cancer cell adhesion to endothelium as a consequence of the MUC1 cell surface polarization and exposure of the cell surface adhesion molecules led us to speculate that change of MUC1 cell surface localization in response to galectin-3 binding may expose a range of cell surface adhesion molecules, some of which may be essential to cancer cell homotypic interactions. Thus an increased interaction between circulating galectin-3 and cancer-associated MUC1 in the circulation of cancer patients may promote the formation of cancer cell aggregates/emboli that would prolong the survival of

disseminated tumour cells in the circulation and thus contribute to haematogenous metastatic spread.

We thus investigated the effect of recombinant galectin-3 at pathologically-relevant concentrations on cancer cell homotypic aggregation

5.3. Materials and Methods

Cell aggregation

Subconfluent cells were released from the culture flask with NECDS 2ml/T25 flask (which releases the cells while keeping the cell membrane proteins intact) and were dispersed in serum-free DMEM containing 0.5mg/ml bovine serum albumin (BSA). Two 0.5 ml ($1x10^6$ cells) aliquots of the cell suspension were incubated, separately, with 5µl/ml DiO and DiI Cell Labelling Solution for 30 min at 37°C. The DIO- and DiI-labelled cells were then mixed in the presence or absence of recombinant galectin-3, antibodies or lactose in DMEM in a rotating incubator (Julabo lab GMBH, Seelbach, Gemerney) at 100 rpm/min at 37°C for 1 hr followed by analysis with flow cytometry (Becton-Dickinson FACSVantage SE).

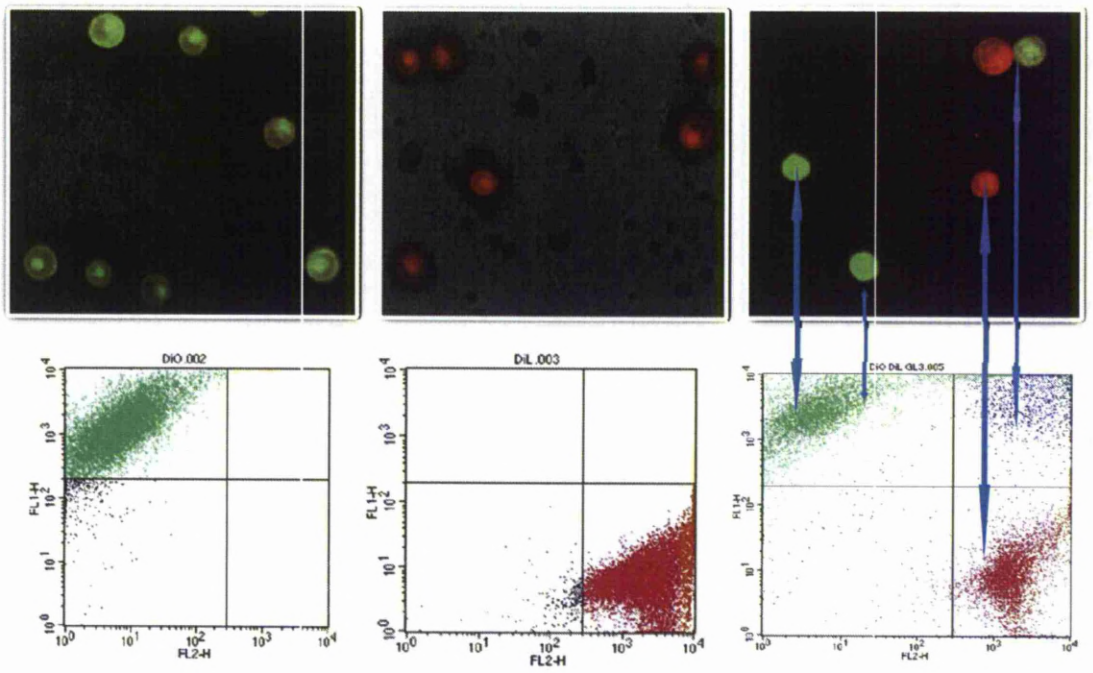

Fig 5-1 Cell aggregation assessed by flowcytometry: The top left(green) and bottom right(red) are cell population labelled with DiO or DiI cell labelling solution separately. The top right in the bivariate correlation plot is the cell population containing cell aggregates that contain both DiO- and DiI-labelled cells and that are defined in this study as cell aggregates.

Cells labelled only with DiI or DiO were used to identify the position of DiO-(upper-left panel) and DiI-(bottom-right panel) labelled cell populations in the bivariate correlation plot and cell populations containing both DiO and DiI fluorescence (top-right panel) in the correlation plot were defined as cell aggregates(Fig5-1).

This method measures cell aggregates containing both DiO- and DiI-labelled cells and does not include cell aggregates formed only by DIO- or DiI-labelled cells. Although this may underestimate the total cell aggregates, it provides a

more accurate assessment of the effect of exogenous galectin-3 by reducing the variations hence the experimental errors due to the differences of initial numbers of cell aggregates in each individual assessment.

Reduction of TF expression by *O*-glycanase treatment

HCA1.7+ cells (10^5 cells) were incubated with 0.02U/ml O-glycanase(which is specific for unsubstituted TF) for 2 hr at 37^0C. The cells were either lysed directly with SDS-sample buffer 100μl for blotting with PNA(1mg/ml, 1:500) following extra-evidin(1:1000) for the purpose testing TF expression, or labelled with DiO and DiI and incubated with recombinant galectin-3 for 1 hr at 37^0C before the cell aggregation assessments.

Electrophoresis and lectin/immunoblotting

SDS-PAGE (4% running gel and 3.5% stack gel for MUC1 blotting and 10% running gel and 4% stack gel for E-Cadherin blotting) electrophoresis and immune/lectin blotting were performed as previously described (248).

MUC1 cell surface localization

Cells released with NECDS were labelled, separately, with DiO and DiI as described above. Two equal cell populations ($5x10^5$) of the labelled cells were mixed in the presence or absence of 1 μg/ml galectin-3, B27.29 antibody or BSA for 1 hr at 37°C. The cell suspensions were applied to poly-lysine coated slides, fixed with 2% paraformaldehyde for 15 min, blocked with 5% normal goat serum for 0.5 hr, probed with B27.29 anti-MUC1 antibody (1:2,000 dilution in 1% goat serum/PBS) and followed by fluorescent-labelled secondary antibody (1:400 dilution in 1% goat serum/PBS). The slides were blind labelled and the number of cells lacking a continuous rim of MUC1 or

the number of small or large aggregates in 500 adjacent cells in randomly selected low power fields was counted using an Olympus B51 fluorescent microscope with 20x objective. To show MUC1 on the cell membrane, cell aggregates labelled with Dio(green colour) and Dil(red colour) were selected, and the localization of MUC1 (blue colour)on the cell membrane was recorded using 25X high power field.

E-Cadherin cell surface distribution

Cells released with NECDS were labelled, separately, with DiO and DiI as described above. Two equal cell populations ($5x10^5$) of the labelled cells were mixed in the presence or absence of 1 μg/ml galectin-3 or BSA for 1 hr at 37°C. The cell suspensions were applied to poly-lysine coated slides, fixed with 2% paraformaldehyde for 15 min, blocked with 5% normal goat serum for 0.5 hr, probed with anti-E-Cadherin antibody (1:400 dilution in 1% goat serum/PBS) and followed by fluorescent-labelled secondary antibody (1:400 dilution in 1% goat serum/PBS). The slides were examined using an Olympus B51 fluorescent microscope with 20x objective. The cell aggregate labelled with Dio(green colour) and Dil(red colour) was selected, the localization of E-Cadherin(blue colour)on the cell membrane was photographed using a high power 25X objective.

E-Cadherin cell surface expression

Cells released with NECDS were fixed in 2% paraformaldehyde for 15 min, blocked with 5% normal goat serum for 0.5 hr, incubated with anti-E-Cadherin antibody (1:1000 dilution with 1% goat serum in PBS) or isotype control immunoglobulin and followed with fluorescent-conjugated secondary

antibodies (1:400 dilution in 1% goat serum/PBS). The cell surface expression of E-Cadherin was analysed by flow cytometry.

siRNA E-Cadherin transfection

HT29-5F7 cells were treated with commercially available siRNA constructs (100nM) against E-Cadherin or scrambled control non-targeting siRNA (siCONTROL non-targeting siRNA, Dhamacon) for 48 hr at 37°C. The cells were either lysed and the expressions of E-Cadherin was analysed by immunoblotting or the cells were labelled with DiO and DiI followed by the assessment of cell aggregation in the presence or absence of 1 μg/ml galectin-3 as described above.

Cell viability in single and aggregated cells under anchorage-independent condition

96 or 24 well plates were coated twice with 200 μl/well (96-well plates) or 5 ml/well (6-well plates) of 10mg/ml poly-2-hydroxyethyl methacrylate (poly-HEMA, Sigma) in 95% ethanol over night at room temperature. After washing, the cells were treated with 1μg/ml recombinant galectin-3 or BSA under suspension culture in serum-free medium for various times at 37°C. The cells in suspension were collected and passed three times through a 40-μm cell strainer (BD Biosciences). The viability of the cells that did and did not pass through the strainers was measured by the CellTiter-Glo® Luminescent Cell Viability Assay (Promega).

Cell anoikis in single and aggregated cells under anchorage-independent condition

For the measurement of cellular anoikis, after separation of the cells by cell strainers as above, the cells were resuspended in FITC-Annexin-V 1×binding buffer and the apoptotic cells were measured FITC-Annexin-V apoptosis detection kit (Cambridge Biosciences, Cambridge, UK) by flow cytometry as the manufacture's instructions.

Statistical analysis

The statistical analyses were performed using the unpaired *t* test for single comparison, one-way analysis of variance (ANOVA) followed by Newman and Keuls test for multiple comparisons or Chi-Square test (StatsDirect for Windows, StatsDirect Ltd; Sale, UK) where appropriate. Differences were considered significant when $p<0.05$.

5.4. Results

5.4.1 Effect of MUC1 expression and MUC1-galectin-3 interaction on cancer cell homotypic aggregation

To test the effect of MUC1 expression on cancer cell homotypic aggregation, we first compared the adhesive properties of human colon cancer HT29 and HT29-5F7 cells.

It was found that spontaneous aggregation of HT29 human colon cancer cells was 2.8-fold greater than that of HT29-5F7 cells (Fig 5-2and Fig5-3),

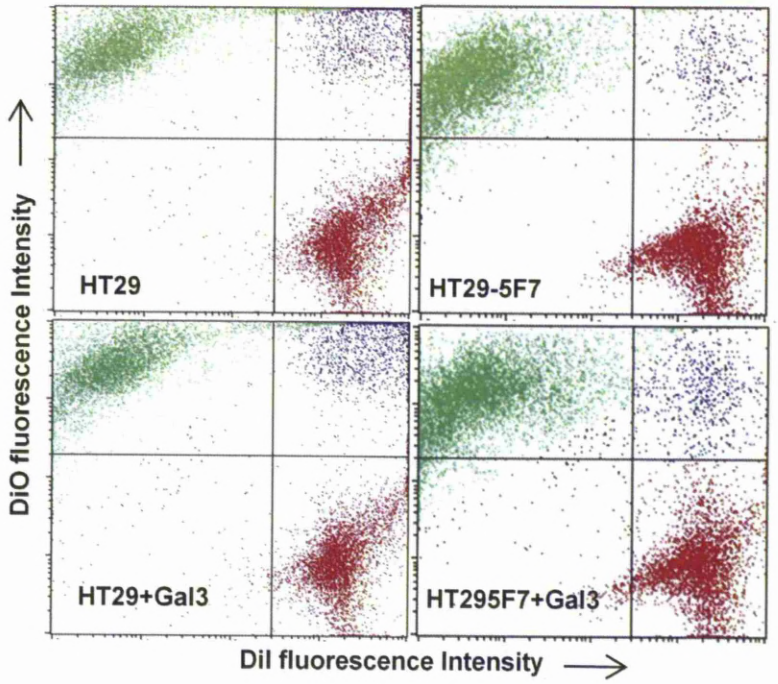

Fig 5-2 MUC1 expression prevents and MUC1-galectin-3 interaction promotes homotypic aggregation of human colon cancer cells: Representative flow cytometry plots from the aggregation assessment of human colon cancer HT29-5F7 and HT29 MUC1 cells in the presence or absence of 1μg/ml recombinant galectin-3. The top right in the bivariate correlation plot are the cell population containing both DiO- and DiI-labelled cells that are defined in this study as cell aggregates.

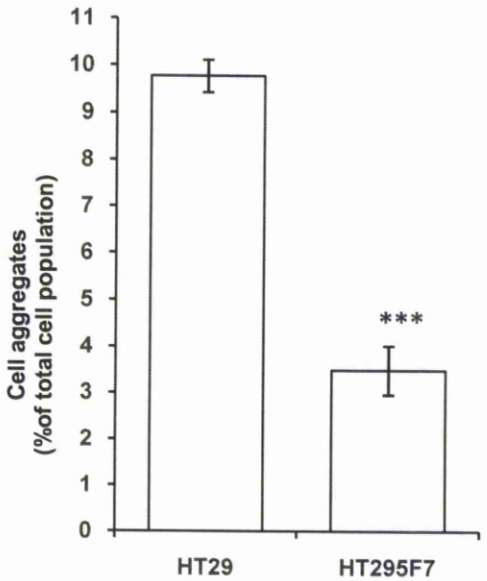

Fig5-3. MUC1 expression prevents homotypic aggregation of human colon cancer cells. The more strongly MUC1-expressing HT29-5F7 cells show less spontaneous cell aggregation than the parental HT29 cells. Data are expressed as mean ± SEM of triplicate determinations from three independent experiments. (one-way ANOVA compare means)

Pre-treatment of HT29-5F7 cells with recombinant galectin-3 at various pathologically-relevant circulating galectin-3 concentrations in the sera of colorectal cancer patients (209) resulted in a dose-dependent increase of HT29-5F7 but not HT29 cell aggregation (Fog 5-4).

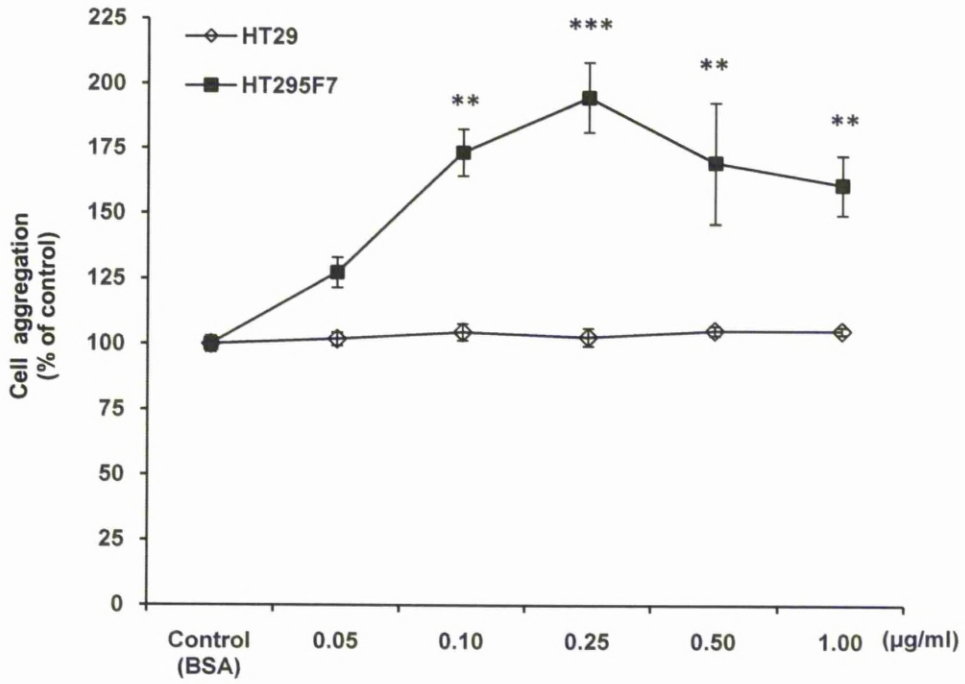

Fig5-4.MUC1-galectin-3 interaction promotes homotypic aggregation of human colon cancer cells. Recombinant galectin-3 treatment induces a dose-dependent increase of HT29-5F7 but not HT29 cell aggregation. Data are expressed as mean ± SEM of triplicate determinations from four independent experiments. **p<0.01, ***p<0.001. (one-way ANOVA followed by Newman-Keuls' test for multiple comparisons)

At 1.0µg/ml, galectin-3 caused 69% increased aggregation [169.2±24.7 (mean ± SEM), p<0.01] of HT29-5F7 but not HT29 cells (91.4±5.9, p=0.2) (Fig 5-2 and Fig5-5)

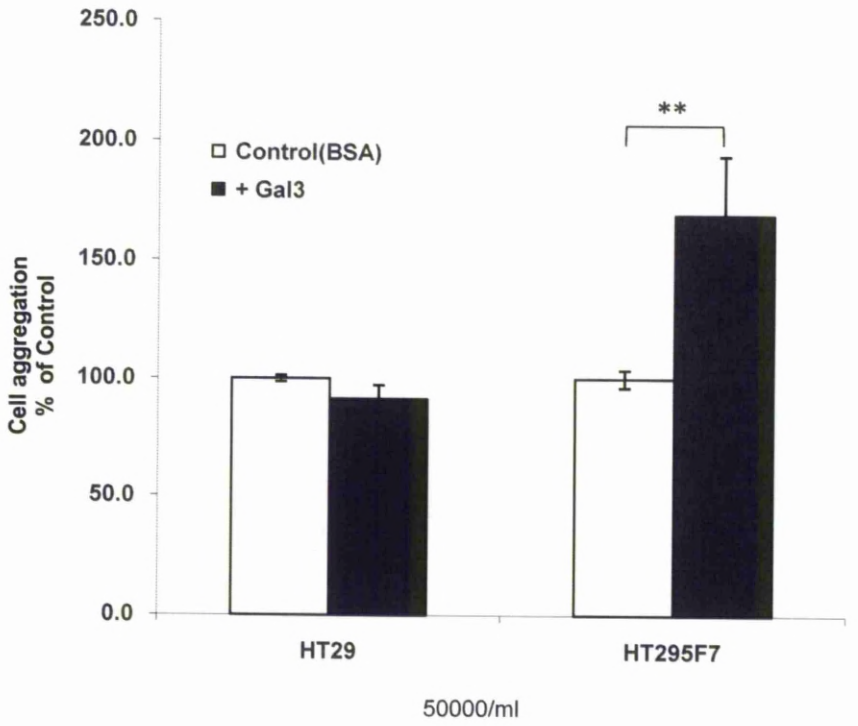

Fig5-5. MUC1 expression prevents and MUC1-galectin-3 interaction promotes homotypic aggregation of human colon cancer cells. Recombinant galectin-3 at 1.0μg/ml induces increase of HT29-5F7 but not HT29 cell aggregation. Data are expressed as mean ± SEM of triplicate determinations from three independent experiments. **p<0.01, ***p<0.001. (one-way ANOVA compare means (bonferroni))

In the flow cytometry plots, the cell population shown at the upper-right quadrant (blue)representative the aggregation cells. The aggregation population of HCA1.7+(Fig 5-6 upper right picture) was significantly less

comparing to HCA1.7- (Fig 5-6 upper left picture) without treatment after 1 hr incubation at 37^0C.

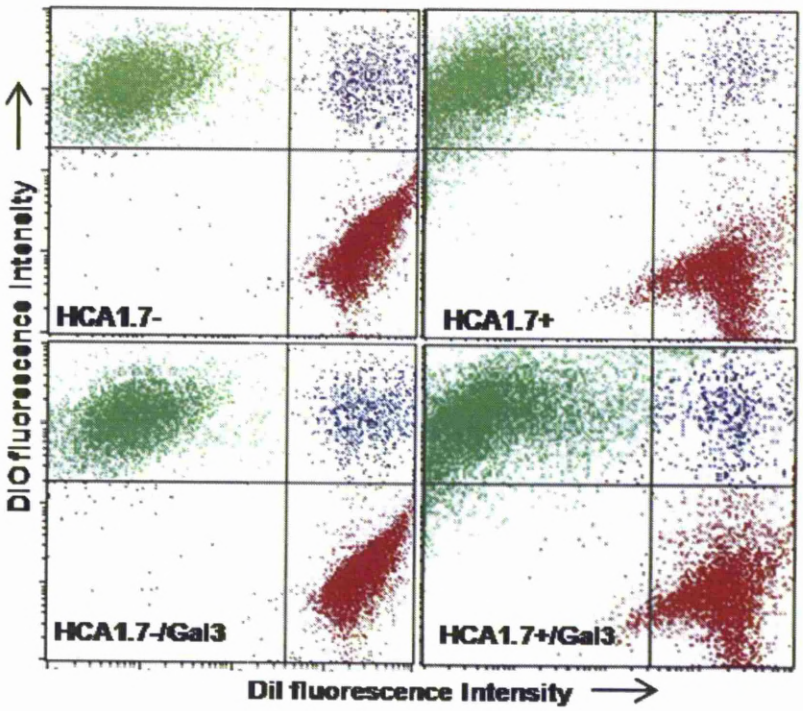

Fig5-6. MUC1 expression prevents and MUC1-galectin-3 interaction promotes homotypic aggregation of MUC1 positively but not negatively transfected human breast epithelial cells. Representative flow cytometry plots from the aggregation assessment of MUC1 positive- transfectants (HCA1.7+) and negative-revertants (HCA1.7-) of HBL-100 human breast epithelial cells in the presence or absence or 1μg/ml recombinant galectin-3.

Spontaneous aggregation of HBL-100 human breast epithelial cells with MUC1-positive transfection (HCA1.7+) (5.1 ± 0.4%) was significantly less comparing to MUC-1-negative transfection (HCA1.7-) (8.0 ± 0.3, $p<0.001$) (Fig 5-6 and Fig5-7).

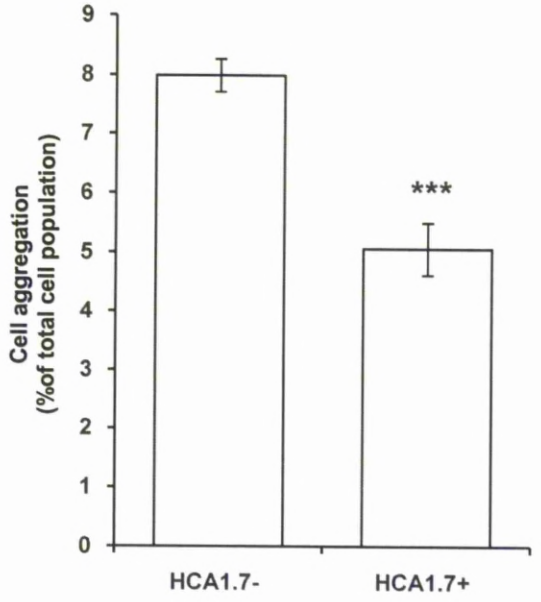

Fig 5-7. MUC1 expression prevents homotypic aggregation of MUC1 positively but not negatively transfected human breast epithelial cells. HCA1.7+ cells show less spontaneous cell-cell aggregation than HCA1.7- cells. Data are expressed as mean ± SEM of triplicate determinations from four independent experiments. Data are expressed as mean ± SEM of triplicate determinations from two independent experiments. *p<0.05, **p<0.01, ***p<0.001. (one-way ANOVA compare means (bonferroni))

Pre-treatment of the cells with galectin-3, 1.0μg/ml, caused 36% increased aggregation of HCA1.7+ (136.6±7.0, p<0.01) but not HCA1.7- cells (94.2±4.2, p=0.2) (Fig 5-8).

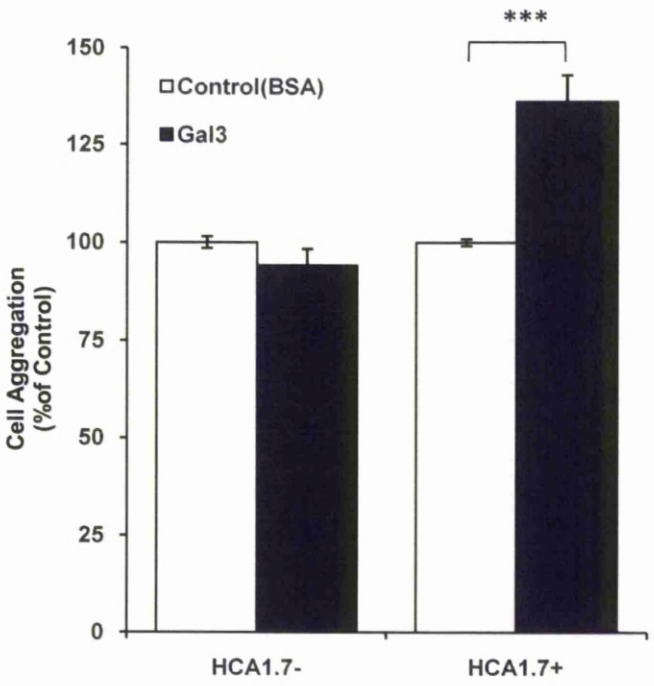

Fig5-8. MUC1-galectin-3 interaction promotes homotypic aggregation of MUC1 positively but not negatively transfected human breast epithelial cells. Galectin-3 (1μg/ml) increases HCA1.7+ but not HCA1.7- cell aggregation. Data are expressed as mean ± SEM of triplicate determinations from four independent experiments. Data are expressed as mean ± SEM of triplicate determinations from two independent experiments. *$p<0.05$, **$p<0.01$, ***$p<0.001$. (one-way ANOVA compare means (bonferroni))

The effect of galectin-3 on HCA1.7+ cell aggregation was dose-dependent (Fig 5-9) and was prevented by the presence of 10 μM lactose (Fig 5-10).

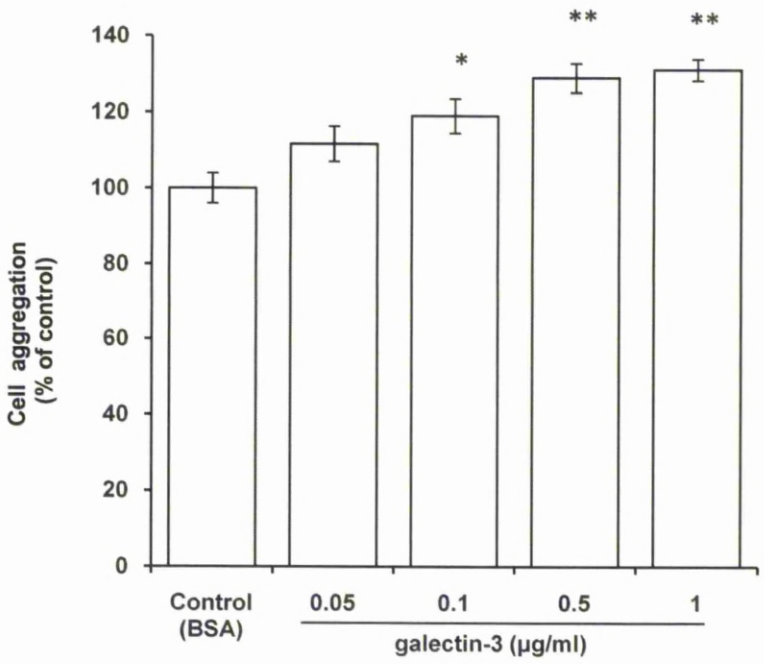

Fig5-9. MUC1-galectin-3 interaction promotes homotypic aggregation of MUC1 positively transfected human breast epithelial cells. Galectin-3 induces dose-dependent aggregation of HCA1.7+ cells. Data are expressed as mean ± SEM of triplicate determinations from two independent experiments. *p<0.05, **p<0.01, ***p<0.001. (one-way ANOVA followed by Newman-Keuls' test for multiple comparisons)

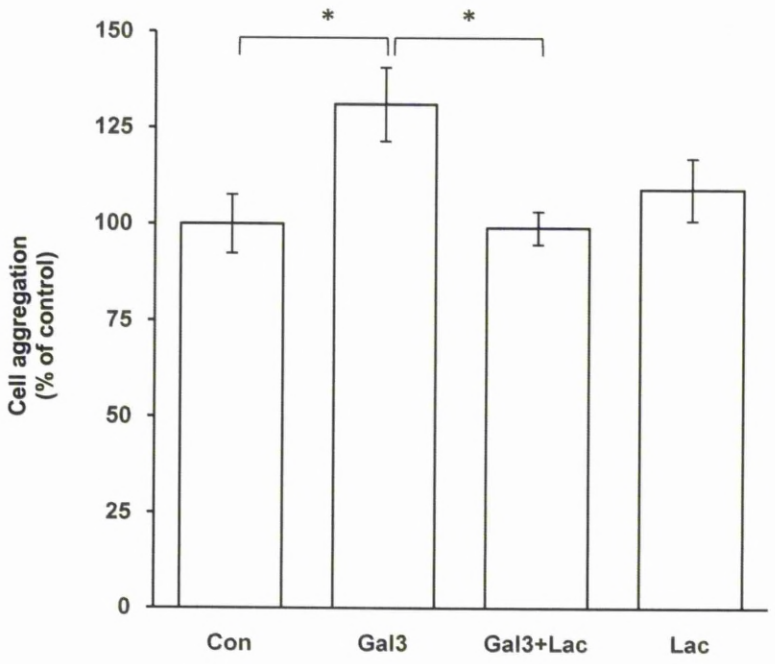

Fig5-10. The effect of MUC1-galectin-3 interaction promotes homotypic aggregation of MUC1 positively transfected human breast epithelial cells blocked by lactose. The presence of lactose (10μM) blocks the increase of HCA1.7+ cell aggregation induced by 1μg/ml galectin-3. Data are expressed as mean ± SEM of triplicate determinations from two independent experiments. *p<0.05, **p<0.01, ***p<0.001. (Two-way ANOVA followed by Newman-Keuls' test for multiple comparisons)

5.4.2 Effect of TF expression in galectin-3-mediated cell aggregation

Pre-treatment of HCA1.7+ cells with *streptococcal O*-glycanase, that specifically removes the unsubstituted TF disaccharide, caused a 58%

reduction of TF expression on MUC1 as assessed by the TF-binding PNA blotting (Fig5-11) and attenuated the effect of galectin-3 on cell aggregation (Fig5-12).

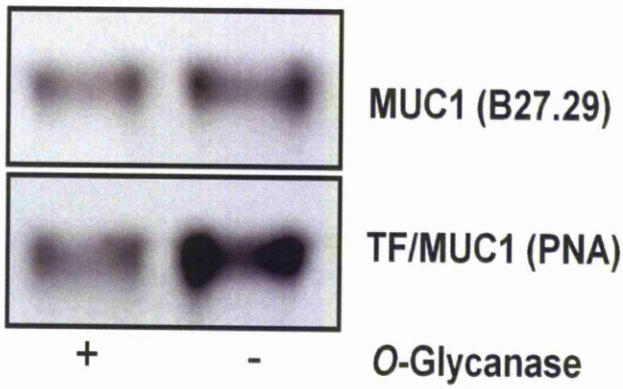

Fig5-11. Effects of O-glycanase treatment on TFexpression. PNA blot show reduction of TF on MUC1 by *O*-Glycanase treatment of HCA1.7+ cells. Data are selected from two independent experiments.

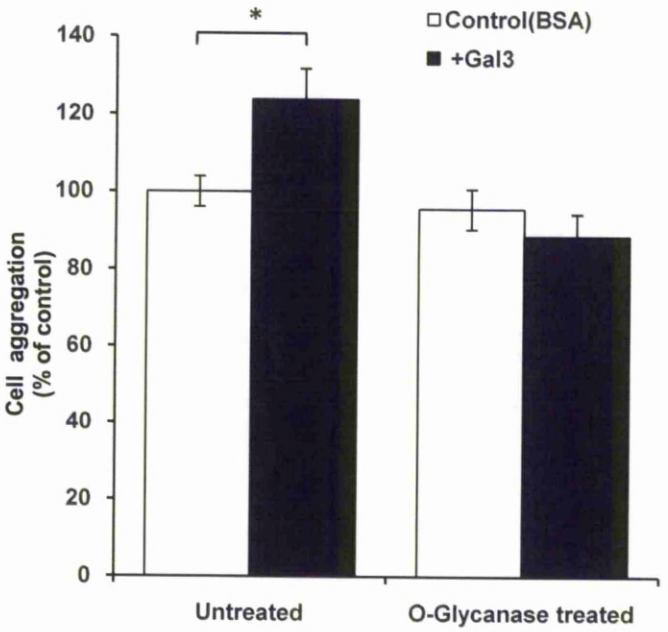

Fig5-12. Effects of TF expression on galectin-3-mediated cell aggregation. Reduction of TF-expression by *O*-glycanase treatment abolishes the effect of galectin-3 (1μg/ml) on HCA1.7+ cell aggregation. Data are expressed as mean ± SEM of triplicate determinations from two independent experiments. * $p<0.05$. (one-way ANOVA followed by Newman-Keuls' test for multiple comparisons)

5.4.3 Effects on B27.29 anti-MUC1 mab on MUC1 cell surface polarization and on cell-cell aggregation

Our previous study demonstrated that B27.29 anti-MUC1 mAb, directed against the PDTRPAP epitope (250) within the VNTR region of MUC1,

induces MUC1 cell surface polarization and increases human melanoma cell adhesion to endothelium(268). The B27.29 anti-MUC1 mAb is known to have an enhanced binding affinity to MUC1 when short sugar chains within the VNTR region are present(251). It was found here that introduction of B27.29 mAb also caused a dose-dependent increase of HCA1.7+ cell aggregation (Fig5-13),

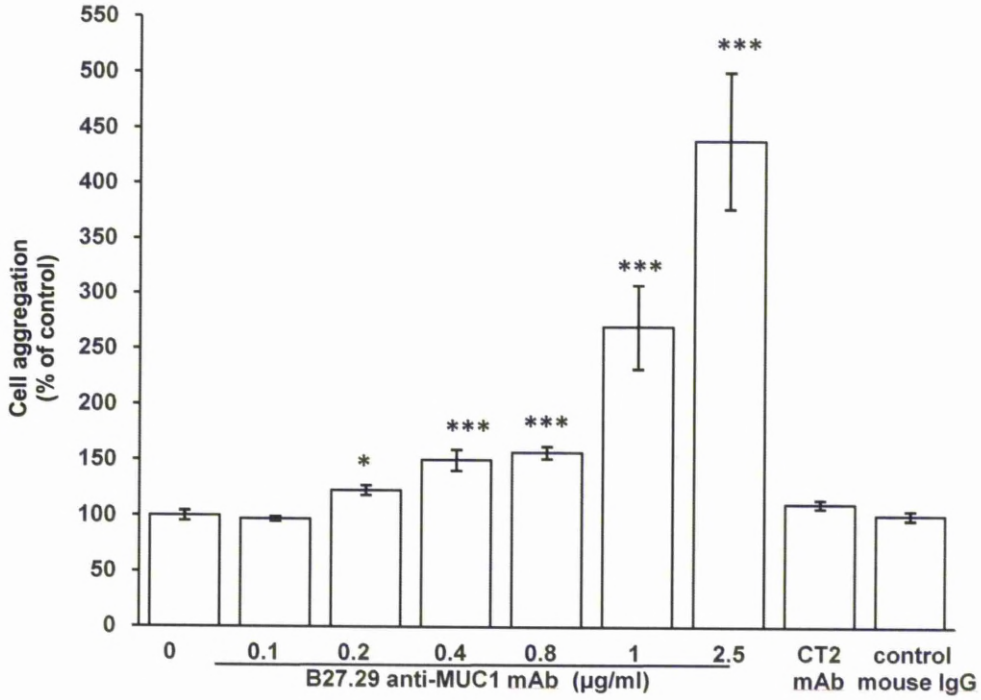

Fig5-13. Galectin-3 and B27.29 anti-MUC1 mAb both induce increase of cell aggregation. B27.29 mAb induces dose-dependent increase of HCA1.7+ cell aggregation. HCA1.7+ cell aggregation was measured after pre-incubation of the cells with or without various concentrations of B27.29, or 1µg/ml control mouse immunoglublin or CT-2 anti-MUC1 antibody. Data are expressed as mean ± SEM of triplicate determinations from three independent experiments. *p<0.05,**p<0.01, ***p<0.001. (one-way ANOVA followed by Newman-Keuls' test for multiple comparisons)

regardless of the presence or absence of recombinant galectin-3 (Fig5-14).

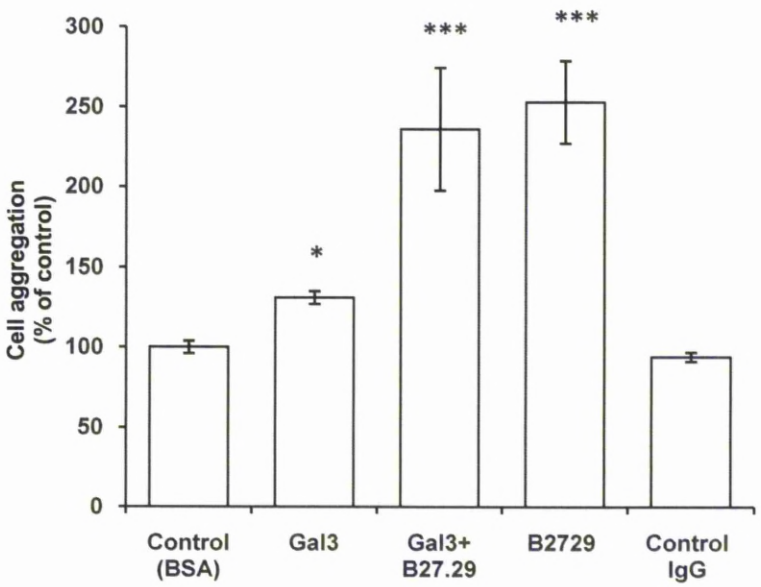

Fig5-14. Galectin-3 and B27.29 anti-MUC1 mAb both induce increase of cell aggregation. B27.29 mAb increases HCA1.7+ cell aggregation regardless of the presence or absence of recombinant galectin-3. HCA1.7+ cell aggregation was measured after pre-incubation of the cells with or without 1μg/ml recombinant galectin-3 in the presence or absence of 1 μg/ml B27.29, BSA or control immunoglublin. Data are expressed mean ± SE of triplicate determinations from three independent experiments. *p<0.05,**p<0.01, ***p<0.001. (Two-way ANOVA followed by Newman-Keuls' test for multiple comparisons)

When the cell aggregates were further analysed, it was found that B27.29 mAb not only induced more cell aggregates but also larger aggregates than recombinant galectin-3 (Table5-1). Because cells may aggregate before treated, in order to make sure the cell aggregates really happen after cells

treated, We defined the aggregates as small or larger one according to the number of cells from different cell groups labelled with different florescence colour rather than total numbers of the whole aggregates. The larger clusters mean no less than two red as well as two green florescence labelling cells. The small clusters contain either one red with one or more green cells or one green cell with one or more red cells. There were 8.8%(including 4.6% of large and 4.2% small) spontaneous HCA1.7+ cell clusters in the 500 consecutive events counted on the slides, when cultured in suspension for 1 hour at 37°C , whilst 16.2 % (include 8.6% of large and 7.6% small, P=0.0004, Chi-square test) or 29.4% (include 18.4% of large and 11% small, P<0.0001) more HCA1.7+ cells clusters, respectively, than control BSA-treated cells clusters after incubation with 1μg/ml recombinant galectin-3 or B27.29 mAb for 1 hr at 37°C.

Table 5-1. Characteristics of the HCA1.7+ cell aggregates in response to galectin-3 and B27.29 anti-MUC1 antibody

	Groups* % of total events (events)	Control % (n)	r-Gal3 % (n)	B27.29 % (n)
	Total	8.8(44)	16.2(81)	29.4(147)
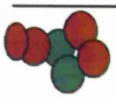	Large clusters (no less than two green as well as two red cells)	4.6 (23)	8.6 (43)	18.4 (92)
	Small clusters (one green with one or more red, or one red with one or more green cells)	4.2 (21)	7.6 (38)	11.0 (55)

*500 events per group were counted

MUC1 is distributed around the whole cell surface in single HCA1.7+ cells without treatment with galectin-3 or b27.29 mab (Picture 5-1 left, blue) After treatment with galectin-3 or b27.29 anti-MUC1 antibody, many cells showed loss of continuous MUC1 cell surface localization .We used MUC1 discontinuity as the criterion for quantifying MUC1 clustering (Picture 5-1 right) in our experiment.

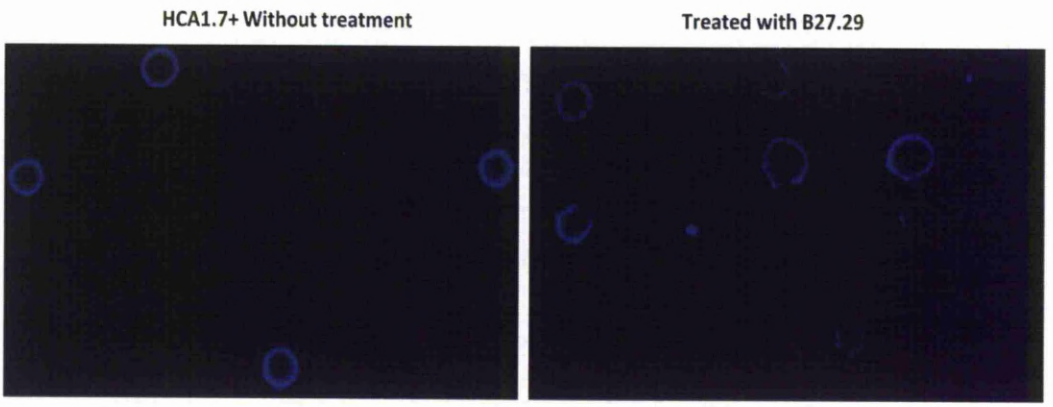

Picture 5-1. MUC1 homogenous distribution on cell surface in single HCA1.7+ cells(Left) showing discontinuity (Right) after addition of MUC1 anti-body(B27.29) implying cell surface clustering.

Fourteen percent (71/500) HCA1.7+ cells showed spontaneous clustering of MUC1 on the cell surface, when cultured in suspension for 1 hour at 37°C whilst 57% (112/500, $P<0.01$, Chi-square test) or 93% (133/500, $P<0.01$) more HCA1.7+ cells, respectively, than control BSA-treated cells demonstrated MUC1 cell surface clustering after incubation with 1μg/ml recombinant galectin-3 or B27.29 mAb for 1 hr at 37°C. Introduction of galectin-3 or mAb B27.29 to the cells at 4°C or to paraformaldehyde pre-fixed cells had no effect on MUC1 localization(Table 5-2) and no significant effect on cell aggregation(Fig 5-15) compared with the control BSA-treated cells,

which suggest liquidity of the cell membrane is important in HCA1.7+ cells MUC1 clustering induced by galectin-3 and B27.29.

Table 5-2. Galectin-3 and B27.29 anti-MUC1 antibody induce discontinuous MUC1 cell surface polarization of HCA1.7+

	37^0C	4^0C	Pre-fixed
	%(n)	%(n)	%(n)
Control (BSA)	14(71)	7(37)	3(16)
Galectin-3 (1μg/ml)	22(112)**	8(38)	3(14)
B27.29 (1μg/ml)	27(133)**	10(49)	3(15)

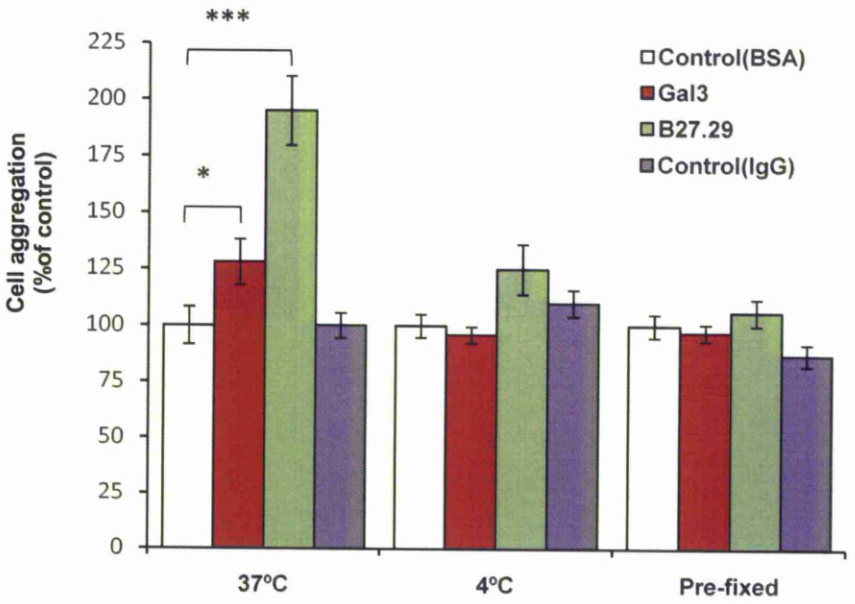

Fig 5-15. Galectin-3 and B27.29 anti-MUC1 mAb both induce increase of cell aggregation. Galectin-3 or B27.29 mAb at 1 μg/ml fails to induce HCA1.7+ cell aggregation at 4^0C or to paraformaldehyde-prefixed cells. Data are expressed as mean ± SE of triplicate determinations from four independent experiments. *p<0.05,**p<0.01, ***p<0.001. (one-way ANOVA followed by Newman-Keuls' test for multiple comparisons)

These results indicate a direct link between discontinuous cell surface localization of MUC1 and the increased cell aggregation in response to galectin-3 and B27.29 mAb. In keeping with this, MUC1 was observed to be absent at the cell-cell contact point within the cell aggregates in the cells treated either with galectin-3 or mAb B27.29 (Picture 5-2). The left picture show cell aggregates composed of cells labelled with Dio(green) or Dil(Red) florescence, the middle picture show the MUC1 distribution (blue florescence)

absent between the cell-cell contact point, the right picture show combination results of the left and the middle picture.

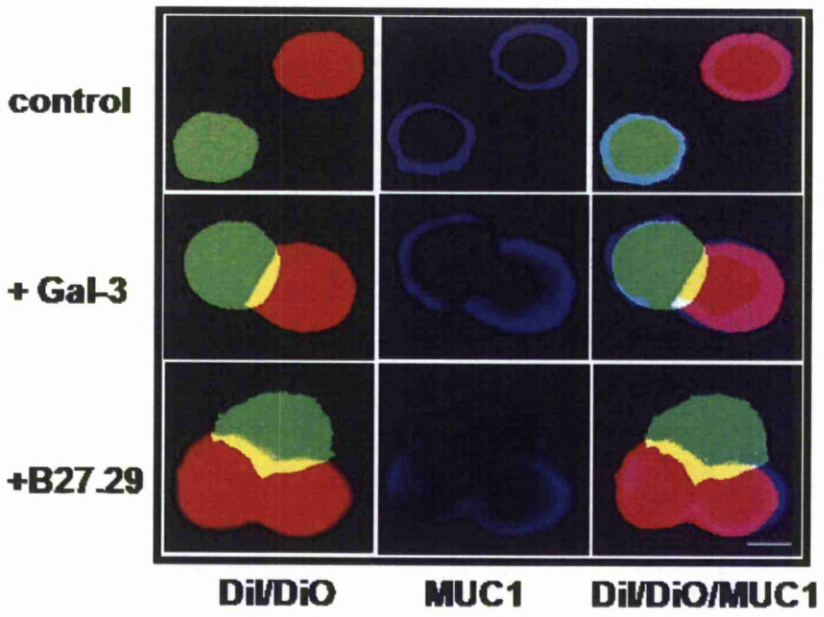

Picture 5-2. Absence of MUC1 at the cell-cell contact point within the cell aggregates of HCA1.7+ . HCA1.7+ cells pre-labelled with Dio (green) and Dil (red) were incubated with or without 1μg/ml recombinant galectin-3 or B27.29 antibody at 370C before the cells were fixed and the MUC1 localization(blue) was determined by immunohistochemistry. Representative images of the MUC1 localization in single and cell aggregates are shown. Bar =10 μm.

Thus, polarization of cell surface MUC1 in response to galectin-3 binding exposes the smaller cell surface adhesion molecules that increases homotypic cell aggregation.

5.4.4 Investigation of the cell surface adhesion molecules in galectin-3-mediated cell aggregation.

E-Cadherin is a member of the Cadherin family that are largely responsible for epithelial cell-cell interaction in the maintenance of epithelial phenotype(269) and has previously been shown to be an important adhesion molecule in epithelial cell-cell interactions (174, 180). It was found here that the presence of the MAB1838 anti-E-Cadherin mAb at 2.5 to 20 μg/ml caused a dose-dependent reduction of the spontaneous aggregation of HT29 but not HT29-5F7 cells (Fig 5-16).

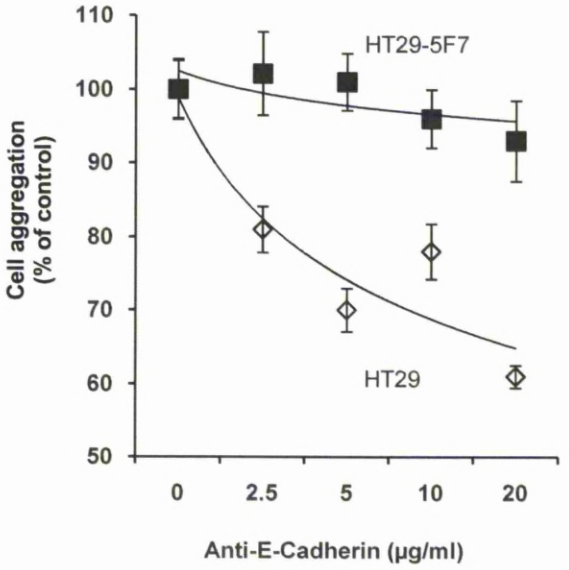

Fig 5-16. Involvement of cell surface E-cadherin in galectin-3-induced cell aggregation. The presence of anti-E-Cadherin antibody (at concentrations between 2.5 and 20µg/ml) reduces spontaneous cell aggregation of HT29 but has little effect on that of HT29-5F7 cells. Data are expressed as mean ± SE of triplicate determinations from three independent experiments. (one-way ANOVA followed by Newman-Keuls' test for multiple comparisons)

However, the presence of this antibody at 20µg/ml inhibited HT29-5F7 cell aggregation induced by galectin-3 (Fig 5-17). This suggests the involvement of the cell surface E-Cadherin in spontaneous aggregation of HT29 and in galectin-3-mediated HT29-5F7 cell aggregation.

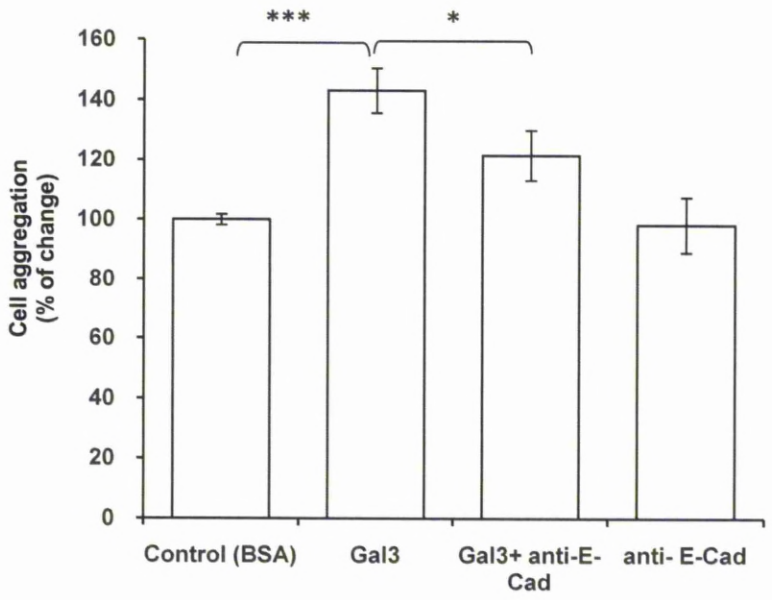

Fig 5-17. Involvement of cell surface E-cadherin in galectin-3-induced cell aggregation. Anti-E-Cadherin antibody at 20μg/ml prevents HT29-5F7 cell aggregation-induced by (1 μg/ml) galectin-3. Data are expressed as mean ± SE of triplicate determinations from three independent experiments. (Two-way ANOVA followed by Newman-Keuls' test for multiple comparisons)

This is supported by the discovery that suppression of E-Cadherin expression by siRNA resulted significant reduction of spontaneous HT29-5F7 cell aggregation and also prevented the increase of cell aggregation in response to galectin-3 (Fig5-18, Fig5-19). We found that treatment of HT29-5F7 cells for 2 or 3 days with E-Cadherin siRNA, but not with the control non-targeting siRNA, caused 74% or 82% reduction of E-Cadherin expression comparing with normal control separately(Fig 5-18).

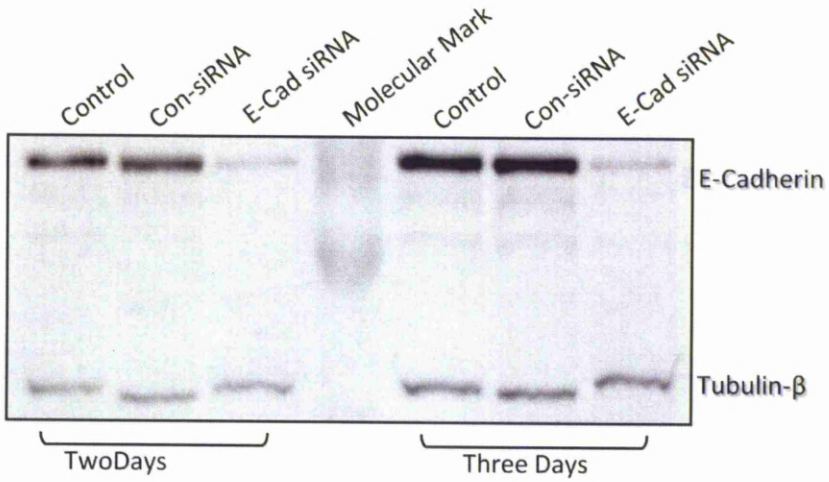

Fig 5-18. SiRNA E-Cadherin knock-down. HT29-5F7 cells were treated with E-Cadherin siRNA or control non-targeting siRNA for two or three days before the cellular E-Cadherin expression was determined by E-Cadherin immunoblotting.

Galectin-3 at 1 μg/ml does not induce HT29-5F7 cell aggregation after E-Cadherin siRNA knock-down after 72 hours though Galectin-3 increase 28±6% ($p=0.0016$) HT295F7 cell aggregation of Con-siRNA groups (Fig 5-19).

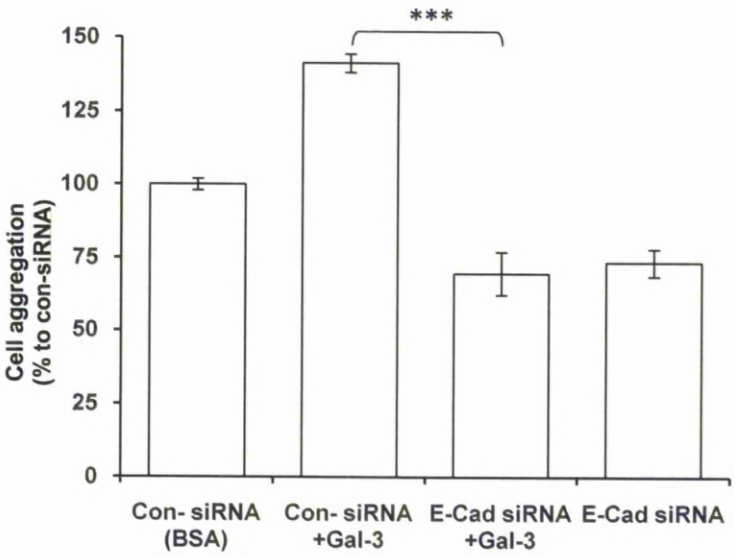

Fig 5-19. Involvement of cell surface E-cadherin in galectin-3-induced cell aggregation. SiRNA suppression of E-Cadherin prevents galectin-3-mediated HT29-5F7 cell aggregation. Data are expressed as mean ±SEM of triplicate determinations from three independent experiments. (one-way ANOVA followed by Newman-Keuls' test for multiple comparisons)

We found that E-Cadherin shows strong localization at the cell-cell contacts in the cell aggregates (Picture5-3). The left two pictures show the single or aggregate cells labelled with Dio(Green) /Dil (Red). The right two pictures show that E-Cadherin(blue) distribute around the single cells(upper-right picture) and accumulate between the cell-cell contact points of the cell aggregates(Lower-right picture).

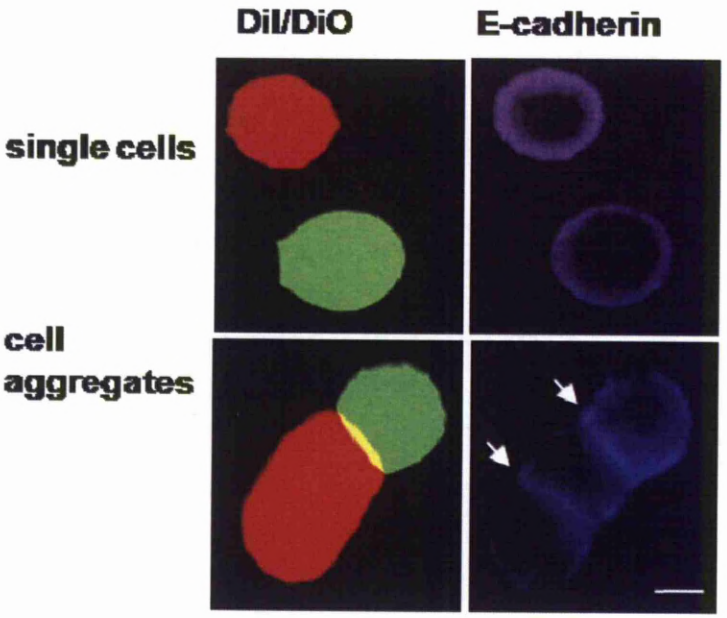

Picture 5-3. Involvement of cell surface E-cadherin in galectin-3-induced cell aggregation. E-Cadherin localization in single and cell aggregates. HT29-5F cells pre-treated with or without 1 μg/ml galectin-3 were analysed for E-Cadherin expression by anti-E-Cadherin immunohistochemistry. E-Cadherin shows strong localization at the cell-cell contacts in the cell aggregates (arrowed). Bar = 10μm.

These findings together imply a critical role of the cell surface E-Cadherin in galectin-3-mediated cell-cell aggregation.

Using anti-E-Cadherin antibody(1μg/ml) 1:400 against E-Cadherin on cell surface of the fixed HT29 and HT295F7 cells followed by a secondary antibody FITC anti-mouse IgG 1:400 incubation, E-Cadherin expression on the cell surface was tested by FACS. We found that HT29 and HT29-5F7 cells have similar levels of cell surface E-Cadherin and similar anti-E-Cadherin antibody accessibility (Fig 5-20).

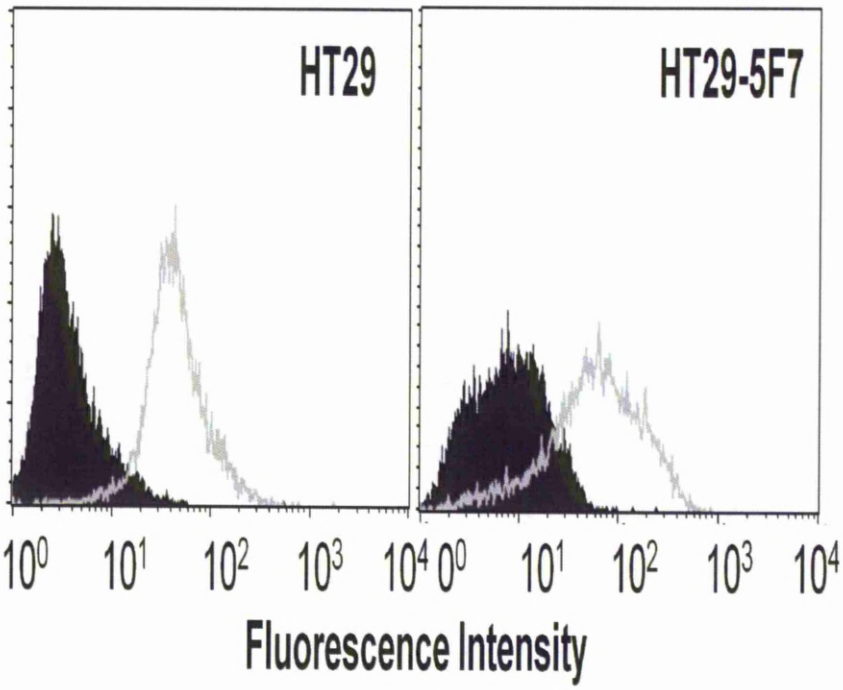

Fig 5-20. Expression of cell surface E-cadherin on HT29 and HT295F7 cells. HT29 and HT29-5F7 cells show similar E-Cadherin cell surface expressions assessed by flow cytometry. Open histogram: E-Cadherin; shaded histogram: immunoglobulin isotype control.

Thus, the inability of the anti-E-Cadherin antibody to prevent HT29-5F7 cell aggregation is most likely due to a functional "concealment" of the cell surface E-Cadherin in HT29-5F7 cells, e.g by the presence of adjacent MUC1. The blockade by the anti-E-Cadherin antibody of galectin-3-mediated HT29-5F7 cell aggregation (Fig 5-17) is in support of this. The fact that the blockade of anti-E-Cadherin antibody on galectin-3-mediated aggregation is only partial implies the likely involvement of other cell surface adhesion molecules, which, like E-Cadherin, may be exposed following MUC1 polarization in response to galectin-3 binding.

5.4.5 Effect of Galectin-3-induced cell aggregation on Anoikis.

As cell aggregation has previously been shown to enhance the ability of cells to avoid Anoikis initiation, we assessed the effect of galectin-3-induced cell aggregation on Anoikis. After 3 days culture under suspension conditions, nearly 4-fold more cells in the cell aggregates obtained from the galectin-3-treated cells were viable than those obtained from the BSA-treated controls (Fig 5-21).

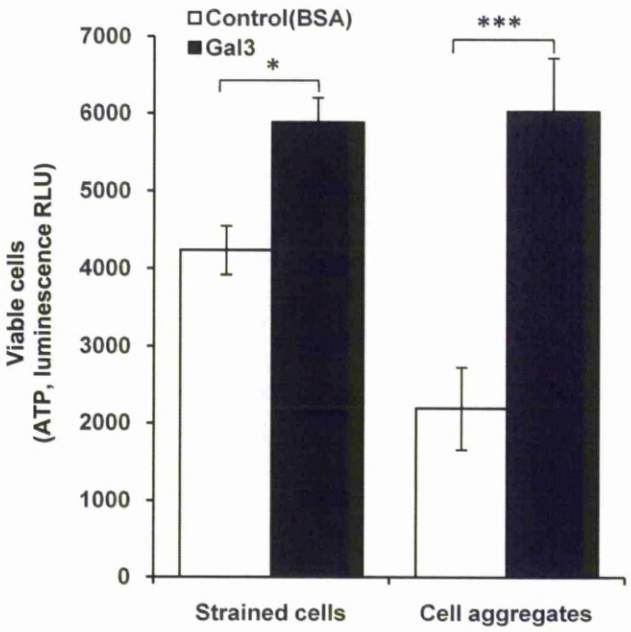

Fig 5-21. Galectin-3-induced cell aggregation enhances survival of cells from escaping Anoikis. Galectin-3-induced cell aggregation increases survival of HT29-5F7 cells under anchorage-independent conditions. HT29-5F7 cells treated with or without 1 μg/ml galectin-3 or BSA by culture of the cells in suspension for 3 days at 37^0C. After separation of the cells using a cell 'strainers', the viability of cells was assessed as described in the Methods section. The data are presented as mean ± SEM of triplicate determinations from two independent experiments.

This indicates that the increase of cell aggregation in response to galectin-3 greatly enhances the survival of the cells under anchorage-independent conditions. A modest 36% increase of the cell viability was also observed in the cell population that passed through the 40μm cell strainers (referred to as

"single" cells in Fig5-21) from the galectin-3-treated cells compared with the BSA-treated controls. As HT29-5F7 cells are 15~ 20 μ m in diameter, this small increase is highly likely due to the inclusion of small cell aggregates, e.g. those formed by 2 to 3 cells, in this cell population. Many small cell aggregates were indeed observed in this population by microscopy (Picture 5-4).

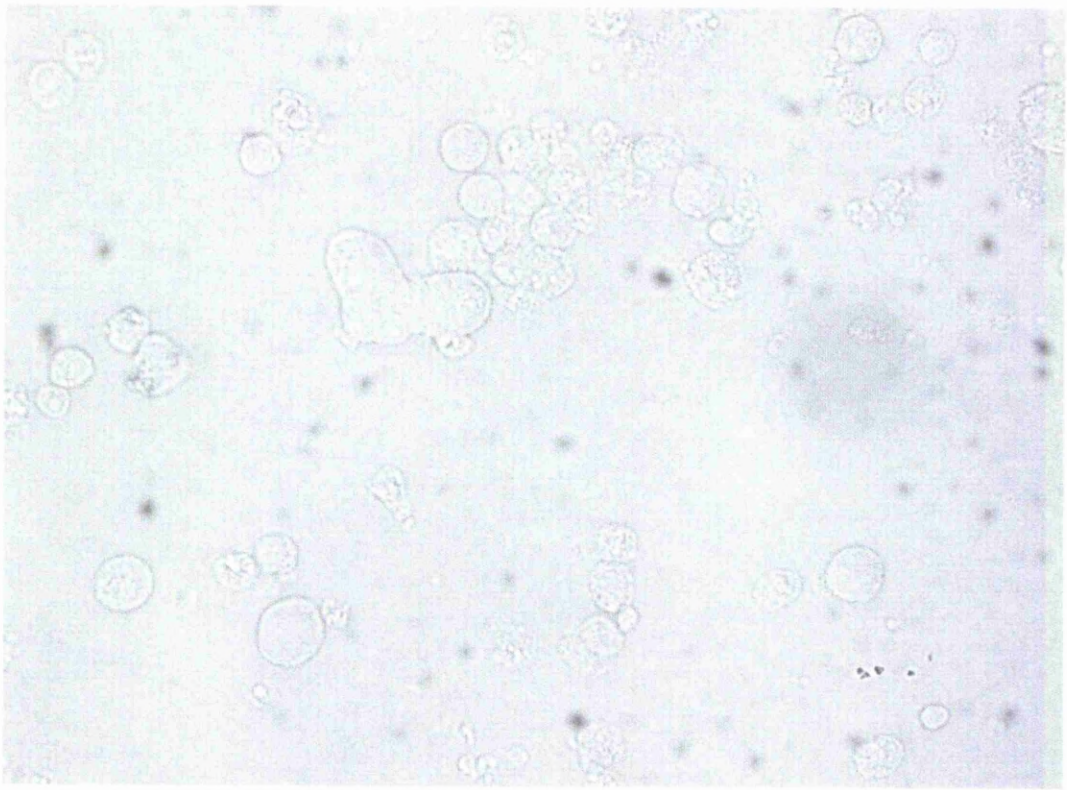

Picture5-4. Images of the strained cell population after straining.

Assessments of Anoikis showed no significant difference between the two strained cell populations obtained from galectin-3-treated and BSA-treated controls within 48 hr culture of the cells under suspension conditions (Fig5-22,5-24).

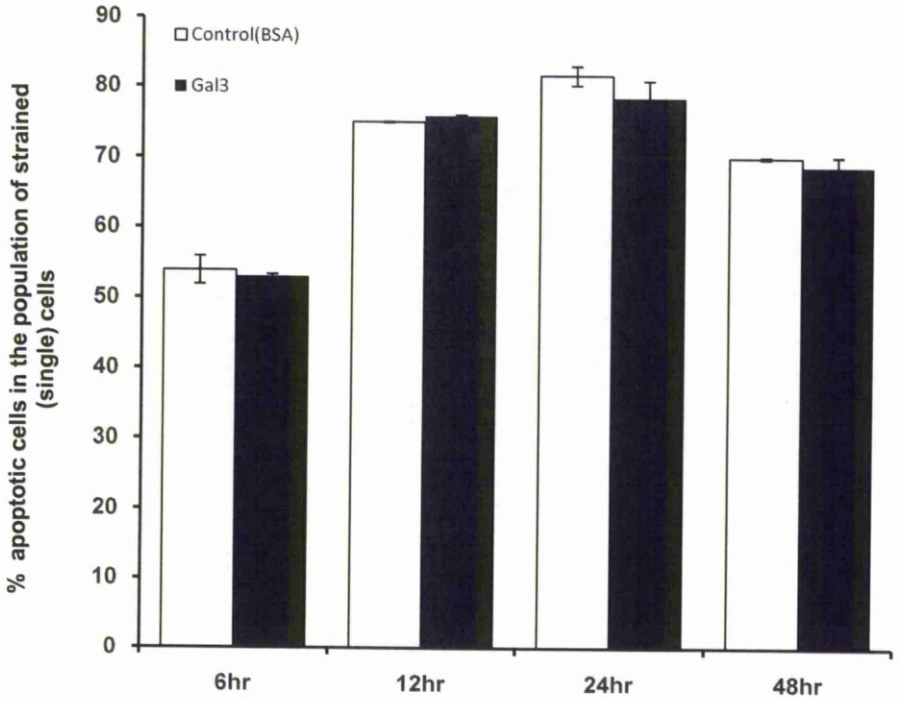

Fig5-22. Galectin-3-induced cell aggregation enhances survival of cells from escaping Anoikis. No significant difference between the two strained cell populations obtained from galectin-3-treated and BSA-treated controls within 48 hr culture of the cells under suspension conditions. (one-way ANOVA followed by Newman-Keuls' test for multiple comparisons)

However, significantly fewer cells in the population of cell aggregates obtained from the galectin-3-treated cells were undergoing Anoikis than from the BSA treated controls (Fig 5-23,Fig5-24).

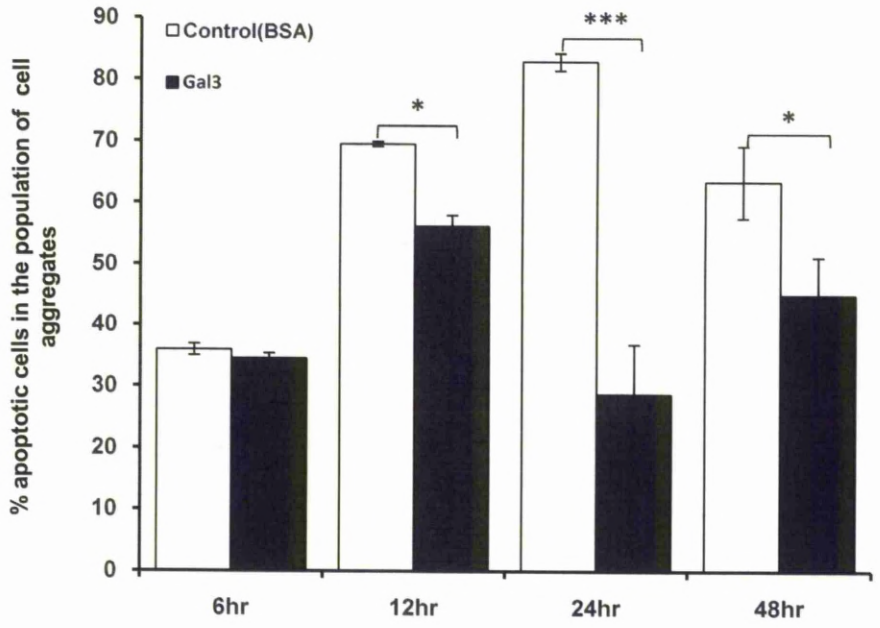

Fig 5-23. Galectin-3-induced cell aggregation enhances survival of cells by escaping Anoikis. Galectin-3-induced cell aggregation is associated with increased resistance of the cells to Anoikis. The data are presented as mean ± SEM of triplicate determinations from two independent experiments. (one-way ANOVA followed by Newman-Keuls' test for multiple comparisons)

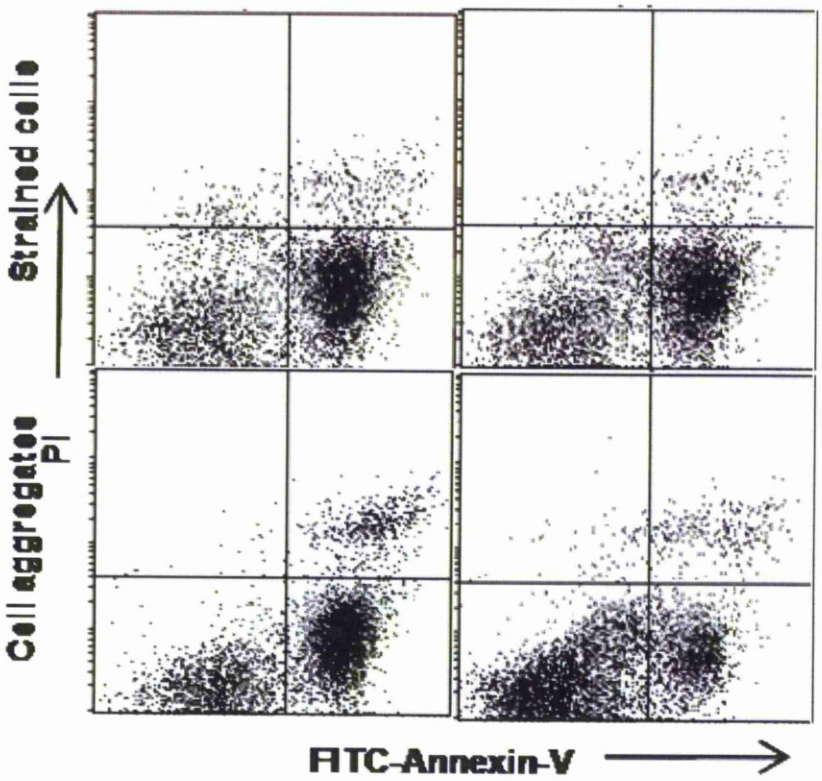

Fig 5-24. Galectin-3-induced cell aggregation enhances survival of cells from escaping Anoikis. Representative flow cytometry plots from the anoikis assessments of HT29-5F7 cells cultured in suspension in the presence of 1 μg/ml galectin-3 or BSA for 2 days at 370C. Annexin-V positive and PI negative (early apoptotic, at the bottom right in the bivariate correlation plot) and Annexin-V positive and PI positive (late apoptotic, at the top right in the correlation plot) cells are considered as apoptotic cells.

A 20% (70.0±0.4% *vs* 56.1±1.8%, p=0.02), 65% (82.8±1.4% *vs* 28.7±8.0%, p=0.0001) and 29% 63.4±5.9% *vs* 44.9±6.2%, p=0.02) reduction of Anoikis were seen in the cell aggregates obtained from the galectin-3 treated than from the BSA-treated control cells after 12, 24 and 48 hr, respectively (Fig 5-23).

This indicates that the galectin-3-induced cell aggregates is associated with resistance of the cells to Anoikis initiation.

5.5. Discussion

This study shows that the presence of galectin-3 at concentrations that can be found in the circulation of patients with metastasis increases cancer cell homotypic aggregation by interaction with cancer-associated MUC1 expressing the TF disaccharide. The interaction between galectin-3 and MUC1 causes MUC1 cell surface clustering and exposes smaller cell surface adhesion molecules including E-Cadherin. The galectin-3-MUC1-induced cell aggregation enhances the survival of the cells under anchorage-independent conditions by preventing initiation of anoikis. This has important implications for our understanding of the molecular mechanisms that underlie cancer metastasis.

Survival of tumour cells in the blood/lymphatic circulation is crucial in cancer cell metastatic spread (5, 267). After invasion of the tumour cells into the blood circulation from the primary tumour sites, only a very small fraction (less than 1 in 10,000 cells) of the invaded cells survive to produce metastasis at distant sites (14, 54). Prolonging the survival of tumour cells in the circulation has been shown previously to directly to increase metastasis (56). Earlier studies have also demonstrated that cells in aggregated form have a much higher survival rate in the circulation than single cells(13, 14). Intraportal injection of aggregated DHD/K12/TRb colon cancer cells into syngeneic BD IX rats produced over 4-times more liver metastases than injection with the same numbers of single cells (12). Thus, an increase of

tumour cell aggregation as a result of the increased interaction between circulating galectin-3 and cancer-associated MUC1 in the bloodstream of cancer patients provides a survival advantage to the circulating tumour cells and enhances their metastatic potential.

Although earlier studies have revealed the association of cell aggregation in survival of the cells under anchorage-independent conditions, the molecular mechanism that underlies such survival advantage is not fully understood. There is evidence that this may be at least partly due to the enhanced ability of aggregated cells to escape anoikis (86). Anoikis is a specific type of apoptotic process induced by loss of cell adhesion or inadequate cell-matrix interactions(50) and has been proposed to be the dominant mechanism in removing disseminating tumour cells from the circulation(51). Resistance to anoikis is considered to be a hallmark of metastatic cancer cells(52). Our discovery that galectin-3-MUC1-induced cell aggregation is associated with enhanced ability of the cells to escape initiation of anoikis supports a role of anoikis resistance in the survival advantage of cell aggregation under anchorage-independent conditions.

The increased formation of cancer cell aggregates by galectin-3-MUC1interaction may also influence physical trapping of the circulating tumour cells in the micro-vasculature. Mechanical as well as "seed-soil" compatibility factors are both known to contribute to the ability of specific types of cancer cells to spread to various target organs (5, 52, 247). It is thought that the initial docking of specific cancer cells to the target organ is predominantly controlled by mechanical factors and that this is then followed by regulation of specific cell adhesion molecules on the cell surface(247).

Thus, an increase of tumour cell homotypic aggregation as a result of the increased interaction between circulating galectin-3 and cancer-associated MUC1 in the bloodstream of cancer patients is likely to enhance physical trapping of the circulating tumour cells in the microvasculature at target organ and this also enhances metastasis.

It has been shown previously that cell surface-associated galectin-3 acts as a cell adhesion molecule and increases cancer cell homotypic aggregation by interaction with TF antigen expressed by unknown cell surface molecules on adjacent cancer cells under anchorage independent conditions(44, 116). As cell surface-associated galectin-3 is relatively small in size, it is likely that such interaction may occur only after MUC1 cell surface polarization and exposure of the cell surface-associated galectin-3.

Thus, the interaction between circulating galectin-3 and TF-expressing MUC1 on the surface of disseminating cancer cells promotes cell-cell aggregation and embolus formation and enhances survival of disseminating tumour cells in the circulation. These findings, together with our previous demonstration that the interaction between circulating galectin-3 and cancer-associated MUC1 enhances cancer-endothelial adhesion(248), indicates that the increased circulation of galectin-3 often found in cancer patients can promote several important steps of the metastatic cascade. Targeting the action of circulating galectin-3 may represent an effective therapeutic approach for preventing metastasis.

CHAPTER 6

6. Effects of TF-binding peanut agglutinin in edible peanuts on factors associated with metastasis

6.1. Hypothesis

The discovery that galectin-3–TF/MUC1 interaction promotes metastasis led us to hypothesize that the presence of other TF binding proteins, such as the peanut agglutinin (PNA) from peanuts, in the bloodstream of cancer patients may also act similarly to galectin-3 and promote metastasis.

6.2. Aims:

- To assess the effect of PNA on cancer cell adhesion to and migration through the monolayer of endothelial cells.
- To assess the effect of PNA on cancer cell homotypic aggregation, survival and anoikis under anchorage-independent conditions.

6.3. Introduction:

A few lectins in foodstuffs recognize the TF antigen. These include the edible mushroom lectin ABL (*Agaricus bisporus* lectin)/ABA (*A. bisporus* agglutinin) (270), jackfruit lectin jacalin (271) and peanut agglutinin (109).

Peanut agglutinin (PNA) is a protein component of the common peanut Arachis hypogaea and binds highly specifically to the oncofetal Thomsen-Friedenreich (Gaβ1,3GalNAc, T or TF) antigen. PNA has a molecular weight of 110,000 dalton with 4 subunits and does not contain covalently bound sugar (272). Peanut lectin increases proliferation in colon cancer cell lines and cultured human colonic mucosal biopsies in vitro (108, 109, 112), causing a 40% increase in rectal mucosal proliferation in individuals who ate peanuts and had TF over-expression in their colonic epithelia in vivo (273). Earlier studies in our group have shown that PNA, which is a tightly globular protein, resists enzymatic attack and is highly resistant to cooking and digestion and rapidly appears in an active form (up to 5 μg/ml) in the systemic blood circulation after peanut ingestion (274). As interaction between the cancer-associated TF antigen and endogenous galactoside-binding galectin-3, whose concentration is increased in the bloodstream of cancer patients, has been shown to increase cancer cell adhesion and metastasis (268), we have hypothesised that the appearance of PNA in the blood circulation of cancer patients who eat peanuts may, like endogenous galectin-3, influence the metastatic behaviour (cancer cell homotypic aggregation and heterotypic aggregation) of disseminating tumour cells.

6.4. Materials and methods

Materials: Biotin-conjugated peanut agglutinin (PNA) was purchased from Vector Laboratories Ltd (Peterborough, UK). O-glycanase was obtained from Prozyme Inc (Oxford, UK).

Cell lines: Human colon cancer HT29-5F7 cells were obtained and cultured as described in Chapter 3 (Yu, Andrews et al., 2007). Macrovascular HUVECs and human microvascular lung endothelial cells (HMVEC-L) were from Cambrex BioSciences and were cultured in EGM endothelial growth medium (EGM Bulletkit) and EGM-2 medium (EGM-2 Bulletkit, Cambrex BioSciences), respectively. Cells that had been passaged less than five times were used in the experiments. Human colon cancer SW620 cells were cultured in complete DMEM medium containing 10% FCS. MUC1 positive transfectants HCA1.7+ human breast epithelial cells and MUC1 negative revertants HCA1.7- were as described previously in Chapter 3 (174).

Cell aggregation

Subconfluent cells were released from the culture plates with NECDS and were dispersed in serum-free DMEM containing 0.5mg/ml bovine serum albumin (BSA). Two 0.5 ml (1X 10^6 cells) aliquots of the cell suspension were incubated, separately, with 5μl/ml DIO and DiI Cell Labelling Solution for 30 mins at 37°C. The DIO- and DiI-labelled cells were then mixed in the presence or absence of PNA in DMEM and incubated at 37°C for 1 hr followed by analysis with flow cytometry.

Cancer cell adhesion to endothelial monolayer

Subconfluent cancer cells were released from the culture plates with NECDS and were dispersed in serum-free DMEM containing 0.5mg/ml bovine serum albumin (BSA). 0.5 ml (1X 10^6 cells) aliquots of the cell suspension were incubated with Calcein AM 10μl/ml for 30 min at 37°C. The Calcein AM-labelled cells were then mixed in the presence or absence of 2.5μg/ml PNA, PNA inhibitor (Asialomucin pre-incubated with PNA for 20 minutes before being added to cells at 37°C), in DMEM. The cell suspension was then added to a monolayer of HMVEC-L (pre-seeded in a 96-well white cell culture plate and cultured for 3 days in EBM2 endothelial growth medium at 37°C) for 1hr at 37°C. The culture medium was then removed and the cells were washed twice with 200μl/well PBS each time to remove the non-adhesion cells. After addition of 100μl PBS/well, the cell adhesion was determined by fluorescent density using a TECAN infinite F200 micro-plate reader.

Cell viability in single and aggregated cells under anchorage-independent conditions

96- or 24-well plates were coated twice with 200 μl/well (96-well plates) or 5 ml/well (6-well plates) of 10mg/ml poly-2-hydroxyethyl methacrylate (poly-HEMA, Sigma) in 95% ethanol overnight at room temperature. After washing, the cells were treated with 2.5μg/ml PNA or BSA under suspension culture in serum-free medium for various times at 37°C. The cells in suspension were collected and passed three times through a 40-μm cell strainer (BD Biosciences). The viability of the cells that did and did not pass through the strainers was measured by the CellTiter-Glo® Luminescent Cell Viability Assay (Promega).

Cell anoikis in single and aggregated cells under anchorage-independent conditions

For the measurement of cellular anoikis, after separation of the cells by cell strainers as above, the cells were re-suspended in FITC-Annexin-V 1×binding buffer and the apoptotic cells were measured by a FITC-Annexin-V apoptosis detection kit (Cambridge Biosciences, Cambridge, UK) by flow cytometry according to the manufacturer's instructions.

Reduction of TF expression by O-glycanase treatment

HT295F7 cells (1×10^6/ml in O-Glycanase 1×buffer) were incubated with 0.02U/ml O-glycanase in O-Glycanase 1×buffer for 3 hrs at 37°C. The cells were then lysed directly with 100μl SDS-sample buffer for 20 mins. The cell lysates were then seperated on 4% gel and analysed for TF expression by PNA blotting with biotin-PNA (1:1000) and extrAvidin Peroxidase (1:2000).

Impact of enzymatic removal of TF on PNA-mediated cell aggregation

HT295F7 cells were incubated with 0.02U/ml O-glycanase for 2.5 hrs at 37°C then labeled with 0.5μg/ml DiO or DiI for 30 minutes at 37°C. After washing with PBS and re-suspension in serum-free DMEM, the cells were incubated with PNA 2.5μg/ml for 1 hr at 37°C before cell aggregation was assessed by flow cytometry, as described in Chapter 3.

6.5. Results:

6.5.1. PNA increases cancer cell homotypic aggregation.

Pre-treatment of HT29-5F7 cells with PNA at physiological concentrations (Wang et al., 1998) increased HT29-5F7 cell aggregation in a dose-dependent way (Fig 6-1).

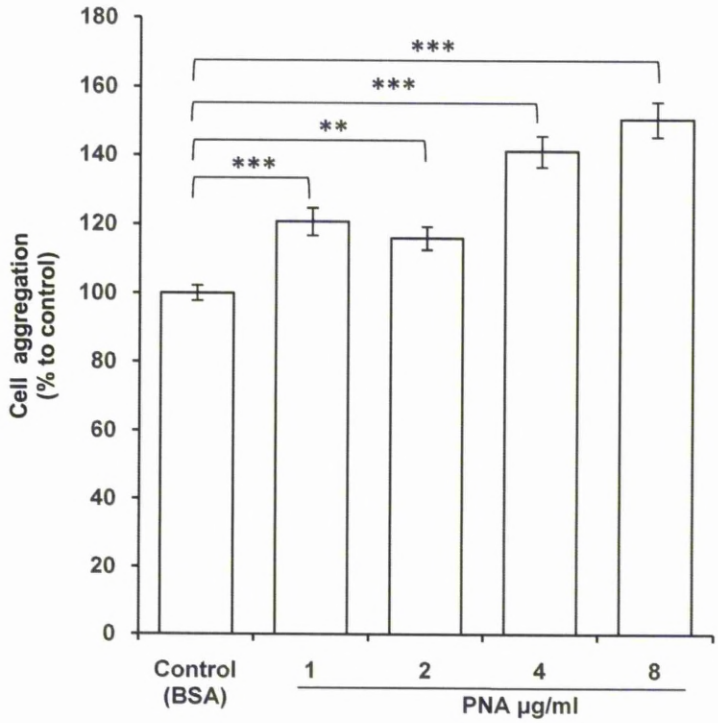

Fig6-1. The presence of PNA increases homotypic aggregation of human colon cancer HT29-5F7 cells. PNA treatment induces a dose-dependent increase of HT29-5F7 cell aggregation. Data are expressed as mean ± SEM of triplicate determinations from three independent experiments. **p<0.01, ***p<0.001 (one-way ANOVA followed by Newman-Keuls' test for multiple comparisons).

At 1 µg/ml and 4 µg/ml PNA caused 21% (p=0.0004) and 41% (p<0.0001) increase of HT29-5F7 cell aggregation, respectively. Fig 6-2 shows representative flow cytometry plots from the aggregation assessment of human colon cancer HT29-5F7 in the presence or absence of 8µg/ml PNA. At

8 μg/ml PNA caused 39% HT295F7 cells aggregation (Fig 6-2 right panel) after 1.5 hrs incubation at 37°C compared to 24% HT295F7 cells spontaneous aggregation (Fig 6-2 left panel) in the control group.

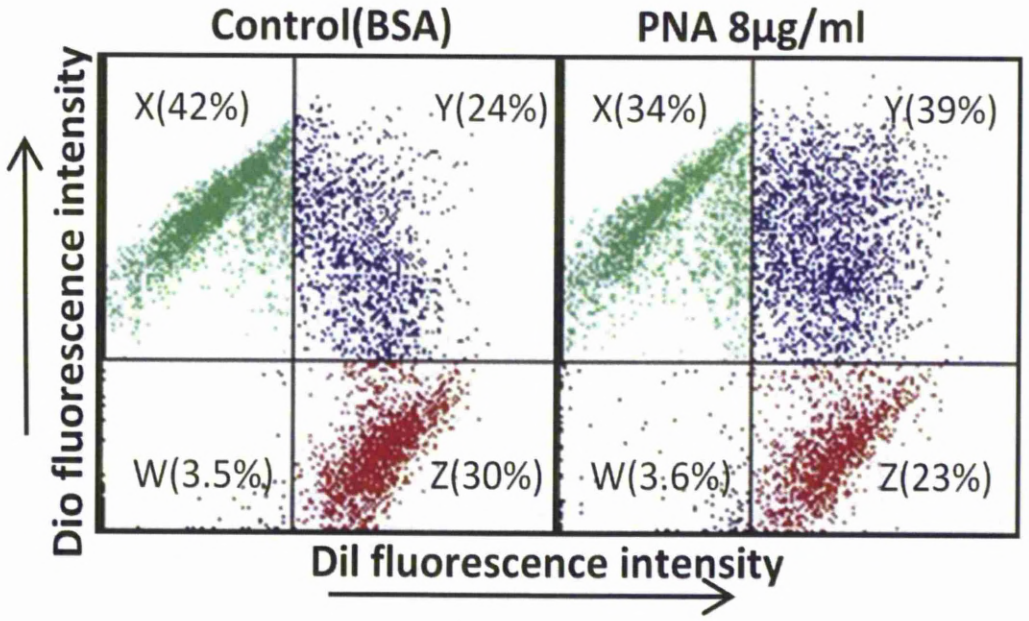

Fig 6-2 Representative flow cytometry plots from the aggregation assessment of human colon cancer HT29-5F7 in the presence or absence of 8μg/ml PNA. The top right in each bivariate correlation plot represents the cell population containing both DiO- and Dil-labelled cells that are defined in this study as cell aggregates.

We then assessed the effect of PNA on aggregation of other human colon cancer SW620 cells. Cell surface binding of anti-MUC1 B27.29 antibody followed by flow cytometry showed high expression of MUC1 by SW620 cells (Fig 6-3).

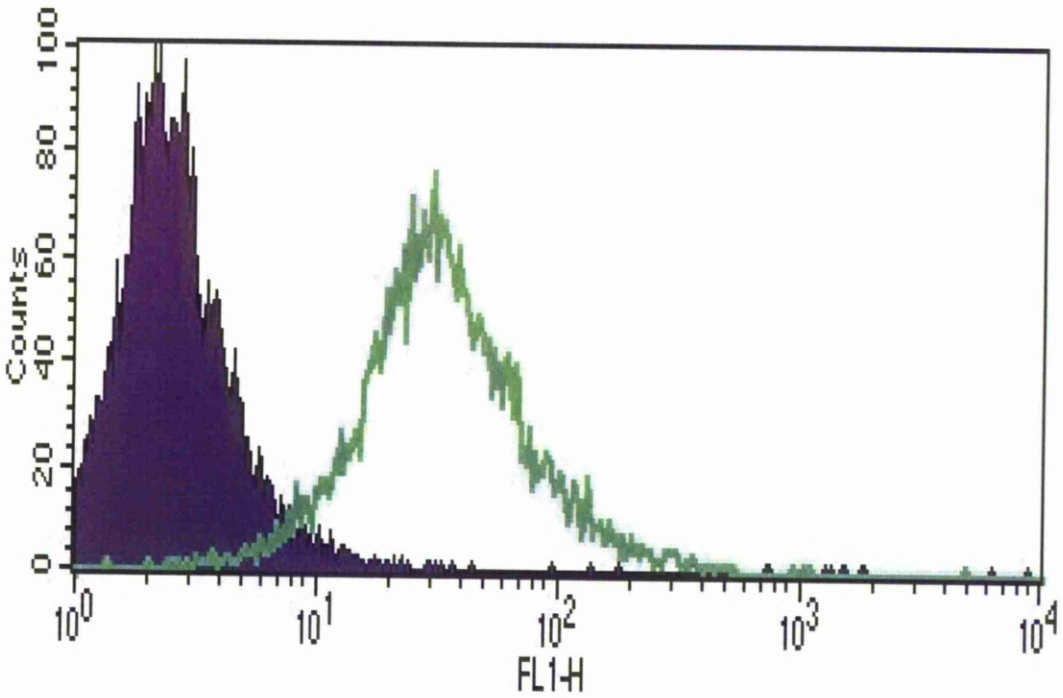

Fig 6-3. SW620 cells express high level of cell surface MUC1 assessed by flow cytometry. Green histogram: MUC1; Blue shaded histogram: immunoglobulin isotype control.

The presence of PNA caused a dose-dependent increase of SW620 cell aggregation (Fig 6-4). At 4 ug/ml, PNA induced 11% increase of cell aggregation compared with non-treated controls ($p=0.0026$).

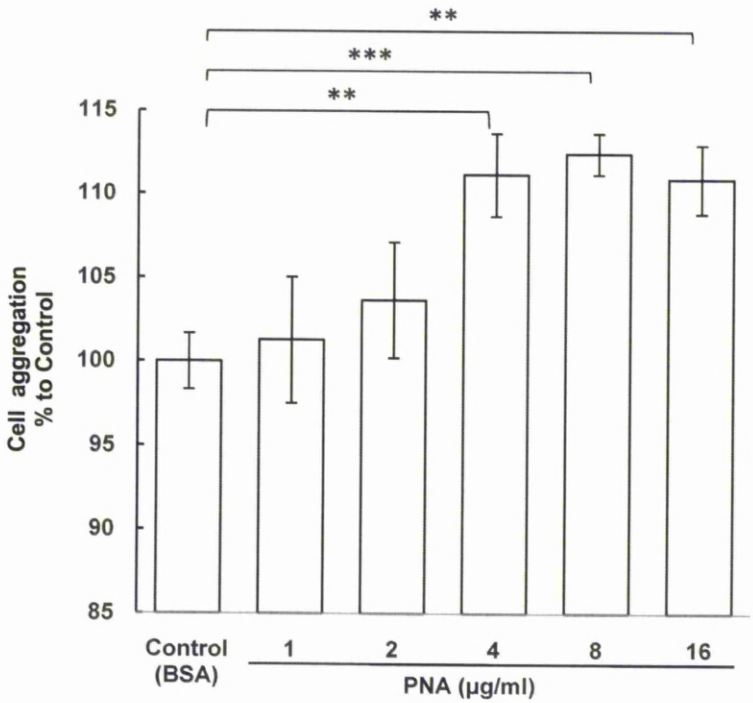

Fig 6-4. PNA increases homotypic aggregation of SW620 cells. PNA treatment induces a dose-dependent increase of SW620 cell aggregation. Data are expressed as mean ± SEM of triplicate determinations from T independent experiments. **p<0.01, ***p<0.001 (one-way ANOVA followed by Newman-Keuls' test for multiple comparisons).

To see if the effect of PNA on cell aggregation is linked with its interaction with MUC1, the effects of PNA on MUC1 positively (HCA1.7+) and negatively transfected (HCA1.7-) human breast epithelial HBL-100 cells were assessed. Pre-treatment of the cells with PNA, at 1, 2, 3, 4 µg/ml, caused dose-dependent increase of aggregation of HCA1.7+ but not HCA1.7- cells compared to a control treated with BSA (Fig 6-5). At 3 ug/ml, PNA induced 656±117% increase of HCA1.7+ cell aggregation.

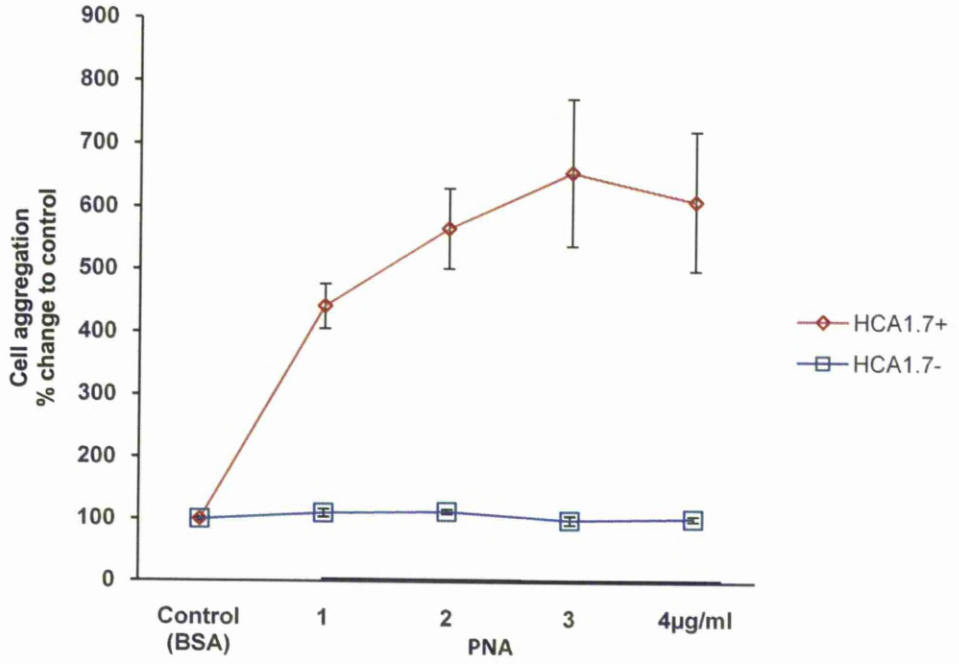

Fig 6-5. PNA induces homotypic aggregation of MUC1 in positively but not negatively transfected human breast epithelial cells. PNA increases HCA1.7+ but not HCA1.7- cell aggregation. Data are expressed as mean ± SEM of triplicate determinations from four independent experiments. Data are expressed as mean ± SEM of triplicate determinations from two independent experiments. *p<0.05, **p<0.01, ***p<0.001 (one-way ANOVA followed by Newman-Keuls' test for multiple comparisons).

6.5.2. PNA-mediated cell aggregation increased cell survival under anchorage-independent conditions

HT295F7 cells were detached with NECDS and suspended in serum-free DMEM (5×10^5/ml), then treated with or without 2.5 μg/ml PNA or BSA by culture in suspension in a Poly-HAMA coated plate for 3 days at 37°C. After separation of the cells by cell strainers, the viability of the cells was assessed. After 3 days' culture under suspension conditions, nearly 2 times more cells in

the cell aggregates obtained from the PNA-treated cells were viable than those obtained from the BSA-treated controls (Fig 6-6).

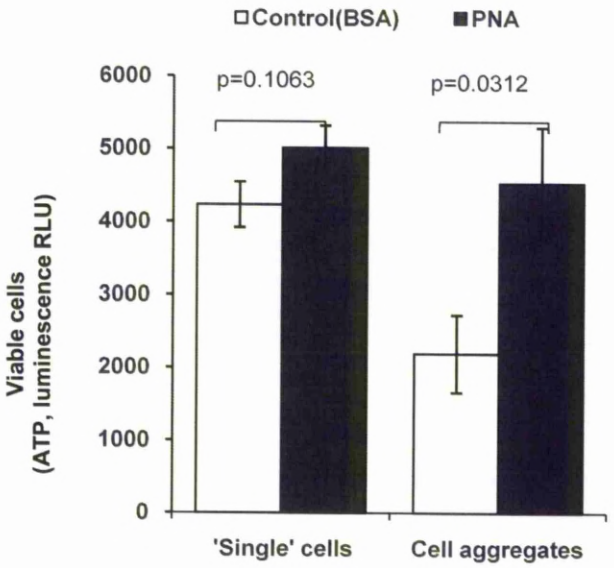

Fig 6-6 PNA-induced cell aggregation enhances survival of cells. PNA-induced cell aggregation increases survival of HT29-5F7 cells under anchorage-independent conditions. HT29-5F7 cells were treated with or without 2.5μg/ml PNA or BSA by culture in suspension in a Poly-HAMA coated plate for 3 days at 37°C. After separation of the cells by cell strainers, the viability of the cells was assessed as described in the Methods section. The data are presented as mean ± SEM of triplicate determinations from two independent experiments (one-way ANOVA to compare means).

These results indicate that the increased aggregation of cells in response to PNA greatly enhances their survival under anchorage-independent conditions.

6.5.3. Effect of PNA-mediated aggregation on anoikis:

To see if the increased survival of the cell aggregates is associated with inhibition of cell anoikis, anoikis in the single and aggregated cell populations was analysed for caspase 3/7 activation and Annexin-V cell surface binding.

After 2 days' incubation of the cells under suspension conditions, significantly fewer cells in the cell aggregates obtained from PNA-treated cells were undergoing apoptosis than amongst the BSA-treated controls (36 ± 3% *vs* 63 ± 6%, p=0.027), whilst apoptosis of the cells that passed through the cell strainers ('single' cells) from PNA-treated and untreated cells showed no statistically significant difference (Fig 6-7). For example, cell aggregates from 2.5 μg/ml PNA-treated cells showed 46% less anoikis (p=0.027) than those from BSA-treated controls under 48 hrs suspension culture.

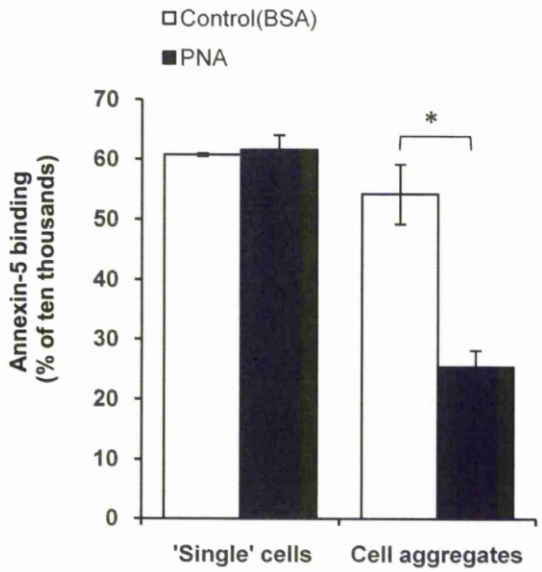

Fig 6-7. PNA-induced cell aggregates show resistance to anoikis initiation. HT29-5F7 cells treated with or without 2.5 μg/ml PNA or BSA followed by culture of the cells in suspension for 3 days at 37°C. After separation of the cells by cell strainers, the apoptosis of cells was assessed by Annexin-V binding with FACs as described in the Methods section. The data are presented as mean ± SEM of triplicate determinations from two independent experiments (one-way ANOVA to compare means).

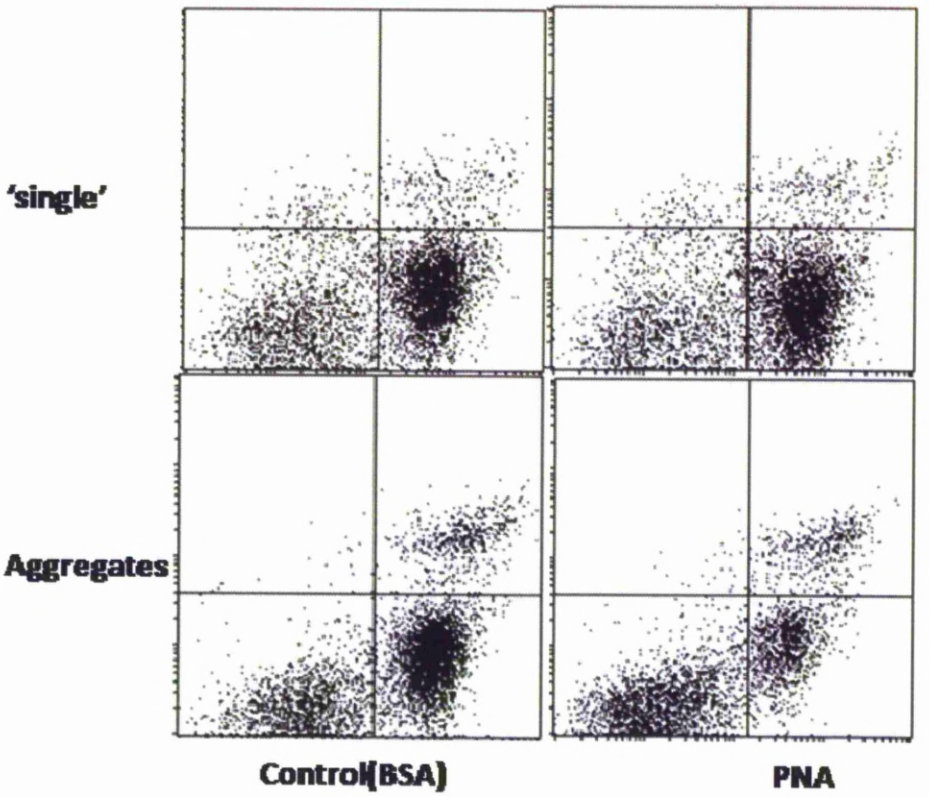

Fig 6-8. PNA-induced cell aggregates show resistance to anoikis initiation. Representative flow cytometry plots from the anoikis assessments of HT29-5F7 cells cultured in suspension in the presence of 2.5 μg/ml PNA or BSA for 2 days at 37°C. Annexin-V positive and PI negative reveal early apoptotic cells (bottom right in the bivariate correlation plot) and Annexin-V positive and PI positive reveal late apoptotic cells (at the top right in the correlation plot).

This indicates that the PNA-induced cell aggregates are associated with increased resistance of the cells to anoikis initiation.

6.5.4. Effects of PNA on HT29-5F7 cell adhesion to HMVEC-L

To determine the effect of PNA on HT295F7 colon cancer cell adhesion to the monolayer of HMVEC-Ls, we pre-treated the HT29-5F7 cells with PNA at several concentrations as seen in the systemic circulation after eating 200g peanuts in human subjects (274). Pre-treatment of the cells with PNA significantly increased adhesion of HT29-5F7 cells to HUVECs in a dose-dependent way (Fig 6-9). At 4 μg/ml, a 67% increased adhesion ($p<0.0001$) was seen.

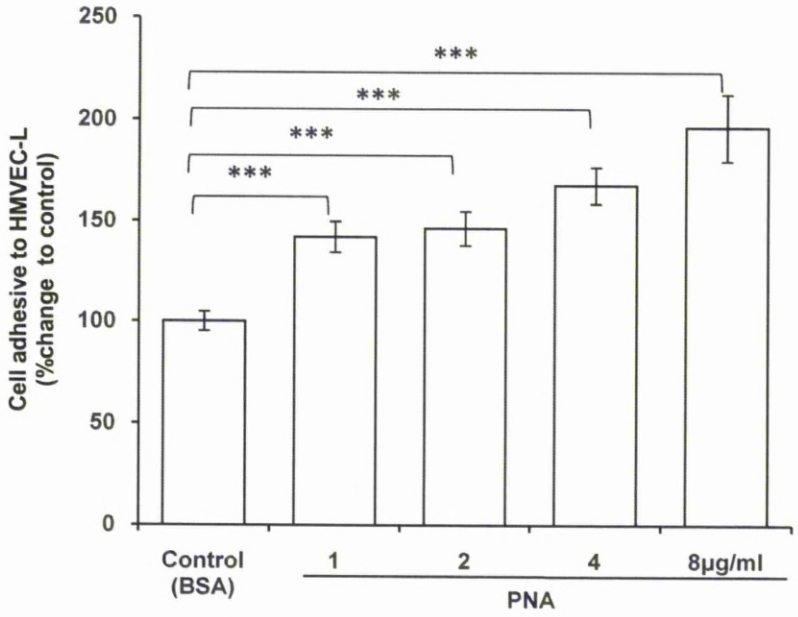

Fig 6-9 Effects of PNA on HT29-5F7 cell adhesion to HMVEC-L. PNA induces a dose-dependent increase of HT29-5F7 cell adhesion to the monolayer of HMVEC-L. Data are expressed as the percentage of the adhered cells compared to that in the controls (mean ± SEM of triplicate determinations from three independent experiments). *$p<0.05$, **$p<0.01$, ***$p<0.001$ (one-way ANOVA followed by Newman-Keuls' test for multiple comparisons).

To determine the role of TF expression in PNA-mediated cell–cell interaction we treated HT295F7 cells with 0.02 U/ml O-glycanase for three hours at 37°C. Subsequent analysis of the cell surface TF expression with Biotinylated-PNA by flow cytometry showed a 50% reduction of TF on the cell surface (Fig 6-10).

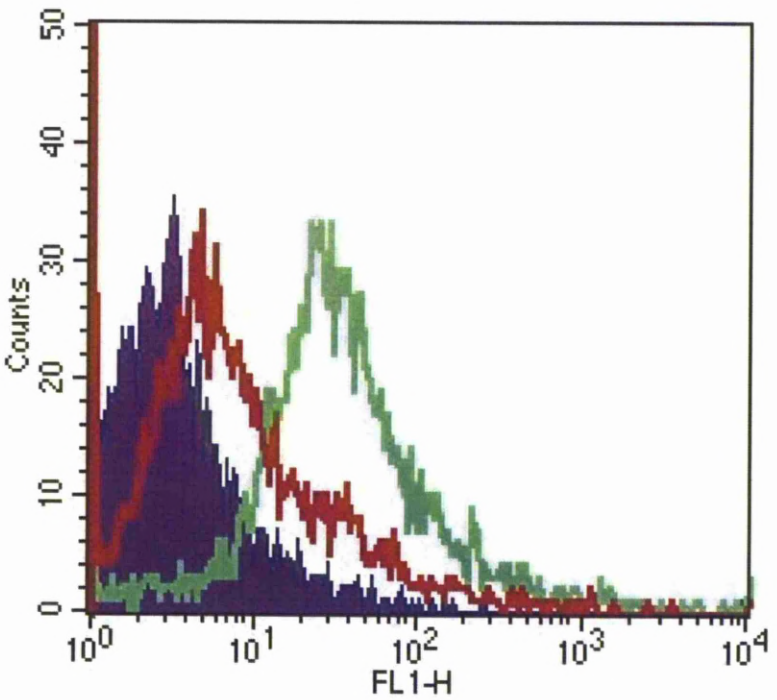

Fig 6-10. Cell surface TF expression in HT295F7 cells in response to treatment of the cells with O-Glycanase. HT295F7 cells incubated with 0.02 U/ml O-Glycanase for 3 hrs at 37°C (red) shows a reduction of TF expressions (compared to the untreated cells (green)) by flow cytometry. Blue: background control without Biotin-PNA and secondary antibody.

Further investigation is needed to see the effect of TF removal from the cell surface on PNA-mediated cell–cell interactions.

6.6. Discussion:

Peanut agglutinin at concentrations similar to that observed in the blood circulation of people who ingested 200g peanuts induces homotypic aggregation and heterotypic adhesion to vascular endothelial cells *in vitro*.

The cell aggregates induced by PNA show increased survival and resistance to anoikis initiation under anchorage-independent conditions.

TF antigen expression occurs in about 90% of all types of human cancer cells. Cancer-associated MUC1 (97) and the cancer-associated high molecular weight splice variant of the adhesion molecule CD44v6 (99) are so far the known cell-surface glycoproteins that carry the unsubstituted TF antigen. It was found here that pre-treatment of the cells with PNA, at 1, 2, 3, 4 μg/ml, caused dose-dependent increases of aggregation of MUC1 positively transfected HCA1.7+ but not MUC1 negatively transfected HCA1.7- cells. This indicates that the expression of MUC1 is crucial in PNA-mediated cell aggregation. Our earlier studies have shown that the MUC1 molecule in HCA1.7+ transfectants also carries many copies of unsubstituted TF antigen (Yu et al., 2007). Thus, it is highly likely that the increased cell–cell interactions induced by PNA shown in this study are through binding of PNA to TF on cell surface MUC1.

Anoikis is a specific type of apoptotic process induced by loss of cell adhesion or inadequate cell-matrix interactions (50) and has been proposed to be the dominant mechanism in removing disseminating tumour cells from the circulation (51). Resistance to anoikis is considered to be a hallmark of metastatic cancer cells (52). Previous studies have shown that squamous cell carcinoma cells, colonic epithelial cells and malignant pleural mesothelioma cells in aggregated forms have a higher ability to resist anoikis initiation (86-88). PNA-mediated cell aggregation in the bloodstream of cancer patients could increase the formation of tumour emboli, thus tumour cell survival in

the circulation. This, together with the enhanced ability of the cancer cells to adhere to vascular endothelial cells by PNA, supports a detrimental effect of the presence of peanuts in the diet of patients on patients' survival.

7. Summary of the main findings of the study

a) Recombinant galectin-3 at pathologically relevant concentrations seen in the circulation of cancer patients increases cancer cell heterotypic adhesion to vascular endothelial cells under static as well as under fluid flow conditions.

b) Recombinant galectin-3 induces cancer cell trans-endothelial migration.

c) Recombinant galectin-3 induces cancer cell homotypic aggregation under anchorage-independent conditions.

d) The aggregation induced by galectin-3 is associated with increased survival and resistance of the cells to anoikis initiation in response to suspension.

e) The effect of galectin-3 on cancer cell homotypic aggregation and heterotypic adhesion to endothelium is via binding of galectin-3 to the Thomsen-Friedenreich carbohydrate antigen on the transmembrane mucin protein MUC1.

f) The galectin-3–MUC1 interaction induces MUC1 cell surface polarization that results in exposure of the cell surface adhesion molecules including E-cadherin, CD44 and ligand for E-selectin.

g) Pre-incubation of galectin-3 with cancer cells before tumour cell inoculation into immunodeficient mice decreases the latency of experimental

metastasis.

h) The TF-binding peanut agglutinin induces cancer cell homotypic aggregation and heterotypic adhesion on vascular endothelial cells in cell culture and promotes tumour cell survival under suspension conditions.

Chapter 8

8. General discussion and implications for future studies

8.1. Discussion

The results presented in this thesis show that recombinant galectin-3 at pathologically-relevant circulating galectin-3 concentrations increases cancer cell homotypic aggregation and heterotypic adhesion to vascular endothelium and trans-endothelium invasion under static and fluid flow conditions, and increases experimental metastasis in athymic nude mice as a result of its interaction with TF antigen on cancer-associated MUC1. The galectin-3–TF/MUC1 interaction causes MUC1 cell surface polarization and exposure of the cell surface adhesion molecules(Fig8-1 and Fig8-2).

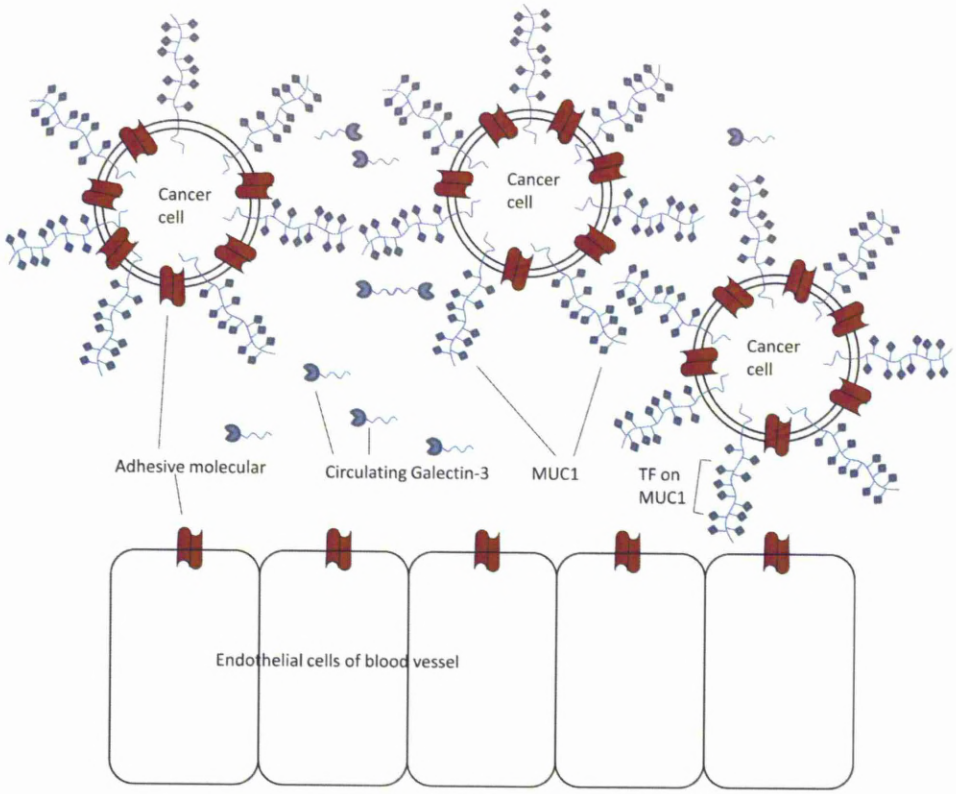

Fig 8-1. Model of the effect of muc1 expression on cancer cell adhesion to vascular endothelium. MUC1 over expression around the cell surface prevent cancer cell adhesion to vacular endothelium. .

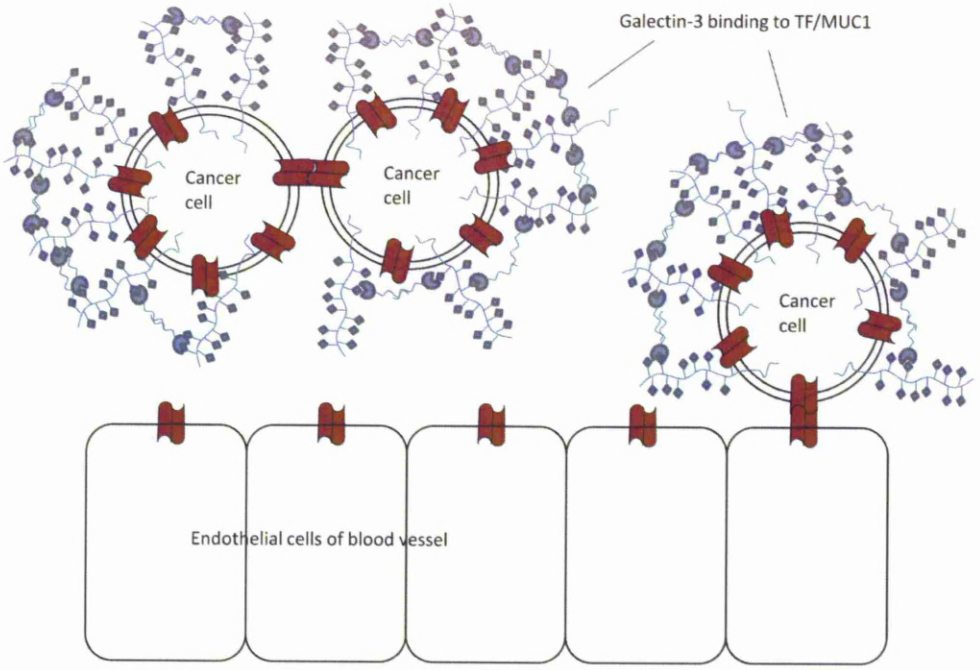

Fig 8-2. Model of the muc1-galectin-3 interaction in promotion of cancer cell homotypic adhesion to vascular endothelium and cancer cell homotypic aggregation. MUC1-galectin-3 interaction causes MUC1 cell surface polarization and exposure of the cell surface adhesion molecules, which causing increased cancer-endothelial adhesion and cancer cell aggregation.

It was already known that the cell surface-associated galectin-3 is involved in many cell–cell and cell–matrix interactions (120, 211) and promotes cancer development and metastasis (211). Cancer cell-associated galectin-3 is reported to play an important role in tumour cell heterotypic adhesion to endothelium(116), cancer cell homotypic aggregation(121), and cancer cell invasion(233, 234). The bivalent and multivalent properties of galectins enable them to bridge two of the same or different cell types, which allows homo- or heterotypic cell–cell interactions, and also interaction of the cells

with extracellular matrix proteins (120). Although the concentration of circulating galectin-3 was previously known to be increased in the serum of patients with many cancers (209, 235, 237) (238), the functional significance of this increased galectin-3 concentration was previously unknown. The results from this study suggest that the increased circulation of galectin-3 plays an important role in promoting tumour cell haematogenous spread to remote organs. Thus, blocking the actions of circulating galectin-3 in the bloodstream of cancer patients may represent a novel therapeutic approach for preventing metastasis.

Tumour recurrence and metastasis are the big problem in cancer patients after surgical treatments of the primary tumour. Circulating tumour cells (CTCs) can be present in patients for 7–20 years without evidence of clinical disease after mastectomy (275). CTCs seem to be non-proliferating cells that persist during chemotherapy and are linked to cancer progression (276). An increase of CTCs in patients is associated with a higher risk of relapse and a poor prognosis (277). The number of circulating tumour cells before any treatment is an independent predictor of progression-free survival and overall survival in patients with metastatic breast cancer (278). Furthermore, detection of elevated CTCs at any time during therapy is an accurate indication of subsequent disease progression and mortality for metastasis breast cancer patients (279). Patients with $\geq$5 CTCs/7.5 mL have shorter mean overall survival than those with <5 CTCs/7.5 mL (278, 279). This study suggests that the aggregation induced by galectin-3 is associated with increased survival and resistance of the cells to anoikis initiation in response to suspension. Thus,

blocking the interaction of circulating galectin-3 with MUC1 in the bloodstream of cancer patients may reduce CTC survival.

Peanut agglutinin binds highly specifically to the TF antigen and has been shown in our previous studies to appear rapidly in the bloodstream after peanut ingestion in a human subject (Wang et al., 1998). The work described in this thesis shows that the presence of PNA at concentrations seen in the serum of people who eat 200g of peanuts increases cancer cell homotypic aggregation and heterotypic adhesion in cell culture and enhances tumour cell survival under anchorage-independent conditions. These *in vitro* data suggest that the presence of PNA in the bloodstream of cancer patients who eat peanuts may represent a detrimental exogenous factor in cancer cell spread. Although further studies are needed, these preliminary data suggest that a recommendation to avoid peanuts in the diet of cancer patients might help to increase the overall survival of those patients.

8.2. Implications for Future Studies

This study reveals a molecular mechanism that promotes metastasis. It has also raised a number of interesting questions which require further investigation. A research project is currently ongoing investigating the expressions of the other galectin members in the circulation of cancer patients and healthy people. As members of the galectin family are widely expressed by many cell types, it is possible that some other galectins members are also altered in the circulation of cancer patients and that these may also act like

galectin-3 and promote metastasis.

It is noted that pre-incubation of galectin-3 with the MUC1 negatively transfected cells before tumour cell injection into nude mice resulted in about 20% decrease of the metastasis-associated animal survival. This indicates that galectin-3 may have other cell surface ligands. Galectin-3 recognizes galactoside-terminated glycans which are known to be expressed by many cell surface molecules (Table8-1). Many of those cell surface molecules are known to be involved in signal transduction and cell adhesion (232). The cell surface-associated galectin-3 has been shown previously to interact with laminin, carcinoembryonic antigen, and lysosome-associated membrane glycoproteins, and increases human colon cancer cell adhesion to extracellular matrix(280). A recent study demonstrated that cell-associated galectin-3 regulates fibronectin polymerization and tumor cell motility by binding to the branched N-glycan ligands and stimulate focal adhesion remodeling, FAK and PI3K activation, local F-actin instability, and alpha5beta1 translocation to fibrillar adhesions(281). Hence, an interaction between circulating galectin-3 and some of these cell surface molecules may also be involved in galectin-3-mediated metastasis promotion.

Table8-1 Ligands recognized by galectin-3

Ligands	Function associated with galectin-3 binding
Laminin	Modulates cell/ECM adhesion
Collagen IV	Modulates cell/ECM adhesion
Fibronectin Vitronectin	Modulates cell/ECM adhesion
Hensin	Maintains terminal differentiation of epithelial cells
Elastin	Promotes adhesion of cells to elastin
Mac-2BP (gp 90)	Promotes cell/cell and cell/ECM adhesion
Cubilin	Adhesions and endocytosis
Cell/ECM adhesion	Cell/ECM adhesion
Colon cancer mucins	Cell/cell and cell/ECM adhesion
Carcino-embrionic antigen (CEA)	Cell/cell and cell/ECM adhesion
Advanced glycosilation end products (AGE)	Mediates endocytosis of AGE
α1β1integrins	Modulates cell/ECM adhesion
αMβ1 (CD11b/18, Mac-1 antigen)(human macrophage)	Modulates cell/ECM adhesion
N-glycans on alpha3beta1 integrin	subsequently activating alpha3beta1-integrin-Rac1 signaling to promote lamellipodia formation(282)
CD66a/CD66b (human neutrophils)	Induces activation NADH oxidase and adhesion of cells to ECM
CD98 (Jurkat cells)	Induces uptake of extracellular Ca2+ and modulates cell ECM adhesion
CD4+/CD8+(T lymphocytes)	Inhibits apoptosis and modulates cell/ECM adhesion
FcgRII (human eosinophilic leukemia cells)	Downregulates of IL-5 gene expression
NCA-160 (human neutrophils)	Induces an oxidative burst in neutrophils
Neural cell adhesion molecules (NCAM) MAG, L1	Modulates cell/ECM adhesion
IgE (rat basophilic leukemia cells)	Triggers degranulation and serotonin release
Lamp-1, Lamp-2 (tumor cells)	Modulates cell/cell, cell/ECM adhesion
Lipopolysaccharides (LPS) (bacteria)	Adhesion of pathogen organisms to host ECM and cells
Mgat5-modified N-glycans	regulates fibronectin matrix remodeling in tumor cells(281)

Table was adapted from Ochieng J, et al(2004) (232).

The likely involvement of circulating galectin-3 in metastasis shown in this study implies that circulating galectin-3 inhibitors could help to reduce cancer

cell metastatic spread and increase survival. Thus, developing novel galectin-3 inhibitors that could be administered directly into the blood circulation of cancer patients may represent a promising therapeutic approach for the prevention of metastasis.

Cancer cells are normally shown to carry shorter and less branched O-linked carbohydrate chains, with increased sialylation and reduced sulfation (Boland and Deshmukh 1990; Lloyd, Burchell et al. 1996; Rhodes 1996). But the expressions of the glycosyltransferase alone may not account for the altered glycosylation changes in cancer cells as discussed in section 1.2.3 of chapter1. Redistribution of the glycotransferases in the Golgi apparatus (130) (131) and the inappropriate Golgi pH may be responsible for altered glycosylation potential (132-134). Further investigations of the mechanisms that lead to the expression of TF/MUC1 will help to design new therapeutic agnets to prevent circulating galectin-3-mediated metastasis promotion.

The discovery that PNA at relevant concentrations increases tumour cell aggregation and adhesion to vascular endothelial cells suggests that the presence of peanuts in the diet of cancer patients may represent an unfavourable factor in patients' survival. An epidemiological investigation into this hypothesis has produced supporting data (see Appendix2).

1. OFNS. Office for National Statistics, 2009 Mortality Statistics: Deaths registered in England & Wales, 2007. . 2009.
2. NISRA. Northern Ireland Statistics and Research Agency, 2009 Registrar General Annual Report 2007 2009.
3. GROFS. General Register Office for Scotland, 2009 Deaths Time Series Data, 1997-2007. 2009.
4. ISD. Cancer Incidence, Mortality and Survival data. Accessed 2009 2009.
5. Fidler IJ. The pathogenesis of cancer metastasis: the 'seed and soil' hypothesis revisited. Nat Rev Cancer 2003;3:453-8.
6. Dittmar T, Heyder C, Gloria-Maercker E, Hatzmann W, Zanker KS. Adhesion molecules and chemokines: the navigation system for circulating tumor (stem) cells to metastasize in an organ-specific manner. Clin Exp Metastasis 2008;25:11-32.
7. Pantel K, Brakenhoff RH, Brandt B. Detection, clinical relevance and specific biological properties of disseminating tumour cells. Nat Rev Cancer 2008;8:329-40.
8. Schluter K, Gassmann P, Enns A, Korb T, Hemping-Bovenkerk A, Holzen J, Haier J. Organ-specific metastatic tumor cell adhesion and extravasation of colon carcinoma cells with different metastatic potential. Am J Pathol 2006;169:1064-73.
9. Paget s. The distribution of secondary growths in cancer of the breast. Lancet 1889:571–3.
10. Fidler IJ, Poste G. The "seed and soil" hypothesis revisited. Lancet Oncol 2008;9:808.
11. Fidler IJ. Review: biologic heterogeneity of cancer metastases. Breast Cancer Res Treat 1987;9:17-26.
12. Topal B, Roskams T, Fevery J, Penninckx F. Aggregated colon cancer cells have a higher metastatic efficiency in the liver compared with nonaggregated cells: an experimental study. J Surg Res 2003;112:31-7.
13. Steuer AF, Ting RC. Formation of larger cell aggregates by transformed cells: an in vitro index of cell transformation. J Natl Cancer Inst 1976;56:1279-80.
14. Steuer AF, Rhim JS, Hentosh PM, Ting RC. Survival of human cells in the aggregate form: potential index of in vitro cell transformation. J Natl Cancer Inst 1977;58:917-21.
15. Brodt P, Fallavollita L, Bresalier RS, Meterissian S, Norton CR, Wolitzky BA. Liver endothelial E-selectin mediates carcinoma cell adhesion and promotes liver metastasis. Int J Cancer 1997;71:612-9.
16. Naor D, Sionov RV, Ish-Shalom D. CD44: structure, function, and association with the malignant process. Adv Cancer Res 1997;71:241-319.
17. Gassmann P, Enns A, Haier J. Role of tumor cell adhesion and migration in organ-specific metastasis formation. Onkologie 2004;27:577-82.
18. Smid M, Wang Y, Zhang Y, Sieuwerts AM, Yu J, Klijn JG, Foekens JA, Martens JW. Subtypes of breast cancer show preferential site of relapse. Cancer Res 2008;68:3108-14.
19. Kobayashi H, Boelte KC, Lin PC. Endothelial cell adhesion molecules and cancer progression. Curr Med Chem 2007;14:377-86.
20. Bevilacqua MP, Pober JS, Mendrick DL, Cotran RS, Gimbrone MA, Jr. Identification of an inducible endothelial-leukocyte adhesion molecule. Proc Natl Acad Sci U S A 1987;84:9238-42.
21. Kansas GS. Selectins and their ligands: current concepts and controversies. Blood 1996;88:3259-87.

22. Kannagi R, Izawa M, Koike T, Miyazaki K, Kimura N. Carbohydrate-mediated cell adhesion in cancer metastasis and angiogenesis. Cancer Sci 2004;95:377-84.
23. Witz IP. The involvement of selectins and their ligands in tumor-progression. Immunol Lett 2006;104:89-93.
24. Sawada R, Tsuboi S, Fukuda M. Differential E-selectin-dependent adhesion efficiency in sublines of a human colon cancer exhibiting distinct metastatic potentials. J Biol Chem 1994;269:1425-31.
25. Mannori G, Santoro D, Carter L, Corless C, Nelson RM, Bevilacqua MP. Inhibition of colon carcinoma cell lung colony formation by a soluble form of E-selectin. Am J Pathol 1997;151:233-43.
26. Goodison S, Urquidi V, Tarin D. CD44 cell adhesion molecules. Mol Pathol 1999;52:189-96.
27. Birch M, Mitchell S, Hart IR. Isolation and characterization of human melanoma cell variants expressing high and low levels of CD44. Cancer Res 1991;51:6660-7.
28. Sy MS, Guo YJ, Stamenkovic I. Distinct effects of two CD44 isoforms on tumor growth in vivo. J Exp Med 1991;174:859-66.
29. Hofmann M, Rudy W, Zoller M, Tolg C, Ponta H, Herrlich P, Gunthert U. CD44 splice variants confer metastatic behavior in rats: homologous sequences are expressed in human tumor cell lines. Cancer Res 1991;51:5292-7.
30. Radotra B, McCormick D, Crockard A. CD44 plays a role in adhesive interactions between glioma cells and extracellular matrix components. Neuropathol Appl Neurobiol 1994;20:399-405.
31. Oliferenko S, Kaverina I, Small JV, Huber LA. Hyaluronic acid (HA) binding to CD44 activates Rac1 and induces lamellipodia outgrowth. J Cell Biol 2000;148:1159-64.
32. Sy MS, Guo YJ, Stamenkovic I. Inhibition of tumor growth in vivo with a soluble CD44-immunoglobulin fusion protein. J Exp Med 1992;176:623-7.
33. Zawadzki V, Perschl A, Rosel M, Hekele A, Zoller M. Blockade of metastasis formation by CD44-receptor globulin. Int J Cancer 1998;75:919-24.
34. Bartolazzi A, Peach R, Aruffo A, Stamenkovic I. Interaction between CD44 and hyaluronate is directly implicated in the regulation of tumor development. J Exp Med 1994;180:53-66.
35. Zeng C, Toole BP, Kinney SD, Kuo JW, Stamenkovic I. Inhibition of tumor growth in vivo by hyaluronan oligomers. Int J Cancer 1998;77:396-401.
36. Bourguignon LY, Xia W, Wong G. Hyaluronan-mediated CD44 interaction with p300 and SIRT1 regulates beta -catenin signaling and NFkappa B -specific transcription activity leading to MDR1 and BCLl-XL gene expression and chemoresistance in breast tumor cells. J Biol Chem 2008.
37. Bourguignon LY. Hyaluronan-mediated CD44 activation of RhoGTPase signaling and cytoskeleton function promotes tumor progression. Semin Cancer Biol 2008;18:251-9.
38. Bourguignon LY, Gilad E, Peyrollier K. Heregulin-mediated ErbB2-ERK signaling activates hyaluronan synthases leading to CD44-dependent ovarian tumor cell growth and migration. J Biol Chem 2007;282:19426-41.
39. Seiter S, Arch R, Reber S, Komitowski D, Hofmann M, Ponta H, Herrlich P, Matzku S, Zoller M. Prevention of tumor metastasis formation by anti-variant CD44. J Exp Med 1993;177:443-55.

40. Sleeman JP, Arming S, Moll JF, Hekele A, Rudy W, Sherman LS, Kreil G, Ponta H, Herrlich P. Hyaluronate-independent metastatic behavior of CD44 variant-expressing pancreatic carcinoma cells. Cancer Res 1996;56:3134-41.
41. Thorne RF, Legg JW, Isacke CM. The role of the CD44 transmembrane and cytoplasmic domains in co-ordinating adhesive and signalling events. J Cell Sci 2004;117:373-80.
42. Peng ST, Su CH, Kuo CC, Shaw CF, Wang HS. CD44 crosslinking-mediated matrix metalloproteinase-9 relocation in breast tumor cells leads to enhanced metastasis. Int J Oncol 2007;31:1119-26.
43. Sugahara KN, Hirata T, Tanaka T, Ogino S, Takeda M, Terasawa H, Shimada I, Tamura J, ten Dam GB, van Kuppevelt TH, Miyasaka M. Chondroitin sulfate E fragments enhance CD44 cleavage and CD44-dependent motility in tumor cells. Cancer Res 2008;68:7191-9.
44. Glinsky VV, Glinsky GV, Glinskii OV, Huxley VH, Turk JR, Mossine VV, Deutscher SL, Pienta KJ, Quinn TP. Intravascular metastatic cancer cell homotypic aggregation at the sites of primary attachment to the endothelium. Cancer Res 2003;63:3805-11.
45. Saiki I, Naito S, Yoneda J, Azuma I, Price JE, Fidler IJ. Characterization of the invasive and metastatic phenotype in human renal cell carcinoma. Clin Exp Metastasis 1991;9:551-66.
46. Meromsky L, Lotan R, Raz A. Implications of endogenous tumor cell surface lectins as mediators of cellular interactions and lung colonization. Cancer Res 1986;46:5270-5.
47. Glinsky GV, Glinsky VV, Ivanova AB, Hueser CJ. Apoptosis and metastasis: increased apoptosis resistance of metastatic cancer cells is associated with the profound deficiency of apoptosis execution mechanisms. Cancer Lett 1997;115:185-93.
48. Fidler IJ. The relationship of embolic homogeneity, number, size and viability to the incidence of experimental metastasis. Eur J Cancer 1973;9:223-7.
49. Zhang Z, Han L, Cao L, Liang X, Liu Y, Liu H, Du J, Qu Z, Zhu C, Liu S, Li H, Sun W. Aggregation formation mediated anoikis resistance of BEL7402 hepatoma cells. Folia Histochem Cytobiol 2008;46:331-6.
50. Frisch SM, Screaton RA. Anoikis mechanisms. Curr Opin Cell Biol 2001;13:555-62.
51. Mehes G, Witt A, Kubista E, Ambros PF. Circulating breast cancer cells are frequently apoptotic. Am J Pathol 2001;159:17-20.
52. Chambers AF, Groom AC, MacDonald IC. Dissemination and growth of cancer cells in metastatic sites. Nat Rev Cancer 2002;2:563-72.
53. Luzzi KJ, MacDonald IC, Schmidt EE, Kerkvliet N, Morris VL, Chambers AF, Groom AC. Multistep nature of metastatic inefficiency: dormancy of solitary cells after successful extravasation and limited survival of early micrometastases. Am J Pathol 1998;153:865-73.
54. Fidler IJ. Metastasis: guantitative analysis of distribution and fate of tumor embolilabeled with 125 I-5-iodo-2'-deoxyuridine. J Natl Cancer Inst 1970;45:773-82.
55. Chambers AF, Naumov GN, Vantyghem SA, Tuck AB. Molecular biology of breast cancer metastasis. Clinical implications of experimental studies on metastatic inefficiency. Breast Cancer Res 2000;2:400-7.

56. Yawata A, Adachi M, Okuda H, Naishiro Y, Takamura T, Hareyama M, Takayama S, Reed JC, Imai K. Prolonged cell survival enhances peritoneal dissemination of gastric cancer cells. Oncogene 1998;16:2681-6.
57. Alattia JR, Kurokawa H, Ikura M. Structural view of cadherin-mediated cell-cell adhesion. Cell Mol Life Sci 1999;55:359-67.
58. Takeichi M. Morphogenetic roles of classic cadherins. Curr Opin Cell Biol 1995;7:619-27.
59. Imai T, Horiuchi A, Shiozawa T, Osada R, Kikuchi N, Ohira S, Oka K, Konishi I. Elevated expression of E-cadherin and alpha-, beta-, and gamma-catenins in metastatic lesions compared with primary epithelial ovarian carcinomas. Hum Pathol 2004;35:1469-76.
60. Kowalski PJ, Rubin MA, Kleer CG. E-cadherin expression in primary carcinomas of the breast and its distant metastases. Breast Cancer Res 2003;5:R217-22.
61. Putz E, Witter K, Offner S, Stosiek P, Zippelius A, Johnson J, Zahn R, Riethmuller G, Pantel K. Phenotypic characteristics of cell lines derived from disseminated cancer cells in bone marrow of patients with solid epithelial tumors: establishment of working models for human micrometastases. Cancer Res 1999;59:241-8.
62. Rubin MA, Mucci NR, Figurski J, Fecko A, Pienta KJ, Day ML. E-cadherin expression in prostate cancer: a broad survey using high-density tissue microarray technology. Hum Pathol 2001;32:690-7.
63. Menter DG, Fitzgerald L, Patton JT, McIntire LV, Nicolson GL. Human melanoma integrins contribute to arrest and stabilization potential while flowing over extracellular matrix. Immunol Cell Biol 1995;73:575-83.
64. Frisch SM, Francis H. Disruption of epithelial cell-matrix interactions induces apoptosis. J Cell Biol 1994;124:619-26.
65. Gassmann P, Haier J. The tumor cell-host organ interface in the early onset of metastatic organ colonisation. Clin Exp Metastasis 2008;25:171-81.
66. Simpson CD, Anyiwe K, Schimmer AD. Anoikis resistance and tumor metastasis. Cancer Lett 2008;272:177-85.
67. Gilmore AP. Anoikis. Cell Death Differ 2005;12 Suppl 2:1473-7.
68. Shimizu S, Narita M, Tsujimoto Y. Bcl-2 family proteins regulate the release of apoptogenic cytochrome c by the mitochondrial channel VDAC. Nature 1999;399:483-7.
69. Bouillet P, Strasser A. BH3-only proteins - evolutionarily conserved proapoptotic Bcl-2 family members essential for initiating programmed cell death. J Cell Sci 2002;115:1567-74.
70. Taylor RC, Cullen SP, Martin SJ. Apoptosis: controlled demolition at the cellular level. Nat Rev Mol Cell Biol 2008;9:231-41.
71. Chiarugi P, Giannoni E. Anoikis: a necessary death program for anchorage-dependent cells. Biochem Pharmacol 2008;76:1352-64.
72. Cohen GM. Caspases: the executioners of apoptosis. Biochem J 1997;326 (Pt 1):1-16.
73. Thornberry NA. Caspases: key mediators of apoptosis. Chem Biol 1998;5:R97-103.
74. Zou H, Henzel WJ, Liu X, Lutschg A, Wang X. Apaf-1, a human protein homologous to C. elegans CED-4, participates in cytochrome c-dependent activation of caspase-3. Cell 1997;90:405-13.

75. Cory S, Huang DC, Adams JM. The Bcl-2 family: roles in cell survival and oncogenesis. Oncogene 2003;22:8590-607.
76. Green DR, Kroemer G. The pathophysiology of mitochondrial cell death. Science 2004;305:626-9.
77. Gazaryan IG, Brown AM. Intersection between mitochondrial permeability pores and mitochondrial fusion/fission. Neurochem Res 2007;32:917-29.
78. Vander Heiden MG, Chandel NS, Williamson EK, Schumacker PT, Thompson CB. Bcl-xL regulates the membrane potential and volume homeostasis of mitochondria. Cell 1997;91:627-37.
79. Kuwana T, Bouchier-Hayes L, Chipuk JE, Bonzon C, Sullivan BA, Green DR, Newmeyer DD. BH3 domains of BH3-only proteins differentially regulate Bax-mediated mitochondrial membrane permeabilization both directly and indirectly. Mol Cell 2005;17:525-35.
80. Letai A, Bassik MC, Walensky LD, Sorcinelli MD, Weiler S, Korsmeyer SJ. Distinct BH3 domains either sensitize or activate mitochondrial apoptosis, serving as prototype cancer therapeutics. Cancer Cell 2002;2:183-92.
81. Wajant H. The Fas signaling pathway: more than a paradigm. Science 2002;296:1635-6.
82. Valentijn AJ, Gilmore AP. Translocation of full-length Bid to mitochondria during anoikis. J Biol Chem 2004;279:32848-57.
83. Rytomaa M, Martins LM, Downward J. Involvement of FADD and caspase-8 signalling in detachment-induced apoptosis. Curr Biol 1999;9:1043-6.
84. Grossmann J, Walther K, Artinger M, Kiessling S, Scholmerich J. Apoptotic signaling during initiation of detachment-induced apoptosis ("anoikis") of primary human intestinal epithelial cells. Cell Growth Differ 2001;12:147-55.
85. Rytomaa M, Lehmann K, Downward J. Matrix detachment induces caspase-dependent cytochrome c release from mitochondria: inhibition by PKB/Akt but not Raf signalling. Oncogene 2000;19:4461-8.
86. Zhang Y, Lu H, Dazin P, Kapila Y. Squamous cell carcinoma cell aggregates escape suspension-induced, p53-mediated anoikis: fibronectin and integrin alphav mediate survival signals through focal adhesion kinase. J Biol Chem 2004;279:48342-9.
87. Daubriac J, Fleury-Feith J, Kheuang L, Galipon J, Saint-Albin A, Renier A, Giovannini M, Galateau-Salle F, Jaurand MC. Malignant pleural mesothelioma cells resist anoikis as quiescent pluricellular aggregates. Cell Death Differ 2009;16:1146-55.
88. Hofmann C, Obermeier F, Artinger M, Hausmann M, Falk W, Schoelmerich J, Rogler G, Grossmann J. Cell-cell contacts prevent anoikis in primary human colonic epithelial cells. Gastroenterology 2007;132:587-600.
89. Brooks SA. Strategies for analysis of the glycosylation of proteins: current status and future perspectives. Mol Biotechnol 2009;43:76-88.
90. Haltiwanger RS, Lowe JB. Role of glycosylation in development. Annu Rev Biochem 2004;73:491-537.
91. Coltart DM, Royyuru AK, Williams LJ, Glunz PW, Sames D, Kuduk SD, Schwarz JB, Chen XT, Danishefsky SJ, Live DH. Principles of mucin architecture: structural studies on synthetic glycopeptides bearing clustered mono-, di-, tri-, and hexasaccharide glycodomains. J Am Chem Soc 2002;124:9833-44.
92. Hang HC, Bertozzi CR. The chemistry and biology of mucin-type O-linked glycosylation. Bioorg Med Chem 2005;13:5021-34.

93. Garner B, Merry AH, Royle L, Harvey DJ, Rudd PM, Thillet J. Structural elucidation of the N- and O-glycans of human apolipoprotein(a): role of o-glycans in conferring protease resistance. J Biol Chem 2001;276:22200-8.
94. Hanisch FG. O-glycosylation of the mucin type. Biol Chem 2001;382:143-9.
95. Brockhausen I. Pathways of O-glycan biosynthesis in cancer cells. Biochim Biophys Acta 1999;1473:67-95.
96. Danishefsky SJ, Allen JR. From the Laboratory to the Clinic: A Retrospective on Fully Synthetic Carbohydrate-Based Anticancer Vaccines Frequently used abbreviations are listed in the appendix. Angew Chem Int Ed Engl 2000;39:836-63.
97. Yu LG. The oncofetal Thomsen-Friedenreich carbohydrate antigen in cancer progression. Glycoconj J 2007;24:411-20.
98. Springer GF. T and Tn, general carcinoma autoantigens. Science 1984;224:1198-206.
99. Singh R, Campbell BJ, Yu LG, Fernig DG, Milton JD, Goodlad RA, FitzGerald AJ, Rhodes JM. Cell surface-expressed Thomsen-Friedenreich antigen in colon cancer is predominantly carried on high molecular weight splice variants of CD44. Glycobiology 2001;11:587-92.
100. Singh R, Subramanian S, Rhodes JM, Campbell BJ. Peanut lectin stimulates proliferation of colon cancer cells by interaction with glycosylated CD44v6 isoforms and consequential activation of c-Met and MAPK: functional implications for disease-associated glycosylation changes. Glycobiology 2006;16:594-601.
101. Hanisch FG, Baldus SE. The Thomsen-Friedenreich (TF) antigen: a critical review on the structural, biosynthetic and histochemical aspects of a pancarcinoma-associated antigen. Histol Histopathol 1997;12:263-81.
102. Baldus SE, Hanisch FG, Monaca E, Karsten UR, Zirbes TK, Thiele J, Dienes HP. Immunoreactivity of Thomsen-Friedenreich (TF) antigen in human neoplasms: the importance of carrier-specific glycotope expression on MUC1. Histol Histopathol 1999;14:1153-8.
103. Hanisch FG, Stadie T, Bosslet K. Monoclonal antibody BW835 defines a site-specific Thomsen-Friedenreich disaccharide linked to threonine within the VTSA motif of MUC1 tandem repeats. Cancer Res 1995;55:4036-40.
104. Karsten U, Butschak G, Cao Y, Goletz S, Hanisch FG. A new monoclonal antibody (A78-G/A7) to the Thomsen-Friedenreich pan-tumor antigen. Hybridoma 1995;14:37-44.
105. Baldus SE, Hanisch FG, Kotlarek GM, Zirbes TK, Thiele J, Isenberg J, Karsten UR, Devine PL, Dienes HP. Coexpression of MUC1 mucin peptide core and the Thomsen-Friedenreich antigen in colorectal neoplasms. Cancer 1998;82:1019-27.
106. Baldus SE, Zirbes TK, Glossmann J, Fromm S, Hanisch FG, Monig SP, Schroder W, Schneider PM, Flucke U, Karsten U, Thiele J, Holscher AH, Dienes HP. Immunoreactivity of monoclonal antibody BW835 represents a marker of progression and prognosis in early gastric cancer. Oncology 2001;61:147-55.
107. Baldus SE, Zirbes TK, Hanisch FG, Kunze D, Shafizadeh ST, Nolden S, Monig SP, Schneider PM, Karsten U, Thiele J, Holscher AH, Dienes HP. Thomsen-Friedenreich antigen presents as a prognostic factor in colorectal carcinoma: A clinicopathologic study of 264 patients. Cancer 2000;88:1536-43.
108. Ryder SD, Smith JA, Rhodes JM. Peanut lectin: a mitogen for normal human colonic epithelium and human HT29 colorectal cancer cells. J Natl Cancer Inst 1992;84:1410-6.

109. Ryder SD, Parker N, Ecclestone D, Haqqani MT, Rhodes JM. Peanut lectin stimulates proliferation in colonic explants from patients with inflammatory bowel disease and colon polyps. Gastroenterology 1994;106:117-24.
110. Yu LG, Milton JD, Fernig DG, Rhodes JM. Opposite effects on human colon cancer cell proliferation of two dietary Thomsen-Friedenreich antigen-binding lectins. J Cell Physiol 2001;186:282-7.
111. Yu LG, Fernig DG, White MR, Spiller DG, Appleton P, Evans RC, Grierson I, Smith JA, Davies H, Gerasimenko OV, Petersen OH, Milton JD, Rhodes JM. Edible mushroom (Agaricus bisporus) lectin, which reversibly inhibits epithelial cell proliferation, blocks nuclear localization sequence-dependent nuclear protein import. J Biol Chem 1999;274:4890-9.
112. Ryder SD, Smith JA, Rhodes EG, Parker N, Rhodes JM. Proliferative responses of HT29 and Caco2 human colorectal cancer cells to a panel of lectins. Gastroenterology 1994;106:85-93.
113. Inohara H, Akahani S, Raz A. Galectin-3 stimulates cell proliferation. Exp Cell Res 1998;245:294-302.
114. Maeda N, Kawada N, Seki S, Arakawa T, Ikeda K, Iwao H, Okuyama H, Hirabayashi J, Kasai K, Yoshizato K. Stimulation of proliferation of rat hepatic stellate cells by galectin-1 and galectin-3 through different intracellular signaling pathways. J Biol Chem 2003;278:18938-44.
115. Honjo Y, Nangia-Makker P, Inohara H, Raz A. Down-regulation of galectin-3 suppresses tumorigenicity of human breast carcinoma cells. Clin Cancer Res 2001;7:661-8.
116. Khaldoyanidi SK, Glinsky VV, Sikora L, Glinskii AB, Mossine VV, Quinn TP, Glinsky GV, Sriramarao P. MDA-MB-435 human breast carcinoma cell homo- and heterotypic adhesion under flow conditions is mediated in part by Thomsen-Friedenreich antigen-galectin-3 interactions. J Biol Chem 2003;278:4127-34.
117. Glinsky VV, Glinsky GV, Rittenhouse-Olson K, Huflejt ME, Glinskii OV, Deutscher SL, Quinn TP. The role of Thomsen-Friedenreich antigen in adhesion of human breast and prostate cancer cells to the endothelium. Cancer Res 2001;61:4851-7.
118. Glinsky VV, Huflejt ME, Glinsky GV, Deutscher SL, Quinn TP. Effects of Thomsen-Friedenreich antigen-specific peptide P-30 on beta-galactoside-mediated homotypic aggregation and adhesion to the endothelium of MDA-MB-435 human breast carcinoma cells. Cancer Res 2000;60:2584-8.
119. Evans RC, Fear S, Ashby D, Hackett A, Williams E, Van Der Vliet M, Dunstan FD, Rhodes JM. Diet and colorectal cancer: an investigation of the lectin/galactose hypothesis. Gastroenterology 2002;122:1784-92.
120. Liu FT, Rabinovich GA. Galectins as modulators of tumour progression. Nat Rev Cancer 2005;5:29-41.
121. Zou J, Glinsky VV, Landon LA, Matthews L, Deutscher SL. Peptides specific to the galectin-3 carbohydrate recognition domain inhibit metastasis-associated cancer cell adhesion. Carcinogenesis 2005;26:309-18.
122. Shigeoka H, Karsten U, Okuno K, Yasutomi M. Inhibition of liver metastases from neuraminidase-treated colon 26 cells by an anti-Thomsen-Friedenreich-specific monoclonal antibody. Tumour Biol 1999;20:139-46.
123. Yamashita K, Ohkura T, Tachibana Y, Takasaki S, Kobata A. Comparative study of the oligosaccharides released from baby hamster kidney cells and their polyoma transformant by hydrazinolysis. J Biol Chem 1984;259:10834-40.

124. Kobata A, Amano J. Altered glycosylation of proteins produced by malignant cells, and application for the diagnosis and immunotherapy of tumours. Immunol Cell Biol 2005;83:429-39.
125. Rhodes JM. Unifying hypothesis for inflammatory bowel disease and associated colon cancer: sticking the pieces together with sugar. Lancet 1996;347:40-4.
126. Boland CR, Deshmukh GD. The carbohydrate composition of mucin in colonic cancer. Gastroenterology 1990;98:1170-7.
127. Lloyd KO, Burchell J, Kudryashov V, Yin BW, Taylor-Papadimitriou J. Comparison of O-linked carbohydrate chains in MUC-1 mucin from normal breast epithelial cell lines and breast carcinoma cell lines. Demonstration of simpler and fewer glycan chains in tumor cells. J Biol Chem 1996;271:33325-34.
128. Brockhausen I, Yang JM, Burchell J, Whitehouse C, Taylor-Papadimitriou J. Mechanisms underlying aberrant glycosylation of MUC1 mucin in breast cancer cells. Eur J Biochem 1995;233:607-17.
129. Dahiya R, Itzkowitz SH, Byrd JC, Kim YS. Mucin oligosaccharide biosynthesis in human colonic cancerous tissues and cell lines. Cancer 1992;70:1467-76.
130. Egea G, Franci C, Gambus G, Lesuffleur T, Zweibaum A, Real FX. cis-Golgi resident proteins and O-glycans are abnormally compartmentalized in the RER of colon cancer cells. J Cell Sci 1993;105 (Pt 3):819-30.
131. Rottger S, White J, Wandall HH, Olivo JC, Stark A, Bennett EP, Whitehouse C, Berger EG, Clausen H, Nilsson T. Localization of three human polypeptide GalNAc-transferases in HeLa cells suggests initiation of O-linked glycosylation throughout the Golgi apparatus. J Cell Sci 1998;111 (Pt 1):45-60.
132. Kellokumpu S, Sormunen R, Kellokumpu I. Abnormal glycosylation and altered Golgi structure in colorectal cancer: dependence on intra-Golgi pH. FEBS Lett 2002;516:217-24.
133. Campbell BJ, Rowe GE, Leiper K, Rhodes JM. Increasing the intra-Golgi pH of cultured LS174T goblet-differentiated cells mimics the decreased mucin sulfation and increased Thomsen-Friedenreich antigen (Gal beta1-3GalNac alpha-) expression seen in colon cancer. Glycobiology 2001;11:385-93.
134. Rivinoja A, Kokkonen N, Kellokumpu I, Kellokumpu S. Elevated Golgi pH in breast and colorectal cancer cells correlates with the expression of oncofetal carbohydrate T-antigen. J Cell Physiol 2006;208:167-74.
135. Axelsson MA, Karlsson NG, Steel DM, Ouwendijk J, Nilsson T, Hansson GC. Neutralization of pH in the Golgi apparatus causes redistribution of glycosyltransferases and changes in the O-glycosylation of mucins. Glycobiology 2001;11:633-44.
136. Kuninaka S, Yano T, Yokoyama H, Fukuyama Y, Terazaki Y, Uehara T, Kanematsu T, Asoh H, Ichinose Y. Direct influences of pro-inflammatory cytokines (IL-1beta, TNF-alpha, IL-6) on the proliferation and cell-surface antigen expression of cancer cells. Cytokine 2000;12:8-11.
137. Campbell BJ, Yu LG, Rhodes JM. Altered glycosylation in inflammatory bowel disease: a possible role in cancer development. Glycoconj J 2001;18:851-8.
138. Flieger D, Hoff AS, Sauerbruch T, Schmidt-Wolf IG. Influence of cytokines, monoclonal antibodies and chemotherapeutic drugs on epithelial cell adhesion molecule (EpCAM) and LewisY antigen expression. Clin Exp Immunol 2001;123:9-14.

139. Wimmenauer S, Steiert A, Wolff-Vorbeck G, Xing B, Baier PK, Ruckauer KD, Kirste G, von Kleist S. Influence of cytokines on the expression of fas ligand and CD44 splice variants in colon carcinoma cells. Tumour Biol 1999;20:294-303.
140. Fernandes B, Sagman U, Auger M, Demetrio M, Dennis JW. Beta 1-6 branched oligosaccharides as a marker of tumor progression in human breast and colon neoplasia. Cancer Res 1991;51:718-23.
141. Granovsky M, Fata J, Pawling J, Muller WJ, Khokha R, Dennis JW. Suppression of tumor growth and metastasis in Mgat5-deficient mice. Nat Med 2000;6:306-12.
142. Asada M, Furukawa K, Segawa K, Endo T, Kobata A. Increased expression of highly branched N-glycans at cell surface is correlated with the malignant phenotypes of mouse tumor cells. Cancer Res 1997;57:1073-80.
143. Demetriou M, Nabi IR, Coppolino M, Dedhar S, Dennis JW. Reduced contact-inhibition and substratum adhesion in epithelial cells expressing GlcNAc-transferase V. J Cell Biol 1995;130:383-92.
144. Ono M, Sakamoto M, Ino Y, Moriya Y, Sugihara K, Muto T, Hirohashi S. Cancer cell morphology at the invasive front and expression of cell adhesion-related carbohydrate in the primary lesion of patients with colorectal carcinoma with liver metastasis. Cancer 1996;78:1179-86.
145. Koprowski H, Herlyn M, Steplewski Z, Sears HF. Specific antigen in serum of patients with colon carcinoma. Science 1981;212:53-5.
146. Nakagoe T, Fukushima K, Hirota M, Kusano H, Kawahara K, Ayabe H, Tomita M, Kamihira S. Immunohistochemical expression of blood group substances and related carbohydrate antigens in breast carcinoma. Jpn J Cancer Res 1991;82:559-68.
147. Magnani JL. The discovery, biology, and drug development of sialyl Lea and sialyl Lex. Arch Biochem Biophys 2004;426:122-31.
148. Irimura T, Nakamori S, Matsushita Y, Taniuchi Y, Todoroki N, Tsuji T, Izumi Y, Kawamura Y, Hoff SD, Cleary KR, et al. Colorectal cancer metastasis determined by carbohydrate-mediated cell adhesion: role of sialyl-LeX antigens. Semin Cancer Biol 1993;4:319-24.
149. Ono M, Hakomori S. Glycosylation defining cancer cell motility and invasiveness. Glycoconj J 2004;20:71-8.
150. Kim YS, Gum J, Jr., Brockhausen I. Mucin glycoproteins in neoplasia. Glycoconj J 1996;13:693-707.
151. Kim YJ, Varki A. Perspectives on the significance of altered glycosylation of glycoproteins in cancer. Glycoconj J 1997;14:569-76.
152. Thor A, Ohuchi N, Szpak CA, Johnston WW, Schlom J. Distribution of oncofetal antigen tumor-associated glycoprotein-72 defined by monoclonal antibody B72.3. Cancer Res 1986;46:3118-24.
153. Miles DW, Happerfield LC, Smith P, Gillibrand R, Bobrow LG, Gregory WM, Rubens RD. Expression of sialyl-Tn predicts the effect of adjuvant chemotherapy in node-positive breast cancer. Br J Cancer 1994;70:1272-5.
154. Kijima-Suda I, Miyamoto Y, Toyoshima S, Itoh M, Osawa T. Inhibition of experimental pulmonary metastasis of mouse colon adenocarcinoma 26 sublines by a sialic acid:nucleoside conjugate having sialyltransferase inhibiting activity. Cancer Res 1986;46:858-62.
155. Bresalier RS, Niv Y, Byrd JC, Duh QY, Toribara NW, Rockwell RW, Dahiya R, Kim YS. Mucin production by human colonic carcinoma cells correlates

with their metastatic potential in animal models of colon cancer metastasis. J Clin Invest 1991;87:1037-45.
156. Engel E, Guth PH, Nishizaki Y, Kaunitz JD. Barrier function of the gastric mucus gel. Am J Physiol 1995;269:G994-9.
157. Byrd JC, Bresalier RS. Mucins and mucin binding proteins in colorectal cancer. Cancer Metastasis Rev 2004;23:77-99.
158. Perez-Vilar J, Hill R, editors. "Mucin Family of Glycoproteins". Encyclopedia of Biological Chemistry (Lennarz & Lane, EDs.) 2004 ed; 2004.
159. Itoh Y, Kamata-Sakurai M, Denda-Nagai K, Nagai S, Tsuiji M, Ishii-Schrade K, Okada K, Goto A, Fukayama M, Irimura T. Identification and expression of human epiglycanin/MUC21: a novel transmembrane mucin. Glycobiology 2008;18:74-83.
160. Kerschner JE, Khampang P, Erbe CB, Kolker A, Cioffi JA. Mucin gene 19 (MUC19) expression and response to inflammatory cytokines in middle ear epithelium. Glycoconj J 2009.
161. Higuchi T, Orita T, Nakanishi S, Katsuya K, Watanabe H, Yamasaki Y, Waga I, Nanayama T, Yamamoto Y, Munger W, Sun HW, Falk RJ, Jennette JC, Alcorta DA, Li H, Yamamoto T, Saito Y, Nakamura M. Molecular cloning, genomic structure, and expression analysis of MUC20, a novel mucin protein, up-regulated in injured kidney. J Biol Chem 2004;279:1968-79.
162. Taylor-Papadimitriou J, Burchell J, Miles DW, Dalziel M. MUC1 and cancer. Biochim Biophys Acta 1999;1455:301-13.
163. Burchell JM, Mungul A, Taylor-Papadimitriou J. O-linked glycosylation in the mammary gland: changes that occur during malignancy. J Mammary Gland Biol Neoplasia 2001;6:355-64.
164. Gendler SJ. MUC1, the renaissance molecule. J Mammary Gland Biol Neoplasia 2001;6:339-53.
165. Bramwell ME, Wiseman G, Shotton DM. Electron-microscopic studies of the CA antigen, epitectin. J Cell Sci 1986;86:249-61.
166. Tarp MA, Clausen H. Mucin-type O-glycosylation and its potential use in drug and vaccine development. Biochim Biophys Acta 2008;1780:546-63.
167. Baldus SE, Engelmann K, Hanisch FG. MUC1 and the MUCs: a family of human mucins with impact in cancer biology. Crit Rev Clin Lab Sci 2004;41:189-231.
168. Kinarsky L, Suryanarayanan G, Prakash O, Paulsen H, Clausen H, Hanisch FG, Hollingsworth MA, Sherman S. Conformational studies on the MUC1 tandem repeat glycopeptides: implication for the enzymatic O-glycosylation of the mucin protein core. Glycobiology 2003;13:929-39.
169. Wandall HH, Hassan H, Mirgorodskaya E, Kristensen AK, Roepstorff P, Bennett EP, Nielsen PA, Hollingsworth MA, Burchell J, Taylor-Papadimitriou J, Clausen H. Substrate specificities of three members of the human UDP-N-acetyl-alpha-D-galactosamine:Polypeptide N-acetylgalactosaminyltransferase family, GalNAc-T1, -T2, and -T3. J Biol Chem 1997;272:23503-14.
170. Hanisch FG, Muller S, Hassan H, Clausen H, Zachara N, Gooley AA, Paulsen H, Alving K, Peter-Katalinic J. Dynamic epigenetic regulation of initial O-glycosylation by UDP-N-Acetylgalactosamine:Peptide N-acetylgalactosaminyltransferases. site-specific glycosylation of MUC1 repeat peptide influences the substrate qualities at adjacent or distant Ser/Thr positions. J Biol Chem 1999;274:9946-54.

171. Bennett EP, Hassan H, Mandel U, Mirgorodskaya E, Roepstorff P, Burchell J, Taylor-Papadimitriou J, Hollingsworth MA, Merkx G, van Kessel AG, Eiberg H, Steffensen R, Clausen H. Cloning of a human UDP-N-acetyl-alpha-D-Galactosamine:polypeptide N-acetylgalactosaminyltransferase that complements other GalNAc-transferases in complete O-glycosylation of the MUC1 tandem repeat. J Biol Chem 1998;273:30472-81.
172. Mather IH, Jack LJ, Madara PJ, Johnson VG. The distribution of MUC1, an apical membrane glycoprotein, in mammary epithelial cells at the resolution of the electron microscope: implications for the mechanism of milk secretion. Cell Tissue Res 2001;304:91-101.
173. Ho SB, Niehans GA, Lyftogt C, Yan PS, Cherwitz DL, Gum ET, Dahiya R, Kim YS. Heterogeneity of mucin gene expression in normal and neoplastic tissues. Cancer Res 1993;53:641-51.
174. Wesseling J, van der Valk SW, Vos HL, Sonnenberg A, Hilkens J. Episialin (MUC1) overexpression inhibits integrin-mediated cell adhesion to extracellular matrix components. J Cell Biol 1995;129:255-65.
175. Wesseling J, van der Valk SW, Hilkens J. A mechanism for inhibition of E-cadherin-mediated cell-cell adhesion by the membrane-associated mucin episialin/MUC1. Mol Biol Cell 1996;7:565-77.
176. Yonezawa S, Goto M, Yamada N, Higashi M, Nomoto M. Expression profiles of MUC1, MUC2, and MUC4 mucins in human neoplasms and their relationship with biological behavior. Proteomics 2008;8:3329-41.
177. Nakamori S, Ota DM, Cleary KR, Shirotani K, Irimura T. MUC1 mucin expression as a marker of progression and metastasis of human colorectal carcinoma. Gastroenterology 1994;106:353-61.
178. Burchell J, Poulsom R, Hanby A, Whitehouse C, Cooper L, Clausen H, Miles D, Taylor-Papadimitriou J. An alpha2,3 sialyltransferase (ST3Gal I) is elevated in primary breast carcinomas. Glycobiology 1999;9:1307-11.
179. Whitehouse C, Burchell J, Gschmeissner S, Brockhausen I, Lloyd KO, Taylor-Papadimitriou J. A transfected sialyltransferase that is elevated in breast cancer and localizes to the medial/trans-Golgi apparatus inhibits the development of core-2-based O-glycans. J Cell Biol 1997;137:1229-41.
180. Kondo K, Kohno N, Yokoyama A, Hiwada K. Decreased MUC1 expression induces E-cadherin-mediated cell adhesion of breast cancer cell lines. Cancer Res 1998;58:2014-9.
181. Hilkens J, Ligtenberg MJ, Vos HL, Litvinov SV. Cell membrane-associated mucins and their adhesion-modulating property. Trends Biochem Sci 1992;17:359-63.
182. Ligtenberg MJ, Buijs F, Vos HL, Hilkens J. Suppression of cellular aggregation by high levels of episialin. Cancer Res 1992;52:2318-24.
183. Hynes RO. Integrins: versatility, modulation, and signaling in cell adhesion. Cell 1992;69:11-25.
184. Becker JW, Erickson HP, Hoffman S, Cunningham BA, Edelman GM. Topology of cell adhesion molecules. Proc Natl Acad Sci U S A 1989;86:1088-92.
185. Regimbald LH, Pilarski LM, Longenecker BM, Reddish MA, Zimmermann G, Hugh JC. The breast mucin MUCI as a novel adhesion ligand for endothelial intercellular adhesion molecule 1 in breast cancer. Cancer Res 1996;56:4244-9.
186. Kam JL, Regimbald LH, Hilgers JH, Hoffman P, Krantz MJ, Longenecker BM, Hugh JC. MUC1 synthetic peptide inhibition of intercellular adhesion

molecule-1 and MUC1 binding requires six tandem repeats. Cancer Res 1998;58:5577-81.
187. Rahn JJ, Shen Q, Mah BK, Hugh JC. MUC1 initiates a calcium signal after ligation by intercellular adhesion molecule-1. J Biol Chem 2004;279:29386-90.
188. Rahn JJ, Chow JW, Horne GJ, Mah BK, Emerman JT, Hoffman P, Hugh JC. MUC1 mediates transendothelial migration in vitro by ligating endothelial cell ICAM-1. Clin Exp Metastasis 2005;22:475-83.
189. Shen Q, Rahn JJ, Zhang J, Gunasekera N, Sun X, Shaw AR, Hendzel MJ, Hoffman P, Bernier A, Hugh JC. MUC1 initiates Src-CrkL-Rac1/Cdc42-mediated actin cytoskeletal protrusive motility after ligating intercellular adhesion molecule-1. Mol Cancer Res 2008;6:555-67.
190. McDermott KM, Crocker PR, Harris A, Burdick MD, Hinoda Y, Hayashi T, Imai K, Hollingsworth MA. Overexpression of MUC1 reconfigures the binding properties of tumor cells. Int J Cancer 2001;94:783-91.
191. Lahav G. Oscillations by the p53-Mdm2 feedback loop. Adv Exp Med Biol 2008;641:28-38.
192. Wei X, Xu H, Kufe D. Human mucin 1 oncoprotein represses transcription of the p53 tumor suppressor gene. Cancer Res 2007;67:1853-8.
193. Yamamoto M, Bharti A, Li Y, Kufe D. Interaction of the DF3/MUC1 breast carcinoma-associated antigen and beta-catenin in cell adhesion. J Biol Chem 1997;272:12492-4.
194. Takahashi-Yanaga F, Sasaguri T. The Wnt/beta-catenin signaling pathway as a target in drug discovery. J Pharmacol Sci 2007;104:293-302.
195. Singh PK, Hollingsworth MA. Cell surface-associated mucins in signal transduction. Trends Cell Biol 2006;16:467-76.
196. Yin L, Li Y, Ren J, Kuwahara H, Kufe D. Human MUC1 carcinoma antigen regulates intracellular oxidant levels and the apoptotic response to oxidative stress. J Biol Chem 2003;278:35458-64.
197. Demetter P, Nagy N, Martin B, Mathieu A, Dumont P, Decaestecker C, Salmon I. The galectin family and digestive disease. J Pathol 2008;215:1-12.
198. Leffler H, Carlsson S, Hedlund M, Qian Y, Poirier F. Introduction to galectins. Glycoconj J 2004;19:433-40.
199. Liu FT, Hsu DK, Zuberi RI, Kuwabara I, Chi EY, Henderson WR, Jr. Expression and function of galectin-3, a beta-galactoside-binding lectin, in human monocytes and macrophages. Am J Pathol 1995;147:1016-28.
200. Lotan R, Ito H, Yasui W, Yokozaki H, Lotan D, Tahara E. Expression of a 31-kDa lactoside-binding lectin in normal human gastric mucosa and in primary and metastatic gastric carcinomas. Int J Cancer 1994;56:474-80.
201. Greco C, Vona R, Cosimelli M, Matarrese P, Straface E, Scordati P, Giannarelli D, Casale V, Assisi D, Mottolese M, Moles A, Malorni W. Cell surface overexpression of galectin-3 and the presence of its ligand 90k in the blood plasma as determinants in colon neoplastic lesions. Glycobiology 2004;14:783-92.
202. Castronovo V, Van Den Brule FA, Jackers P, Clausse N, Liu FT, Gillet C, Sobel ME. Decreased expression of galectin-3 is associated with progression of human breast cancer. J Pathol 1996;179:43-8.
203. Pacis RA, Pilat MJ, Pienta KJ, Wojno K, Raz A, Hogan V, Cooper CR. Decreased galectin-3 expression in prostate cancer. Prostate 2000;44:118-23.
204. Konstantinov KN, Robbins BA, Liu FT. Galectin-3, a beta-galactoside-binding animal lectin, is a marker of anaplastic large-cell lymphoma. Am J Pathol 1996;148:25-30.

205. Xu XC, el-Naggar AK, Lotan R. Differential expression of galectin-1 and galectin-3 in thyroid tumors. Potential diagnostic implications. Am J Pathol 1995;147:815-22.
206. Idikio H. Galectin-3 expression in human breast carcinoma: correlation with cancer histologic grade. Int J Oncol 1998;12:1287-90.
207. van den Brule FA, Buicu C, Berchuck A, Bast RC, Deprez M, Liu FT, Cooper DN, Pieters C, Sobel ME, Castronovo V. Expression of the 67-kD laminin receptor, galectin-1, and galectin-3 in advanced human uterine adenocarcinoma. Hum Pathol 1996;27:1185-91.
208. Inohara H, Raz A. Identification of human melanoma cellular and secreted ligands for galectin-3. Biochem Biophys Res Commun 1994;201:1366-75.
209. Iurisci I, Tinari N, Natoli C, Angelucci D, Cianchetti E, Iacobelli S. Concentrations of galectin-3 in the sera of normal controls and cancer patients. Clin Cancer Res 2000;6:1389-93.
210. Hughes RC. Secretion of the galectin family of mammalian carbohydrate-binding proteins. Biochim Biophys Acta 1999;1473:172-85.
211. Takenaka Y, Fukumori T, Raz A. Galectin-3 and metastasis. Glycoconj J 2004;19:543-9.
212. Yang RY, Hsu DK, Liu FT. Expression of galectin-3 modulates T-cell growth and apoptosis. Proc Natl Acad Sci U S A 1996;93:6737-42.
213. Nakahara S, Oka N, Raz A. On the role of galectin-3 in cancer apoptosis. Apoptosis 2005;10:267-75.
214. Cecchinelli B, Lavra L, Rinaldo C, Iacovelli S, Gurtner A, Gasbarri A, Ulivieri A, Del Prete F, Trovato M, Piaggio G, Bartolazzi A, Soddu S, Sciacchitano S. Repression of the antiapoptotic molecule galectin-3 by homeodomain-interacting protein kinase 2-activated p53 is required for p53-induced apoptosis. Mol Cell Biol 2006;26:4746-57.
215. Elad-Sfadia G, Haklai R, Balan E, Kloog Y. Galectin-3 augments K-Ras activation and triggers a Ras signal that attenuates ERK but not phosphoinositide 3-kinase activity. J Biol Chem 2004;279:34922-30.
216. Delhalle S, Blasius R, Dicato M, Diederich M. A beginner's guide to NF-kappaB signaling pathways. Ann N Y Acad Sci 2004;1030:1-13.
217. Dumic J, Lauc G, Flogel M. Expression of galectin-3 in cells exposed to stress-roles of jun and NF-kappaB. Cell Physiol Biochem 2000;10:149-58.
218. Liu L, Sakai T, Sano N, Fukui K. Nucling mediates apoptosis by inhibiting expression of galectin-3 through interference with nuclear factor kappaB signalling. Biochem J 2004;380:31-41.
219. Moon BK, Lee YJ, Battle P, Jessup JM, Raz A, Kim HR. Galectin-3 protects human breast carcinoma cells against nitric oxide-induced apoptosis: implication of galectin-3 function during metastasis. Am J Pathol 2001;159:1055-60.
220. Dagher SF, Wang JL, Patterson RJ. Identification of galectin-3 as a factor in pre-mRNA splicing. Proc Natl Acad Sci U S A 1995;92:1213-7.
221. Yoshii T, Inohara H, Takenaka Y, Honjo Y, Akahani S, Nomura T, Raz A, Kubo T. Galectin-3 maintains the transformed phenotype of thyroid papillary carcinoma cells. Int J Oncol 2001;18:787-92.
222. Takenaka Y, Inohara H, Yoshii T, Oshima K, Nakahara S, Akahani S, Honjo Y, Yamamoto Y, Raz A, Kubo T. Malignant transformation of thyroid follicular cells by galectin-3. Cancer Lett 2003;195:111-9.

223. Ballin M, Gomez DE, Sinha CC, Thorgeirsson UP. Ras oncogene mediated induction of a 92 kDa metalloproteinase; strong correlation with the malignant phenotype. Biochem Biophys Res Commun 1988;154:832-8.
224. Fridman M, Tikoo A, Varga M, Murphy A, Nur EKMS, Maruta H. The minimal fragments of c-Raf-1 and NF1 that can suppress v-Ha-Ras-induced malignant phenotype. J Biol Chem 1994;269:30105-8.
225. Rabinovich GA, Cumashi A, Bianco GA, Ciavardelli D, Iurisci I, D'Egidio M, Piccolo E, Tinari N, Nifantiev N, Iacobelli S. Synthetic lactulose amines: novel class of anticancer agents that induce tumor-cell apoptosis and inhibit galectin-mediated homotypic cell aggregation and endothelial cell morphogenesis. Glycobiology 2006;16:210-20.
226. Inufusa H, Nakamura M, Adachi T, Aga M, Kurimoto M, Nakatani Y, Wakano T, Miyake M, Okuno K, Shiozaki H, Yasutomi M. Role of galectin-3 in adenocarcinoma liver metastasis. Int J Oncol 2001;19:913-9.
227. O'Driscoll L, Linehan R, Liang YH, Joyce H, Oglesby I, Clynes M. Galectin-3 expression alters adhesion, motility and invasion in a lung cell line (DLKP), in vitro. Anticancer Res 2002;22:3117-25.
228. Matarrese P, Fusco O, Tinari N, Natoli C, Liu FT, Semeraro ML, Malorni W, Iacobelli S. Galectin-3 overexpression protects from apoptosis by improving cell adhesion properties. Int J Cancer 2000;85:545-54.
229. Ochieng J, Leite-Browning ML, Warfield P. Regulation of cellular adhesion to extracellular matrix proteins by galectin-3. Biochem Biophys Res Commun 1998;246:788-91.
230. Hughes RC. Galectins as modulators of cell adhesion. Biochimie 2001;83:667-76.
231. Kuwabara I, Sano H, Liu FT. Functions of galectins in cell adhesion and chemotaxis. Methods Enzymol 2003;363:532-52.
232. Ochieng J, Furtak V, Lukyanov P. Extracellular functions of galectin-3. Glycoconj J 2004;19:527-35.
233. Le Marer N, Hughes RC. Effects of the carbohydrate-binding protein galectin-3 on the invasiveness of human breast carcinoma cells. J Cell Physiol 1996;168:51-8.
234. Hittelet A, Legendre H, Nagy N, Bronckart Y, Pector JC, Salmon I, Yeaton P, Gabius HJ, Kiss R, Camby I. Upregulation of galectins-1 and -3 in human colon cancer and their role in regulating cell migration. Int J Cancer 2003;103:370-9.
235. Vereecken P, Zouaoui Boudjeltia K, Debray C, Awada A, Legssyer I, Sales F, Petein M, Vanhaeverbeek M, Ghanem G, Heenen M. High serum galectin-3 in advanced melanoma: preliminary results. Clin Exp Dermatol 2006;31:105-9.
236. Saussez S, Glinoer D, Chantrain G, Pattou F, Carnaille B, Andre S, Gabius HJ, Laurent G. Serum galectin-1 and galectin-3 levels in benign and malignant nodular thyroid disease. Thyroid 2008;18:705-12.
237. Sakaki M, Oka N, Nakanishi R, Yamaguchi K, Fukumori T, Kanayama HO. Serum level of galectin-3 in human bladder cancer. J Med Invest 2008;55:127-32.
238. Saussez S, Lorfevre F, Lequeux T, Laurent G, Chantrain G, Vertongen F, Toubeau G, Decaestecker C, Kiss R. The determination of the levels of circulating galectin-1 and -3 in HNSCC patients could be used to monitor tumor progression and/or responses to therapy. Oral Oncol 2008;44:86-93.
239. Vereecken P, Heenen M. Serum galectin-3 in advanced melanoma patients: a hypothesis on a possible role in melanoma progression and inflammation. J Int Med Res 2006;34:119-20.

240. Petrakou E, Murray A, Price MR. Epitope mapping of anti-MUC1 mucin protein core monoclonal antibodies. Tumour Biol 1998;19 Suppl 1:21-9.
241. Yu LG, Jansson B, Fernig DG, Milton JD, Smith JA, Gerasimenko OV, Jones M, Rhodes JM. Stimulation of proliferation in human colon cancer cells by human monoclonal antibodies against the TF antigen (galactose beta1-3 N-acetyl-galactosamine). Int J Cancer 1997;73:424-31.
242. Brattain MG, Brattain DE, Sarrif AM, McRae LJ, Fine WD, Hawkins JG. Enhancement of growth of human colon tumor cell lines by feeder layers of murine fibroblasts. J Natl Cancer Inst 1982;69:767-71.
243. Sheikh S, Rainger GE, Gale Z, Rahman M, Nash GB. Exposure to fluid shear stress modulates the ability of endothelial cells to recruit neutrophils in response to tumor necrosis factor-alpha: a basis for local variations in vascular sensitivity to inflammation. Blood 2003;102:2828-34.
244. Sheikh S, Rahman M, Gale Z, Luu NT, Stone PC, Matharu NM, Rainger GE, Nash GB. Differing mechanisms of leukocyte recruitment and sensitivity to conditioning by shear stress for endothelial cells treated with tumour necrosis factor-alpha or interleukin-1beta. Br J Pharmacol 2005;145:1052-61.
245. Jaffe EA, Nachman RL, Becker CG, Minick CR. Culture of human endothelial cells derived from umbilical veins. Identification by morphologic and immunologic criteria. J Clin Invest 1973;52:2745-56.
246. Cooke BM, Usami S, Perry I, Nash GB. A simplified method for culture of endothelial cells and analysis of adhesion of blood cells under conditions of flow. Microvasc Res 1993;45:33-45.
247. Miles FL, Pruitt FL, van Golen KL, Cooper CR. Stepping out of the flow: capillary extravasation in cancer metastasis. Clin Exp Metastasis 2008;25:305-24.
248. Yu LG, Andrews N, Zhao Q, McKean D, Williams JF, Connor LJ, Gerasimenko OV, Hilkens J, Hirabayashi J, Kasai K, Rhodes JM. Galectin-3 interaction with Thomsen-Friedenreich disaccharide on cancer-associated MUC1 causes increased cancer cell endothelial adhesion. J Biol Chem 2007;282:773-81.
249. Leteurtre E, Gouyer V, Rousseau K, Moreau O, Barbat A, Swallow D, Huet G, Lesuffleur T. Differential mucin expression in colon carcinoma HT-29 clones with variable resistance to 5-fluorouracil and methotrexate. Biol Cell 2004;96:145-51.
250. Schol DJ, Meulenbroek MF, Snijdewint FG, von Mensdorff-Pouilly S, Verstraeten RA, Murakami F, Kenemans P, Hilgers J. 'Epitope fingerprinting' using overlapping 20-mer peptides of the MUC1 tandem repeat sequence. Tumour Biol 1998;19 Suppl 1:35-45.
251. Grinstead JS, Koganty RR, Krantz MJ, Longenecker BM, Campbell AP. Effect of glycosylation on MUC1 humoral immune recognition: NMR studies of MUC1 glycopeptide-antibody interactions. Biochemistry 2002;41:9946-61.
252. Draffin JE, McFarlane S, Hill A, Johnston PG, Waugh DJ. CD44 potentiates the adherence of metastatic prostate and breast cancer cells to bone marrow endothelial cells. Cancer Res 2004;64:5702-11.
253. Fujisaki T, Tanaka Y, Fujii K, Mine S, Saito K, Yamada S, Yamashita U, Irimura T, Eto S. CD44 stimulation induces integrin-mediated adhesion of colon cancer cell lines to endothelial cells by up-regulation of integrins and c-Met and activation of integrins. Cancer Res 1999;59:4427-34.
254. Ligtenberg MJ, Vos HL, Gennissen AM, Hilkens J. Episialin, a carcinoma-associated mucin, is generated by a polymorphic gene encoding splice variants with alternative amino termini. J Biol Chem 1990;265:5573-8.

255. Krause T, Turner GA. Are selectins involved in metastasis? Clin Exp Metastasis 1999;17:183-92.
256. Zhang K, Baeckstrom D, Brevinge H, Hansson GC. Secreted MUC1 mucins lacking their cytoplasmic part and carrying sialyl-Lewis a and x epitopes from a tumor cell line and sera of colon carcinoma patients can inhibit HL-60 leukocyte adhesion to E-selectin-expressing endothelial cells. J Cell Biochem 1996;60:538-49.
257. Lowe JB. Glycan-dependent leukocyte adhesion and recruitment in inflammation. Curr Opin Cell Biol 2003;15:531-8.
258. Li YS, Kaneko M, Sakamoto DG, Takeshima Y, Inai K. The reversed apical pattern of MUC1 expression is characteristics of invasive micropapillary carcinoma of the breast. Breast Cancer 2006;13:58-63.
259. Kurtenkov O, Klaamas K, Mensdorff-Pouilly S, Miljukhina L, Shljapnikova L, Chuzmarov V. Humoral immune response to MUC1 and to the Thomsen-Friedenreich (TF) glycotope in patients with gastric cancer: relation to survival. Acta Oncol 2007;46:316-23.
260. Baldus SE, Wienand JR, Werner JP, Landsberg S, Drebber U, Hanisch FG, Dienes HP. Expression of MUC1, MUC2 and oligosaccharide epitopes in breast cancer: prognostic significance of a sialylated MUC1 epitope. Int J Oncol 2005;27:1289-97.
261. Heimburg J, Yan J, Morey S, Glinskii OV, Huxley VH, Wild L, Klick R, Roy R, Glinsky VV, Rittenhouse-Olson K. Inhibition of spontaneous breast cancer metastasis by anti-Thomsen-Friedenreich antigen monoclonal antibody JAA-F11. Neoplasia 2006;8:939-48.
262. Gorelik E, Galili U, Raz A. On the role of cell surface carbohydrates and their binding proteins (lectins) in tumor metastasis. Cancer Metastasis Rev 2001;20:245-77.
263. Albini A, Mirisola V, Pfeffer U. Metastasis signatures: genes regulating tumor-microenvironment interactions predict metastatic behavior. Cancer Metastasis Rev 2008;27:75-83.
264. Finak G, Bertos N, Pepin F, Sadekova S, Souleimanova M, Zhao H, Chen H, Omeroglu G, Meterissian S, Omeroglu A, Hallett M, Park M. Stromal gene expression predicts clinical outcome in breast cancer. Nat Med 2008;14:518-27.
265. Bresalier RS, Mazurek N, Sternberg LR, Byrd JC, Yunker CK, Nangia-Makker P, Raz A. Metastasis of human colon cancer is altered by modifying expression of the beta-galactoside-binding protein galectin 3. Gastroenterology 1998;115:287-96.
266. Mourad-Zeidan AA, Melnikova VO, Wang H, Raz A, Bar-Eli M. Expression profiling of Galectin-3-depleted melanoma cells reveals its major role in melanoma cell plasticity and vasculogenic mimicry. Am J Pathol 2008;173:1839-52.
267. Pantel K, Brakenhoff RH. Dissecting the metastatic cascade. Nat Rev Cancer 2004;4:448-56.
268. Zhao Q, Guo X, Nash GB, Stone PC, Hilkens J, Rhodes JM, Yu LG. Circulating galectin-3 promotes metastasis by modifying MUC1 localization on cancer cell surface. Cancer Res 2009;69:6799-806.
269. Larue L, Ohsugi M, Hirchenhain J, Kemler R. E-cadherin null mutant embryos fail to form a trophectoderm epithelium. Proc Natl Acad Sci U S A 1994;91:8263-7.
270. Yu L, Fernig DG, Smith JA, Milton JD, Rhodes JM. Reversible inhibition of proliferation of epithelial cell lines by Agaricus bisporus (edible mushroom) lectin. Cancer Res 1993;53:4627-32.

271. Yu LG, Packman LC, Weldon M, Hamlett J, Rhodes JM. Protein phosphatase 2A, a negative regulator of the ERK signaling pathway, is activated by tyrosine phosphorylation of putative HLA class II-associated protein I (PHAPI)/pp32 in response to the antiproliferative lectin, jacalin. J Biol Chem 2004;279:41377-83.
272. Lotan R, Skutelsky E, Danon D, Sharon N. The purification, composition, and specificity of the anti-T lectin from peanut (Arachis hypogaea). J Biol Chem 1975;250:8518-23.
273. Ryder SD, Jacyna MR, Levi AJ, Rizzi PM, Rhodes JM. Peanut ingestion increases rectal proliferation in individuals with mucosal expression of peanut lectin receptor. Gastroenterology 1998;114:44-9.
274. Wang Q, Yu LG, Campbell BJ, Milton JD, Rhodes JM. Identification of intact peanut lectin in peripheral venous blood. Lancet 1998;352:1831-2.
275. Meng S, Tripathy D, Frenkel EP, Shete S, Naftalis EZ, Huth JF, Beitsch PD, Leitch M, Hoover S, Euhus D, Haley B, Morrison L, Fleming TP, Herlyn D, Terstappen LW, Fehm T, Tucker TF, Lane N, Wang J, Uhr JW. Circulating tumor cells in patients with breast cancer dormancy. Clin Cancer Res 2004;10:8152-62.
276. Muller V, Stahmann N, Riethdorf S, Rau T, Zabel T, Goetz A, Janicke F, Pantel K. Circulating tumor cells in breast cancer: correlation to bone marrow micrometastases, heterogeneous response to systemic therapy and low proliferative activity. Clin Cancer Res 2005;11:3678-85.
277. Paterlini-Brechot P, Benali NL. Circulating tumor cells (CTC) detection: clinical impact and future directions. Cancer Lett 2007;253:180-204.
278. Cristofanilli M, Budd GT, Ellis MJ, Stopeck A, Matera J, Miller MC, Reuben JM, Doyle GV, Allard WJ, Terstappen LW, Hayes DF. Circulating tumor cells, disease progression, and survival in metastatic breast cancer. N Engl J Med 2004;351:781-91.
279. Hayes DF, Cristofanilli M, Budd GT, Ellis MJ, Stopeck A, Miller MC, Matera J, Allard WJ, Doyle GV, Terstappen LW. Circulating tumor cells at each follow-up time point during therapy of metastatic breast cancer patients predict progression-free and overall survival. Clin Cancer Res 2006;12:4218-24.
280. Ohannesian DW, Lotan D, Thomas P, Jessup JM, Fukuda M, Gabius HJ, Lotan R. Carcinoembryonic antigen and other glycoconjugates act as ligands for galectin-3 in human colon carcinoma cells. Cancer Res 1995;55:2191-9.
281. Lagana A, Goetz JG, Cheung P, Raz A, Dennis JW, Nabi IR. Galectin binding to Mgat5-modified N-glycans regulates fibronectin matrix remodeling in tumor cells. Mol Cell Biol 2006;26:3181-93.
282. Saravanan C, Liu FT, Gipson IK, Panjwani N. Galectin-3 promotes lamellipodia formation in epithelial cells by interacting with complex N-glycans on alpha3beta1 integrin. J Cell Sci 2009;122:3684-93.

Appendix 1

Effect of MUC1 expression and MUC1-galectin-3 interaction on metastasis in vivo in nude mice (conducted by Prof Xiuli Guo et al in Shangdong University of China)

Methods: Eight-week-old female BALB/c athymic (*nu*$^{+}$/*nu*$^{+}$) nude mice were obtained from the Shanghai SLAC Laboratory Animals (Shanghai Institute for Biological Sciences) and maintained and used in accordance with the animal care protocol approved by Shandong University.

Suspensions (1.0 x 10^6 cells/mL with PBS) of ACA19^{+} and ACA19^{-} cells were passed through a 20-μm nylon mesh and incubated with or without galectin-3 (1 μg galectin-3 per 0.25 x 10^6 cells) with gentle shaking (30–60 rpm) for 1 h at 37°C before injection of the whole-cell suspension into the lateral tail vein of the experimental mice. Forty-eight experimental animals were randomly divided into four groups: 11 animals per group were injected with or without galectin-3–pretreated ACA19^{-} and 13 animals per group were injected with or without galectin-3–treated ACA19^{+} cells. The animals were maintained under standard conditions and observed daily. Two animals per group were randomly picked and sacrificed under ether anesthesia at days 20, 40, 60, and 80 (only the two ACA19^{+} groups at the last time point), and tumor metastases in lung, liver, and kidney were assessed by light microscopy. The remainder of the animals (five animals per group) were killed when considered by an independent blinded observer to be moribund, and the animal survival time from metastasis-associated death was recorded.

Immediate dissections of these animals were also done, and metastases to lung, liver, and kidney were examined by light microscope.

Results and discussion:

Forty-seven of the 48 experimental animals developed metastasis after inoculation of $ACA19^+$ or $ACA19^-$ cells with or without galectin-3 pretreatment. Metastatic foci were seen in the lungs but not in the other organs. At day 20, several metastatic foci in the edges of the lung lobes appeared in animals injected with $ACA19^-$. Metastatic foci were not visible in those injected with $ACA19^+$ at day 20 but were visible at day 40(Fig4-27C , Fig4-27D,Table4-1)

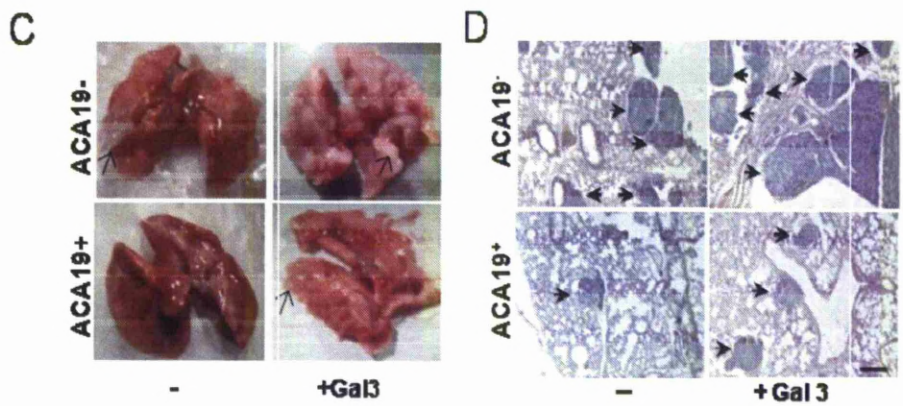

Fig4-27. Effects of MUC1 and MUC1-galectin-3 on ACA19 cell metastasis in athymic mice.*C,* macroscopic appearance of representative lungs 40 d after tumor cell injections. *Arrows,* metastatic foci. *D,* H&E staining of representative lung sections from animals 40 d after tumor cell injection. *Arrows,* metastatic lesions. *Bar,* 200 μm.

Table S1. the numbers of metastatic foci on surface of the lungs in two of the sacrificed experimental animals in each group

Animal groups	Average numbers of foci			
	Day 20	day 40	day 60	day 80
ACA19+	2±0	19±4	36±5	66±10
ACA19+/Gal3	18±3	41±6	70±6	131±13
ACA19-	32±8	99±5	166±46	
ACA19-/Gal3	172±23	217±11	192±18	

Table 4-1. Metastatic foci on the surface of the lungs of the experimental animals. The numbers of metastatic foci on the surface of lungs in the two sacrificed experimental animals at day 20, 40, 60 and 80 in each group were counted under a dissecting microscope. The data are expressed as mean numbers (the actual numbers for each animal are shown in the brackets) of the metastatic foci. It was noted that there were huge variations of the sizes of the metastatic foci in each experimental animals.

Animals bearing ACA19$^+$ cells survived significantly longer (164 ± 52 days) than those bearing ACA19$^-$ cells (85 ± 22 days; $P = 0.006$; Fig4-28).

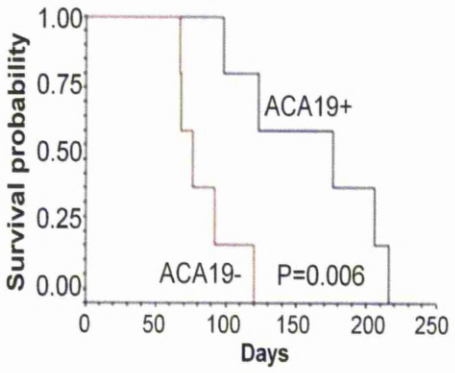

Fig4-28. Effects of MUC1 and MUC1-galectin-3 on ACA19 cell metastasis in athymic mice. *A*, animals injected with ACA19$^+$ cells have markedly increased survival compared with those injected with ACA19$^-$ cells.

Pretreatment of ACA19$^+$ cells with galectin-3 resulted in 35% reduction in animal survival (107 ± 31 days; P = 0.05;Fig4-29).

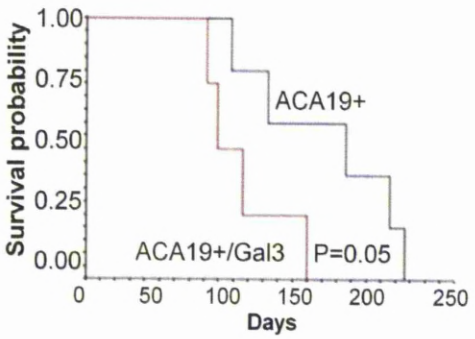

Fig4-29. Effects of MUC1 and MUC1-galectin-3 on ACA19 cell metastasis in athymic mice. Pretreatment of ACA19$^+$ cells with galectin-3 before injection led to shortened animal survival.

These results provide proof of concept that the effects of MUC1 expression and galectin-3-MUC1 interaction on cancer cell-endothelial adhesion are associated with decreased and increased metastasis, respectively. Pretreatment of ACA19$^-$ cells with galectin-3 resulted in a small but statistically nonsignificant reduction of animal survival from metastasis-associated death (62 ± 12 days; P = 0.1) compared with those injected with ACA19$^-$ cells alone. This suggests that recombinant/circulating galectin-3 may interact with other cell-surface molecules apart from MUC1 and that such interaction, although not affecting endothelial adhesion, may also contribute to metastasis.

Appendix 2

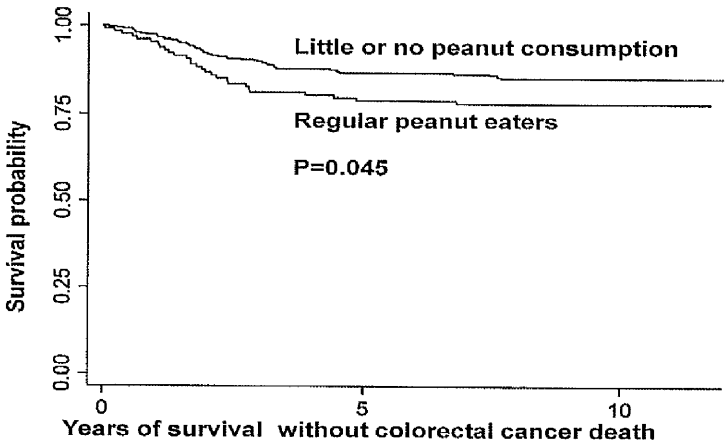

Retrospective analysis of mortality amongst the patients studied in an earlier case-controlled epidemiological study conducted by our group (Evens et al, 2002) shows a weak but significant correlation between regular consumption of peanut and poor survival of patients with colorectal cancer (the analysis are corrected for age, site of cancer, intakes of calories, alcohol, protein and fat). This earlier epidemiological study covered a population of 1,276,092 people residing in 62 postal codes and included 512 cancer patients in the Merseyside and Cheshire Cancer Registry and 512 matched controls.

PUBLICATION

Zhao Q, Guo X, Nash GB, Stone PC, Hilkens J, Rhodes JM, Yu LG(2009). Circulating galectin-3 promotes metastasis by modifying MUC1 localization on cancer cell surface." Cancer Res 69(17): 6799-806.

Qicheng Zhao, Monica Barclay, John Hilkens, Hannah Barrow, Jonathan Rhodes and Lu-Gang Yu. (2010). Interaction between galectin-3 and cancer-associated MUC1 enhances tumour cell homotypic aggregation and prevents Anoikis. Submitted to Molecular Cancer, (in press)

Published abstracts:

Qicheng Zhao, Xiuli Guo, Gerard Nash, Philip Stone, John Hilkens, Jonathan Rhodes, Lu-Gang Yu. Circulating galectin-3 promotes metastasis by modifying MUC1 localization on cancer cell surface. [abstract]. In: National Cancer Research Institute (NCRI) Cancer Conference 2007; 30 Sep -3 Oct 2007; Birmingham, UK. NCRI; Nov 2007. Abstract A95. Available from http://www.ncri.org.uk/ncriconference/2009abstracts/abstracts/A95.htm

Q Zhao, M Barclay, J Hilkens, JM Rhodes, LG Yu. Extracellular galectin-3 interacts with cell surface MUC1 to promote cancer cell aggregation, adhesion and trans-endothelial invasion: an important mechanism for metastasis. Gut 2008;57(Suppl I):A27. Available from http://gut.bmj.com/content/57/Suppl_1#Abstracts

Qicheng Zhao, Monica Barclay, Jonathan M. Rhodes, Lu-gang Yu. Galectin-3-Muc1 Interaction Promotes Epithelial Cancer Cell Aggregation: Potential Role of Circulating Galectin-3 in Colon Cancer Metastasis. Gastroenterology, Volume 132, Issue 4, Supplement 2, April 2007, Pages A306

Presentations in conferences:

Qicheng Zhao, Xiuli Guo, Gerard B. Nash, Philip C. Stone, John Hilkens, Jonathan M. Rhodes and Lu-Gang Yu. Circulating galectin-3 promotes metastasis by modifying MUC1 localization on cancer cell surface. Poster presentation, National Cancer Research Institute (NCRI) Cancer Conference, 4-7 October 2009, The ICC, Birmingham, UK

Q Zhao, M Barclay, J Hilkens, JM Rhodes, LG Yu. Extracellular galectin-3 interacts with cell surface MUC1 to promote cancer cell aggregation, adhesion and trans-endothelial invasion: an important mechanism for metastasis. Oral presentation, the British Society of Gastroenterology (BSG) annual meeting, 10-13 MARCH 2008, The ICC, Birmingham, UK

Qicheng Zhao, Monica Barclay, Jonathan M. Rhodes, Lu-gang Yu. Galectin-3-Muc1 Interaction Promotes Epithelial Cancer Cell Aggregation: Potential Role of Circulating Galectin-3 in Colon Cancer Metastasis. Poster presentation, Digestive Disease Week (DDW) 2007, May 19-24, 2007, Washington, DC, American.

Circulating Galectin-3 Promotes Metastasis by Modifying MUC1 Localization on Cancer Cell Surface

Qicheng Zhao,[1] Xiuli Guo,[2] Gerard B. Nash,[3] Philip C. Stone,[3] John Hilkens,[4] Jonathan M. Rhodes,[1] and Lu-Gang Yu[1]

[1]Gastroenterology Research Unit, School of Clinical Sciences, University of Liverpool, Liverpool, United Kingdom; [2]Department of Pharmacology, School of Pharmacy, Shandong University, Shandong, China; [3]Division of Medical Sciences, School of Medicine, University of Birmingham, Birmingham, United Kingdom; and [4]Division of Molecular Genetics, the Netherlands Cancer Institute, Amsterdam, the Netherlands

Abstract

Adhesion of circulating tumor cells to the blood vessel endothelium is a critical step in cancer metastasis. We show in this study that galectin-3, the concentration of which is greatly increased in the circulation of cancer patients, increases cancer cell adhesion to macrovascular and microvascular endothelial cells under static and flow conditions, increases transendothelial invasion, and decreases the latency of experimental metastasis in athymic mice. These effects of galectin-3 are shown to be a consequence of its interaction with cancer-associated MUC1, which breaks the "protective shield" of the cell-surface MUC1 by causing MUC1 polarization, leading to exposure of smaller cell-surface adhesion molecules/ligands including CD44 and ligand(s) for E-selectin. Thus, the interaction in the bloodstream of cancer patients between circulating galectin-3 and cancer cells expressing MUC1 bearing the galectin-3 ligand TF (Galβ1,3GalNAc-) promotes metastasis. This provides insight into the molecular regulation of metastasis and has important implications for the development of novel therapeutic strategies for prevention of metastasis. [Cancer Res 2009;69(17):6799–806]

Introduction

One of the critical steps in cancer metastasis is the adhesion of disseminating tumor cells to the blood vessel endothelium in distant organs. This process is thought to be regulated by the mechanical properties of the cancer cells and also by the specific expression of various adhesion molecules and/or ligands to adhesion molecules on the surface of cancer cells and endothelial cells (1).

MUC1 is a large transmembrane mucin protein that is expressed on the apical surface of most secretory epithelia. The extracellular domain of MUC1 consists of variable numbers of 20-amino-acid tandem repeat (VNTR) peptides that are heavily glycosylated (up to 50% of the molecule weight) with complex *O*-glycans (2). The expression of MUC1 is increased up to 10-fold in epithelial cancers (3), and this increased MUC1 expression is associated with high metastatic potential and poor prognosis (4, 5). The cancer-associated MUC1 loses its apical membrane polarization, becoming expressed over the entire cell surface (6, 7), and shows reduced expression of complex *O*-glycans and increased expression of short oligosaccharides such as GalNAcα- (Tn antigen), sialylated GalNAcα- (sialyl-Tn), and Galβ1,3GalNAcα-, the oncofetal Thomsen-Friedenreich (TF) antigen (8). The TF antigen, which is concealed by more extensive glycosylation and sialylation in normal epithelium, is revealed on ~90% of human epithelial cancer cells (9). Cancer-associated MUC1 and the cancer-associated high molecular weight splice variant of the adhesion molecule CD44v6 (10) are probably the major cell-surface glycoproteins that carry the unsubstituted TF antigen, but the secreted mucin, MUC2, has also been shown to carry the unsubstituted TF in LSLiM6 human colon cancer cells (4). In gastric and colorectal adenocarcinomas, MUC1 is the predominant carrier of TF (11, 12), and the expression of TF on MUC1 correlates with increased pathologic tumor-node-metastasis staging, histologic grading, and unfavorable prognosis (13, 14).

Because of its huge size and length (protruded >10 times higher above the cell surface than the typical cell-surface molecules), overexpression of MUC1 promotes tumor cell release from primary tumor sites by inhibiting E-cadherin–mediated cell-cell and integrin-mediated cancer-matrix interactions (6, 7). Binding of cell-surface MUC1 by intercellular adhesion molecule-1 increases cancer cell interaction with B lymphocytes (15), fibroblasts (16), and endothelial cells (17) in cell culture under static conditions. Cell-surface MUC1 is also involved in signal transduction via interaction of its cytoplasmic tail with important intracellular signaling proteins, such as p53 and β-catenin, and suppresses cellular apoptosis in response to DNA damage (18, 19).

Galectin-3 is a galactoside-binding protein that is expressed in many cell types (20) and is found inside cells, extracellularly (but still cell surface associated) and in the circulation. Intracellular galectin-3 is an apoptosis inhibitor and mRNA splicing promoter, whereas extracellular cell surface–associated galectin-3 acts as an adhesion molecule during cell-cell interactions and is associated with metastasis (20, 21). For example, galectin-3 expressed on the surface of breast cancer cells as well as on endothelial cells promotes adhesion of breast cancer cells to endothelium by interaction with cancer-associated TF antigen expressed by unknown cell-surface molecules (22, 23). Concentrations of circulating galectin-3 are markedly increased in the sera of cancer patients, and patients with metastatic disease have higher concentrations of circulating galectin-3 than those with localized tumors (24–26).

Recently, we reported that MUC1 is a natural ligand of galectin-3 in human cancer cells and that binding of recombinant galectin-3 to cancer-associated MUC1, via the TF antigen, induces MUC1 cell-surface polarization and increases the adhesion of human epithelial cells to human umbilical vein endothelial cells (HUVEC)

Note: Supplementary data for this article are available at Cancer Research Online (http://cancerres.aacrjournals.org/).

Requests for reprints: Lu-Gang Yu, The Henry Wellcome Laboratory, School of Clinical Sciences, University of Liverpool, Liverpool L69 3GE, United Kingdom. Phone: 44-151-794-6820; Fax: 44-151-794-6825; E-mail: lgyu@liv.ac.uk.

doi:10.1158/0008-5472.CAN-09-1096

under static cell culture conditions (27). Previous investigations have indicated that the great size and length of MUC1 allows it to form a protective shield on the cell surface and inhibit cell-cell and cell-matrix interactions (6, 7). We therefore suggested that interaction between circulating galectin-3 and cancer-associated MUC1 in the bloodstream of cancer patients may break the "protective shield" of MUC1 and reveal smaller cell-surface adhesion molecules/ligands that enhance cancer cell-endothelial adhesion and, hence, promote metastasis (27).

The present study provides *in vitro* and *in vivo* evidence that strongly supports this hypothesis. It shows that overexpression of cell-surface MUC1 is associated with reduced cancer cell-endothelial adhesion under static and flow conditions and with decreased cancer cell transendothelial invasion and increased survival of athymic nude mice inoculated i.v. with malignant melanoma cells. The interaction of cell surface MUC1 with recombinant galectin-3 at pathologically-relevant circulating galectin-3 concentrations markedly reduces the protective effects of cell surface MUC1 on cancer cell adhesion, trans-endothelial invasion and metastasis-free survival as a consequence of MUC1 cell surface polarization and subsequent exposure of cell-surface adhesion molecules/ligands including CD44 and ligand(s) for E-selectin.

Materials and Methods

Materials. Recombinant full-length human galectin-3 and monoclonal antibodies (mAb) against human CD44H (BBA10) and E-selectin (BBA16) were from R&D Systems. B27.29 anti-MUC1 mAb was kindly provided by Dr. Mark Reddish (Biomira, Inc.). Nonenzymatic Cell Dissociation Solution was from Sigma. Vybrant DiO Cell-Labeling Solutions were from Molecular Probes.

Cell lines. Human colon cancer HT29 and HT29-5F7 cells were obtained and cultured as described previously (27). Macrovascular HUVECs and human microvascular lung endothelial cells (HMVEC-L) were from Cambrex BioSciences and were cultured in EGM endothelial growth medium (EGM Bulletkit) and EGM-2 medium (EGM-2 Bulletkit, Cambrex BioSciences), respectively. Cells that had been passaged less than five times were used in the experiments. MUC1 transfection of human melanoma A375 cells with full-length cDNA encoding MUC1 resulted in the MUC1-positive transfectants ACA19$^+$, and the subsequent bulk selection of the MUC1-negative revertants ACA19$^-$ was as described previously (6).

Cancer cell-endothelial adhesion. Cancer cell-endothelial adhesion was done as described previously (27). At the end of the experiments, the samples were blinded and the fluorescently labeled cells remaining on the endothelial monolayer were counted in 10 randomly selected fields of view using fluorescent microscopy (Olympus B51). The ability of the cells to be labeled by the fluorescent dye was different between any two human cell lines tested in our pilot experiment. As comparison of

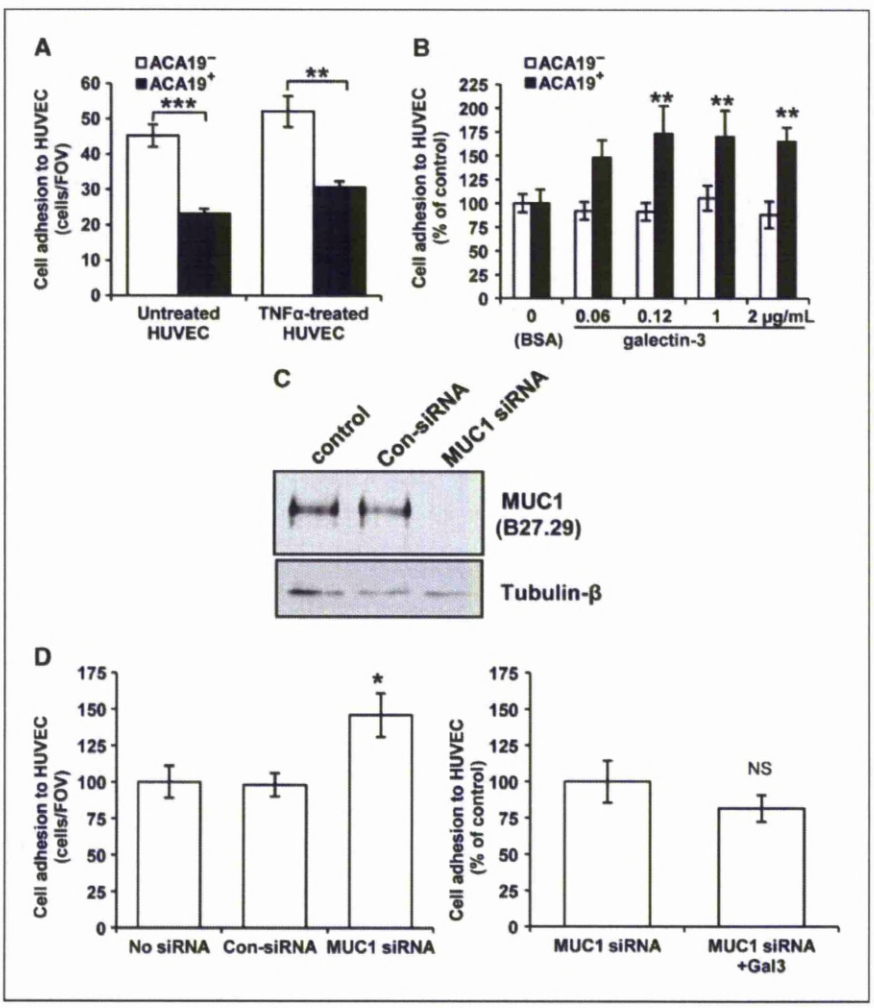

Figure 1. Effects of MUC1 and MUC1-galectin-3 on cancer cell-HUVEC adhesion under static conditions. *A*, ACA19$^+$ cells adhere less than ACA19$^-$ cells to HUVECs. *Columns*, mean of triplicate determinations from three independent experiments; *bars*, SE. *B*, pretreatment of the cells with galectin-3 increases ACA19$^+$, but not ACA19$^-$, cell adhesion to HUVECs. *Columns*, mean of three independent experiments; *bars*, SE. *C*, siRNA MUC1 suppression in ACA19$^+$ cells. Representative blots of three experiments. *D*, MUC1 suppression increases ACA19$^+$ cell adhesion (*left*) and abolishes galectin-3–induced cell adhesion (*right*). *Columns*, mean of three independent experiments; *bars*, SE. *, $P < 0.05$; **, $P < 0.01$; ***, $P < 0.001$.

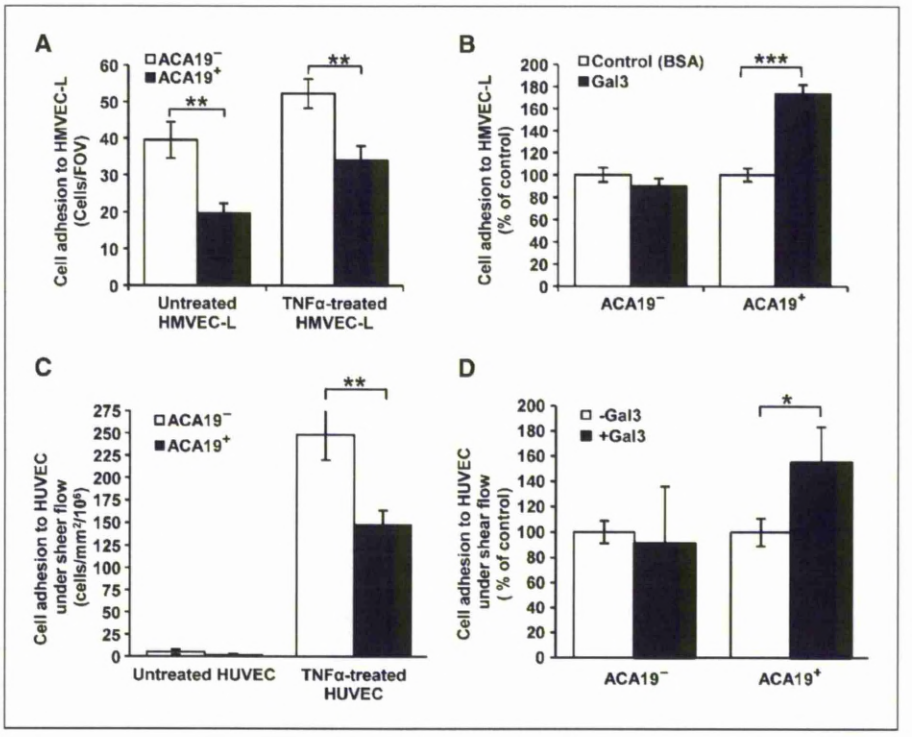

Figure 2. Effects of MUC1 and MUC1-galectin-3 on cancer cell-HMVEC-Ls adhesion under static conditions and on cancer cell-HUVEC adhesion under flow conditions. *A*, ACA19$^+$ cells adhere less than ACA19$^-$ cells to HMVEC-Ls. *Columns*, mean of three independent experiments; *bars*, SE. *B*, galectin-3 (1 μg/mL) increases ACA19$^+$, but not ACA19$^-$, cell adhesion to HMVEC-Ls. *Columns*, mean of two independent experiments; *bars*, SE. *C*, ACA19$^+$ cells adhere less than ACA19$^-$ cells to HUVECs at 0.05-Pa shear stress flow conditions. *Columns*, mean of seven independent experiments; *bars*, SE. *D*, galectin-3 (1 μg/mL) treatment increases adhesion of ACA19$^+$, but not ACA19$^-$, cells to HUVECs under flow conditions. *Columns*, mean of five ACA19$^+$ and six ACA19$^-$ independent assessments; *bars*, SE. *, $P < 0.05$; **, $P < 0.01$; ***, $P < 0.001$.

the cell adhesion between different MUC1-expressing cells is an important part of this study, the actual number of the fluorescently labeled cells adhered to endothelial monolayer, rather than the reading of the fluorescent density, was used as the end point.

MUC1 small interfering RNA knockdown. ACA19$^+$ cells were transfected with 100 nmol/L MUC1 small interfering RNA (siRNA) or scrambled control nontargeting siRNA (siCONTROL, Dharmacon) for 48 h at 37°C. The cells were lysed and the expression of MUC1 was assessed by MUC1 immunoblotting with the B27.29 anti-MUC1 antibody.

Cell adhesion under flow conditions. HUVECs, cultured in flattened glass capillaries for 24 h at 37°C to allow the cells to form monolayers as described previously (28), were unstimulated or stimulated with 10 ng/mL tumor necrosis factor-α (TNF-α) for 24 h at 37°C before the introduction of cancer cells. ACA19$^{+/-}$ cells were incubated with or without 1 μg/mL galectin-3 for 30 min at 37°C. The cells were then perfused through glass capillaries at a flow rate to deliver 0.05-Pa shear wall stress. After 4 min of washing with PBS, the capillaries were video-recorded and the number of adherent cells was quantified and expressed as the number of adherent cells per square millimeter per 10^6 cells perfused.

Cell-surface expressions of E-selectin and CD44. Cells released with Nonenzymatic Cell Dissociation Solution were fixed with 2% paraformaldehyde for 0.5 h, blocked with 5% normal goat serum/PBS for 0.5 h, and incubated with antibodies against E-selectin or CD44H for 1 h at room temperature. After application of fluorescein-conjugated secondary antibody for 0.5 h, the expression of cell-surface E-selectin or CD44 was analyzed by flow cytometry.

Transendothelial invasion. HUVECs were cultured in Transwell inserts with 8-μm-pore filters (BD Falcon) for 3 d to allow tight formation of cell monolayers. Monolayer integrity was monitored by measuring transendothelial electrical resistance using a volt-ohm meter (EVOM, World Precision Instruments), and monolayers with transendothelial electrical resistance >800 Ω/cm^2 were used for transendothelial assessment. Epithelial cells, labeled with DiO, were incubated with or without galectin-3 for 30 min at 37°C before application of the cells to the HUVECs for 16 h at 37°C. The cells at the upper side of the Transwell membrane were removed with a cotton swab and fluorescent cells migrated to the bottom side of the Transwell membrane were counted using an Olympus B51 fluorescence microscope.

Metastasis and survival. Eight-week-old female BALB/c athymic (*nu*$^+$/*nu*$^+$) nude mice were obtained from the Shanghai SLAC Laboratory Animals (Shanghai Institute for Biological Sciences) and maintained and used in accordance with the animal care protocol approved by Shandong University.

Suspensions (5.0×10^6 cells/mL with PBS) of ACA19$^+$ and ACA19$^-$ cells were passed through a 20-μm nylon mesh and incubated with or without galectin-3 (1 μg galectin-3 per 0.25×10^6 cells) with gentle shaking (30–60 rpm) for 1 h at 37°C before injection of the whole-cell suspension into the lateral tail vein of the experimental mice. Forty-eight experimental animals were randomly divided into four groups: 11 animals per group were injected with or without galectin-3–pretreated ACA19$^-$ and 13 animals per group were injected with or without galectin-3–treated ACA19$^+$ cells. The animals were maintained under standard conditions and observed daily. Two animals per group were randomly picked and sacrificed under ether anesthesia at days 20, 40, 60, and 80 (only the two ACA19$^+$ groups at the last time point), and tumor metastases in lung, liver, and kidney were assessed by light microscopy. The remainder of the animals (five animals per group) were killed when considered by an independent blinded observer to be moribund, and the animal survival time from metastasis-associated death was recorded. Immediate dissections of these animals were also done, and metastases to lung, liver, and kidney were examined by light microscopy.

Statistical analysis. Paired or unpaired *t* test for single-comparison, one-way ANOVA followed by Newman-Keuls' test for multiple comparisons, χ^2 test, and Kaplan-Meier analysis followed by log-rank test (StatsDirect for Windows, StatsDirect) were used where appropriate. Differences were considered significant when $P < 0.05$.

Results

Cancer cell-endothelial adhesion is inhibited by MUC1 expression but increased by MUC1-galectin-3 interaction. A375 human melanoma cells transfected with MUC1 (ACA19$^+$)

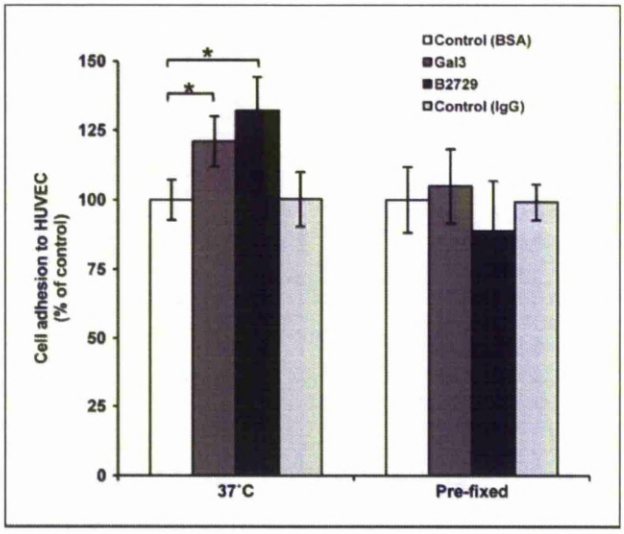

Figure 3. Galectin-3 and B27.29 anti-MUC1 mAb both induce increased adhesion to HUVECs of live, but not prefixed, ACA19$^+$ or ACA19$^-$ cells. Live or paraformaldehyde-prefixed ACA19$^{+/-}$ cells were pretreated with 1 μg/mL recombinant galectin-3, B27.29 mAb, bovine serum albumin (*BSA*), or control mouse IgG before adhesion to HUVECs. *Columns*, mean of four independent experiments; *bars*, SE. *, $P < 0.05$.

showed significantly less adhesion to unstimulated and TNF-α–prestimulated HUVECs compared with the MUC1-negative revertants (ACA19$^-$; Fig. 1*A*). To determine the effect of circulating galectin-3 on cancer cell adhesion to endothelium, we pretreated the cells with recombinant galectin-3 at several pathologically relevant circulating galectin-3 concentrations. Earlier investigation by Iurisci and colleagues (24) has shown that the concentration of circulating galectin-3 increases up to 5-fold in the sera of cancer patients with melanoma, breast, or gastrointestinal cancer (range, 20–950 ng/mL) compared with healthy people. Our own investigation has indicated that the concentrations of circulating galectin-3 in the sera of colorectal cancer patients are >14-fold higher (up to 5 μg/mL) than in healthy people.[5] We found that pretreatment of the cells with galectin-3 at concentrations >100 ng/mL resulted in significant increase of ACA19$^+$, but not ACA19$^-$, cell adhesion to HUVECs (Fig. 1*B*). Immuno/lectin blots of ACA19$^+$ and ACA19$^-$ cells with B27.29 anti-MUC1 mAb and TF-binding DNA showed that MUC1 in ACA19$^+$ cells is abundantly decorated with TF antigens (Supplementary Fig. S1). Suppression of MUC1 expression by siRNA in ACA19$^+$ cells was associated with 47% increased adhesion of the cells to HUVECs, and this prevented the increase of cell adhesion in response to galectin-3 (Fig. 1*C* and *D*). Thus, the presence of extracellular free galectin-3, by its interaction with MUC1, counteracts the antiadhesive effect of MUC1 expression on cancer cell adhesion.

To determine whether MUC1-galectin-3 interaction has similar effects on cell adhesion in cancer cells that naturally express MUC1, we compared the adhesion of human colon cancer HT29 and HT29-5F7 cells in the presence or absence of recombinant galectin-3. HT29-5F7 is a HT29 subline selected by its resistance to 5-fluorouracil and has much greater MUC1 than the parental HT29 cells (ref. 29; Supplementary Fig. S2). HT29 cells showed significantly more adhesion to unstimulated and TNF-α–prestimulated HUVECs than HT29-5F7 cells (Supplementary Fig. S3*A*). Pretreatment of the cells with galectin-3 significantly increased adhesion of HT29-5F7, but not HT29, cells to HUVECs, and this effect was abolished by the presence of TF-expressing asialofetuin (Supplementary Fig. S3).

We also assessed whether galectin-3 may have been secreted into the medium by the cancer cells, but we found no detectable endogenously secreted galectin-3 (<0.325 ng/mL, the detectable limit of the assay) in the medium during the 1.5-hour assessment period. Thus, the contribution of endogenously secreted galectin-3 to recombinant galectin-3–mediated cell adhesion in these assessments is minimal.

To see whether the effects of MUC1–galectin-3 interaction on cancer cell adhesion to HUVECs also occur with microvascular endothelium, a model that is probably closer to the *in vivo* situation in metastasis, we analyzed cell adhesion to HMVEC-L. Again, ACA19$^+$ cells showed significantly less adhesion to unstimulated and TNF-α–prestimulated HMVEC-Ls than ACA19$^-$ cells (Fig. 2*A*). Pretreatment of the cells with galectin-3 (1 μg/mL) increased adhesion of ACA19$^+$ cells but not of ACA19$^-$ cells (Fig. 2*B*).

Collectively, these results indicate that MUC1 expression prevents cancer cell adhesion to macrovascular and microvascular endothelium and that MUC1-galectin-3 interaction reduces this protective effect of MUC1.

Cancer cell-endothelial adhesion under flow conditions is inhibited by MUC1 expression but increased by MUC1-galectin-3 interaction. Under shear flow conditions, very few ACA19$^+$ or ACA19$^-$ cells showed adhesion to unstimulated HUVECs, but their adhesion was markedly increased when HUVECs were pretreated with TNF-α (Fig. 2*C*). Moreover, ACA19$^+$ cells showed 68% less adhesion than ACA19$^-$ cells to TNF-α–stimulated HUVECs under such conditions. Pretreatment of the cells with 1 μg/mL galectin-3 resulted in 55% increased adhesion of ACA19$^+$ cells but not of ACA19$^-$ cells (Fig. 2*D*). Thus, the effects of MUC1 expression and galectin-3-MUC1 interaction on cancer cell-endothelial adhesion seen under static conditions also hold true under flow conditions.

Galectin-3 and B27.29 anti-MUC1 mAb have similar effects on MUC1 cell-surface polarization and on cell adhesion. We have previously shown that galectin-3-MUC1 interaction induces change in MUC1 cell-surface localization (27). To see whether this change in MUC1 localization is associated with altered cell adhesion to endothelium, we compared MUC1 cell-surface clustering in response to galectin-3 and cell adhesion to HUVECs.

It was found that 10% (48 of 500) ACA19$^+$ cells showed spontaneous clustering of MUC1 on the cell surface, as illustrated by discontinuity of MUC1 cell-surface staining when cultured in suspension for 1 h at 37°C. After pretreatment with galectin-3 (1 μg/mL) at 37°C for 1 h, 40% more (68 of 500; $P < 0.05$) cells showed MUC1 cell-surface polarization than control cells. Introduction of B27.29 anti-MUC1 mAb also resulted in significant increase (128 of 500; $P < 0.01$) in the number of cells showing MUC1 cell-surface polarization. This effect of B27.29 on MUC1 cell-surface polarization is in keeping with previous reports that the presence of 214D4 anti-MUC1 mAb, which also recognizes the VNTR region of MUC1, induces MUC1 cell-surface polarization in MUC1-transfected human melanoma cells (6). The B27.29 mAb recognizes the PDTRPAP epitope in the VNTR region of MUC1 (30), and nuclear magnetic resonance analysis has indicated an enhanced binding affinity of B27.29 to MUC1 in the presence of short sugar chains within the VNTR region (31).

[5] H. Barrow, J.M. Rhodes, and L.G. Yu, in preparation.

It was found that the increases of MUC1 cell-surface polarization in response to galectin-3 and to B27.29 mAb are both associated with increased adhesion of ACA19$^+$ cells to HUVECs (Fig. 3). Furthermore, introduction of galectin-3 or B27.29 mAb to paraformaldehyde-prefixed cells, which could not affect the MUC1 cell-surface localization, failed to induce cell adhesion to HUVECs compared with the control cells. These results support a direct link of discontinuous cell-surface localization of MUC1 and increased cell adhesion in response to galectin-3 and B27.29 mAb.

Involvement of cancer-associated CD44 and endothelial-E-selectin in MUC1-galectin-3–induced cancer cell-endothelial adhesion. The presence of 25 μg/mL anti-CD44H mAb (BBA10), which recognizes all CD44 isoforms, caused 26% ($P < 0.05$) inhibition of ACA19$^-$, but not ACA19$^+$, adhesion to HUVECs, but largely blocked ACA19$^+$ cell adhesion induced by galectin-3 (Fig. 4*A*). The presence of 25 μg/mL anti–E-selectin antibody, however, failed to block the adhesion of either ACA19$^-$ or ACA19$^+$ cells and also showed no significant inhibition ($P = 0.47$) of galectin-3–induced ACA19$^+$ adhesion (Fig. 4*A*). The presence of either anti-CD44H or anti–E-selectin antibody inhibited HT29 cell adhesion to HUVECs (Fig. 4*B*). Neither of these antibodies at this concentration showed significant inhibition of HT29-5F7 cell adhesion to HUVECs, but their presence completely prevented the increase of HT29-5F7 cell adhesion in response to galectin-3.

Antibody binding followed by flow cytometry analysis showed similar CD44 cell-surface expression and antibody accessibility between HT29 and HT29-5F7 and between ACA19$^-$ and ACA19$^+$ cells (Fig. 4*C*). Thus, the lack of effect of the anti-CD44H antibody on the adhesion of HT29-5F7 and ACA19$^+$ cells to HUVECs is likely due to the inability of cell-surface CD44 to gain access to its receptor on HUVECs as a result of functional concealment of cell-surface CD44, for example, by the presence of adjacent MUC1. The inhibition by the anti-CD44H antibody of galectin-3–induced cell adhesion, in which cell-surface CD44 is functionally exposed following MUC1 cell-surface polarization, supports this conclusion. The relatively modest inhibition of the anti-CD44 antibody at 25 μg/mL on ACA19$^-$ adhesion indicates that cell-surface CD44 may represent just one of several cell adhesion molecules involved in melanoma cell-endothelial adhesion.

We found that anti-CD44H antibody pretreatment of HT29 cells, but not of HUVECs, caused a significant inhibition of subsequent HT29 cell adhesion to HUVECs (Fig. 4*D*). This indicates the involvement of HT29-associated, but not HUVEC-associated, CD44 molecules in HT29-endothelial interaction and in galectin-3–mediated cancer cell-endothelial adhesion. This is in keeping with earlier reports of a role for cancer-associated CD44 in the initial endothelial adhesion of human prostate, breast, and colon cancer cells (32, 33).

Neither HT29/HT29-5F7 nor ACA19$^-$/ACA19$^+$ cells express E-selectin on their cell surface (Fig. 4*C*). The HT29 cell adhesion to HUVECs and the HT29-5F7 adhesion to HUVECs induced by galectin-3 were, however, inhibited by the presence of the anti–E-selectin antibody (Fig. 4*A* and *B*). This suggests the involvement of endothelial-E-selectin in these cell adhesion events. The different effects of the anti–E-selectin antibody on HT29/HT29-5F7 and ACA19$^{-/+}$ adhesions to HUVECs likely reflect differences in the expression of E-selectin ligands on the surface of HT29 colon and ACA19 melanoma cells.

Cancer cell transendothelial invasion is inhibited by MUC1 expression and increased by MUC1-galectin-3 interaction. ACA19$^-$ showed 46% greater trans-HUVEC invasion than ACA19$^+$

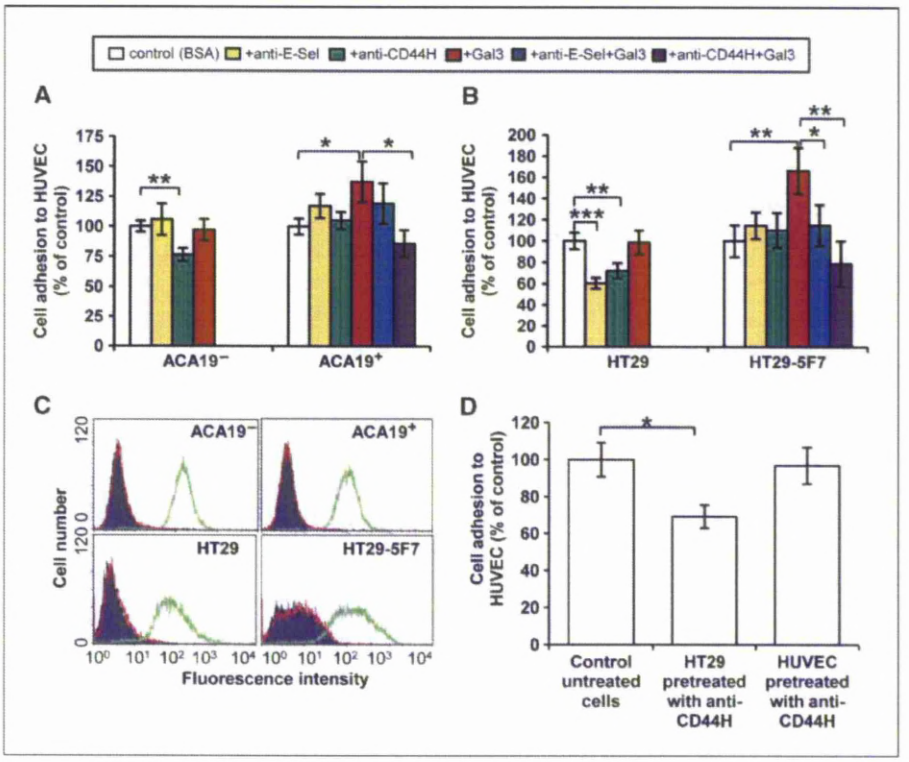

Figure 4. Involvement of cell-surface CD44 and ligand(s) to endothelial-E-selectin in galectin-3–induced cancer cell-endothelial adhesion. *A*, the presence of 25 μg/mL anti-CD44H, but not anti–E-selectin, mAb reduces ACA19$^-$ cell adhesion and adhesion of ACA19$^+$ cells induced by 1 μg/mL galectin-3. *Columns*, mean of three independent experiments; *bars*, SE. *B*, the presence of 25 μg/mL anti-CD44H or anti–E-selectin antibody inhibits HT29 and HT29-5F7 cell adhesion and adhesion of HT29-5F7 cells induced by 1 μg/mL recombinant galectin-3. *Columns*, mean of three independent experiments; *bars*, SE. *C*, cell-surface expression of E-selectin and CD44 are similar between HT29 and HT29-5F7 cells and between ACA19$^+$ and ACA19$^-$ cells. *Green*, CD44; *red*, E-selectin; *purple*, isotype control. *D*, pretreatment of HT29 cells, but not of HUVECs, with 25 μg/mL anti-CD44H antibody inhibits HT29 cell adhesion to HUVECs. *Columns*, mean of three independent experiments; *bars*, SE. *, $P < 0.05$; **, $P < 0.01$; ***, $P < 0.001$.

cells (Fig. 5*A*). Pretreatment of the cells with galectin-3 (1 μg/mL) resulted in 64% increased invasion of ACA19$^+$ cells but not of ACA19$^-$ cells (Fig. 5*B*). This effect of galectin-3 was completely prevented by the presence of lactose (Fig. 5*C*).

Galectin-3 promotes metastasis of ACA19$^+$ MUC1-expressing cells *in vivo*. Forty-seven of the 48 experimental animals developed metastasis after inoculation of ACA19$^+$ or ACA19$^-$ cells with or without galectin-3 pretreatment. Metastatic foci were seen in the lungs but not in the other organs. At day 20, several metastatic foci in the edges of the lung lobes appeared in animals injected with ACA19$^-$. Metastatic foci were not visible in those injected with ACA19$^+$ at day 20 but were visible at day 40 (Fig. 6*C* and *D*; Supplementary Table S1). Animals bearing ACA19$^+$ cells survived significantly longer (164 ± 52 days) than those bearing ACA19$^-$ cells (85 ± 22 days; $P = 0.006$; Fig. 6*A*). Pretreatment of ACA19$^+$ cells with galectin-3 resulted in 35% reduction in animal survival (107 ± 31 days; $P = 0.05$; Fig. 6*B*). These results provide proof of concept that the effects of MUC1 expression and galectin-3-MUC1 interaction on cancer cell-endothelial adhesion are associated with decreased and increased metastasis, respectively. Pretreatment of ACA19$^-$ cells with galectin-3 resulted in a small but statistically nonsignificant reduction of animal survival from metastasis-associated death (62 ± 12 days; $P = 0.1$) compared with those injected with ACA19$^-$ cells alone. This suggests that recombinant/circulating galectin-3 may interact with other cell-surface molecules apart from MUC1 and that such interaction, although not affecting endothelial adhesion, may also contribute to metastasis.

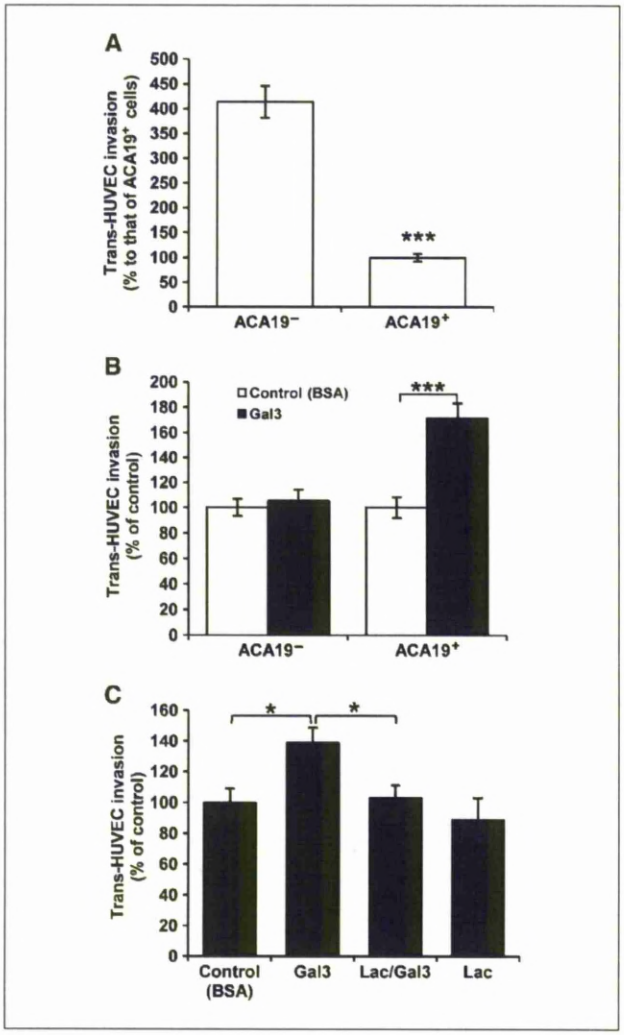

Figure 5. Effects of MUC1 and MUC1-galectin-3 on cancer cell transendothelial invasion. *A*, ACA19$^+$ cells show less trans-HUVEC invasion than ACA19$^-$ cells. *Columns*, mean of triplicate determinations from six independent experiments; *bars*, SE. *B*, galectin-3 (1 μg/mL) pretreatment increases ACA19$^+$, but not ACA19$^-$, cell trans-HUVEC invasion. *Columns*, mean of six independent experiments; *bars*, SE. *C*, galectin-3–mediated transendothelial invasion of ACA19$^+$ is inhibited by the presence of (10 μg/mL) lactose. *Columns*, mean of four independent assessments; *bars*, SE. *, $P < 0.05$; ***, $P < 0.0001$.

Discussion

This study shows that overexpression of cell-surface MUC1 is associated with reduced cancer cell-endothelial adhesion under static and flow conditions and with decreased cancer cell transendothelial invasion and increased survival of athymic nude mice inoculated i.v. with malignant melanoma cells. The interaction of cell-surface MUC1 with circulating galectin-3 at pathologically relevant concentrations reduces the protective effects of MUC1 on cancer cell adhesion, transendothelial invasion, and metastasis. These effects of galectin-3 are mediated by MUC1 cell-surface clustering and the consequent exposure of cell-surface adhesion molecules including CD44 and the ligand(s) for endothelial-E-selectin. Thus, the enhanced molecular interaction between circulating galectin-3 and cancer-associated MUC1 in the bloodstream of cancer patients, occurring as a result of the increased expression of MUC1 by cancer cells, the increased expression of the galectin-3-ligand TF antigen by cancer-associated MUC1, and the increased concentration of circulating galectin-3, all of which are common features in cancer, promotes metastasis.

Cancer cell adhesion to endothelium is a vital step in metastasis and is mediated by a range of adhesion molecules and their ligands, including selectins and integrins expressed on cancer cells and endothelial cells, which in turn are regulated by circulating molecules such as cytokines (1). The inhibitory effect of MUC1 expression and the stimulatory effect of galectin-3-MUC1 interaction on cancer cell-endothelial adhesion shown in this study suggest that MUC1 cell-surface polarization, which leads to uncovering of the smaller adhesion molecules and/or ligands to adhesion molecules, represents an essential first step in the process of cancer cell-endothelial adhesion. Given the variable expression of MUC1 in different cancer cell lines (34), the lack of inhibitory effect of anti-selectin antibodies on cancer cell-endothelial adhesion observed in several previous investigations (35) may be, to a large extent, due to the concealment of the cell-surface selectin ligands by MUC1.

MUC1 can carry sialyl Lewis–related carbohydrate structures that act as ligands for selectins (36). However, an interaction between cancer-associated MUC1 and endothelial-E-selectin will probably not induce tight cell adhesion, a process that is believed to require the involvement of cell-surface integrins as has been well established for leukocyte-endothelial adhesion (37). Tight cancer cell-endothelial adhesion may only occur after MUC1 cell-surface polarization and exposure of integrins and other smaller cell adhesion molecules. Our previous demonstration (27) that MUC1 is absent at the cancer cell-endothelial contact point supports this.

The protective effect of the MUC1 "shield" and the "deprotective" effect of the galectin-3-TF/MUC1 interaction on cancer cell adhesion provide explanations at the molecular level for several

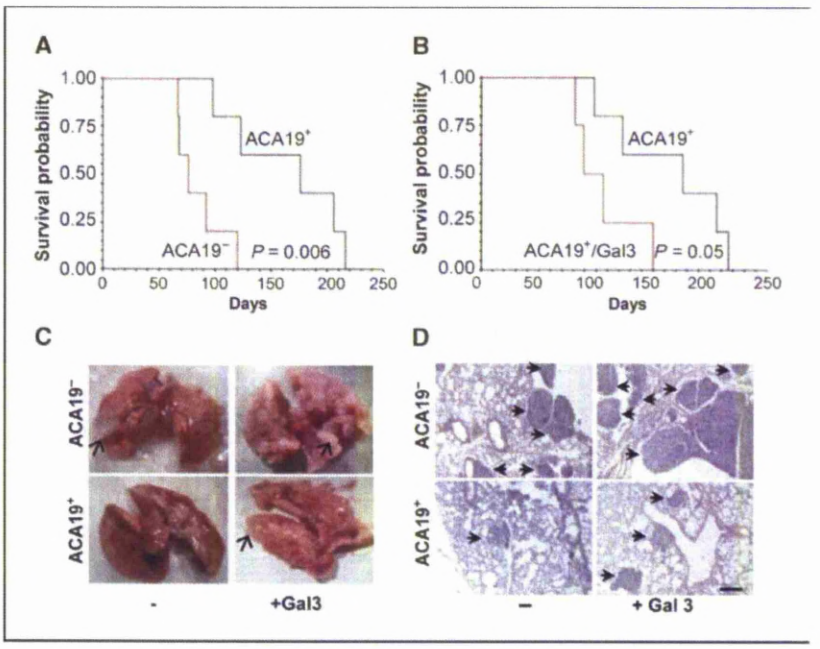

Figure 6. Effects of MUC1 and MUC1-galectin-3 on ACA19 cell metastasis in athymic mice. *A*, animals injected with ACA19$^+$ cells have markedly increased survival compared with those injected with ACA19$^-$ cells. *B*, pretreatment of ACA19$^+$ cells with galectin-3 before injection led to shortened animal survival. *C*, macroscopic appearance of representative lungs 40 d after tumor cell injections. *Arrows*, metastatic foci. *D*, H&E staining of representative lung sections from animals 40 d after tumor cell injection. *Arrows*, metastatic lesions. *Bar*, 200 μm.

recent clinical and experimental observations related to metastasis, for example, the correlation between increased apical MUC1 cell-surface polarization and increased lymphatic invasion, recurrence rate, and lower overall survival in breast cancer patients (38). The correlation of increased concentrations of circulating anti-TF antibodies, which would inhibit galectin-3–mediated TF/MUC1 interactions, with improved prognosis in gastric cancer (39) is also consistent with our model. The association of MUC1 sialylation with a better prognosis in breast cancer (40) is also in keeping with a reduced galectin-3-TF/MUC1 interaction as a consequence of concealment of TF by sialic acid, thus inhibiting MUC1-galectin-3 interaction (27). The significant extension of animal survival induced by i.p. coinjection of an anti-TF antibody with metastatic 4T1 breast cancer cells (41) could be the consequence of the blockade of the galectin-3-TF/MUC1 interaction.

Because increased occurrence of the TF glycan is one of the commonest glycosylation changes in cancer (9), this study also highlights the functional importance of cancer-associated changes in cellular glycosylation (42, 43) and indicates a potential for glycan profiling in predicting cancer metastasis and prognosis. Furthermore, as the increased concentrations of circulating galectin-3 in cancer patients are probably produced not only by the tumor cells but also by the peritumoral inflammatory and stromal cells (24), this also reinforces the importance of the tumor microenvironment for metastasis (44, 45).

It should be emphasized that this study focuses on the role of circulating galectin-3 on cancer cell adhesion and metastasis. The functional importance of cancer cell-associated galectin-3 in metastasis is well documented (20, 21). For example, antisense suppression of galectin-3 in metastatic LSLiM6 human colon cancer cells before inoculation of the cells into athymic mice results in reduced liver colonization and metastasis (46), whereas suppression of galectin-3 expression by short hairpin RNA in melanoma cells reduces tumor cell invasiveness and capacity to form tube-like structures on collagen, so-called vasculogenic mimicry (47). Similarly, reduction of galectin-3 expression in highly malignant human breast cancer MDA-MB-435 cells leads to loss of serum- and anchorage-independent growth *in vitro* and tumor growth in nude mice (48).

Thus, galectin-3 released into the bloodstream of cancer patients promotes cancer cell hematogenous dissemination by its interaction with TF-expressing MUC1 on cancer cell surface. This provides insight into the molecular regulation of metastasis and has important implications for the development of therapeutic strategies to prevent metastasis.

Disclosure of Potential Conflicts of Interest

No potential conflicts of interest were disclosed.

Acknowledgments

Received 3/24/09; revised 5/29/09; accepted 6/23/09; published OnlineFirst 8/18/09.

Grant support: Cancer Research UK grant C7596 and North West Cancer Research Fund grant CR777 (L-G. Yu).

The costs of publication of this article were defrayed in part by the payment of page charges. This article must therefore be hereby marked *advertisement* in accordance with 18 U.S.C. Section 1734 solely to indicate this fact.

We thank Dr. Thecla Lesuffleur (INSERM U560, Lille, France) for the HT29-5F7 cells and Dr. Mark Reddish (Biomira, Edmonton, Canada) for the B27.29 mAb.

References

1. Miles FL, Pruitt FL, van-Golen KL, Cooper CR. Stepping out of the flow: capillary extravasation in cancer metastasis. Clin Exp Metastasis 2008;25:305–24.
2. Kim YS, Gum JR, Jr., Brockhausen I. Mucin glycoproteins in neoplasia. Glycoconj J 1996;13:693–707.
3. Hilkens J, Ligtenberg MJ, Vos HL, Litvinov SV. Cell membrane-associated mucins and their adhesion-modulating property. Trends Biochem Sci 1992;17:359–63.
4. Bresalier RS, Niv Y, Byrd JC, et al. Mucin production by human colonic carcinoma cells correlates with their metastatic potential in animal models of colon cancer metastasis. J Clin Invest 1991;87:1037–45.
5. Nakamori S, Ota DM, Cleary KR, Shirotani K, Irimura

T. MUC1 mucin expression as a marker of progression and metastasis of human colorectal carcinoma. Gastroenterology 1994;106:353–61.
6. Wesseling J, van der Valk SW, Hilkens J. A mechanism for inhibition of E-cadherin-mediated cell-cell adhesion by the membrane-associated mucin episialin/MUC1. Mol Biol Cell 1996;7:565–77.
7. Wesseling J, van der walk SW, Vos HJ, Sonnenberg A, Hilkens J. Epithelin (MUC1) overexpression inhibits integrin-mediated cell adhesion to extracellular matrix components. J Cell Biol 1995;129:255–65.
8. Lloyd KO, Burchell J, Kudryashov V, Yin BW, Taylor-Papadimitriou J. Comparison of *O*-linked carbohydrate chains in MUC-1 mucin from normal breast epithelial cell lines and breast carcinoma cell lines. Demonstration of simpler and fewer glycan chains in tumor cells. J Biol Chem 1996;271:33325–34.
9. Yu LG. The oncofetal Thomsen-Friedenreich carbohydrate antigen in cancer progression. Glycoconj J 2007;24:411–20.
10. Singh R, Campbell BJ, Yu LG, et al. Cell surface-expressed Thomsen-Friedenreich antigen in colon cancer is predominantly carried on high molecular weight splice variants of CD44. Glycobiology 2001;11:587–92.
11. Baldus SE, Hanisch FG, Kotlarek GM, et al. Coexpression of MUC1 mucin peptide core and the Thomsen-Friedenreich antigen in colorectal neoplasms. Cancer 1998;82:1019–27.
12. Baldus SE, Hanisch FG, Monaca E, et al. Immunoreactivity of Thomsen-Friedenreich (TF) antigen in human neoplasms: the importance of carrier-specific glycotope expression on MUC1. Histol Histopathol 1999;14:1153–8.
13. Baldus SE, Wienand JR, Werner JP, et al. Thomsen-Friedenreich antigen presents as a prognostic factor in colorectal carcinoma: a clinicopathologic study of 264 patients. Cancer 2000;88:1536–43.
14. Baldus SE, Zirbes TK, Glossmann J, et al. Immunoreactivity of monoclonal antibody BW835 represents a marker of progression and prognosis in early gastric cancer. Oncology 2001;61:147–55.
15. McDermott KM, Crocker PR, Harris A, et al. Overexpression of MUC1 reconfigures the binding properties of tumor cells. Int J Cancer 2001;94:783–91.
16. Rahn JJ, Shen Q, Mah BK, Hugh JC. MUC1 initiates a calcium signal after ligation by intercellular adhesion molecule-1. J Biol Chem 2004;279:29386–90.
17. Rahn JJ, Chow JW, Horne GJ, et al. MUC1 mediates transendothelial migration *in vitro* by ligating endothelial cell ICAM-1. Clin Exp Metastasis 2005;22:475–83.
18. Wei X, Xu H, Kufe D. MUC1 oncoprotein regulates p53-responsive gene transcription in the genotoxic stress response. Cancer Cell 2005;7:167–78.
19. Singh PK, Hollingsworth MA. Cell surface-associated mucins in signal transduction. Trends Cell Biol 2006;16:467–76.
20. Liu FT, Rabinovich GA. Galectins as modulators of tumour progression. Nat Rev Cancer 2005;5:29–41.
21. Takenaka Y, Fukumori T, Raz A. Galectin-3 and metastasis. Glycoconj J 2004;19:543–9.
22. Glinsky VV, Glinsky GV, Rittenhouse-Olson K, et al. The role of Thomsen-Friedenreich antigen in adhesion of human breast and prostate cancer cells to the endothelium. Cancer Res 2001;61:4851–7.
23. Khaldoyanidi SK, Glinsky VV, Sikora L, et al. MDA-MB-435 human breast carcinoma cell homo- and heterotypic adhesion under flow conditions is mediated in part by Thomsen-Friedenreich antigen-galectin-3 interactions. J Biol Chem 2003;278:4127–34.
24. Iurisci I, Tinari N, Natoli C, et al. Concentrations of galectin-3 in the sera of normal controls and cancer patients. Clin Cancer Res 2000;6:1389–93.
25. Saussez S, Lorfevre F, Lequeux T, et al. The determination of the levels of circulating galectin-1 and -3 in HNSCC patients could be used to monitor tumour progression and/or responses to therapy. Oral Oncol 2008;44:86–93.
26. Vereecken P, Zouaoui Boudjeltia K, Debray C, et al. High serum galectin-3 in advanced melanoma: preliminary results. Clin Exp Dermatol 2006;31:105–9.
27. Yu LG, Andrews N, Zhao Q, et al. Galectin-3 interaction with Thomsen-Friedenreich disaccharide on cancer-associated MUC1 causes increased cancer cell endothelial adhesion. J Biol Chem 2007;282:773–81.
28. Sheikh S, Rainger GE, Gale Z, Rahman M, Nash GB. Exposure to fluid shear stress modulates the ability of endothelial cells to recruit neutrophils in response to tumor necrosis factor-α: a basis for local variations in vascular sensitivity to inflammation. Blood 2003;102:2828–34.
29. Leteurtre E, Gouyer V, Rousseau K, et al. Differential mucin expression in colon carcinoma HT-29 clones with variable resistance to 5-fluorouracil and methotrexate. Biol Cell 2004;96:145–51.
30. Schol DJ, Meulenbroek MFA, Snijdewint FGM, et al. 'Epitope fingerprinting' using overlapping 20-mer peptides of the MUC1 tandem repeat sequence. Tumor Biol 1998;19:35–45.
31. Grinstead JS, Koganty RR, Krantz MJ, Longenecker BM, Campbell AP. Effect of glycosylation on MUC1 humoral immune recognition: NMR studies of MUC1 glycopeptide-antibody interactions. Biochemistry 2002;41:9946–61.
32. Draffin JE, McFarlane S, Hill A, et al. CD44 potentiates the adherence of metastatic prostate and breast cancer cells to bone marrow endothelial cells. Cancer Res 2004;64:5702–11.
33. Fujisaki T, Tanaka Y, Fujii K, et al. CD44 stimulation induces integrin-mediated adhesion of colon cancer cell lines to endothelial cells by up-regulation of integrins and c-Met and activation of integrins. Cancer Res 1999;59:4427–34.
34. Ligtenberg MJ, Vos HL, Gennissen AM, Hilkens J. Episialin, a carcinoma-associated mucin, is generated by a polymorphic gene encoding splice variants with alternative amino termini. J Biol Chem 1990;265:5573–8.
35. Krause T, Turner GA. Are selectins involved in metastasis? Clin Exp Metastasis 1999;17:181–92.
36. Zhang K, Baeckström D, Brevinge H, Hansson GC. Secreted MUC1 mucins lacking their cytoplasmic part and carrying sialyl-Lewis a and x epitopes from a tumor cell line and sera of colon carcinoma patients can inhibit HL-60 leukocyte adhesion to E-selectin-expressing endothelial cells. J Cell Biochem 1996;60:538–49.
37. Lowe JB. Glycan-dependent leukocyte adhesion and recruitment in inflammation. Curr Opin Cell Biol 2003;15:531–8.
38. Li YS, Kaneko M, Sakamoto DG, Takeshima Y, Inai K. The reversed apical pattern of MUC1 expression is characteristics of invasive micropapillary carcinoma of the breast. Breast Cancer 2006;13:58–63.
39. Kurtenkov O, Klaamas K, Mensdorff-Pouilly S, Miljukhina L, Shljapnikova L, Chuzmarov V. Humoral immune response to MUC1 and to the Thomsen-Friedenreich (TF) glycotope in patients with gastric cancer: relation to survival. Acta Oncol 2007;46:316–23.
40. Baldus SE, Wienand JR, Werner JP, et al. Expression of MUC1, MUC2 and oligosaccharide epitopes in breast cancer: prognostic significance of a sialylated MUC1 epitope. Int J Oncol 2005;27:1289–97.
41. Heimburg J, Yan J, Morey S, et al. Inhibition of spontaneous breast cancer metastasis by anti-Thomsen-Friedenreich antigen monoclonal antibody JAA-F11. Neoplasia 2006;8:939–48.
42. Kim YJ, Varki A. Perspectives on the significance of altered glycosylation of glycoproteins in cancer. Glycoconj J 1997;14:569–76.
43. Gorelik E, Galili U, Raz A. On the role of cell surface carbohydrates and their binding proteins (lectins) in tumor metastasis. Cancer Metastasis Rev 2001;20:245–77.
44. Albini A, Mirisola V, Pfeffer U. Metastasis signatures: genes regulating tumor-microenvironment interactions predict metastatic behavior. Cancer Metastasis Rev 2008;27:75–83.
45. Finak G, Bertos N, Pepin F, et al. Stromal gene expression predicts clinical outcome in breast cancer. Nat Med 2008;14:518–27.
46. Bresalier RS, Mazurek N, Sternberg LR, et al. Metastasis of human colon cancer is altered by modifying expression of the β-galactoside-binding protein galectin 3. Gastroenterology 1998;115:287–96.
47. Mourad-Zeidan AA, Melnikova VO, Wang H, Raz A, Bar-Eli M. Expression profiling of galectin-3-depleted melanoma cells reveals its major role in melanoma cell plasticity and vasculogenic mimicry. Am J Pathol 2008;173:1839–52.
48. Honjo Y, Nangia-Makker P, Inohara H, Raz A. Down-regulation of galectin-3 suppresses tumorigenicity of human breast carcinoma cells. Clin Cancer Res 2001;7:661–8.